Wissenschaftszentrum Weihenstephan für Ernährung, Landnutzung und Umwelt

Lehrstuhl für Entwicklungsgenetik

Characterization of the interaction of CRHR1 with MAGUKs via the PDZ binding motif

Julia Bender

Vollständiger Abdruck der von der Fakultät Wissenschaftszentrum Weihenstephan für Ernährung, Landnutzung und Umwelt der Technischen Universität München zur Erlangung des akademischen Grades eines

Doktors der Naturwissenschaften

genehmigten Dissertation.

Vorsitzender: Univ.-Prof. Dr. S. Scherer

Prüfer der Dissertation:

1. Univ.-Prof. Dr. W. Wurst
2. Priv.-Doz. Dr. T. Rein,
   Ludwig-Maximilians-Universität München

Die Dissertation wurde am 02.02.2015 bei der Technischen Universität München eingereicht und durch die Fakultät Wissenschaftszentrum Weihenstephan für Ernährung, Landnutzung und Umwelt am 20.04.2015 angenommen.

Table of Contents

Summary

The corticotropin-releasing hormone receptor type 1 (CRHR1) plays an important role in orchestrating neuroendocrine, behavioral and autonomic responses to stress. Recently, our group demonstrated a bidirectional control of anxiety-related behavior by CRHR1 in anxiogenic glutamatergic and in anxiolytic dopaminergic circuits suggesting circuit-specific CRHR1 signaling mechanisms. To understand CRHR1 function and signaling on the molecular level this study focused on the characterization of the intracellular C-terminal PDZ (PSD-95, discs large, zona occludens 1) binding motif of CRHR1. This motif represents a potential site for the interaction with PDZ domains. Previous yeast two-hybrid screens using the C-terminal tail of CRHR1 identified several PDZ domain containing proteins including the membrane-associated guanylate kinases (MAGUKs) postsynaptic density protein 95 (PSD95), synapse-associated protein 102 (SAP102), membrane-associated guanylate kinase, WW and PDZ domain containing 2 (MAGI2), SAP97 as well as the syndecan binding protein 1 (Syntenin-1) and transmembrane protein 106B (TMEM106B) which is devoid of PDZ domains.

Western blot analysis of CRHR1 revealed two distinct bands which were identified as glycosylated monomers and oligomers. The MAGUKs - including the additionally investigated PSD93 - were validated as CRHR1 interaction partners by co-immunoprecipitation studies which also unraveled the PDZ domains relevant for the CRHR1-MAGUK interaction. The PDZ binding motif of CRHR1 is essential for the physical interaction with MAGUKs as revealed by the CRHR1-STAVA mutant which harbors a functionally impaired PDZ binding motif. In contrast, CRHR1 did not interact with Syntenin-1, while the interaction with TMEM106B appeared to be unspecific. A CRHR1 mutant lacking its C-terminal portion including the last two transmembrane domains still interacted with TMEM106B.

The co-expression of CRHR1 and respective interacting MAGUK in HEK293 cells resulted in a clustered co-localization, which depended on an intact PDZ binding motif. The clustering, which occurred intracellulary and partially also at the plasma membrane, provided first evidence for a functional relevance of the identified interaction.

Moreover, CRHR1 was co-expressed with identified MAGUKs in neurons of the adult mouse brain and in cultured primary hippocampal neurons supporting the probability of a physiological interaction *in vivo*.

Primary neurons were verified as a cell culture model suitable for investigating the CRHR1/CRH system and its interactions with identified MAGUKs by different techniques.

CRH was found to be expressed exclusively in GABAergic neurons in primary cultures of cortex and hippocampus. CRHR1 expressing neurons were identified as glutamatergic, of which a small proportion was also calbindin D28-K positive. The rather low endogenous mRNA expression of CRHR1 was in line with the failure to detect endogenous CRHR1 by immunostaining. Consequently, the CRHR1 had to be overexpressed for further functional studies. To exclude intrinsic toxic properties the wild-type receptor and different CRHR1 variants were overexpressed *in vitro* and *in vivo* indicating that overexpression is in general possible. These CRHR1 variants revealed also neither the PDZ binding motif itself nor the entire intracellular C-terminus was necessary for cAMP production or localization to the plasma membrane in HEK293 cells.

Expression of CRHR1 in primary neurons was established via adeno-associated viruses which demonstrated that the receptor is localized throughout the neuronal plasma membrane in the soma, axon and dendrites including the excitatory post synapse where the receptor co-localized with PSD95 and SAP97 albeit independent of the intact PDZ binding motif.

Taken together, this study validated the previously predicted C-terminal PDZ binding motif of CRHR1 as the mediator of protein-protein interactions with multiple MAGUKs. This interaction directly impacts on receptor function as demonstrated by the PDZ binding motif-dependent clustering of CRHR1 with different MAGUKs.

Zusammenfassung

Der Corticotropin-releasing Hormon Receptor Typ 1 (CRHR1) ist unentbehrlich für die Koordination der neuroendokrinen, verhaltensbiologischen und autonomen Stressantwort. Vor kurzem konnte unsere Gruppe nachweisen, dass CRHR1 in anxiogenen glutamatergen und anxiolytischen dopaminergen Schaltkreisen für eine bidirektionale Kontrolle des Angstverhaltens verantwortlich ist, was schaltkreisspezifische CRHR1 Signalwege nahelegt. Um die CRHR1 Mechanismen der Signaltransduktion auf molekularer Ebene zu verstehen, wurden das intrazellulare C-terminale PDZ (PSD-95, discs large, zona occludens 1)-Bindemotiv des CRHR1 näher untersucht. Dieses Motiv stellt eine potentielle Interaktionsstelle für PDZ Domänen enthaltende Proteine dar. Mit Hilfe eines Hefe-Zwei-Hybrid-System, bei dem die C-terminale intrazelluläre Sequenz des CRHR1 benutzt wurde, konnten einige PDZ Domänen enthaltende Membran-assoziierte Guanylat-Kinasen (MAGUKs) identifiziert werden: PSD95 (postsynaptic density protein 95), SAP102 (synapse-associated protein 102), MAGI2 (membrane-associated guanylate kinase, WW and PDZ domain containing 2), SAP97 und auch Syntenin-1 (syndecan binding protein 1) und das TMEM106B (transmembrane protein 106B), das keine PDZ Domänen enthält.

Der CRHR1 zeigte in der Western Blot-Analyse zwei verschiedene Banden, die als glykosilierte Monomere und Oligomere identifiziert werden konnten. Alle MAGUKs – inklusive dem zusätzlich untersuchten PSD93 – konnten mit Hilfe von Ko-immunopräzipitationsstudien als CRHR1-Interaktionspartner verifiziert werden. Verschiedene PDZ Domänen innerhalb der MAGUKs sind in den Interaktionen involviert. Das PDZ-Bindemotiv des CRHR1 ist essentiell für die physische Interaktion mit den MAGUKs, was durch die CRHR1-STAVA Mutante deutlich gemacht werden konnte, die ein funktionell inaktives PDZ-Bindemotiv trägt. Ko-immunopräzipitationsstudien konnten weiterhin offenlegen, dass der CRHR1 nicht mit Syntenin-1 interagierte, während sich die Interaktion mit TMEM106B als unspezifisch herausstellte. Denn eine Mutante des CRHR1, welcher der C-terminale Anteil inklusive der letzten beiden Transmembran-domänen fehlte, interagierte immer noch mit TMEM106B.

Die Ko-Expression des CRHR1 mit den jeweiligen MAGUKs in HEK293 Zellen führte zu einer aggregatförmigen Ko-Lokalisation, welche ein intaktes PDZ-Bindemotiv benötigte. Die Aggregatbildung, die intrazellulär in Vesikeln und teilweise an der Membran auftrat, deutet zum ersten Mal auf eine funktionelle Relevanz der identifizierten Interaktion hin.

Des Weiteren war der CRHR1 mit den identifizierten MAGUKs in Neuronen des adulten murinen Gehirns und in primären hippokampalen Neuronen ko-exprimiert, was die Möglichkeit einer physiologischen Interaktion *in vivo* unterstützt.

Die primären Neuronen wurden mit verschiedenen Techniken als nützliches Zellkultur-Modell etabliert, um das CRHR1/CRH System inklusive der Interaktionen mit den identifizierten MAGUKs zu untersuchen. Im Zuge dieser Untersuchungen wurde gezeigt, dass CRH in GABAergen primären Neuronen des Hippokampus und Cortex exprimiert wurde. CRHR1 positive Neurone waren glutamaterg und gleichzeitig auch zu einem kleinen Anteil Calbindin D28-K positiv. Das geringe endogene mRNA Expressionsniveau des CRHR1 stimmt mit der Tatsache überein, dass es nicht möglich war, den endogenen CRHR1 mit Antikörpern zu detektieren. Daher wurde der Rezeptor in den weiteren Studien überexprimiert. Um eine intrinsische Toxizität auszuschließen, wurden der Wildtyp und verschiedene CRHR1 Varianten *in vitro* und *in vivo* überexprimiert, was die Möglichkeit der Über-Exprimierung im Allgemeinen beweist. Diese CRHR1 Varianten offenbarten auch, dass weder das PDZ-Bindemotiv noch der gesamte C-Terminus für die cAMP Produktion oder für die Membranverteilung in HEK293 Zellen wichtig war.

Die Expression des CRHR1 in primären Neurone mit Hilfe von adeno-assoziierten Viren zeigte eine Verteilung des Rezeptors in der neuronalen Plasmamembran des Soma, Axons und der Dendriten und insbesondere in der exzitatorischen Post-synapse, wo der Rezeptor mit PSD95 und SAP97 unabhängig vom intakten PDZ-Bindemotiv ko-lokalisierte.

Zusammenfassend validiert diese Studie das zuvor vorhergesagte C-terminale PDZ-Bindemotiv des CRHR1 als Mediator für eine Protein-Protein-Interaktion mit verschiedenen MAGUKs. Diese Interaktion wirkt sich direkt auf die Rezeptorfunktion aus, wie die PDZ-Bindemotiv-vermittelte Aggregatbildung des CRHR1 mit verschiedenen MAGUKs gezeigt hat.

1 Introduction

Already the Egyptian in 1550 BC tried to understand the human brain and to date it is still an immediate requirement to decipher the molecular correlations of the healthy and diseased brain processes (Lopez-Munoz and Alamo 2009, Vargas et al. 2012). Proteins are essential for all mechanisms in the human body because e.g. they pump ions, catalyze chemical reactions and recognize signals (Alberts 2007). The signal transduction is mediated to a large extent by proteins residing within the cell membrane, so-called membrane proteins. They can consist of multiple transmembrane domains, whereat G protein-coupled receptors (GPCRs) always harbor seven transmembrane domains.

1.1 G protein-coupled receptors (GPCR)

GPCRs constitute the largest family of cell surface receptors in mammals with approximately 800 GPCR genes identified in the human genome (Venter et al. 2001, Luttrell 2008). The number of GPCR genes represents more than 1 % of the human genome and including alternative splicing, 1000-2000 discrete proteins may be expressed. The evolutionary diversity is responsible for the wide spectrum of detected extracellular signals, from photons of light and odorants to ions, small organic molecules and entire proteins (Venkatakrishnan et al. 2013). GPCRs function in regulation of important physiological processes such as neurotransmission and reproduction that is why many pathophysiological processes are affected from GPCR malfunction (Magalhaes et al. 2011). Therefore, approximately 30-40 % of currently marketed drugs target GPCRs, acting either to modify ligand production, to mimic endogenous ligands or to block ligand binding to the GPCR. Structurally GPCRs consist always of seven transmembrane domains and respectively four connecting extra- and intracellular domains. Based on sequence similarity and pharmacological properties, GPCRs are classified into class A (rhodopsin), class B (secretin), class C (metabotropic) and frizzled receptors (Venkatakrishnan et al. 2013).

In the classical signaling paradigm, ligand binding results in conformational changes of GPCRs including their intracellular domains, causing coupling to heterotrimeric guanosine triphosphate (GTP)-binding proteins (G proteins) (Magalhaes et al. 2011). Then GPCRs function as GTP exchange factors (GEFs) facilitating the replacement of guanosine diphosphate (GDP) to GTP at the G protein´s α subunit. This leads to dissociation of the functional activated Gα-subunit and Gβγ-subunit, which can regulate a variety of downstream effectors such as ion channels, phospholipases and adenylyl cyclases (Tang and Gilman

1991, Neer 1995) resulting in activation of diverse signaling pathways e.g. adenylyl cyclase/protein kinase A (AC-PKA), phospholipase C-protein kinase C (PLC-PKC) and extracellular signal-regulated kinase/mitogen-activated protein kinase (ERK-MAPK) (Peralta et al. 1988). The activated state of G protein subunits is terminated by the intrinsic GTPase activity of the Gα-subunit hydrolyzing GTP to GDP. Afterwards the subunits re-associate, become inactive and can return to the ligand-activated receptor. The original signal can be largely amplified due to activation of many G proteins via one GPCR. To terminate the signaling despite continuous agonist stimulation, the receptor responsiveness can be adapted by desensitization (Rockman et al. 2002). The receptor can be downregulated due to reduction of receptor synthesis, destabilization of receptor messenger RNA or increase in receptor degradation (Lefkowitz 1998). More rapidly – seconds to minutes instead of hours – the receptor can be uncoupled from its Gα-subunit by phosphorylation (Rockman et al. 2002). The conformational changes after ligand binding result in phosphorylation of a specific pattern of serines and threonines in the GPCR´s third intracellular loop (IC3) and/or C terminus via protein kinases e.g. PKA or PKC (Moore et al. 2007). This process is called heterologous desensitization because also non-activated GPCRs are phosphorylated (Rockman et al. 2002). In contrast, homologous desensitization is mediated via G protein-coupled kinases (GRKs), which phosphorylate only agonist-stimulated GPCRs. GRK-catalyzed phosphorylation of the receptor enhances the affinity for β-arrestins, which binds to the GPCR and facilitates the uncoupling of the receptor from its Gα-subunit by a steric barricade. There are also phosphorylation-independent sequences, which can be bound by β-arrestin in a high-affinity manner leading to a sterically uncoupling of the receptor from its Gα-subunit (Hanson and Gurevich 2006). This terminates signal transduction by steric hindrance without GRK phosphorylation. In addition to this termination, β-arrestin 1 and β-arrestin 2 binding promotes receptor endocytosis since β-arrestins function as endocytic adaptor proteins for clathrin-mediated endocytosis (Goodman et al. 1996). β-arrestin 1 and β-arrestin 2 specifically bind to both, the clathrin heavy chain and the β2-adaptin subunit, mediating endocytosis. β-arrestins also recruit proteins, which regulate the clathrin-mediated endocytic machinery, like E3 ubiquitin ligases e.g. MDM2 (Shenoy et al. 2001). Thus, β-arrestins are essential for the internalization of GPCRs as well as for the regulation of their endocytosis. There are two different pattern of temporal stability of the arrestin-GPCR complexes. Class A GPCRs preferentially bind to β-arrestin 2 than to β-arrestin 1 and dissociate from the arrestins before internalization. Class B GPCRs bind both β-arrestins with similar affinities and form stable complexes with β-arrestins internalizing to endocytic vesicles as a unit (Oakley et al. 2000). GPCRs that do not internalize with β-arrestins in a complex are dephosphorylated by specific phosphatases and recycled to the membrane. In contrast,

GPCRs that internalize with β-arrestins in a complex are either inefficiently transported back to the plasma membrane or are not recycled at all (Magalhaes et al. 2011).

Beside the stimulation via ligands, GPCRs can be constitutively active in the absence of any stimulus (Tao 2008). In pathological context receptor splice variants and single nucleotide polymorphisms can affect GPCRs´ coding regions, which can result in diverse levels of constitutive activity (Bond and Ijzerman 2006).

G protein independent signaling can be mediated via an antagonist (selective agonist), which induce a change in receptor conformation that favors β-arrestin binding and inhibits G protein binding. A variety of signaling pathways are scaffolded by β-arrestins to the receptor like the Src kinases and ERK-MAPK components (Magalhaes et al. 2011). In contrast to the classical signaling paradigm, GPCR can be activated selectively by ligands that favor a conformation either for the binding with G proteins or β-arrestins resulting in activation of different signaling pathways. G protein independent signaling can be consequence from β-arrestin signaling but can also depend on other GPCR interacting proteins (GIP).

1.2 GPCR interacting proteins (GIP)

GPCR traditionally signal via G proteins but recently emerging data indicate that the G protein independent signaling is not only a marginal phenomenon (Sun et al. 2007). GIPs have various important functions since they are essential for the targeting of GPCRs to specific cellular compartments as intracellular vesicles or the plasma membrane and they modulate their ligand specificity and signaling properties. Furthermore, GIPs scaffold GPCR into large functional complexes, which are called receptosomes or signalosomes (Bockaert et al. 2004, Magalhaes et al. 2011). There are different types of GIPs: transmembrane proteins with one or more transmembrane domains, ionic channels, ionotropic receptors and soluble proteins, which often interact with the extreme C-terminal tail of GPCRs. According to their function GIPs are classified into receptor activity-modifying proteins (RAMPs), regulators of G protein signaling (RGS), GPCR-associated sorting proteins (GASPs), small G proteins and PSD95/discs large/zona occludens 1 (PDZ) proteins.

RAMPs are single transmembrane proteins, which interact with class B GPCRs including the receptors for calcitonin (CT), glucagon and vasoactive intestinal peptide (VIP), the calcitonin receptor-like receptor (CRLR) (Sexton et al. 2006) and also with the class C calcium sensing receptor (CaSR) (Bouschet et al. 2005). The first RAMP was detected in *Xenopus* oocytes during pharmacology studies for the calcitonin peptide. There the heterologous expression of either CT or CRLR in cell lines did not recapitulate the pharmacology observed *in vivo*

(McLatchie et al. 1998). It is speculated that RAMPs influence the pharmacology of calcitonin family peptides by e.g. contributing to the calcitonin family receptors ligand binding site or by influencing allosterically the structure of calcitonin family receptors (Magalhaes et al. 2011). The study of McLatchie and colleagues also showed that RAMPs allow the receptors´ terminal glycosylation in the endoplasmatic reticulum (ER) necessary for the transport to the cell surface by allosterically influencing the structure of calcitonin family receptors (McLatchie et al. 1998). Thus, without an appropriate RAMP CT and also CaSR are retained in the ER (Bouschet et al. 2005).

RGS proteins modulate GPCR signaling by accelerating the intrinsic GTPase activity of the Gα-subunit of Gq and Gi/o proteins hydrolyzing GTP to GDP (Magalhaes et al. 2011). Therefore, they act as GTPase activating proteins (GAPs) terminating the G protein signaling. All RGS proteins contain a RGS box consisting of 130 amino acids, which is critical for the GAP activity. The amino acid sequence flanking the RGS box differs for every RGS protein and can contain other domains as e.g. for protein-protein interactions (Sjogren and Neubig 2010). These different domains can be important for the regulation of protein localization and intracellular trafficking as well as receptor selectivity (Sethakorn et al. 2010). The subgroup R4 of RGS proteins contain a membrane targeting signal at their N-terminus, an amphipathic α-helix, which enables them to localize next to their targets (Sethakorn et al. 2010). Besides, RGS2 protein which is a member of subgroup R4 has been shown to interact directly with tubulin via its N-terminus enhancing microtubule polymerization and thereby neurite outgrowth (Heo et al. 2006). The R12 subgroup of RGS proteins contains in addition a functional GoLoco motif and a Rap binding domain at the very C-terminus. The GoLoco motif blocks the dissociation of the guanine nucleotide inhibiting the exchange of GDP to GTP when bound to Gαi. With this motif R12 proteins have an additional domain beyond the RGS box, which terminates or inhibits G protein signaling. Moreover, the extra N-terminal domains harboring interaction sites with GPCRs and other signal transduction proteins suggest that RGS proteins can be important to scaffold diverse proteins into signalosomes.

The members of the GASP family share a conserved 250 amino acids domain and seem to be important for the post-endocytic sorting of GPCRs (Magalhaes et al. 2011). GASP-1 was detected to be responsible for the rapid degradation of δ opioid, but not μ opioid receptors after agonist stimulation (Whistler et al. 2002). In the course of the agonist-dependent desensitization of dopamine D2 receptors, GASP-1 inhibits the resensitization of the receptor back to the membrane (Bartlett et al. 2005).

The small GTP-binding protein superfamily consists of over 100 members that are classified by structural similarity in Ras, Rho, Rab, Sar1/Arf, and Ran families with an intrinsic GTPase

activity (Takai et al. 2001). They are also called biological timers since they initiate and terminate specific cell functions. The Ras family function as a regulator for gene expression, the Rho family for cytoskeletal reorganization and gene expression, the Rab and Sar1/Arf families for the formation, fusion and movement of vesicle traffic between different membrane compartments, and the Ran family for nucleocytoplasmic transport and microtubule organization. Multiple Rab GTPases were shown to regulate GPCRs transport between ER and Golgi as well as the GPCRs endocytosis and trafficking between early, late and recycling endosomes and lysosomes. Many Rab GTPases interact directly with the C-terminal tail of GPCRs (Seachrist et al. 2002, Esseltine et al. 2011). For example Rab5 was found in a yeast two-hybrid screen using the C-terminus of angiotensin II type 1 receptor (AT1R). Furthermore, Rab5 can be co-immunoprecipitated with the AT1R and agonist activation results in the exchange of GDP for GTP on Rab5 what suggests that the receptor itself function as a GEF. The interaction of Rab5 and AT1R leads to a retention of the receptor in endosomes. However, binding studies of Rab GTPases with different GPCRs did not reveal any clearly defined consensus sequence until now.

Many GPCRs contain at their extreme C-terminal tail a PDZ binding motif, which enables PDZ proteins to scaffold them into signalosomes. Thus, receptor properties as trafficking, signaling and localization are modulated. PDZ domain-containing proteins have been shown to directly relay signals from GPCRs independent of G proteins, whereat PDZ containing proteins also gain more functional features beyond their scaffolding function e.g. postsynaptic density protein 95 (PSD95) can suppress the activity of the inward rectifier K+ channel (Nehring et al. 2000b). PSD95 belongs to the family of membrane-associated guanylate kinases (MAGUKs) which are discussed below including their interactions with GPCRs (see paragraph 1.6).

In the following other GIPs are described which are not listed above. For the recycling of GPCRs, specific protein phosphatases have to dephosphorylate the receptors in endosomes before they can be transported back to the plasma membrane. This process is as highly regulated as the phosphorylation process. The β2-adrenergic receptor (β2AR) e.g. is dephosphorylated by protein phosphatase 2A (PP2A) (Krueger et al. 1997). Although G proteins bind to the IC3 of GPCRs, there are only few other GIPs detected until now, which also bind to the IC3. The calcium-binding protein calmodulin was detected to interact with the IC3 of dopamine D2 receptors blocking G protein signaling (Bofill-Cardona et al. 2000). Additionally, cytoskeletal-associated proteins interact with the IC3 of GPCRs like filamin A and spinophilin. They interact with dopamine receptors and regulate their trafficking to the plasma membrane (Smith et al. 1999, Li et al. 2000, Lin et al. 2001). An electron microscopy study showed that the microtubule-associated protein 1A (MAP1A), which interacts with

5-hydroxytryptamine receptor 2A (5-HT2A) co-localized in the same cortical dendrites with 5-HT2A (Cornea-Hebert et al. 2002). Homer proteins encompass a 120 amino acid N-terminal domain containing an enabled/VASP homology (EVH) domain, which binds to a PP-X-X-F motif. Metabotropic glutamate receptors (mGluRs) 1 and 5 as well as the α_{1D} adrenergic receptor contain in their C-terminal tails such a PP-X-X-F motif (Tu et al. 1998) enabling them to be scaffolded by Homer proteins. Long Homer isoforms contain additionally a C-terminal coiled-coiled domain, which facilitates selfmultimerization and heteromultimerization. Moreover, the EVH domain interacts also with a variety of mGluR effector proteins including inositol 1,4,5 triphosphate receptors, ryanodine receptors, store-operated transient receptor channels 1 and 4, P/Q type Ca^{2+} channels, Shank, dynamin III and phosphoinositide 3-kinase enhancer long (Rong et al. 2003, Fagni et al. 2004). The complex built by mGluR, Homer, store-operated transient receptor channels 1 and 4, IP3 (inositol-triphosphate) or ryanodine receptors, and P/Q type Ca^{2+} channels represents an ideal signalosome for intracellular Ca^{2+} release (Bockaert et al. 2004). The long isoforms of Homer were shown to scaffold their substrates in the post-synaptic density (PSD) via dimerization of the Homer coiled-coiled domain (Hayashi et al. 2006). In contrast, the shorter Homer 1a does not possess a coiled-coiled domain and behaves as a negative competitor of this scaffolding during its upregulation in response to synaptic activity (Kammermeier and Worley 2007).

In contrast to the classical signaling paradigm, in which GPCRs signal via G proteins and generate second messengers influencing downstream effectors, GPCRs also interact with a large variety of GIPs. The interactions with GIPs not only modulate G protein signaling, desensitization and the subcellular localizations of GPCRs, but the interactions also facilitate diverse novel signaling pathways.

1.3 The Corticotropin-releasing hormone receptor type 1 (CRHR1) in health and disease

The corticotropin-releasing hormone receptor type 1 (CRHR1) is an important regulator of the neuroendocrine, behavioral and autonomic response to stress. It is the main activator of the hypothalamic-pituitary-adrenal (HPA) axis, which is central for the stress response in vertebrates (Tonon et al. 1986, Reul and Holsboer 2002). In the course of the stress response and circadian rhythm of the HPA axis the ligand corticotropin-releasing hormone (CRH) is released from the paraventricular nucleus of the hypothalamus to the portal capillary zone of the median eminence. Afterwards, CRH is transported to the anterior

pituitary, where it binds to CRHR1 expressed on endocrine cells. CRHR1 activation triggers secretion of adrenocorticotropic hormone (ACTH), which is transported to the adrenal cortex and activates ACTH receptors provoking the synthesis and release of glucocorticoids (GC, cortisol in humans and corticosterone in rodents). Finally, GCs mediate the stress response by modulating gluconeogenesis, lipolysis, proteolysis and blood pressure (Wallerath et al. 1999). The HPA axis is regulated by a negative feedback loop, in which GCs bind to GC receptors in the pituitary, paraventricular nucleus and in the hippocampus (Herman and Cullinan 1997) and suppress further CRH and ACTH production.

Besides, a dysregulation of CRHR1 and its ligand CRH have been causally linked to stress-related pathologies including mood and anxiety disorders (Arborelius et al. 1999, Holsboer 2000, de Kloet et al. 2005). The HPA axis in depressed patients was observed to be dysregulated because the magnitude of ACTH and cortisol secretory episodes is elevated, which is also manifested in increased urinary cortisol production rates (Rubin et al. 1987). Furthermore, increased levels of CRH in the cerebrospinal fluid have also been reported in depressed subjects (Nemeroff et al. 1984) illustrating the HPA hyperactivity in major depression. The CRH-expressing neurons in depressed patients were demonstrated to be hyperactivated in the paraventricular nucleus (Raadsheer et al. 1994). Moreover, in suicide victims CRH binding sites in the frontal cortex were reduced probably secondary to elevated CRH levels (Nemeroff et al. 1988).

To study the physiological HPA axis regulation and pathological HPA axis dysregulation in major depression, genetically engineered mice are widely used to model alterations of the CRH system and the HPA axis. Two different constitutive CRHR1 knockout mice showed increased exploratory activity and reduced anxiety-related behaviour (Smith et al. 1998, Timpl et al. 1998). The HPA axis is also disrupted in these models due to the complete loss of CRHR1, which is also reflected in a chronic decrease of plasma corticosterone. For this reason tissue-specific conditional approaches were consulted to disrupt the CRHR1 only in a spatially restricted manner. The conditional inactivation of CRHR1 within the murine anterior forebrain, using floxed CRHR1 mice bred to CaMKIIαCre (calcium/calmodulin-dependent protein kinase II) mice, revealing that limbic CRHR1 signaling modulates anxiety-related behavior independent of its role in the neuroendocrine stress response via the HPA axis (Muller et al. 2003). Recently, our group demonstrated the bidirectional control of anxiety-related behavior by CRHR1 in anxiogenic glutamatergic and in anxiolytic dopaminergic circuits (Refojo et al. 2011) suggesting distinct CRHR1-dependent signaling pathways. CRH overexpression was studied in gain-of-function approaches in genetic mouse lines e.g. with restriction of CRH overexpression to the central nervous system (CNS). These CNS-specific

CRH overexpressing mice showed increased active stress-coping behavior and stress-induced hypersecretion of corticosterone (Lu et al. 2008).

Since the CRHR1/CRH system appears to be dysregulated in depressed patients, CRHR1 antagonists have been developed to treat depression. Clinical studies with CRHR1 antagonists were partially successful dependent on the genetic background of the patients and subtype of the depression (Holsboer 2014). Until now many small molecule CRHR1 antagonists have been developed, nevertheless, only few of them entered clinical development and none of them is available on the drug market yet (Valdez 2006). For example the antagonist NBI-30775/R121919 reduced cognitive symptoms of depression, sleep disturbances and suicidality in a study of limited sample size (Holsboer and Ising 2008). In contrast, a different CRHR1 antagonist, CP-316211, failed to show any antidepressant effect (Binneman et al. 2008). Difficulties of CRHR1 antagonists impeded further progress like suboptimal pharmacokinetics, bioavailability as well as toxicity of highly lipophilic small molecules (Hauger et al. 2009).

CRHR1 is highly expressed throughout the mammalian brain and pituitary (Chen et al. 2000b, Van Pett et al. 2000, Refojo et al. 2011, Kuhne et al. 2012). Regions with the highest expression are the cerebral cortex, cerebellum, amygdala, hippocampus, olfactory bulb, and anterior pituitary. In the periphery CRHR1 is mainly expressed in the testis, ovary and adrenal gland (Muller et al. 2001, Xu et al. 2006, McDowell et al. 2012). At molecular level hippocampal long-term potentiation (LTP) of synaptic efficacy can be facilitated by a preincubation with CRH, which was also elicited when animals had been subjected to restraint stress. This effect was blocked by CRHR1 antagonist treatment (Blank et al. 2002). To measure induced LTP at slices, CA1 (cornu ammonis area 1) population spikes (PS) can be assessed. Studies showed that CRH increases PS and raises the spontaneous firing frequency of rat hippocampal neurons (Aldenhoff et al. 1983, Sillaber et al. 2002). Using transgenic mice a CRH-mediated increase in PS was exclusively initiated by CRHR1 expressed on glutamatergic neurons (Kratzer et al. 2013). It was observed that activation of CRHR1 changed voltage-gated ion currents, which are important for the generation of action potentials. CRH rather shows neuroregulatory and neuromodulatory actions than neurotransmitter features because it does not induce any membrane potential change or change in electrical excitability of the neuronal membrane by itself (Gallagher et al. 2008). Additionally, CRHR1 is responsible for spine dynamics because following CRH treatment or stress, spine loss was induced, an effect which could be abolished by blocking CRHR1 (Chen et al. 2008, Chen et al. 2012b). But until now the accountable molecular mechanisms how CRHR1 influences synaptic transmission are not unraveled. This knowledge would

provide new starting points to develop specific drugs for the treatment of anxiety and mood disorders.

1.4   CRHR1-mediated signaling

CRHR1 is a G protein-coupled receptor (GPCR) of the B1 family and can be activated via CRH and Urocortin 1 (Figure 1). The members of the class B family of GPCRs in general have diverse splicing variants, which may account for different ligand or tissue specificities in signaling (Bonfiglio et al. 2011). CRHR1α is the dominantly expressed and functional form among several alternative splice variants like β, c-g and h, which have been identified in rodents and humans (Zmijewski and Slominski 2010). Only in humans, the complete gene product consisting of its 14 exons exists. This CRHR1β splicing variant has impaired agonist-binding and signaling properties (Chen et al. 1993). The excision of exon 6 results in the expression of CRHR1α containing 415 instead of 444 amino acids (Hillhouse and Grammatopoulos 2006). In rodents CRHR1β is absent; here CRHR1 contains only 13 exons.
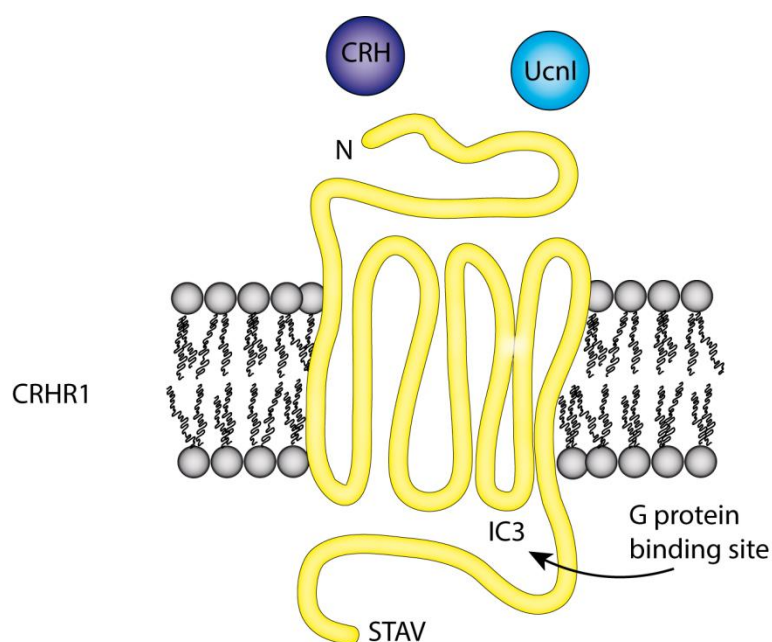
Figure 1: Corticotropin-releasing hormone receptor type 1 (CRHR1) with its ligands and the PDZ binding motif S^{412}-T^{413}-A^{414}-V^{415}.
CRH, corticotropin-releasing hormone; UcnI, urocortin I.

Commonly the other CRHR1 variants also lack exon 6 and entire or various parts of exons, some of which result in a frame-shift in the open reading frame what can alter e.g. the C terminal sequence. In human keratinocytes splicing variants of CRHR1 showed diverse

cellular localizations, as CRHR1α and c localized at the cell membrane, whereat only CRHR1α was functionally active (Zmijewski and Slominski 2009). CRHR1d, f and g were intracellularly localized, but the soluble variants e and h showed a diffuse cytosolic localization or localized to the ER and additionally were found secreted to the culture medium. It is speculated that alternatively spliced CRHR1 variants can dimerize with CRHR1α and thereby change its intracellular localization and activity.

CRHR1 preferentially signals via coupling of Gsα to its IC3 resulting in the activation of the AC-PKA pathway but it can also signal via coupling of Gq to its IC3 resulting in ERK-MAPK pathway activation (Figure 2) (Grammatopoulos et al. 1996, Grammatopoulos et al. 2000, Hauger et al. 2009). Specific amino acids within the highly conserved hydrophobic N- and C terminal microdomains of IC3 are important for the selectivity in coupling of Gα or Gq and subsequent signaling via AC-PKA or ERK-MAPK (Punn et al. 2012). The Serin301 within the IC3 is critical for efficient G protein coupling; its mutation ends e.g. in reduced cAMP production (Papadopoulou et al. 2004). The AC-PKA signaling is stringently regulated by GRKs and β-arrestin mediated homologous desensitization. GRK3 and GRK6 were demonstrated to phosphorylate CRHR1 after activation with high concentrations of CRH (Dautzenberg et al. 2002, Teli et al. 2005). GRK-catalyzed phosphorylation of the receptor immediately increases the affinity for β-arrestins (~30 fold) causing its internalization. CRHR1 preferentially recruits β-arrestin 2 rather than β-arrestin 1 to the membrane as disclosed in transfected HEK293 and primary cortical neurons (Rasmussen et al. 2004, Holmes et al. 2006, Oakley et al. 2007). Like class A GPCRs CRHR1 dissociates from β-arrestin before internalization (Hauger et al. 2009). Studies using truncated and mutated versions of the receptor revealed that the recruitment and binding of β-arrestin 2 by the agonist-activated CRHR1 is conveyed by distinct motifs like a phosphorylation-dependent motif in the C terminus and a phosphorylation-independent motif in one or more of the ICs. Besides their role in desensitization, GRKs and β-arrestins can also mediate G protein independent signaling selectively via the ERK-MAPK or AKT pathways. However, depending on its cellular localization and context, CRHR1 can also activate multiple G proteins, which can trigger alternative second messengers (Grammatopoulos and Chrousos 2002). For example the coupling to Gsα can result in the activation of the ERK1/2 signaling pathway, which can also be activated by Gqα (Kovalovsky et al. 2002, Papadopoulou et al. 2004, Refojo et al. 2005). Coupling to Gsα can also end into intracellular calcium mobilization via the activation of AC, which activates the ε isoform of phospholipase C (PLCε) (Gutknecht et al. 2009).
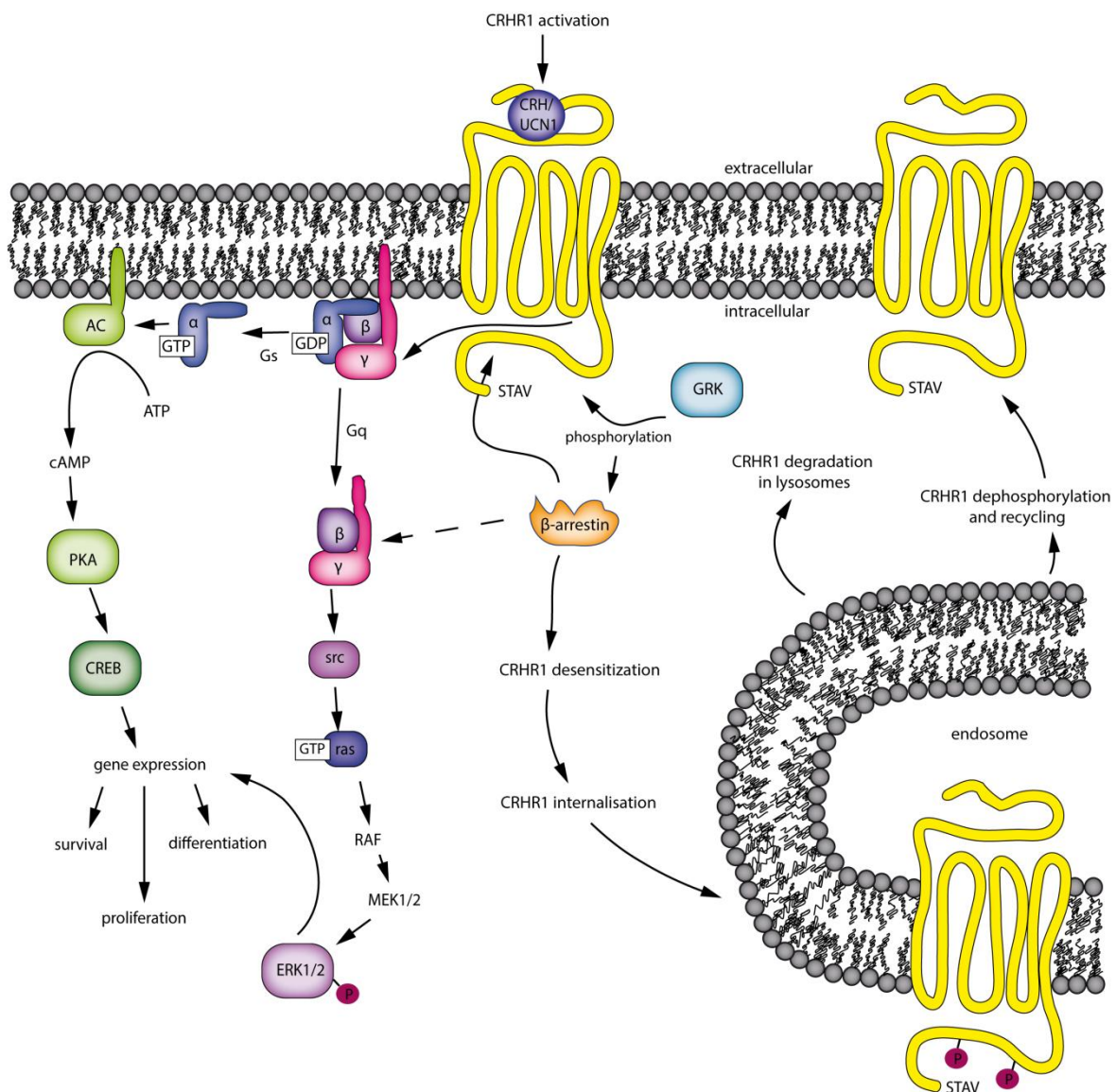
Figure 2: Corticotropin-releasing hormone receptor type 1 (CRHR1) signaling pathways.
AC, adenylyl cyclase; ATP, adenosine triphosphate; cAMP, cyclic adenosine monophosphate; CREB, cAMP response element-binding protein; CRH, corticotropin-releasing hormone; ERK1/2, extracellular signal-regulated kinase 1/2; GDP, guanosine diphosphate; GRK, G protein-coupled kinases; GTP, guanosine triphosphate; MEK, mitogen-activated protein kinase kinase; PKA, protein kinase A; UCN1, urocortin 1.

In general, there are selective agonist (antagonists) also called biased agonists that induce receptor conformations resulting in specific signal transduction pathways like β-arrestin signaling (Violin and Lefkowitz 2007). Up to now CRHR1 interactions with G proteins, GRKs and β-arrestins have extensively been studied (Oakley et al. 2007, Punn et al. 2012), whereas interactions with other proteins that would provide further specificity to CRHR1 signaling or determine the activation of particular downstream pathways are largely

unknown. Interestingly, the amino acid sequence S^{412}-T^{413}-A^{414}-V^{415} at the C-terminus of murine and human CRHR1 (Figure 1) resembles a C-terminal class I PDZ-binding motif, which was for the first time suggested by comparison with other C-terminal sequences (Kornau et al. 1995).

1.5 Oligomerization of G protein-coupled receptors

Besides the monomeric form, GPCRs build homo- and hetero-dimers as well as oligomeric complexes (Angers et al. 2001, Lee et al. 2003, Szidonya et al. 2008, Ferre et al. 2014). The used methods for detection of oligomers are diverse but have also different drawbacks. Co-immunoprecipitation (Co-IP) is the most frequently used method to reveal oligomerization of GPCRs based on differentially epitope-tagged molecules expressed in heterologous systems (Szidonya et al. 2008, Skieterska et al. 2013). But the lysis and solubilization of the proteins out of the membrane needs high concentrations of detergents, which potentially can disrupt existing interactions between receptors. Here, a crosslinking step can stabilize the oligomers (Hebert et al. 1996, Cvejic and Devi 1997). Furthermore, the production of free sulfydryl groups e.g. with β-mercaptoethanol during the lysis can lead to artificial associations in terms of oligomerized complexes, what can be prevented by the use of capping agents like iodoacetamide. Additionally, incomplete solubilization can result in small remaining membrane patches that also result in artificial oligomerizations. This artifact can be avoided by centrifugation after detergent extraction for at least 60 min over 100000 g (Gines et al. 2000). Glycosylated GPCRs can also lead to artificial aggregates during boiling what can be solved by using lower temperatures (Gines et al. 2000).

Another obvious problem of the Co-IP detection is that the dynamics and fluctuations of interactions cannot be monitored. This issue is investigated with resonance energy transfer (RET) in living cells in real time, which is based on fluorescent molecules (FRET) or involves an enzyme as energy trigger (bioluminescence RET, BRET) (Maurel et al. 2008, Szidonya et al. 2008, Vidi and Watts 2009, Cottet et al. 2011, Ferre et al. 2014). There are different models proposed for the functions of the oligomerization of GPCRs like the dimer-cooperativity model, in which one unit can allosteric communicate with the other unit of the oligomer allowing negative cooperativity meaning that the binding of a ligand to the first unit decreases the affinity of the ligand for the second unit (Ferre et al. 2014). This effect has been detected for adenosine receptors (May et al. 2011, Orru et al. 2011) and is thought to be important to protect the system against acute increases of the endogenous ligand (Agnati et al. 2005). Similarly, inhibition of β2AR in a hetero-dimer inhibits also the signaling of AT1R

(Barki-Harrington et al. 2003). Tetrameric oligomers of β2AR were changed in number of oligomeric complexes after agonist treatment showing the importance for physiological receptor signaling (Angers et al. 2001, Fung et al. 2009), although others detected that monomeric β2AR in a lipid bilayer is sufficient to activate the G protein (Whorton et al. 2007). The early dimerization of GPCRs is also essential for the efficient folding and maturation including cell surface delivery (Milligan 2010). This was also observed for hetero-dimers as the mouse 71 olfactory receptor (M71OR) needs the association with β2AR for surface expression (Hague et al. 2004). Interestingly, for the adenosine receptor the fifth transmembrane domain was found to be able to self-associate and build stable oligomers (Thevenin et al. 2005). The CRHR1 can also oligomerize and was found to cluster forming dimers and high molecular weight complexes (Young et al. 2007, Zmijewski and Slominski 2009). In contrast to β2AR, dimerization of CRHR1 was revealed to be independent of ligand binding (Kraetke et al. 2005).

Recent data describe that heterodimerization of GPCRs is essential for neuropsychiatric diseases (Szafran et al. 2013). The heteromers of serotonin receptor 5-hydroxytryptamine receptor 2A (5-HT2A) and mGluR2 were shown to be probably involved in altered cortical processes of schizophrenia (Gonzalez-Maeso et al. 2008), since drugs that activated mGluR2 abolished 5-HT2A signaling and behavioral responses evoked by hallucinogenic drugs. Additionally, the receptor densities in schizophrenic subjects were changed showing downregulated mGluR2 and upregulated 5-HT2A in post-mortem human brain, a receptor expression pattern that might predispose to psychosis. Heteromers of CRHR1 and vasopressin V1b receptor (V1bR) have been associated with depression and anxiety disorders because both are co-expressed as functional heteromers in corticotropes in the pituitary where they act as key regulators of the HPA axis (Young et al. 2007). The heterodimerization is not ligand dependent and does not alter the binding properties of these receptors, but because both receptor ligands act synergistically on the release of ACTH, the interaction may play an important role in stress-related diseases like depression and anxiety disorders.

The functional crosstalk between GPCR hetero-complexes imply different pharmacological properties including the opportunity to design new therapeutic drugs (Gonzalez-Maeso 2011).

1.6 Membrane-associated guanylate kinases (MAGUKs) of the post-synaptic density

Cells of multicellular eukaryotes communicate with their environment through junctional complexes that consist of adhesion proteins and receptors connected via scaffolds to actin bundles (Good et al. 2011, Zheng et al. 2011). Therefore, cells can integrate external signals and react with a developmental or functional change. Junctional complexes are essential for the apical-basal polarity of epithelial cells developed as tight junctions, adherens junctions and desmosomes and of sensory cells e.g. the photoreceptor cells in retinas (Kaplan et al. 2009, Kevany and Palczewski 2010). Moreover, the neuronal PSD and pre-synaptic active zone display also classical examples of junctional complexes (Mushynski et al. 1978). Within the PSD the membrane-associated guanylate kinases (MAGUKs) are synaptic scaffolds proteins that are important to assemble receptors, adhesion proteins and intracellular signaling proteins (Kim and Sheng 2004). MAGUKs consist of PDZ domains and an enzymatically inactive guanylate kinase (GuK) like domain, they can contain also a L27 (MAGUK Lin-2 + Lin-7) and a SRC homology 3 (SH3) domain (Figure 3).

Figure 3: Structure of a typical MAGUK (Membrane-associated guanylate kinase).
PSD95, SAP97, SAP102 and PSD93 share the same domain structure with three PDZ (PSD95/discs large/zona occludens 1) domains, a SRC homology 3 (SH3) domain and an enzymatically inactive guanylate kinase (GuK) like domain, but they are different in their total amino acid sequence composition.

The MAGI (membrane-associated guanylate kinase inverted) subgroup of MAGUKs does not contain SH3 domains but contains two tryptophan residues (WW) reflecting the diversity of the structure of MAGUK family proteins (Shoji et al. 2000). The structure of MAGIs is inverted with the GuK domain at the N-terminus followed by two WW domains and five PDZ domains (Montgomery et al. 2004). There are three MAGI isoforms called MAGI1, MAGI2 and MAGI3, which are expressed broadly in neural and non-neural cells (Laura et al. 2002, Montgomery et al. 2004). MAGI2 - also called synaptic scaffolding molecule (S-SCAM) or activin receptor-interacting protein 1 (ARIP1) - is dominantly expressed in neurons where it localizes to the PSD of excitatory synapses (Yao et al. 2003). Nevertheless, MAGI2 was detected to be essential for the integrity of the kidney barrier, presumably because it interacts with the slit diaphragm protein nephrin in podocytes (Lehtonen et al. 2005, Balbas et al. 2014). The

isoforms MAGI1 and MAGI3 are located next to tight junctions between epithelial cells in mostly non-neural tissue (Ide et al. 1999, Laura et al. 2002).

The MAGUK Discs-large (DLG) in *Drosophila melanogaster* is one of the first proteins detected to possess PDZ domains (Woods and Bryant 1991, Bilder 2001). DLG is essential for the regulation of apical-basal polarity and has tumor suppressor properties since a loss of DLG results in over-proliferation and neoplastic transformation of epithelial cells (Woods and Bryant 1989, Woods et al. 1996, Roberts et al. 2012).

MAGUKs in the PSD are essential for synaptic development and plasticity, since they influence the clustering of e.g. glutamate receptors (Kornau et al. 1995, Kim and Sheng 2004, Zheng et al. 2011). They perform their diverse actions by scaffolding proteins together via their different protein interaction domains like the PDZ domains. PDZ domains are the best characterized protein interaction modules and one of the most common protein-protein interaction domains in mammals (Chi et al. 2012): they are approximately 90 amino acids long, consist of 5 or 6 β-stranded and 2 or 3 α- helical structures and often recognize short amino acid motifs at the C-termini of interacting proteins (Fanning and Anderson 1996, Lee and Zheng 2010, Ye and Zhang 2013). MAGUKs can bind to many surface receptors via their PDZ domains, which directly interact with the receptors´ C-terminal PDZ binding motif (Kim and Sheng 2004). PDZ domains are classified according to the observed binding motif. Class I PDZ domains recognize the motif S/T-X-Φ, class II PDZ domains recognize the motif Φ-X-Φ and class III PDZ domains recognize the motif D/E-X-Φ, where Φ represents a bulky hydrophobic residue (Skelton et al. 2003, Lee and Zheng 2010). This original classification has been challenged because of observations that more amino acids upstream of the very C-terminus are also important for the interaction (Kurakin et al. 2007, Tonikian et al. 2008). The members of the PSD95 subfamily of MAGUKs (PSD95, SAP97, SAP102 and PSD93) contain only class I PDZ domains (Oliva et al. 2011) and they are alternatively spliced changing for example the N-terminal amino acid composition (Funke et al. 2005, Zheng et al. 2011). At this position cysteines constitute a potential palmitoylation site, which can have dramatically functional consequences as palmitoylated members are less mobile in dendritic spines than non-palmitoylated members and palmitoylated members are targeted to the PSD instead of peri-synaptic regions (Craven and Bredt 1998, Waites et al. 2009). Palmitoylation is a highly dynamic, reversible protein modification of palmitic acid-attachment, which increases the membrane association of proteins and can modulate protein interactions (Smotrys and Linder 2004, Salaun et al. 2010). Alternatively, the N-terminus can also contain a L27 domain, which is important for homo- and heteromultimerization, what can enhance the clustering of interaction proteins (Feng et al. 2004, Zheng et al. 2011).

The PSD95 subfamily of MAGUKs is developmentally differentially regulated. SAP102 is highly expressed early in postnatal development, whereas PSD95, PSD93 and SAP97 expression dramatically increases at later time points (Sans et al. 2000). They are all found in the PSD but are also located at non-synaptic sites, e.g. SAP102 and PSD95 are associated with extra-synaptic NMDA (N-methyl-d-aspartate) receptors (Valtschanoff et al. 2000, Petralia et al. 2010).

1.6.1 The role of MAGUKs in the post-synaptic density (PSD)

MAGUKs in the PSD are essential for synaptic development and plasticity, because they scaffold proteins together via their different protein interaction domains and consequently increase the efficiency of interactions between signaling molecules as e.g. membrane receptors (Good et al. 2011). Besides, MAGUKs themselves are target of regulation and can influence the signaling processes as for example phosphorylation of a MAGUK can result in a reduced or abolished interaction (Lee and Zheng 2010). In the PSD synaptic plasticity is changed amongst others via spine dynamics, for which MAGUKs are important (Tada and Sheng 2006). Herein, MAGUKs regulate spine morphogenesis by scaffolding actin-coordinating proteins. Spines are actin-rich protrusions; therefore, spine dynamics in volume and shape depend on organization of actin filaments. LTP and long-term depression (LTD) are two major effects in signal transmission underlying synaptic plasticity (Cooke and Bliss 2006). LTP results from stimulation of a synapse over an extended period and can terminate in a synapse strengthening over weeks *in vivo* (Bliss and Gardner-Medwin 1973, Abraham et al. 2002), whereas LTD ends in a long-lasting diminishment of synaptic efficacy (Nishiyama et al. 2000, Malenka and Bear 2004). It is known that LTP is connected to an increase in actin-based spine volume depending on PSD95 signaling via PDZ and GuK domains (Steiner et al. 2008, Meyer et al. 2014). Meanwhile the reduction of endogenous PSD95 expression during LTP results in a shrinkage of spine volume, but over-expression of PSD95 after knockdown rescues this effect (Zheng et al. 2011). Furthermore, the over-expression of PSD95 leads to a synaptic potentiation mimicking LTP because silent synapses are converted into functional synapses and GluA1 glutamate receptors are delivered to synapses. Concurrently LTP is occluded while PSD95 overexpression and LTD is enhanced, possibly because of a secondary overload of the synaptic membrane with AMPA (α-amino-3-hydroxy-5-methyl-4-isoxazole propionic acid) receptors due to PSD95 expression (Stein et al. 2003, Ehrlich and Malinow 2004). In detail the AMPAR-mediated excitatory post-synaptic currents (EPSCs) of synaptic transmission are also regulated by PSD95, because after acute over-expression of PSD95 they were potentiated what depends on two palmitoylated

N-terminal cysteines in PSD95 (El-Husseini et al. 2000a, Beique and Andrade 2003, Ehrlich and Malinow 2004). Here, EPSCs mediated by NMDARs, which are glutamate receptors mediating long-term synaptic plasticity, were not enhanced during PSD95 over-expression. Controversial to above PSD95 effects, mice lacking the protein showed no altered basal synaptic transmission (Migaud et al. 1998), but studies excluding the possibility of compensation by other MAGUKs revealed a PSD95-dependent basal synaptic transmission (Xu et al. 2008, Yudowski et al. 2013). The redundancy and high homology of PSD95 subfamily members could explain why many interaction partners can bind to more than one member of the PSD95 subfamily and double or triple knockouts are necessary to investigate phenotypes (Dakoji et al. 2003, Perez-Perez et al. 2009). The increased or decreased levels of synaptic AMPARs after increasing or decreasing PSD95 were also observed for the MAGUK PSD93 (Elias et al. 2006). Whereas similar effects for the MAGUKs SAP102 and SAP97 are less dramatic and more variable (Huganir and Nicoll 2013). The deficits in synaptic AMPARs of PSD93/PSD95 double-knockout mice were rescued by SAP97 (Howard et al. 2010), underlining the importance of partly overlapping functions of PSD95 subfamily members. On the other hand functions are also very specialized since the SAP102 knockout mice showed an enhancement of LTP depending on the ERK signaling pathway, but in PSD95 knockout mice the enhancement of LTP is ERK-pathway independent (Opazo et al. 2003, Cuthbert et al. 2007, Xu 2011). These findings demonstrate comparable effects on LTP regulation but with distinct mechanisms suggesting a complex relationship between MAGUK proteins and synaptic plasticity.

Because of overlapping but not identical sets of interacting proteins, two members of the PSD95 subfamily, PSD95 and PSD93, are thought to be more specifically associated with synaptic functions, whereas the two other members, SAP97 and SAP102, could be more important in trafficking (Kim and Sheng 2004).

1.6.2 MAGUKs modulate the neuronal synapse via PDZ domain interactions

MAGUKs execute their diverse effects by scaffolding interaction partners and tethering them to the right place at the right time (Good et al. 2011). The protein-protein interaction take place via their protein domains as for example the PDZ, SH3, GuK and WW domains. Many surface receptors and adhesion proteins interact with the PDZ domains of MAGUKs via their C-terminal PDZ binding motif as classified in paragraph 1.6. But some proteins interact also via an internal sequence with PDZ domains like neuronal nitric oxide synthase (nNOS), which interacts with the PDZ domains of PSD95 and PSD93 (Brenman et al. 1996).

For the majority of protein interactions the SH3 domain is not responsible, nevertheless the ionotropic glutamate kainate receptor 5 (GluK5) can interact via its C-terminus with the SH3 and GuK domain of PSD95 (Garcia et al. 1998, Maximov et al. 1999). Conversely, the GuK domain of MAGUKs is necessary for interaction with numerous ligands including the guanylate kinase-associated protein (GKAP), which connects the GuK domain of PSD95 with the PDZ domain of Shank (Kim et al. 1997, Takeuchi et al. 1997, Gerrow et al. 2006). Moreover, PSD93 interacts with the microtubule-associated protein 1A (MAP1A) via its GuK domain (Brenman et al. 1998). The WW domains bind as SH3 domains to proline-rich domains (Zheng et al. 2011). MAGI2 has been shown to interact via WW domains with β-dystroglycan at inhibitory synapses in rat hippocampal neurons (Sumita et al. 2007).

MAGUKs contain often more than one PDZ domain and two or more PDZ domains arranged in tandem were shown to display binding properties distinct from those of each isolated domain. This discrepancy arises from interactions between these PDZ domains and resulting folding changes e.g. between the N-terminal tandem PDZ domains of PSD-95 that is why the structural and functional units are termed PDZ supramodules (Long et al. 2003, Feng and Zhang 2009). A supramodule can act synergistically with oligomeric proteins enhancing the binding affinity and supplying higher specificity than a single PDZ domain-dependent interaction. Every MAGUK except the MAGIs shares a common heterotypic supramodule composed sequentially into a PDZ-SH3-GuK tandem (Ye and Zhang 2013). Previously this supramodular organization was functionally validated for zona occludens 1 (ZO-1) revealing that the PDZ domain directly interacts with the SH3 and GuK module changing the binding properties (Pan et al. 2011). This suggests that other MAGUKs also form PDZ-SH3-GuK supramodules.

MAGUKs interact via their PDZ domains with various surface receptors and adhesion proteins, thus clustering them for example at distinct membrane locations. But they also scaffold surface receptors to distinct downstream pathways such as the actin and microtubule cytoskeleton, thereby modulating synapse morphology: PSD95 interacts with Kalirin-7, a guanine nucleotide exchange factor for Rac1, which regulates spine morphogenesis through the actin cytoskeleton (Penzes et al. 2001). Furthermore, cypin (cytosolic PSD-95 interactor) interacts with PSD95 and regulates dendrite branching by promoting microtubule polymerization (Firestein et al. 1999, Akum et al. 2004). PSD95 can also bind to the cysteine-rich PDZ-binding protein (CRIPT), which is a microtubule-binding protein (Passafaro et al. 1999).

Besides, MAGUKs interact also with various membrane receptors, especially GPCRs (Magalhaes et al. 2011). There are many class I PDZ domain-dependent interactions between members of the PSD95 subfamily or MAGI2 and membrane receptors (Table 1)

coordinating neuronal synapse-related events including synaptic transmission. MAGUKs influence the pre-synaptic excitability through calcium dynamics, since PSD95, SAP97, SAP102 and PSD93 interact with plasma membrane calcium ATPase isoform 4b (PMCA4b), whereas SAP97 also binds to PMCA2b (Kim et al. 1998, DeMarco and Strehler 2001, Oliva et al. 2011). PMCAs are responsible for the calcium expulsion and intracellular maintenance of calcium levels influencing the pre-synaptic vesicle fusion with the membrane (Rizzoli and Betz 2005).

PSD95 and MAGI2 interact with neuroligin, a postsynaptic membrane protein, which interacts trans-synaptically with β-neurexins (Irie et al. 1997, Sumita et al. 2007, Rosenberg et al. 2010). This neuroligin-β-neurexin interaction mediates cell adhesion, but also seems to induce presynaptic differentiation (Dean et al. 2003, Li and Sheng 2003), probably with the influence of PSD95 and/or MAGI2 (Kim and Sheng 2004). Additionally, MAGI2 induces synaptic accumulation of neuroligin and subsequently recruits PSD95 to the ternary complex (Iida et al. 2004).

The post-synaptic excitability is influenced by many PDZ domain-mediated interactions of membrane receptors with MAGUKs. For example the isoform 2 of the NMDAR subunit GluN1 and many of the GluN2 subunits interact with each member of the PSD95 subfamily resulting in a synaptic clustering (Kornau et al. 1995, Kim et al. 1996, Muller et al. 1996, Niethammer et al. 1996, Standley et al. 2000, Lim et al. 2002, Chung et al. 2004, Chen et al. 2006, Zheng et al. 2011, Fiorentini et al. 2013). The C-terminal truncation of GluN2A inhibited the synaptic but not extra synaptic localization of NMDA receptors indicating the importance of a MAGUK interaction (Steigerwald et al. 2000). Besides, the NMDAR C-terminal tail is sufficient to induce robust dendritic branching in mature hippocampal neurons, suggesting that the GluN2B tail is important in recruiting calcium-dependent signaling proteins and scaffolding proteins like PSD95 necessary for dendritogenesis (Bustos et al. 2014). Only SAP97 is able to interact directly with AMPARs (Leonard et al. 1998, von Ossowski et al. 2006a, von Ossowski et al. 2006b, Zhou et al. 2008). Surprisingly, the direct link is important for SAP97 targeting to the plasma membrane where both proteins together promote dendrite branching upon receptor activation. But PSD95 and SAP97 recruit the tetraspanning membrane protein stargazin, which connects AMPARs with PSD95 (Chen et al. 2000a). This interaction between PSD95, stargazin and AMPARs is important for synaptic AMPAR targeting due to surface expression and synaptic targeting. The overexpression of PSD93 or SAP102 leads to a selectively enhancement of AMPAR synaptic currents showing the importance of additional MAGUKs for synaptic modulation (Zheng et al. 2011).

The 5-HT2Rs, which are GPCRs, interact with PSD95, SAP97, SAP102 and MAGI2 and thereby influence the dendritic targeting and signal transduction of these receptors (Xia et al.

2003a, Xia et al. 2003b, Becamel et al. 2004, Dunn et al. 2014). PSD95 stabilizes also the receptor turnover *in vivo* (Abbas et al. 2009) suggesting that PDZ proteins may regulate the life span of GPCRs (Magalhaes et al. 2011). This interaction is also of particular interest, since CRHR1 activation leads to a significant potentiation of 5-HT2R signaling (Magalhaes et al. 2010). Moreover, this GPCR sensitization depends on intact PDZ binding motifs of both receptors, indicating an example of PDZ protein-mediated crosstalk of GPCRs.

MAGI2 and PSD95 are known to bind to the β1-adrenergic receptor 1 (β1AR) (Hu et al. 2000, He et al. 2006). The agonist-induced internalization of β1AR is increased by MAGI2 overexpression, but PSD95 overexpression has the opposite effect (Xu et al. 2001). Whereas, the interaction of β1AR with MAGI3 abolished the β1AR-mediated ERK1/2 activation with no effect on agonist dependent receptor internalization or agonist stimulated cAMP formation (He et al. 2006). This is one example for the diverging regulation of GPCR signaling through distinct MAGUKs.

Another GPCR, the somatostatin receptor (SSTR), interacts with PSD95, PSD93 and SAP97 and is involved in the regulation of growth cone dynamics (Christenn et al. 2007, Cai et al. 2008, Moller et al. 2013). Our laboratory recently showed that SSTR1 clearly co-localized with PSD95 in primary murine hippocampal neurons suggesting a possible PDZ domain-dependent clustering (Moller et al. 2013).

PSD95 interacts and clusters also with the G protein-coupled estrogen receptor 1 (GPR30) via the N-terminal tandem PDZ domains (Akama et al. 2013). The estrogen receptor is found in dendritic spines of the hippocampus and thought to mediate the estrogen-modulating effects to the synaptic plasticity in the hippocampus.

Although SAP102 contains only class I PDZ domains (Oliva et al. 2011), SAP102 connects to the receptor tyrosine kinase EphrinB2, which contains with the C-terminal amino acids V-E-V a class II PDZ binding motif and regulates cortical synapse development (Murata and Constantine-Paton 2013). Simultaneously, the actin binding afadin interacts with the EphrinB2 receptor (Hock et al. 1998) through PDZ domain interactions and SAP102 also co-immunoprecipitates like PSD95 with Kalirin-7 modulating the actin cytoskeleton (Penzes et al. 2001). This can explain the inhibited reorganization of actin filaments, synapse formation and synaptic AMPAR trafficking after EphrinB2 activation due to knockdown of SAP102.

These example shows that MAGUKs can induce membrane clustering, synaptic targeting, stabilization of protein turnover and influence signaling of interacting partners via PDZ domains. Furthermore, MAGUKs can also induce dendritic branching and control synapse formation and morphology. In conclusion, these multiple PDZ domain-dependent interactions of MAGUKs with membrane receptors indicate that MAGUKs are more than just scaffolding

proteins and modulate the synaptic plasticity in various and complex manners that are far from being fully understood.

PDZ Protein	Interacting PDZ domains	Membrane receptor	Reference
PSD95	n.d.	5-hydroxytryptamine receptor (5-HT2A/5-HT2C)	(Xia et al. 2003a, Becamel et al. 2004)
	n.d.	β1-adrenergic receptor 1 (β1AR)	(Hu et al. 2000, He et al. 2006)
	PDZ1+2	Brain-specific angiogenesis inhibitor 1 (Bai1)	(Lim et al. 2002)
	n.d.	Corticotropin-releasing hormone receptor type 1 (CRHR1)	(Akama et al. 2013)
	n.d.	C-X-C chemokine receptor type 2 (CXCR2)	(Moller et al. 2013)
	PDZ1+2	G protein-coupled estrogen receptor 1 (GPR30)	(Akama et al. 2013)
	n.d.	Inward rectifier potassium channel (Kir2.1/Kir2.3/Kir5.1)	(Cohen et al. 1996, Nehring et al. 2000a)
	n.d.	LDL receptor-related protein 4 (LRP4)	(Tian et al. 2006)
	PDZ3	Neuroligin	(Irie et al. 1997)
	n.d.	Neuropeptide Y receptor type 2 (NPY2-R)	(Moller et al. 2013)
	PDZ1+2	NMDA receptor subunits (GluN1/GluN2A/GluN2B/GluN2C)	(Kornau et al. 1995, Niethammer et al. 1996, Standley et al. 2000, Lim et al. 2002, Chen et al. 2006)
	PDZ1+2+3	Plasma membrane calcium ATPase isoform 4b (PMCA4b)	(Kim et al. 1998)
	PDZ1+2	Receptor tyrosine-protein kinase erbB-4	(Garcia et al. 2000)
	PDZ2	Shaker-type K+ channel (Kv1.4)	(Kim et al. 1995, Jugloff et al. 2000, Imamura et al. 2002)
	PDZ1+2	Somatostatin receptor (SSTR1/SSTR4)	(Christenn et al. 2007, Moller et al. 2013)
	n.d.	Synaptic adhesion-like molecules (SALM3/SALM5)	(Mah et al. 2010)
PSD93	PDZ1+2	Glutamate receptor ionotropic, delta (GluRδ1/GluRδ2)	(Roche et al. 1999)
	PDZ1+2	NMDA receptor subunits (GluN1/GluN2A/GluN2B)	(Kim et al. 1996, Standley et al. 2000, Fiorentini et al. 2013)
	PDZ1+2+3	Plasma membrane calcium ATPase isoform 4b (PMCA4b)	(Kim et al. 1998)
	n.d.	Receptor tyrosine-protein kinase erbB-4	(Garcia et al. 2000)
	n.d.	Shaker-type K+ channel (Kv1.4)	(Kim et al. 1996)
	PDZ1+2	Somatostatin receptor (SSTR1/SSTR4)	(Christenn et al. 2007)

PDZ Protein	Interacting PDZ domains	Membrane receptor	Reference
SAP97	n.d.	5-hydroxytryptamine receptor (5-HT2A)	(Dunn et al. 2014)
	PDZ2	AMPA receptor subunit (GluA1)	(Leonard et al. 1998, von Ossowski et al. 2006a, von Ossowski et al. 2006b, Zhou et al. 2008)
	n.d.	ATP-sensitive inward rectifier potassium channel 12 (Kir2.2)	(Leonoudakis et al. 2001)
	n.d.	β1-adrenergic receptor 1 (β1AR)	(He et al. 2006)
	PDZ1+2	Corticotropin-releasing hormone receptor type 1 (CRHR1)	(Dunn et al. 2013)
	n.d.	LDL receptor-related protein 4 (LRP4)	(Tian et al. 2006)
	PDZ1+2	NMDA receptor subunits (GluN1/GluN2A/GluN2B)	(Niethammer et al. 1996, Standley et al. 2000)
	PDZ1+2(+3)	Plasma membrane calcium ATPase isoforms (PMCA2b/ PMCA4b)	(Kim et al. 1998, DeMarco and Strehler 2001)
	n.d.	Somatostatin receptor (SSTR1)	(Cai et al. 2008)
SAP102	n.d.	5-hydroxytryptamine receptor (5-HT2A/5-HT2C)	(Becamel et al. 2004)
	PDZ1+2	NMDA receptor subunit (GluN1/GluN2B/GluN2C)	(Muller et al. 1996, Standley et al. 2000, Lim et al. 2002, Chung et al. 2004, Chen et al. 2006)
	n.d.	Receptor tyrosine-protein kinase erbB-4	(Garcia et al. 2000)
	n.d.	Plasma membrane calcium ATPase isoform 4b (PMCA4b)	(DeMarco and Strehler 2001)
MAGI2	n.d.	5-hydroxytryptamine receptor (5-HT2C)	(Becamel et al. 2004)
	n.d.	Activin type II A receptor	(Shoji et al. 2000)
	PDZ0	β1-adrenergic receptor 1 (β1AR)	(Xu et al. 2001, He et al. 2006)
	n.d.	Dendrite arborization and synapse maturation 1 (Dasm1)	(Shi et al. 2004)
	PDZ5	Glutamate receptor ionotropic, delta (GluRδ2)	(Yap et al. 2003)
	PDZ1	Neuroligin 1 and 2	(Iida et al. 2004, Sumita et al. 2007, Rosenberg et al. 2010)
	PDZ4	NMDA receptor subunit (GluN2A/GluN2C)	(Hirao et al. 1998, Hirao et al. 2000, Montgomery et al. 2004)
	n.d.	Vasoactive intestinal polypeptide type-1 receptor (VPAC1)	(Gee et al. 2009)

Table 1: Class I PDZ domain-dependent interactions of MAGUKs with membrane receptors.
n.d. not determined.

2   Aim of the thesis

The aim of the thesis was to unravel molecular mechanisms of corticotropin-releasing hormone receptor type 1 (CRHR1) signaling, particularly the interactions with other proteins via its putative C-terminal PDZ binding motif.

Starting point were candidate interaction partners identified in two yeast two-hybrid screens using the cytoplasmic C-terminal tail of CRHR1 as a bait (Figure 4): Postsynaptic density protein 95 (PSD95), synapse-associated protein 97 (SAP97), SAP102, membrane-associated guanylate kinase, WW and PDZ domain containing 2 (MAGI2; also called ARIP1, activin receptor-interacting protein 1 or S-SCAM, synaptic scaffolding molecule), transmembrane protein 106B (TMEM106B) and syndecan binding protein 1 (abbreviated as SDCBP or Syntenin-1).
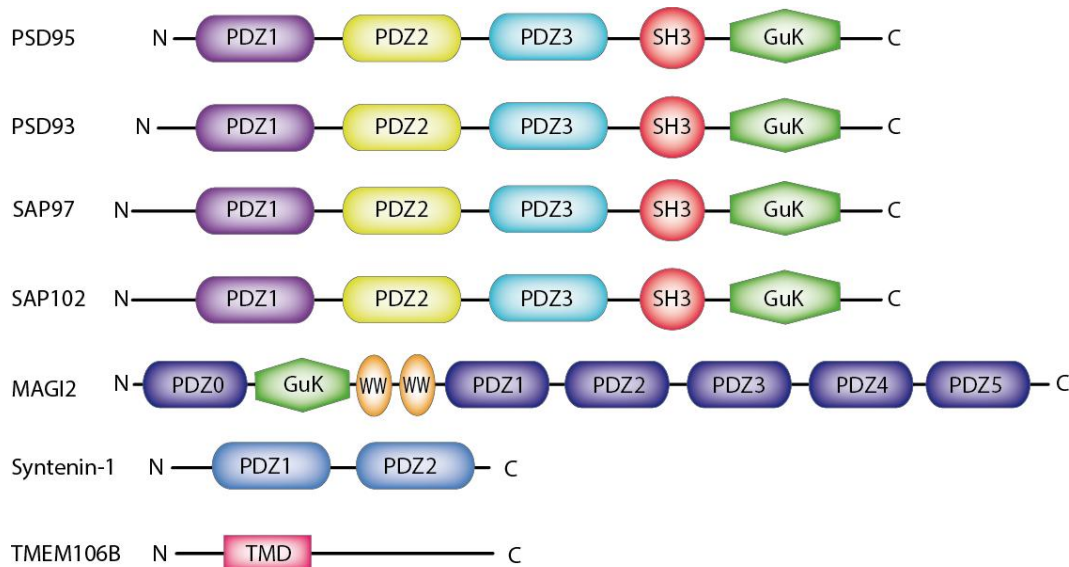
Figure 4: Candidate interaction partners of CRHR1.
PSD95, PSD93, SAP97, SAP102 and MAGI2 belong to the membrane-associated guanylate kinases (MAGUK) family. PSD93 was included into further studies because of its high homology to the other members of the PSD95 subfamily of MAGUKs identified in the Y2H screen. PDZ, PSD95/discs large/zona occludens 1; SH3, SRC homology 3; GuK; guanylate kinase; W, tryptophan; TMD, transmembrane.

The following specific questions were addressed in the course of this thesis.

I)   Can the putative CRHR1 interaction partners be verified and what are the important protein domains mediating the interaction?

To verify the putative interaction partners of CRHR1, co-immunoprecipitations were established and performed in human embryonic kidney 293 (HEK293) cells. Moreover,

mutants of CRHR1 and of the interaction partners were constructed and used to determine the interacting domains.

II)   What is the functional relevance of the PDZ binding motif-dependent interaction *in vitro*?

To elucidate the functional relevance of the interaction of CRHR1 with the candidate interaction partners *in vitro*, the subcellular localization of CRHR1 and interaction partner was assessed in dependence of their interaction.

III)   Are the putative interaction partners co-expressed with CRHR1 *in vivo* in order that a physiologically interaction is possible?

The co-expression of CRHR1 and interaction partners represents a prerequisite for their physical interaction. For this purpose single and double *in situ* hybridization methods were established and conducted throughout the mouse brain.

IV)   Is primary neuronal culture a suitable cellular model to investigate the CRHR1/CRH system?

Primary hippocampal neurons were examined in terms of their utility as a cell culture model to investigate the CRHR1/CRH system. Consequently, the expression of CRHR1, its ligand CRH and the candidate interaction partners were explored on mRNA level. Additionally, CRHR1 and CRH expression was elucidated using primary neurons derived from transgenic reporter mouse lines.

V)   Does the CRHR1 PDZ binding motif have a physiological role in mature neurons?

The role of the CRHR1 PDZ binding motif in localization of the receptor was studied in primary neurons. Different transfection and transduction methods were established and used for over-expression of wild-type and mutants variants of CRHR1.

The in-depth characterization of CRHR1 interactions with other proteins via its C-terminal PDZ binding motif will help to understand on the molecular level how CRHR1 modulates synaptic plasticity. Thereby this study will provide additional insight how CRHR1 is involved in the pathoethiology of stress-related neuropsychiatric disorders.

3 Materials and Methods

3.1 Material

3.1.1 Plasmids

Name	Backbone	Purpose	Source
HA-hCRHR1	pcDNA3	HA-hCRHR1 expression plasmid	Cloned
HA-hCRHR1- STAVA	pcDNA3	HA-hCRHR1- STAVA expression plasmid	Cloned
flag-hCRHR1	pcDNA3	flag-hCRHR1 expression plasmid	F. Hausch
flag-hCRHR1-STAVA	pcDNA3	flag-hCRHR1-STAVA expression plasmid	Cloned
myc-GFP-mCRHR1	pcDNA3	Expression plasmid for mCRHR1 WT with enhanced expression by using signal sequence of larval cuticle protein 3 (LCP3)	J. Breu
myc-GFP-mCRHR1-STAVA	pcDNA3	Expression plasmid for mCRHR1-STAVA	J. Breu
myc-GFP-CRHR1 CRHR1Δ C-term	pcDNA3	myc-GFP-CRHR1 CRHR1Δ C-term expression plasmid	Cloned
myc-GFP-CRHR1-S301V	pcDNA3	CRHR1 mutant expression plasmid	Cloned
myc-GFP-CRHR1Δ 2TM	pcDNA3	CRHR1 mutant expression plasmid	Cloned
myc-GFP-mCRHR1	pAAV-EF1a-DIO -WPRE-IRES	myc-GFP-mCRHR1 expression plasmid	Cloned
myc-GFP-mCRHR1-STAVA	pAAV-EF1a-DIO -WPRE-IRES	CRHR1 mutant expression plasmid	Cloned
myc-GFP-mCRHR1	Lentiviralbackbone	mCRHR1 WT expression plasmid	Cloned
myc-GFP-mCRHR1-STAVA	Lentiviralbackbone	CRHR1 mutant expression plasmid	Cloned
myc-GFP-mCRHR1	pCRII	Transfer vector for cloning	Cloned
myc-GFP-mCRHR1-STAVA	pCRII	Transfer vector for cloning	Cloned
pCRII-TOPO	pCRII	TOPO cloning vector	Invitrogen
pcDNA3	pcDNA3	Control expression vector	Invitrogen

Name	Backbone	Purpose	Source
pAAV-EF1a-DIO EYFP-WPRE-IRES	pAAV-EF1a-DIO -WPRE-IRES	double-floxed inverse open reading frame (DIO)-AAV expression plasmid for cloning	K. Deisseroth, C. Ramakrishnan
EGFP	pcDNA3	Cloning of GFP-fusion proteins	R. Sprengel
IRES GFP	pSKSP (+)	Lentiviral expression plasmid for cloning	D. Vogt-Weisenhorn
pmaxGFP	unknown	Control expression vector	Lonza
myc-MAGI2	pCIneomycS	myc-MAGI2 expression vector	N. Brose
myc- MAGI2-PDZ0+GuK	pCIneomycS	myc- MAGI2-PDZ0+GuK expression vector	N. Brose
myc- MAGI2-WW+PDZ1	pCIneomycS	myc- MAGI2-WW+PDZ1 expression vector	N. Brose
myc- MAGI2-PDZ2-PDZ5	pCIneomycS	myc- MAGI2-PDZ2-PDZ5 expression vector	N. Brose
PSD93-GFP	pcDNA3	PSD93-GFP expression vector	D. Refojo
PSD95 PDZ1flag	pcDNA3	PSD95 PDZ1flag expression vector	M. Engeholm
PSD95 PDZ2-3flag	pcDNA3	PSD95 PDZ2-3flag expression vector	M. Engeholm
PSD95 PDZ3flag	pcDNA3	PSD95 PDZ3flag expression vector	M. Engeholm
PSD95 ΔPDZ1-3flag	pcDNA3	PSD95 ΔPDZ1-3flag expression vector	M. Engeholm
PSD95flag	pcDNA3	PSD95flag expression vector	D. Refojo
HA-SAP97	pcDNA3	HA-SAP97 expression vector	D. Gardiol
HA-SAP97-NT-PDZ1-2	pcDNA3	HA-SAP97-NT-PDZ1-2 expression vector	D. Gardiol
HA-SAP97-NT-PDZ1	pcDNA3	HA-SAP97-NT-PDZ1 expression vector	D. Gardiol
HA-SAP97-3PDZ	pcDNA3	HA-SAP97-3PDZ expression vector	D. Gardiol
SAP102-flag	pCMV3TAG1A	SAP102-flag expression vector	R. Zalm
SAP102ΔPDZ1-2-flag	pCMV3TAG1A	SAP102ΔPDZ1-2-flag expression vector	Cloned
Syntenin-myc	pcDNA3.1/Zeo+	Syntenin-myc expression vector	P. Zimmermann
HA-hTMEM106B	pcDNA3.1/Hygro	HA-hTMEM106B expression vector	Cloned from plasmid from A. Capell

Table 2: Plasmids used in this work.
List of plasmids including their backbone, purpose and source.

3.1.2 Antibodies

Name	Source, cat #	Species	Application	Dilution
α-ankyrin G	UCDavis/ NIH NeuroMab Facility, #75-147	mouse	IF	1:500
α-calbindin D28-K	Swant, #CB38	rabbit	IF	1:2000
α-calretinin	Swant, #7699/3H	rabbit	IF	1:5000-1:10000
α-CRHR1	Santa Cruz, #sc1757	goat	IF	1:500
α-flag M2	Sigma-Aldrich, #F3165	mouse	IF/ WB	1:3000/1:5000
α-Gad67	Millipore, #MAB5406	mouse	IF	1:2000
α-Gad65/67	Abcam, # ab49832	rabbit	IF	1:10000
α-GFP	Abcam, #ab13970	chicken	IF	1:3000
α-GFP	Abcam, #ab 6556	mouse	WB	1:5000
α-gephyrin	Synaptic Systems, #147111	mouse	IF	1:1000
α-HA	Cell Signaling, #C29F4	rabbit	IF/ WB	1:2000/1:750-1:3000
α-MAP2	Abcam, # ab5622	rabbit	IF	1:1000
α-myc	Santa Cruz, #sc798B	rabbit	IF	1:250
α-myc	Abcam, #ab 9106	rabbit	IF/WB	1:2000/1:5000
α-NeuN	Millipore, #MAB377	mouse	IF	1:1000
α-PSD95	UCDavis/ NIH NeuroMab Facility, #75-028	mouse	IF	1:500
α-SAP97	Thermo Fisher Scientific, #PA1-741	rabbit	IF	1:2000
α-SMI-312	Abcam, #ab24574	mouse	IF	1:2000
α-synapsin	Synaptic Systems, #106001	mouse	IF	1:1000
α-V-Glut	UCDavis/ NIH NeuroMab Facility, #75-066	mouse	IF	1:500

Table 3: List of primary antibodies used in this work.
cat #, catalog number; IF, immunofluorescence; WB, Western blot.

Name	Source, cat #	Application	Dilution
Alexa Fluor 488 goat α-chicken IgG	Invitrogen, #A11039	IF	1:1000
Alexa Fluor 488 goat α- mouse IgG	Invitrogen, #A11029	IF	1:1000
Alexa Fluor 488 goat α-rabbit IgG	Invitrogen, #A11034	IF	1:1000

Name	Source, cat #	Appli-cation	Dilution
Alexa Fluor 594 donkey α-goat IgG	Invitrogen, #A11058	IF	1:1000
Alexa Fluor 594 goat α-mouse IgG	Invitrogen, #A11032	IF	1:1000
Alexa Fluor 594 goat α-rabbit IgG	Invitrogen, #A11037	IF	1:1000
α-mouse-IgG horseradish-peroxidase	Cell Signaling, #7076	WB	1:3000- 1:5000
α-rabbit-IgG horseradish-peroxidase	Cell Signaling, #7074	WB	1:3000- 1:5000

Table 4: List of secondary antibodies used in this work.
cat #, catalog number; IF, immunofluorescence; WB, Western blot.

3.1.3 Buffers and Solutions

All chemicals and solutions were purchased from Sigma, Roth and Merck unless indicated otherwise.

Appli-cation	Name	Composition
general buffers	10x PBS	1.37 M NaCl 27 mM KCl 200 mM Na_2HPO_4 x 12 H_2O 20 mM KH_2PO_4 adjust pH to 7.4
	20 % Paraformaldehyde (PFA)	20 % w/v Paraformaldehyde in 1 x PBS-DEPC adjust pH to 7.4
	20 x standard saline citrate (SSC)	3 M NaCl 300 mM Sodium citrate adjust pH to 7.4
	DEPC- H_2O	2 ml DEPC ad 2 l $H_2O_{bidest.}$, shake the solution, incubate for 4 h at room temperature and autoclave twice
bacterial culture	LB (lysogeny broth) medium	1 % (w/v) Bacto-tryptone 0.5 % (w/v) Bacto-yeast extract 1.5 % (w/v) NaCl adjust pH to 7.4

Appli-cation	Name	Composition
bacterial culture	LB agar medium	1 % (w/v) Bacto-tryptone 0.5 % (w/v) Bacto-yeast extract 1.5 % (w/v) NaCl 1.5 % (w/v) Bacto-agar adjust pH to 7.4
	TSS	25 ml 2x LB, adjusted pH to 7.0 and autoclaved 16.5 ml 30 % PEG8000, freshly prepared, slightly heated 2.5 ml DMSO (dimethylsulfoxide) 2.5 ml 1M $MgCl_2$, adjusted pH to 6.5 3.5 ml H_2O, filtrate with 0.2 µm pore size
agarose gel electrophoresis	1x Tris acetate EDTA (TAE) buffer	4.84 g tris(hydroxylmethyl)-aminomethan (Tris) 1.142 ml acetic acid 20 ml 0.5 M ethylenediaminetetraacetic acid (EDTA), pH 8.0 800 ml H_2O_{bidest}. adjust pH to 8.3 with acetic acid and volume to 1 liter with H_2O_{bidest}.
	6x DNA loading buffer (orange)	1 g orange G 10 ml 2 M Tris-HCl, pH 7.5 150 ml glycerol adjust volume to 1 liter with H_2O_{bidest}.
in situ hybridization (ISH)	10x triethanolamine (TEA)	1 M TEA, pH 8.0 adjust H_2O_{bidest}., add 1 ml DEPC/liter incubate overnight, 2x autoclave
	Hybridization-mix (hybmix)	50 ml formamide 1 ml 2 M Tris-HCl, pH 8.0 1.775 g NaCl 1 ml 0.5 M EDTA, pH 8.0 10 g dextransulphate 0.02 g ficoll 400 0.02 g polyvinylpyrrolidone 40 (PVP40) 0.02 g bovine serum albumin (BSA) 5 ml tRNA (10 mg/ml) 1 ml carrier DNA (salmon sperm, 10 mg/ml) 4 ml 5 M dithiothreitol (DTT) store as 1 to 5 ml aliquots at -80°C
	Hybridization chamber fluid	250 ml formamide 50 ml 20x SSC 200 ml H_2O_{bidest}.

Appli-cation	Name	Composition
in situ hybridization (ISH)	5 M DTT/diethyl pyrocarbonate (DEPC)	7.715 g DTT 4 ml DEPC-H_2O shake the falcon tube until the powder is nearly solved adjust volume to 10 ml with DEPC-H_2O
	10x proteinase K buffer/DEPC	500 ml 1 M Tris-HCl, pH 7.5 100 ml 0.5 M EDTA, pH 8.0 adjust volume to 1 liter with DEPC-H_2O, autoclave
	5x NTE	146.1 g NaCl 50 ml 1 M Tris-HCl, pH 8.0 50 ml 0.5 M EDTA, pH 8.0 adjust volume to 1 liter with $H_2O_{bidest.}$, add 1 ml DEPC incubate overnight
	Hybridization chamber fluid	250 ml Formamide 50 ml 20 x SSC 200 ml $H_2O_{bidest.}$
	3 M NH4OAc	3.0 M Ammonium acetate (NH_4OAc) add $H_2O_{bidest.}$
double *in situ* hybridization (DISH)	TNT buffer	0.15 M NaCl 0.1 M Tris-HCl 0.05 % Tween 20 solved in $H_2O_{bidest.}$ adjust pH to 7.6
	NEN-TNB	0.5 % blocking reagent (TSA™-Biotin System) solved in TNT buffer
	DIG blocking buffer	Roche
	DIG washing buffer	Roche
Western blot	Protein lysis buffer	50 mM Tris HCl pH 8 150 mM NaCl 0.1 % SDS 1 % Triton X100 1 mM EDTA pH 8
	Transfer buffer	25 mM Tris-HCl 190 mM Glycine 200 ml MeOH adjust volume to 1 l with $H_2O_{bidest.}$

Appli-cation	Name	Composition
Western blot	Running buffer	25 mM Tris-HCl 190 mM Glycine 0.1 % Sodium dodecyl sulfate (SDS) adjust volume to 1 l with H_2O_{bidest}.
	10 x TBS	200 mM Tris /HCl 1.35 M NaCl adjust pH to 7.6 and volume with H_2O_{bidest}.
	TBS-T 0.01 % (TBS-Tween20)	100 ml 10 x TBS 1 ml Tween20 (BioRad) adjust volume to 1 l with H_2O_{bidest}.
co-immunoprecipitation	Washing buffer I	50 mM Tris HCl pH 8 500 mM NaCl 0.1 % SDS 0.5 % Triton X100 1 mM EDTA pH 8
	Washing buffer II	50 mM Tris HCl pH 7.4 0.1 % SDS 0.5 % Triton X100 1 mM EDTA pH 8

Table 5: Buffers and solutions used in this study.

3.1.4 Oligonucleotides

The DNA oligos nucleotides were purchased from Metabion (Planegg/Steinkirchen, Germany).

3.1.4.1 Oligonucleotides used for cloning procedures

Name		Oligonucleotides sequence	Comment
PSD93	fwd. rev.	5´-GCA-CTC-CGG-ACT-AAC-GTA-AAG-3` 5´-GCA-AAA-TAG-AGC-CGG-CTT-cc-3`	For ISH probe

Name		Oligonucleotides sequence	Comment
PSD95	fwd.	5`-GCA-GGT-GGC-ACC-GAC-AAC-C-3`	For ISH probe
	rev.	5´-GCC-TTC-ACC-GTC-CTC-GCC-3`	
MAGI2	fwd.	5´-CGT-AAG-TCA-GAA-TTT-TGC-AGG-3`	For ISH probe
	rev.	5´-GAA-TAT-CTG-AAG-AGT-TGA-AGC-3`	
CRHR1Δ C-term	fwd.	5´-CCG-GTG-AGA-TAT-CGT-GCG-3`	For cloning of CRHR1 mutant missing the C-terminus
	rev.	5´-CCG-GCG-CAC-GAT-ATC-TCA-3`	
CRHR1-S301V	fwd.	5´-CCT-CAT-GAC-CAA-ACT-CCG-AGC-AGT-CAC-CAC-ATC-TGA-GAC-3`	For cloning of CRHR1 mutant harboring a point mutation at aa 301
	rev.	5´-GTC-TCA-GAT-GTG-GTG-ACT-GCT-CGG-AGT-TTG-GTC-ATG-AGG-3`	
CRHR1-HA	fwd.	5`-GAT-CCA-CCG-CCA-TGA-AGA-CCA-TCA-TCG-CCC-TGA-GCT-ACA-TCT-TCT-GCC-TGG-TGT-TCG-CCT-ACC-CAT-ACG-ATG-TTC-CAG-ATT-ACG-CTG-CCG-3`	For HA tag of CRHR1
	rev.	5`-AAT-TCG-GCA-GCG-TAA-TCT-GGA-ACA-TCG-TAT-GGG-TAG-GCG-AAC-ACC-AGG-CAG-AAG-ATG-TAG-CTC-AGG-GCG-ATG-ATG-GTC-TTC-ATG-GCG-GTG-3`	
CRHR1-virus	fwd.	5`-GCT-AGC-GGC-CGC-CTG-GGC-CCT-CGA-GCC-ACC-ATG-TTC-AAG-3`	For cloning of CRHR1 in lentiviral and AAV backbone
	rev.	5´-GGC-GCG-CCG-TTT-AAA-CGA-ATA-GGG-CCC-TCT-AGA-TCA-3`	
SAP102 PDZ3	fwd.	5´-AAT-TCG-CCG-CCG-C-3`	For cloning and ligation of SAP102 mutant
	rev.	5´-TCG-GCG-GCG-GCG-3´	

Table 6: List of oligonucleotides used in this study for cloning procedures.
ISH, *in situ* hybridization; AAV, adeno-associated virus.

3.1.4.2 Primers used for quantitative real time PCR

Name		Primer sequence	GenBank acc. no.
CRHR1	fwd.	5´-GGG-CCA-TTG-GGA-AAC-TTT-A-3´	NM_007762
	rev.	5´-ATC-AGC-AGG-ACC-AGG-ATC-A-3	
CRH	fwd.	5´-GAG-GCA-TCC-TGA-GAG-AAG-TCC-3´	NM_205769
	rev.	5´-TGT-TAG-GGG-CGC-TCT-CTT-C-3´	
CRHR2	fwd.	5´-TGT-GGA-CAC-TTT-TGG-AGC-AG-3´	NM_009953
	rev.	5´-TGC-AGT-AGG-TGT-AGG-GAC-CTG-3´	

Name		Primer sequence	GenBank acc. no.
MAGI2	fwd. rev.	5´-CAG-GTC-CCG-GAG-TAT-GGA-3´ 5´-TGC-TTG-TCA-CTT-TTC-ATG-CAC-3´	NM_001170746
PSD93	fwd. rev.	5´-CAA-TCA-GAA-ACG-CTC-CCT-GT-3´ 5´-CCC-ACT-GTC-CCT-GCT-CTT-GT-3´	NM_011807
PSD95	fwd. rev.	5´-TCT-GTG-CGA-GAG-GTA-GCA-GA-3´ 5´-CGG-ATG-AAG-ATG-GCG-ATA-G-3´	NM_007864
SAP97	fwd. rev.	5´-TTT-CCC-GAA-AAT-TTC-CCT-TC-3´ 5´-TGG-CAT-TAG-AAG-TTA-CGT-GCT-G-3´	NM_007862
SAP102	fwd. rev.	5´-GGG-CCA-GTT-CAA-TGA-TAA-TCT-C-3´ 5´-CGT-TGC-CGG-AGA-CAT-CTA-AG-3´	NM_001177779

Table 7: Primers used for quantitative real time PCR.
PCR, polymerase chain reaction; acc. no., accession number. fwd. forward; rev. reverse.

3.1.4.3 Oligonucleotides used for single and double *in situ* hybridization (ISH)

Name	Antisense	Vector	insert size [bp]	complem. region [bp]	GenBank acc. no.
CRHR1	T7	pBluescript II SK (+)	702	1728-2428	NM_007762
PSD93	Sp6	pCRII-TOPO	512	243-754	NM_011807
PSD95	Sp6	pCRII-TOPO	731	572-1302	NM_007864
SAP97	T3	PT7T3D	1098	27-1124	NM_001252436
SAP102	T3	PT7T3D	906	3883-4788	NM_016747
MAGI2	Sp6	pCRII-TOPO	623	5336-5958	NM_001170746
GFP	T7	pCRII-TOPO	632	1757-2388	JX679622

Table 8: List of oligonucleotides used in this study for single and double in situ hybridization.
bp, base pairs; complem., complementary; acc. no., accession number.

38

3.2 Methods

3.2.1 Animal experiments

3.2.1.1 Animals and Housing

Mice were housed under standard laboratory conditions (22 ± 1 °C, 55 ± 5 % humidity, 12 h light :12 h dark cycle) with food and water ad libitum. For staging of embryos the day of the appearance of a vaginal plug was treated as embryonic day 0 (E0). Animal experiments were conducted in accordance with the Guide for the Care and Use of Laboratory Animals of the Government of Upper Bavaria (Germany) as well as by the Animal Care and Use Committee of the Max Planck Institute of Psychiatry (Munich, Germany).

3.2.1.2 Transgenic animals used in this study

In this study wild-type and transgenic mice were used, which are described in more detail at the particular experiment. Briefly, for single *in situ* hybridization (ISH) and primary hippocampal cell culture wild-type CD1 mice were used. For double ISH and primary hippocampal cell culture brains of CRHR1-GFP reporter mice (Justice et al. 2008) were utilized. To investigate the CRH expression in primary neurons, CRH-Cre mice (Taniguchi et al. 2011) breeded with the Ai9 reporter mouse line (Madisen et al. 2010) were used. Timed CD1 breedings for standard *in utero* electroporation experiments were conducted. For adeno-associated virus (AAV)-mediated expression of CRHR1-WT (wild-type) or CRHR1-STAVA, primary neurons from homozygous Nex-Cre mice (Goebbels et al. 2006) were prepared.

3.2.2 Microbiological methods

3.2.2.1 Preparation of chemically competent bacteria

For chemically competent bacteria 5 ml of DH5α *E. coli* culture was grown overnight in LB medium. On the next day, 100 ml LB medium was inoculated with 1 ml of the overnight culture and grown on a shaker at 37°C until bacteria were grown to an optical density (OD) of OD_{600nm}= 0.3 – 0.4. Bacteria were then centrifuged for 10 min at 3000 rpm at 4°C. The supernatant was discarded and the pellet was gently resuspended on ice in 10 ml cold TSS.

50 µl aliquots were prepared and snap-frozen on dry ice. Competent bacteria were stored at - 80°C.

3.2.2.2 Transformation

Chemically competent DH5α or XL1-Blue *E. coli* bacteria, stored at -80°C, were thawn on ice. 50-200 ng of DNA was added and mixed with the bacteria by gently tapping the tube. Bacteria were incubated for 30 min on ice. For uptake of plasmid DNA, competent cells were heat-shocked at 42°C for 90 sec and subsequently put on ice. 1 ml LB medium was added and cells were incubated on a shaker at 37°C for 1 h. Cells were plated on LB plates containing the appropriate antibiotic for selection (100 µg/ml ampicillin or 50 µg/ml kanamycin) and incubated overnight at 37°C. Single colonies were picked and inoculated in 5 ml LB medium containing the appropriate selection marker (100 µg/ml ampicillin or 50 µg/ml kanamycin) and grown overnight at 37°C on a shaker at 250 rpm for subsequent DNA preparation.

3.2.2.3 Glycerol stocks

For long-term storage, 500 µl of an overnight bacteria culture was mixed with 500 µl 80 % glycerol and frozen at -80°C.

3.2.3 Preparation and analysis of nucleic acids

3.2.3.1 Preparation of plasmid DNA

E. coli bacteria containing plasmid DNA were usually grown in autoclaved, sterile LB medium with a selective antibiotic, ampicillin (100 µg/ml) or kanamycin (50 µg/ml), overnight at 37°C. Small (5 ml culture), medium (25 ml culture) and large (100 ml culture) scale preparations of plasmid DNA were carried out by means of the respectively Plasmid Mini-, Midi and Plasmid Maxi-Kit from Qiagen, according to the manufacturer´s protocol.

3.2.3.2 RNA isolation

RNA was isolated from mammalian cells using the TRIzol protocol (Invitrogen). Harvested cells were homogenized in 1 ml/mg TRIzol reagent per 10 cm^2 using a 1 ml pipette and

mixed vigorously. Solutions were incubated at room temperature for 5 min. After addition of 200 µl chloroform, tubes were shaken vigorously and incubated for 3 min at room temperature (RT). By centrifugation for 15 min at 13000 rpm (12000g) at 4°C the phenol and water phases were separated. The aqueous upper phase containing the RNA was transferred into a fresh 1.5 ml Eppendorf tube and RNA was precipitated with 500 µl isopropanol/ml TRIzol for 10 min at RT. Precipitated RNA was centrifuged for 10 min at 13000 rpm at 4°C. The pellet was washed with 1 ml of 70 % ethanol, mixed and centrifuged at 9000 rpm (7500 g) at 4°C for 5 min. RNA pellet was dried at 37°C and dissolved in 20-50 µl H_2O_{bidest} at 37°C for 10 min.

3.2.3.3 Agarose gel electrophoresis

For separation of DNA by gel electrophoresis, agarose (Invitrogen) was boiled in 1x TAE buffer with agarose concentration depending on the DNA fragment size. For fragments between 100 and 1000 bp 2 % agarose gels were chosen. For bigger fragments 0.8-1 % agarose gels were applied. 0.1 µg/ml ethidiumbromide was added to boiled and liquid agarose in 1x TAE, which was distributed in a gel electrophoresis chamber (PeqLab). DNA samples mixed with 1/6 of 6x sample loading buffer were loaded. As size marker smart ladder (Eurogentec, Brussels, Belgium) was used. Electrophoresis was carried out with 80-140 V for 1-2 h. The DNA fragments were detected with an UV light camera (QUANTUM ST5, Vilber Eberhardzell, Germany).

3.2.3.4 Photometric determination of DNA concentrations

Optical density (OD) values were measured with the Nanophotometer P330 (Implen, München, Germany) at 260 nm. Samples were diluted in distilled water and DNA concentrations were calculated automatically using the following equation:

DNA concentration [µg/ml] = OD_{260} x f x n

OD_{260} =   Optical density of a strongly diluted DNA solution determined with a spectrophotometer at a wavelength of 260 nm

f =   Dilution factor

n =   Set by default 50 µg/ml for DNA

The ratio of the absorbance readings at 260 nm and 280 nm was used to estimate the purity of nucleic acid preparations. The expected 260/280 ratio of a very pure DNA preparation is ~1.8.

3.2.3.5 Analysis of RNA quality

The quality and concentration of RNA was determined with the Agilent 2100 bioanalyzer (Agilent Technologies) using the Agilent RNA 6000 Nano Kit (Agilent Technologies) according to the manufacturer´s protocol. The method is based on electrophoresis through microchannels measuring the integrity of the RNA.

3.2.3.6 Restriction digestions of DNA samples for analytical purposes

Restriction enzymes from Fermentas or New England Biolabs (NEB) were used. Enzyme units added to a reaction were empirically determined and working buffers were chosen in accordance to the information provided by the suppliers. 1-2 µl of DNA samples were incubated for 1-2 h at 37°C (unless a different temperature was recommended for the used enzyme) and fragment sizes subsequently analyzed on an agarose gel.

3.2.3.7 Sequencing

Sequencing reactions were performed at GATC Biotech (Konstanz, Germany) or Sequiserve (Vaterstetten, Germany). The sequencing results were analyzed using Vector NTI software (Invitrogen).

3.2.4 Polymerase chain reaction (PCR)

To amplify DNA standard polymerase chain reactions were performed using the Thermoprime Plus DNA polymerase (ABgene, Hamburg, Germany) as follows:

1-2 µl	DNA
5 µl	10 x reaction buffer IV (Thermo Scientific)
3 µl	25 mM $MgCl_2$ (Thermo Scientific)
1 µl	dNTPs (dATP, dTTP, dCTP and dGTP, 10 mM each, Roche Applied Science)
2 µl	10 µM primer fwd.
2 µl	10 µM primer rev.
0.5 µl	Thermoprime Plus DNA polymerase (5 U/µl, Thermo Scientific)
ad 50µl	$H_2O_{bidest.}$

PCR was carried out in a PCR machine (Thermal Cycler T100 (Biorad)) with the temperature settings displayed in Table 9.

Program name		Cycles	Temperature [°C]	hold
preincubation		1	94	2 min
amplification	denaturation	30-35	94	30 sec
	annealing		x	30 sec
	elongation		72	y
elongation		1	72	12 min
cooling		1	8	∞

Table 9: Program of a standard PCR (polymerase chain reaction).

Annealing temperature (x) and elongation time (y) were adjusted according to the melting temperature of the primers and the amplicon size.

3.2.4.1 cDNA synthesis

First strand cDNA synthesis from RNA was performed using the SuperScript II Reverse Transcriptase Kit (Invitrogen, Karlsruhe, Germany) according to the provided protocol. To test for genomic DNA contaminations, one control reaction lacking the reverse transcriptase was carried out for each RNA sample. 500-1000 ng of total RNA was incubated together with 0.5 µg/µl oligo d(T) primers (Invitrogen) and 1 µl 10 mM dNTPs in a total volume of 12 µl (H_2O) at 65°C for 5 min and subsequently chilled on ice. Per sample 4 µl 5 x buffer (Invitrogen) and 2 µl 0.1 M DTT (Invitrogen) were added, mixed and tubes were incubated at 42°C for 2 min. Afterwards, samples were incubated with 1 µl SuperScript II at 42°C for 50 min followed by 70°C for 15 min to inactivate the enzyme. cDNA was stored at -20°C.

3.2.4.2 Quantitative real time PCR

For detection of mRNA levels quantitative real time PCR (qPCR) was conducted as previously described (Graf et al. 2012). Aliquots of the reverse transcribed cDNA were utilized as templates. qPCR was performed with a Light Cycler 2.0 System (Roche) using QuantiFast SYBR Green PCR Kit (Qiagen, Hilden, Germany) according to manufacturer´s protocol and relative expression was calculated via the 2Δ method and results were

normalized to the housekeeping gene ribosomal protein L19 (RPL-19). Mastermix was prepared as follows:

5.0 µl   QuantiFast SYBR Green PCR Mix (Qiagen, Hilden, Germany)

1.0 µl   primer forward (10 µM)

1.0 µl   primer reverse (10 µM)

1.0 µl H_2O_{bidest}

8 µl mastermix were pipetted in each capillary, which was fixed in the LightCycler carousel, 2 µl DNA (1/10 diluted) were added and capillaries were closed immediately. A standard qPCR program was applied (Table 10).

Program name		Cycles	Temperature [°C]	hold	Slope [°C/sec]	Sec target	Step size	Step delay	Acquisition mode
preincubation		1	95	5 min	20	0	0	0	none
amplification	denaturation	40	95	10 sec	20	0	0	0	none
	annealing + elongation		60	30 sec	20	0	0	0	single
Melting curve		1	95	0	20	0	0	0	none
			50	10 sec	20	0	0	0	none
			95	0	0.1	0	0	0	continuous
cooling		1	42	30	20	0	0	0	none

Table 10: Program of a quantitative real time PCR (polymerase chain reaction).

3.2.5 Cloning techniques

3.2.5.1 Restriction digestions of DNA samples for preparative purposes

For digestion of plasmid DNA or PCR products restriction enzymes from Fermentas or New England Biolabs (NEB) were used. Enzyme units added to a reaction were empirically determined and reaction conditions and working buffers were chosen in accordance to the information provided by the suppliers. The restriction digest was incubated at 37 °C (unless a different temperature was recommended for the used enzyme). In order to prevent unwanted

religation of the opened plasmid, the terminal phosphates of the digested vector were removed by adding simultaneously 0,5 U FastAP Thermosensitive alkaline phosphatase (Thermo Scientific). The digestion was stopped in general by heating the sample to 65°C or 80°C for 10 min according to the manufacturer's recommendations.

Afterwards, if it was necessary, DNA fragments were separated by gel electrophoresis and the desired fragment was purified by gel extraction, when necessary.

3.2.5.2 Gelextraction

For purification of DNA fragments out of an agarose gel the QIAquick Gel Extraction Kit (Qiagen) was used according to manufacturer´s instructions. DNA was eluted using 30 µl of H_2O_{bidest}. DNA concentration was photometrically determinated and DNA quality was checked by agarose gel electrophoresis of a small aliquot of the eluted DNA.

3.2.5.3 Ligation

For ligation of linearized vector and insert, different molar ratios of 1:3, 1:5 or 1:6 of vector:insert were used. In general, 50 ng of vector DNA and 3 x, 5 x or 6 x of insert, in molar ratio, were mixed. T4 DNA ligase buffer, 50 % PEG4000 and 5 U of T4 DNA ligase (Fermentas or Roche) were added in a total volume of 15 µl. Before mixing the DNA was decoiled by heating to 55°C for 5 min and shortly cooled on ice. The reaction was incubated o.n. at 16 °C. Afterwards, 5 µl of the ligation reaction were used for transformation into chemocompetent bacteria. Usually 5- 10 colonies were inoculated for MiniPreps and the recovered plasmid DNA was subjected to restriction digestion with appropriate restriction enzymes. To verify the sequence of the cloned insert, positive clones were sent for sequencing.

3.2.5.4 Direct cloning of PCR products

For direct cloning of PCR products, e.g. cloning of in situ hybridization probes, the TOPO TA kit from Invitrogen was used. PCR products, amplified with Taq DNA polymerase (5 U/µl, ABgene), therefore containing 3'-A overhangs, were mixed with TOPO pCRII vector, which carries T-overhangs with covalently bound topoisomerase, and salt solution, following the manufacturer's protocol. The reaction was incubated 30 min at RT, and subsequently transformed into chemocompetent bacteria. For blue-white selection (LacZ (β-galactosidase gene) complementation assay) bacteria were plated on LB agar plates containing X-Gal (1

mg/ml LB agar) and ampicillin or kanamycin as antibiotic selection. Usually 5-10 white or light blue colonies were analyzed by MiniPrep and restriction digestion of the recovered plasmid DNA with EcoRI, releasing the inserted PCR product. To determine the orientation of the insert in the pcRII vector, either a restriction digestion with an appropriate enzyme was performed or a positive colony was sent for sequencing with T7 (5'-TAA-TAC-GAC-TCA-CTA-TAG-G-3') or Sp6 (5'-ATT-TAG-GTG-ACA-CTA-TAG-3') primers.

3.2.5.5 Site directed mutagenesis

To introduce point mutations into plasmid DNA the QuikChange Lightning Site Directed Mutagenesis-Kit from Stratagene was used accordingly to the manufacturer's protocol. For generation of CRHR1-S301V the appropriate primers were used (Table 6). Successful mutagenesis was confirmed by sequencing (GATC Biotech or Sequiserve).

3.2.6 Single *in situ* hybridization

For *in situ* hybridization (ISH) brains were dissected from 2-3 months old male wild-type mice sacrificed by an overdose of isoflurane (Forene®, Abbott). The single ISH was conducted as previously described (Refojo et al.). Brains were carefully removed and immediately shock-frozen on dry ice and stored at -80°C until further processing. Frozen brains were mounted on polyfreeze tissue freezing medium (Polyscience Inc.) and cut coronally on a cryostat (HM 560 M, Microm) in 20-µm thick sections and mounted on SuperFrost Plus slides (Menzel GmbH). Specific riboprobes were generated by Standard PCR (paragraph 3.2.4) using T7 and T3 or SP6 primers using plasmids containing respective cDNAs fragments (Table 8) as templates. Radiolabeled sense and antisense cRNA probes were generated from the respective PCR products by *in vitro* transcription with ^{35}S-UTP (Perkin Elmer) using T7 and T3 or SP6 RNA polymerases (Roche). To prevent RNA degradation all precautions were taken to avoid RNase activity.

The *in vitro* transcription was pipetted as follows:

2 µl	PCR product (1.5 µg)
13 µl	H$_2$O-DEPC
3 µl	10 x transcription buffer (Roche)
3 µl	NTP-mix (rATP/rCTP/rGTP 10mM, Roche)
1 µl	0.5 M DTT
1 µl	RNasin (RNAse-inhibitor, 40 U/µl, Roche)
6 µl	^{35}S-thio-rUTP (12.5 mCi/mM, 1250 Ci/mmol, Amersham)
2 µl	T7 or sp6 RNA polymerase (20 U/µl, Roche)

The reaction samples were gently mixed. Afterwards, samples were incubated at 37°C for 3 hours in total; after 1 h another 1.5 µl of RNA polymerase was added.

To destroy the DNA template, 2 µl RNase-free DNase I (10 U/µl, Roche) were added and samples were incubated for 15 min at 37°C.

3.2.6.1 Purification of riboprobes

For purification of riboprobes the RNeasy Mini Kit (Qiagen) was used according to the manufacturer´s protocol. RNA was diluted in 100 µl RNase-free water and 1 µl of the probe was measured in 2 ml scintillation fluid (Zinsser Analytic, Frankfurt, Germany) in a beta-counter (LS 6000 IC, Beckmann Coulter). For in situ hybridization 35000 to 70000 cpm/µl and 90 µl/slide (7 million cpm/slide) were required.

3.2.6.2 Pre-treatment of cryo-slides

Slides were taken out of the -20°C freezer and warmed up for least 1 h while still in the box. Then they were spread out on clean cotton tissue and dried for another 15 min. For pretreatment the following protocol was applied.

Step	Description	Duration	Chemical	Comment
1	fix	10 min	4 % PFA/PBS	ice-cold (4°C)
2	rinse	3 x 5 min	PBS/DEPC	
3		10 min	0.1 M triethanolamine-HCl (TEA) (pH 8.0) 200 ml	add 600 µl acetic anhydride (Sigma-Aldrich) to rapidly rotating stirring bar of TEA
4	rinse	2 x 5 min	2 x SSC/DEPC	
5	dehydrate	1 min	60 % EtOH/DEPC	
6		1 min	75 % EtOH/DEPC	
7		1 min	95 % EtOH/DEPC	
8		1 min	100 % EtOH	
9		1 min	CHCl3	
10		1 min	100 % EtOH	
11	air dry (dust free)			

Table 11: Protocol for pre-treatment of cryo-slides.

3.2.6.3 Hybridization

An appropriate amount of hybridization mix (hybmix) containing the riboprobe of interest was prepared. 90 to 100 µl hybmix and 3.5 to 7 million counts per slide were required.

The hybridization mix containing the probe was heated to 90°C for 2 min and snap cooled on ice. The solution was pipetted onto the slides and coverslips were carefully mounted, avoiding air bubbles in between. The slides were carefully placed into a hybridization chamber containing hybridization chamber fluid to prevent drying of the hybmix and the chamber was sealed with adhesive tape. The slides were incubated in an oven (Memmert, Schwabach, Germany) at 55-68°C o.n. (up to 20 h).

3.2.6.4 Washing

After hybridization the coverslips were carefully removed and the following protocol was applied.

Step	Duration	Temperature [°C]	Chemical	Comment
1	4x 5 min	RT	4x SSC	
2	20 min	37	NTE (20 µg/ml RNaseA)	Add 500 µl RNaseA (10 mg/ml) to 250 ml of NTE
3	2x 5 min	RT	2x SSC/1 mM DTT	50 µl of 5 M DTT/250 ml
4	10 min	RT	1x SSC/1 mM DTT	50 µl of 5 M DTT/250 ml
5	10 min	RT	0.5x SSC/1 mM DTT	50 µl of 5 M DTT/250 ml
6	2x 30 min	64	0.1x SSC/1 mM DTT	50 µl of 5 M DTT/250 ml
7	2x 10 min	RT	0.1x SSC	
8	1 min	RT	30 % ethanol in 300 mM NH_4OAc	
9	1 min	RT	50 % ethanol in 300 mM NH_4Oac	
10	1 min	RT	70 % ethanol in 300 mM NH_4Oac	
11	1 min	RT	95 % ethanol	
12	2x 1 min	RT	100 % ethanol	
13	air dry (dust free)			

Table 12: Washing procedure for hybridized sections on cryo-slides.
RT, room temperature; DTT, Dithiothreitol.

3.2.6.5 Autoradiography

Dried in situ sections were exposed to a special high performance X-ray film (BioMax MR from Kodak) for one to seven days and developed.

Photomicrographs were captured with Zeiss AxioCam MRc5 digital cameras adapted to a stereomicroscope Leica MZ Apo (Leica). Images were digitalized using Axio Vision 4.5., and afterwards photomicrographs were integrated into figures using Adobe Photoshop CS2 9.0 and Adobe Illustrator CS2 12.0.0 image-editing software. Only sharpness, brightness and contrast were adjusted. Brain slices were digitally cut out and set onto an artificial black background.

3.2.7 Double *in situ* hybridization

For detection of co-localization on single cell level double ISH (DISH) was performed as previously described (Refojo et al.). Therefore, two different probes were used, which were individually labeled. One probe was radioactivly labeled as described above in paragraph

3.2.6. Into the other probe Digoxigenin (DIG)-labeled dUTP was incorporated, which can be detected by a DIG specific enzyme antibody coupled to phosphatase. The *in vitro* transcription of DIG-labeled riboprobes was performed with the DIG RNA Labeling Kit (Roche) and was pipetted as follows:

2 µl	PCR product (1.5 µg)
13 µl	H_2O-DEPC
2 µl	10 x DIG RNA labeling mix, Roche)
2 µl	10 x transcription buffer (Roche)
1 µl	RNasin (RNAse-inhibitor, 40 U/µl, Roche)
1 µl	T7 or sp6 RNA polymerase (20 U/µl, Roche)

The reaction samples were gently mixed. Afterwards, samples were incubated at 37°C for 3 hours in total; after 1 h another 0.5 µl of RNA polymerase was added.

To destroy the DNA template, 2 µl RNase-free DNase I (10 U/µl, Roche) were added and samples were incubated for 15 min at 37°C.

For purification of riboprobes the RNeasy Mini Kit (Qiagen) was used according to the manufacturer´s protocol identical to the protocol of ISH.

3.2.7.1 Measuring concentrations of DIG-riboprobes

To determine the efficacy of DIG-labeling the probe was spotted in several dilutions on a nylon membrane (Amersham Hybond-N[+]-Membrane). The spotted probe was visualized by immunoreaction and the intensity of staining was compared with a standard of defined concentration. The detection resulted from enzymatic reaction of a phosphatase coupled anti-DIG antibody, which transferred the substrate nitroblue tetrazolium /5-bromo-4-chloro-3-indolyl-phosphate (NBT/BCIP) into a blue precipitate.

3.2.7.2 Pre-treatment of cryo-slides

Slides were taken out of the -20°C freezer and warmed up for least 1 h while still in the box. Then they were spread out on clean cotton tissue and dried for another 15 min. For pretreatment the following protocol was applied.

Step	Description	Duration	Chemical	Comment
1	fix	15 min	4 % PFA/PBS	ice-cold (4°C)
2	wash	2 x 5 min	PBS/DEPC	
3	quench endogenous peroxidase	15 min	1 % H_2O_2 in 100 % MeOH	
4	wash	2 x 5 min	PBS/DEPC	
5	reduce background	8 min	0.2 M HCl/DEPC	Can be reused up to 3 times
6	wash	2 x 5 min	PBS/DEPC	
7	acetylate	10 min	0,1 M triethanolamine-HCl pH 8.0	add 600 µl acetic anhydride (Sigma-Aldrich) to rapidly rotating stirring bar of TEA
8	wash	5 min	PBS/DEPC	
9	dehydrate	1 min	60 % EtOH/DEPC	
10		1 min	70 % EtOH/DEPC	
11		1 min	96 % EtOH/DEPC	
12		1 min	100 % EtOH	
13	air dry (dust free)			

Table 13: Pre-treatment of cryo-slides for DISH.

3.2.7.3 Hybridization

An appropriate amount of hybridization mix (hybmix) containing the both differently labeled riboprobes was prepared. For hybridization 90 to 100 µl hybmix per slide was required containing a radioactive labeled riboprobe concentration of 8.5×10^6 c.p.m. μl^{-1} and a DIG labeled riboprobe concentration of 0,75 µg/ml.

The hybridization mix containing the probe was heated to 92°C for 2 min and snap cooled on ice. The solution was pipetted onto the slides and coverslips were carefully mounted, avoiding air bubbles in between. The slides were carefully placed into a hybridization chamber containing hybridization chamber fluid to prevent drying out of the hybmix and the chamber was sealed with adhesive tape. The slides were incubated in an oven (Memmert, Schwabach, Germany) at 56°C o.n. (up to 20 h).

3.2.7.4 Washing

After hybridization the coverslips were carefully removed and the following protocol was applied.

Step	Duration	Tempera-ture [°C]	Chemical	Comment
1	25 min	42	4 x SSC/0.05 % Tween 20/1 mM DTT	50 µl of 5 M DTT/200 ml freshly
2	25 min	42	2 x SSC/50 %/formamide/0.05 % Tween 20/1 mM DTT	50 µl of 5 M DTT/200 ml freshly
3	25 min	42	1 x SSC/50 %/formamide/0.05 % Tween 20/1 mM DTT	50 µl of 5 M DTT/200 ml freshly
4	30 min	62	0.1 x SSC/0.05 % Tween 20/1 mM DTT	50 µl of 5 M DTT/200 ml freshly
5	30 min	37	NTE/0.05 % Tween 20	Add 500 µl RNaseA (10 mg/ml) to 250 ml of NTE
6	15 min	30	15 mM iodoacetamide	
7	2x 5 min	30	NTE/0,05 % Tween 20	
8	1 h	30	4 % BSA in TNT	blocking step
9	3 x 2-5 min	30	TNT	
10	30 min	30	NEN-TNB	blocking step
11	o.n.	4	anti-DIG (Fab)-POD (Roche) in TNB, 1:400	

Table 14: Washing procedure of hybridized sections on cryo-slides.
DTT, Dithiothreitol; o.n., overnight.

3.2.7.5 Development of the DIG signal

Step	Duration	Tempera-ture [°C]	Chemical	Comment
1	3 x 2-5 min	30	TNT	
2	15 min	30	TSA mix (=tyramide-biotin in 0.3 ml DMSO) (TSA™-Biotin System)	dilute TSA mix 1:50 with amplification diluent (keep dark)
3	3 x 2-5 min	30	1 x Roche washing buffer	
4	1 h	30	Roche streptavidin-AP in 1 x Roche washing buffer	1:400 diluted

Step	Duration	Tempera-ture [°C]	Chemical	Comment
5	3 x 2-5 min	30	1 x Roche washing buffer	
6	5 min	RT	100 mM Tris/HCl	pH 8.2-.8.5
7	10–30 min	RT	Vector Red: 5 ml 1 x Tris/HCl + 5 µl 1 M levamisole, add 2 drops of reagent 1, vortex, add 2 drops of reagent 2, vortex, add 2 drops of reagent 3, vortex and pipet onto the slides, check red staining intensity under stereomicroscope	
8	2 min	RT	$H_2O_{bidest.}$	
9	10 min	RT	1 x PBS	Stop reaction
10	20 min	RT	2.5 % glutaraldehyd in 1 x PBS	20 ml in 200 ml, freshly prepared
11	3 x 5 min	RT	0.1 x SSC	
12	15 sec	RT	30 % EtOH	
13	15 sec	RT	50 % EtOH	
14	15 sec	RT	70 % EtOH	
15	10 sec	RT	96 % EtOH	
16	air dry (dust free)			

Table 15: Procedure for development of the DIG signal.
RT, room temperature.

3.2.7.6 Dipping

Dried in situ sections were exposed to a special high performance X-ray film (BioMax MR from Kodak) for three days and developed.

The slides were dipped in a pre-warmed photographic emulsion (KODAK NTB2 emulsion, Rochester, NY, USA) for about 4 sec and dried overnight at RT. Then they were packed into light-tight black boxes with sufficient desiccant (silica gel capsules), labeled and sealed with tape. The slides were exposed for one to four weeks at 4°C depending on the signal intensity of the X-ray film.

3.2.7.7 Development

The boxes were equilibrated to room temperature for 2 h while still sealed. The slides were developed in KODAK D 19 developer (Sigma P5670) for 3 min at RT, rinsed 30 sec in tap water and fixed in KODAK fixer (cat # 197 1720) for 6 min. Then they were rinsed in running

tap water for 15 min. Using a strong razor blade the emulsion was scratched from the back side of the slides and the slides were air dried.

After 1-2 days drying at the air the slides were dehydrated again for 30 sec in 30 % Ethanol, 50 % Ethanol and 70 % Ethanol and for 20 sec in 96 % Ethanol. After 2 x 5 min incubation in xylol the slides were covered with DPX (contains xylene, mixture of isomers, dibutylphthalate, VWR international, England) and coverslips.

Dark-field photomicrographs were captured with Zeiss AxioCam MRm digital camera adapted to a Zeiss axioplan 2 imaging microscope. Images were digitalized using Axio Vision 4.5. and afterwards photomicrographs were integrated into figures using Adobe Photoshop CS2 9.0 and Adobe Illustrator CS2 12.0.0 image-editing software. Only sharpness, brightness and contrast were adjusted.

3.2.8 Cell culture

All cell culture reagents were purchased from Invitrogen except as otherwise stated, and all cell culture dishes were purchased from Nunc except otherwise stated.

To avoid bacteria, fungi or yeast contaminations cell culture experiments were carried out under sterile conditions using a sterile hood (Heraeus Instruments, Hanau, Germany).

3.2.8.1 Maintaining of cell lines

Human embryonic kidney (HEK293) cells were maintained in DMEM (Dulbecco's Modified Eagle's Medium) (Invitrogen) supplemented with 10 % fetal bovine serum and 1 % penicillin (100 units/ml)/streptomycin (100 µg/ml) (growth medium) at 37°C with 5 % CO_2 in a sterile incubator (Heraeus). Every third day cells were passaged or medium was refreshed.

3.2.8.2 Thawing of cells

A frozen vial of cells was thawed quickly at 37°C, diluted in growth medium and centrifuged at 1200 rpm for 5 min. The cell pellet was resuspended gently in 5 ml growth medium and cells were seeded onto 10 cm plates.

3.2.8.3 Splitting of cells

Medium was removed from the plates and the monolayer was washed with 5 ml DPBS (Dulbecco's phosphate-buffered saline). 1 ml 0.5 % trypsin/EDTA (Ethylenediaminetetra-

acetic acid) was added and plates were incubated for about 5 min at 37°C until the cells were detached. To stop the reaction, 9 ml DMEM was added and cells were resuspended. An appropriate amount of the cells was plated immediately on new dishes containing growth medium.

3.2.8.4 Freezing of cells

For long-term storage of cell lines freshly thawed cells were passaged at least twice until they were refrozen. Therefore, a confluent plate was trypsinized and cells harvested by centrifugation. Cells were resuspended in 1 ml of freezing medium consisting of 10 % DMSO and 90 % fetal calf serum (FCS) and aliquoted in three cryo tubes (Nalgene, Roskilde, Denmark). The tubes were cooled down slowly overnight wrapped in wet tissue surrounded by aluminum foil at - 80°C or freezing containers (Nalgene) were used. Afterwards cell tubes were stored at – 80°C.

3.2.8.5 Counting of cells

For determination of the cell number a Neubauer chamber (Roth, Karlsruhe) was used. One chamber of this hemocytometer consists of nine squares with the dimension of 1 x 1 mm and a total volume over each square of 10^{-4} ml. After trypsinization cells were resuspended in growth medium and 10 μl of the suspension were counted. The mean value (m) of two counted quadrants was used to calculate the cell number: cells/ml = m x 10000.

3.2.8.6 Plasmid DNA transfection in cell lines

For transfections HEK293 cells were plated on Poly-D-Lysine (Sigma Aldrich)-coated (only for 10 cm plates) cell culture plates in antibiotic-free DMEM and transfected with Lipofectamine 2000 (Invitrogen) according to the manufacturer´s protocol. Cells were transfected at high cell density of 80 % for high efficiency, high expression levels, and to minimize cytotoxicity. For each transfection sample, complexes were prepared as follows: DNA was diluted in Opti-MEM (Minimal Essential Medium), which is a reduced serum medium without serum and mixed gently. Lipofectamine 2000 was mixed gently before use, then the appropriate amount was diluted in Opti-MEM medium and incubated for 5 min at RT. After the incubation, the diluted DNA was combined with diluted Lipofectamine 2000, mixed gently and incubated for 20 min at RT. Complexes were added to each well containing cells and medium and mixed gently by rocking the plate back and forth. After 5-6 h the

medium was changed to normal growth medium. Cells were incubated at 37°C in a 5 % CO_2 incubator for 24 h.

3.2.8.7 cAMP measurement

The cAMP production of transfected HEK293 in a 96 well plate was measured with the cyclic AMP cell-based assay kit (Cisbioassays) according to the manufacturer's instructions by Serena Cuboni. This kit is based on a competitive immunoassay between native cAMP and cAMP labeled with the acceptor dye d2. Both cAMP variants compete for a cryptate-labeled anti-cAMP antibody, which is detected by fluorescence resonance energy transfer (FRET) that is inversely proportional to the concentration of cAMP in the sample. The fluorescence was measured with Tecan Genios Pro (Tecan).

3.2.8.8 Preparation of hippocampal neuronal cultures

Primary hippocampal cultures were prepared from embryonic day 17-18 mouse brains as recently described (Moller et al.). Hippocampi were digested with 0.25 % trypsin containing 1 mM EDTA for 20 min at 37°C with gentle shaking and grown in Neurobasal A medium supplemented with 2 % B27 and 0,25 % GlutaMAXI (growth medium). Tissue pieces were then washed 3x with DMEM supplemented with 10 % FCS and afterwards dissociated with a fire-polished Pasteur-pipette. Cells were centrifuged at 90x g for 5 min, cell pellet was carefully resuspended in Neurobasal-A medium supplemented with B27, cell number and viability were assessed by counting the number of living cells of a trypan blue stained cell dilution. Neurons were plated at 24 well plates on coverslips (Menzel) coated with 50 µg/ml Poly-D-Lysine (Sigma) and 5 µg/ml Laminin (Invitrogen) at a density of 65000 cells per coverslip.

3.2.8.9 Transfection of primary neurons

Once plated neurons were transfected with expression plasmids at the desired days *in vitro* (DIV) via a modified calcium phosphate protocol (Jiang and Chen, 2006). 1 ml transfection mixtures (5-8 µg plasmid DNA, adjusted with Ampuwa H_2O to 50 µl, 12.5 µl 1 M $CaCl_2$, 50 µl 2x BBS (50 mM BES, 280 mM NaCl, 1.5 mM Na_2HPO_4, pH 7.26) and 900 µl Neurobasal-A medium supplemented with 2 % B27-supplement and 0.5 mM GlutaMAXI) were prepared in sterile 1.5 ml eppendorf tubes. Ampuwa water was mixed with $CaCl_2$ by vortexing at full speed, then plasmid DNA, isolated with MAXI-Preps (Qiagen) and dissolved in Ampuwa

water at a minimal concentration of ≥ 0.5 µg/µl, was added and mixed by pipetting up and down for 10 times. 2x BBS buffer was added drop-wise into the H_2O-$CaCl_2$-DNA mixture during slow vortexing. Neurobasal-A medium, preincubated in the cell culture incubator, was added and the complete transfection mix was vortexed at full speed for 10 seconds and incubated 15 min at RT. The conditioned medium from the neurons was collected and the transfection mix was applied to the neurons for 1 to 4 h depending on the age and density of the neuronal culture and based on the size and appearance of the precipitate formed by the transfection. Neurons were then washed 8 to 12 times with warm HBSS (Hanks´s balanced salt solution) buffer containing 0.01 M HEPES (4-(2-Hydroxyethyl)piperazine-1-ethanesulfonic acid), and the conditioned medium, filled up with new Neurobasal-A medium, was pipetted back onto the neurons. To avoid any damage of the neurons, the time outside of the incubator was minimized during and after transfection. Expression efficiency, usually between 0.5 and 1 % of neurons, was checked 24 h after transfection and was evaluated by expression of fluorescent proteins.

Primary neurons were also transfected with an adapted Lipofectamine protocol. Therefore, 0.5 µl Lipofectamine was mixed with 50 µl growth medium per coverslip and incubated for 5 min. 2 µg DNA/well was mixed with 50 µl growth medium and incubated with the Lipofectamine-growth medium mixture for 20 min. The medium of one well was stored and exchanged with 400 µl of fresh Neurobasal A medium. The conditioned medium was filtrated with a 0,2 µm filter and 20 % fresh Neurobasal A medium was added. After the 20 min incubation the transfection mix was added slowly at the edge and the plate was incubated for 1,5 h at the incubator. Then the transfection mix was exchanged against the prepared conditioned medium.

Primary neurons were also transfected via electroporation according to the protocol provided by the manufacturer (Nepa Gene, Chiba, Japan).

3.2.8.10   Production of lentiviruses

Primary neurons were also transduced by viruses. For transduction with lentiviruses myc-GFP-CRHR1 and myc-GFP-CRHR1-STAVA the respective fragment was cloned with PmeI and SfiI into pSKSP (+)-IRES-GFP (internal ribosome entry site). Annerose Kurz-Drexler (Institute of Developmental Genetics, Helmholtz Center Munich, German Research Center for Environmental Health, Neuherberg, Germany) produced lentiviruses using Lipofectamine as described recently (Glasl et al. 2012). Therefore, HEK293 cells were seeded on 12 x 10 cm plates at 5 x 10^6 cell per plate. The other day cells were transfected with a mixture of Opti-MEM, myc-GFP-CRHR1 or myc-GFP-CRHR1-STAVA and the packaging, expression

regulating and envelope plasmids pMDL, RS.REV and CMV-vsvg (cytomegalovirus-vesicular stomatitis virus). After 5 hours the supernatant was replace with fresh medium. After two days the virus was collected in the supernatant centrifuged at 2000 rpm for 2-3 min and filtered through a 0.22 µm filter. Then the virus was ultracentrifuged for 2 hours at 19400 rpm at 4°C. The resuspended virus was eluted in PBS overnight. The next day the virus was resuspended, ultracentrifuged as the day before and resuspended in PBS-sucrose. After a quick spin the supernatant was stored at – 80°C. For myc-GFP-CRHR1 1.3×10^9 gc/ ml (genome copies/ml) and myc-GFP-CRHR1-STAVA 1×10^9 gc/ ml were achieved.

3.2.8.11   Production of rAAV (adeno-associated virus)

For production of AAV8 for myc-GFP-CRHR1 and myc-GFP-CRHR1-STAVA the respective fragment was cloned with NheI and AscI into pAAV-EF1a-DIO-EYFP-WPRE provided by Karl Deisseroth and Charu Ramakrishnan (Stanford University). This approach allows for Cre recombinase-mediated induction of CRHR1 expression. Stylianos Michalakis (Ludwig-Maximilians-Universität München, Department Pharmazie, Munich, Germany) produced AAV8Y733F-pseudotyped single-strand AAV2 vectors as described recently (Koch et al. 2012). In brief, 293T cells were transfected with the trans plasmids pAdDeltaF6, pAAV2/8Y733F, and a cis plasmid (pAAV-myc-GFP-CRHR1 WT or STAVA) using the calcium phosphate method. rAAV2/8Y7333F particles were harvested after 48 h followed by iodixanol-gradient purification. The 40–60 % iodixanol interface was further purified and concentrated by ion exchange chromatography on a 5 ml HiTrap Q Sepharose column using an ÄKTA Basic FPLC system (GE Healthcare, Munich, Germany) according to previously described procedures, followed by further concentration using Amicon Ultra-4 Centrifugal Filter Units (Millipore, Schwalbach, Germany). Physical titers were determined by quantitative PCR on a LightCycler 480 (Roche Applied Science, Mannheim, Germany) using KAPPA SYBR FAST kit (Peqlab, Erlangen, Germany) and the following primer set: WPREF: 5′-AGT-TGT-GGC-CCG-TTG-TCA-GG-3′ and WPRER: 5′-AGT-TCC-GCC-GTG-GCA-ATA-GG-3′. For myc-GFP-CRHR1 1.2×10^{12} gc/ ml and myc-GFP-CRHR1-STAVA 3×10^{12} gc/ ml were achieved.

3.2.9 Immunocytochemistry

For detection of a protein of interest, immunocytochemistry was carried out as described earlier (Refojo et al. 2011). Briefly, neurons after different days in culture or HEK293 cells

24 h after transfection were fixed with 4 % PFA containing 4 % sucrose for 30 min, washed three times with PBS and permeabilized with 0,1 % Triton X-100 in PBS for 3 × 5 min. After the cells were washed with PBS for 5 min, they were blocked with 0,1 % Triton X-100 in PBS containing 5 % BSA for 1 h and additionally washed two times. Cells were incubated overnight at 4 °C with the respective antibody. Then cells were washed three times with PBS and subsequently incubated with a secondary antibody conjugated with an Alexa-Fluorophore. After secondary antibody treatment cells were washed for 5 min three times, stained with DAPI (4`,6-diamidino-2-phenylindole) (Sigma Aldrich, #D8417, 20 mg/ml, 1:10000) for 5 min and mounted using VectaShield medium (Vector). Labeled cells were imaged by Zeiss AxioCam MRm digital camera adapted to a Zeiss axioplan 2 imaging microscope or laser-scanning confocal microscopy using a 40× and 60× objective with 4 times zoom. Images were subsequently analyzed using Axio Vision 4.5. or FLUOVIEW (FV10-ASW, Version 2.0a), Image J and Adobe Photoshop CS2.

3.2.10 Co-immunoprecipitation

24-48 h post transfection cells seeded onto 6-well plates or 10 cm dishes were washed twice with ice-cold PBS and lysed in lysis buffer supplemented with protease inhibitors (1 tablet complete mini (ROCHE)/ 10 ml) for 1 h on a rocking platform at 4 °C. Lysates were scrape-collected with a cell scraper M (TPP, Trasadingen, Switzerland) and transferred to a 2 ml tube. The lysates were sheared to separate the proteins from the DNA by using syringe tip with Gr. 18 G1/2 and Gr. 25G1 applying each three times per sample. Then, the lysates were centrifuged for 20 min at 40,000 g (19700 rpm for SW55Ti Rotor). Clarified lysates were precleared by incubation with 10 or 15 µl Dynabeads Protein G (#100-04D, Life Technologies) for 30 min that were washed three times with 0.5 ml or 1 ml washing buffer I. After removing the beads similar protein amounts (around 200 µl or 500 µl) assessed in a test Western blot were used for overnight incubation at 4 °C with 0.5 µl of the relevant antibody (0.5 µg - 2 µg antibody/ 1 ml lysate). Lysates with antibody were incubated with pre-equilibrated Protein G Dynabeads for 4 h at 4 °C rotating. The beads were washed with 0.5 ml or 1 ml of washing buffer I for 3 x 10 min and 1 x 10 min with washing buffer II. For elution beads were incubated with 65 µl or 120 µl of 1× Roti-Load (Roth) at 37 °C for 30 min or at 95 °C for 10 min. Preferentially the receptor was only heated to 37°C at this step and directly before loading the gel. Samples were separated by 10 % SDS-PAGE gels and transferred to Immobilon-P PVDF membranes (Millipore) and immunoblotted as indicated in the figures.

3.2.10.1 Western blot

For immunoblotting, protein samples were separated by 10 % SDS-PAGE and transferred to 0.45-µm Immobilon-P PVDF membranes (Millipore). Membranes were blocked in 5 % nonfat milk (Roth) in TBS-Tween 20 0.01 % (Sigma Aldrich) for 1h at RT, followed by incubation with primary antibodies overnight at 4ºC. Membranes were washed 3x 8 min with TBS-T 0.01 % and then incubated with the appropriate secondary horseradish peroxidase-IgG-conjugated antibody for 2 h at RT. After 3x 8 min washing of membranes, signals were revealed by enhanced chemiluminescence (Millipore) and membranes were developed by using ChemiDoc imaging system (Biorad, München).

3.2.10.2 Deglycosylation treatment

The proteins were deglycosylated according the protocol provided by the manufacturer for PNGaseF (NEB, Frankfurt am Main). Therefore, 2 µg protein was heated with 10 x glycoprotein denaturing buffer at 95°C for 10 min and after cooling down incubated with PNGaseF, 10 x G7 reaction buffer, NP40 (10 %) and additionally proteinase inhibitors at 37°C for 1.5 h. The reaction was stopped by adding Rotiload (Roth) and heating again at 95°C for 10 min.

3.2.11 *In utero* intraventricular injection and electroporation

For in vivo expression of CRHR1 Annette Vogl and Anna Möbus (Max Planck Institute of Psychiatry, Munich, Germany) injected expression plasmids for WT and mutant CRHR1 *in utero* and electroporated the plasmid according to the following protocol: Timed pregnant female CD1 mice were anesthetized via i.p. (intraperitoneal) injection with a mixture of ketamine (100 mg/kg body weight) and xylazine (10 mg/kg body weight). The eyes of the pregnant dam were protected from drying during the surgery by a drop of eye cream (Bepanthen eye and nose cream). After shaving, the abdomen was cleaned with 70 % ethanol and 3 cm long midline laparotomy was performed. The uterine horns were carefully exposed, placed on sterile gauze and hydrated with saline (0.9 % NaCl solution), prewarmed to 37ºC. 1-2 µl of high concentrated expression plasmids (2-4 µg/µl), mixed with fast green dye (for visualization of the injection), were microinjected into the lateral ventricle of E13.5-E14.5 mouse embryos using a glass micropipet and plunger (Drummond PCR micropipets, 1-10 µl). After DNA injection, electroporations were performed using an Electro Square Porator ECM830 and tweezertrodes (BTX Genetronics). Five pulses with 40V, 50 ms

duration and with 950 ms intervals, were delivered to each embryo. The developing cortex or hippocampus was targeted by electroporations with 7-mm diameter tweezertrodes (BTX Genetronics) as described in (Nakahira and Yuasa 2005). After the embryos had been injected and electroporated, the uterine horns were placed back in the abdominal cavity and antibiotic/antimitotic solution (100x stock solution, Invitrogen), diluted 1:100 in saline, was administered to reduce the chance of infection. The abdominal wall and skin were sewed up with surgical sutures (Johnson & Johnson), and 7.5 % povidone-idonine solution (Braunol) was applied to the abdominal skin around the sutures. For pain management, Metacam (1 mg/kg body weight), diluted in saline, was injected subcutaneously in the neck after surgery and again 18 to 24 h later. The pregnant mouse was allowed to recover from the anesthesia on a heating plate at 30 ºC. Then it was placed back into a new clean cage. The embryos were allowed to develop up to two month after birth (Noctor et al. 2001, Saito and Nakatsuji 2001, Tabata and Nakajima 2001).

3.2.12 Preparation of brain slices

Electroporated and stereotactically injected animals were sacrificed by an overdose of with isoflurane (Forene®, Abbott) and transcardially perfused with a peristaltic pump for 1 min with PBS, 5 min with 4 % PFA (w/v) in PBS, pH7.4, and 1 min with PBS at a flow of 10 ml/min. Brains were removed, post-fixed for 1 or 2 days in 4 % PFA at 4ºC, washed three times with PBS and cryoprotected in 15 % (w/v) Saccharose in PBS, pH7.6 o.n. at 4 ºC. Brains were embedded in warm 4 % (w/v) agarose (Invitrogen) in PBS for vibratome-sections (MICROM HM 650V, ThermoScientific). 50 µm thick vibratome-sections were stored at -20 ºC in cryopreservation solution (25 % (v/v) glycerol, 25 % (v/v) Ethylenglycol, 50 % (v/v) PBS, pH 7.4) until immunohistochemistry, DAPI staining and mounting.

3.2.13 Immunohistochemistry

Brain sections were washed 2 x 5 min with PBS and again incubated for 10 min in 4 % PFA. After washing for 3 x 5 min with PBS and brain sections were blocked with 5 % BSA (w/v) in PBS-TritonX-100 0.3 % for 1 h at room temperature. Then, sections were incubated with primary antibodies diluted in an appropriate concentration in 5 % BSA (w/v) in PBS-TritonX-100 0.01 % overnight at 4 ºC. After washing 3 x 10 min with PBS sections were incubated with secondary antibodies, Alexa dye conjugated antibodies (Invitrogen), diluted 1:1000 in 5 % BSA (w/v) in PBS-TritonX- 100 0.01 % for 1-2 h at RT. Brain sections were washed 3 x

10 min with PBS, stained with DAPI (1:10000 in H_2O), washed again with PBS and mounted on super frost plus slides (Menzel) with anti-fading fluorescence VectaShield medium (Vector).

4 Results

To unravel the molecular components of corticotropin-releasing hormone receptor 1 (CRHR1) signaling, candidate interaction partners were identified in a previous yeast two-hybrid (Y2H) screen by using the C-terminal cytoplasmic tail of CRHR1 including the amino acids 368-415 as a bait (Engeholm 2004). Interestingly, several positive clones were identified, which belong to the family of membrane-associated guanylate kinases (MAGUKs) including: postsynaptic density protein 95 (PSD95), synapse-associated protein 97 (SAP97), SAP102 and membrane-associated guanylate kinase, WW and PDZ domain containing 2 (MAGI2). In collaboration with Tamas Rasko and Erich Wanker (Max Delbrück Center for Molecular Medicine, Proteomics and Molecular Mechanisms of Neurodegenerative Diseases, Berlin) a second high-throughput Y2H screen verified PSD95 and found the C-terminus binding protein β-arrestin 1 as an anticipated interactor highlighting the specificity of the method. Furthermore, this screen identified also transmembrane protein 106B (TMEM106B) and syndecan binding protein 1 (Syntenin-1) as positive clones. In the further studies PSD93 was included because of its affiliation to the PSD95 subfamily of MAGUKs. In the following, the interaction of CRHR1 with candidate interaction partners was investigated by co-expression analysis in human embryonic kidney 293 cells (HEK293), in the adult mouse brain and in primary cultured neurons.

4.1 *In vitro* investigation of the interaction of CRHR1 with the candidate proteins

In a first step to verify the candidate interaction partners, the proteins and their mutant variants were co-transfected together with CRHR1 into HEK293 cells. The interaction was examined by co-immunoprecipitation (Co-IP) studies to confirm the identified candidate proteins of the Y2H screen in a mammalian cell line with an independent method. The mutant variants additionally revealed the domains important for the interaction. Afterwards, the PDZ binding motif-dependent interaction was elucidated by co-localization studies to uncover the impact of this motif.

4.1.1 Biochemical analysis of CRHR1

To investigate the interaction by Co-IP, first, the method for detection of CRHR1 by Western blot (WB) was established. For the IP, magnetic beads covered with Protein G, which detect

the Fc region of IgG were used. The protein elution from magnetic beads after immunoprecipitation (IP) had to be adjusted to improve CRHR1 detection.

The transmembrane CRHR1 appeared as two distinct bands when homogenates of transiently transfected HEK293 cells were analyzed by WB. The band at ~75 kDa resembles the calculated weight of the myc-GFP-CRHR1 fusion protein of 75.8 kDa (Figure 5). In comparison to this monomeric form there were always high molecular weight complexes (HMWCs) detected at around 170 kDa (Figure 5). The CRHR1 monomer was best observed when the lysate was treated at room temperature (RT) and not boiled at 95 °C.
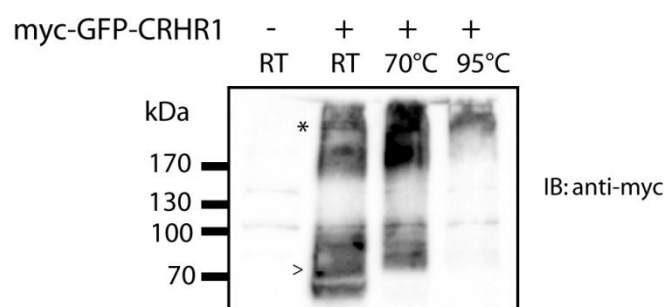
Figure 5: Separation characteristics of CRHR1 are temperature-dependent.
myc-GFP-CRHR1 was transiently transfected in HEK293 cells as indicated and the lysates were incubated for ten minutes with different temperatures in a reducing agents containing buffer. Samples were run on SDS-PAGE and immunoblotted (IB) with anti-myc. The anti-myc antibody detected high molecular weight complexes (*) and the monomer (>). RT, room temperature.

Different to the direct detection in the lysate, the CRHR1 monomer was also visible after an elution at 95 °C, when CRHR1 was previously immunoprecipitated. To validate the two distinct CRHR1 bands, the receptor was deglycosylated with PNGase F. The deglycosylation resulted in a shift of the bands of approximately 15 kDa but did not resolve the CRHR1 HMWCs (Figure 6).

The identity of the CRHR1 bands was confirmed, since it is known that CRHR1 dimerization does not depend on ligand binding, and it can even oligomerize under denaturing conditions using standard SDS-PAGE electrophoresis (Kraetke et al. 2005, Zmijewski and Slominski 2009). Moreover, Alken et colleagues revealed that CRHR1 oligomers show a similar shift in size after deglycosylation (Alken et al. 2005).
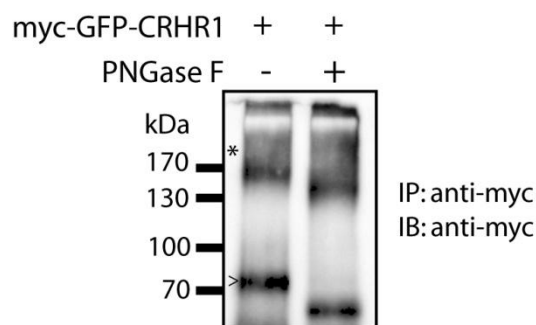
Figure 6: CRHR1 is highly glycosylated.
myc-GFP-CRHR1 was transiently transfected in HEK293 cells as indicated and treated for 1.5 h with PNGase F following immunoprecipitation (IP) with anti-myc and elution at 95 °C. After heating for 10 min at 95°C samples were run on SDS-PAGE and immunoblotted (IB) with anti-myc. CRHR1 was detected as high molecular weight complexes (*) and as a monomer (>).

4.1.2 Establishing the detection of CRHR1 monomers

Partly in opposition to Figure 6 it was later not possible to detect the CRHR1 monomer following IP and elution from magnetic beads at 95°C. Therefore, different conditions were tested for the elution of the proteins from the magnetic beads covered with Protein G while still using the denaturing loading buffer. The proteins were eluted by acetic acid with pH 2.8 for 2 and 20 min at RT or by 0.1 M citrate with pH 3.1 for 2 min at RT without subsequent heating. These low pH elutions did not result in detectable protein amounts (data not shown). CRHR1 was also eluted by different temperature treatments. The elution at 37 °C for 30 min resulted in similar protein amounts as the elution at RT following overnight incubation (Figure 7).
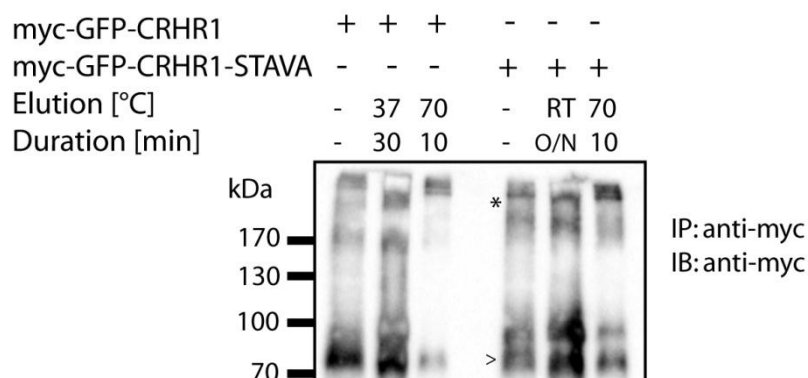
Figure 7: Evaluation of elution conditions for CRHR1 following immunoprecipitation (IP).
myc-GFP-CRHR1 was transiently transfected in HEK293 cells as indicated and immunoprecipitated with anti-myc. For elution different conditions were tested. Samples were run on SDS-PAGE and immunoblotted (IB) with anti-myc. CRHR1 was detected as high molecular weight complexes (*) and as a monomer (>). RT, room temperature.

This low temperature elution was more effective in comparison to elution at 70 °C for 10 min especially with regards to the CRHR1 monomer. The antibody against myc detected for the CRHR1-STAVA mutant similar separation characteristics. Consequently, the IP elution was in the following performed at 37 °C for 30 min and the samples were handled for 10 min at RT before the Western blot.

4.1.3 CRHR1 interacts with PSD95 via the PDZ binding motif

In order to confirm the candidate interaction partners PSD95, SAP97, SAP102, MAGI2, Syntenin-1 and TMEM106B identified in the yeast two-hybrid screen, the proteins were co-transfected with CRHR1 transiently in HEK293, and co-immunoprecipitation studies were executed to test the binding capabilities.

The analysis of the murine and human CRHR1 amino acid sequences S^{412}-T^{413}-A^{414}-V^{415} at the C-terminus revealed a C-terminal class I PDZ (PSD95/discs large 1/zona occludens 1) -binding motif that in general has the consensus sequence S/T-X-Φ, where Φ represents a bulky hydrophobic residue. For the validation and detailed characterization of the interplay with potential interactors, C-terminal CRHR1 mutants with a functionally disrupted PDZ binding motif were generated. Interactions were probed by co-immunoprecipitation (Co-IP) using lysates of HEK293 cells transiently co-transfected with CRHR1 and MAGUK variants. First, the capacity of mutant CRHR1 variants to co-immunoprecipitate PSD95 PDZ1-3 were tested (Figure 8A, lanes 2–5), which was originally identified in the Y2H screen and comprises the three PDZ domains and the SH3 domain of PSD95. PSD95 PDZ1-3 was readily co-immunoprecipitated with wild-type (WT) CRHR1 (Figure 8A, lane 1). Moreover, the CRHR1-STAVA mutant, which contains an additional alanine at the C-terminus, most efficiently disrupted the interaction of CRHR1 with PSD95 PDZ1-3 (Figure 8A, lane 5). Another advantage of this particular mutant compared, for example, to the deletion of the entire PDZ binding motif is the fact that it does not interfere with S^{412} and T^{413}, which are potential GRK or PKC phosphorylation sites (Hauger et al. 2009). Thus, the CRHR1-STAVA mutant was used in subsequent experiments in addition to the wild-type receptor to further characterize the interaction of CRHR1 with MAGUKs.
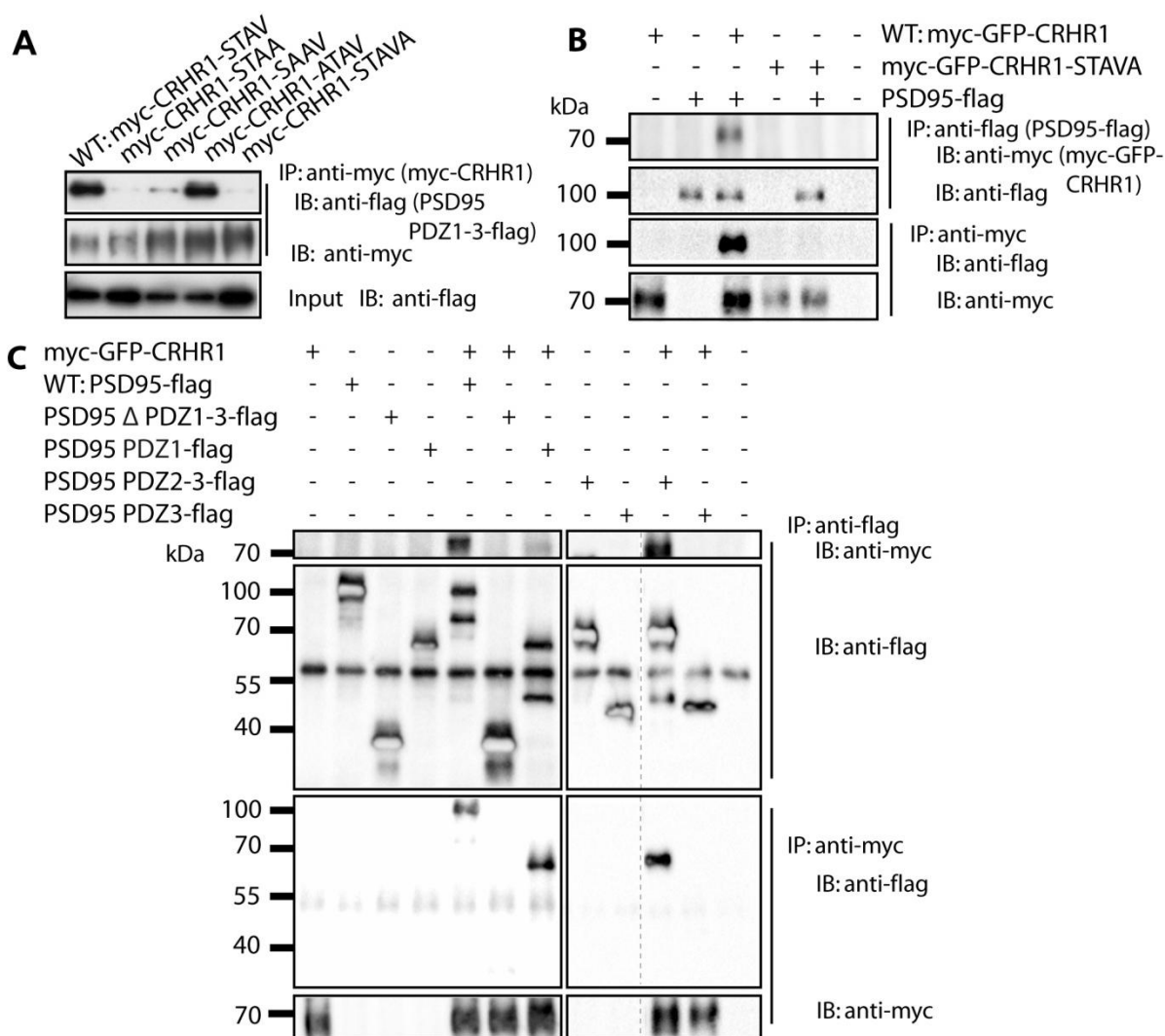
Figure 8: CRHR1 interacts with PSD95 via the PDZ binding motif and PDZ1 and PDZ2.
Co-immunoprecipitations (Co-IPs) were performed using lysates of HEK293 cells transiently transfected as indicated. (**A**) PSD95 PDZ1-3-flag was co-immunoprecipitated with wild-type myc-CRHR1-STAV and to variable degrees with myc-CRHR1-STAA, myc-CRHR1-SAAV, and myc-CRHR1-ATAV but not with the myc-CRHR1-STAVA mutant (This particular experiment was executed by Maik Engeholm (Engeholm 2004)). (**B**) myc-GFP-CRHR1 was co-immunoprecipitated with PSD95-flag but not myc-GFP-CRHR1-STAVA, which has a disrupted PDZ binding motif. Accordingly, PSD95-flag was co-immunoprecipitated with myc-GFP-CRHR1 but not with myc-GFP-CRHR1-STAVA. (**C**) myc-GFP-CRHR1 was co-immunoprecipitated with the PSD95 mutants PSD95 PDZ1-flag, PSD95 PDZ2-3-flag, but not with PSD95Δ PDZ1-3-flag or PSD95 PDZ3-flag. Complementary results were obtained when the Co-IP was performed against myc-GFP-CRHR1. Samples were run on SDS-PAGE and immunoblotted (IB) with anti-myc or anti-flag. The IP and IB with the same antibody respectively showed similar expression levels of the proteins. Dashed lines indicate that the samples were run on the same immunoblot (IB), however, not in adjacent lanes. Continuous lines separate different IBs from the same experiment. The ~55 kDa band in the anti-flag IB represents the heavy chain of the primary antibody. IP, immunoprecipitation.

For the candidate protein PSD95, Co-IPs were performed also with the full length version indicating that CRHR1 interacted also with native PSD95 (Figure 8B, lane 3). Co-IPs

succeeded in both directions; i.e., PSD95 was detected in the Western blot (WB) following immunoprecipitation (IP) against CRHR1, and CRHR1 was detected in the WB following an IP against PSD95. However, the CRHR1-STAVA mutant carrying a functionally impaired PDZ binding motif did not interact with PSD95 (Figure 8B, lane 5), verifying the importance of the PDZ binding motif of CRHR1 in the interaction with PSD95. The members of the PSD95 subfamily of MAGUKs comprise three PDZ domains and each of them interacts specifically with the C-terminus of different membrane receptors and adhesion proteins (Zheng et al. 2011). Therefore, PSD95 mutants were investigated to further specify the PDZ domains relevant for the interaction with the CRHR1 PDZ binding motif. Co-IPs against CRHR1 and against PSD95 mutants revealed interactions of CRHR1 with PSD95 PDZ1-flag (Figure 8C, lane 7) and PSD95 PDZ2-3-flag (Figure 8C, lane 10). By contrast, no interaction of CRHR1 was detected with PSD95Δ PDZ1-3-flag (Figure 8C, lane 6) or PSD95 PDZ3-flag (Figure 8C, lane 11). These results underline the importance of the PDZ1 and PDZ2 domains of PSD95 for the interaction with CRHR1.

4.1.4 CRHR1 interacts with SAP97 via the PDZ binding motif

For the second candidate MAGUK SAP97, Co-IPs were performed against HA or myc tag using lysates of HEK293 cells transiently transfected. Co-IPs against CRHR1 and SAP97, respectively, disclosed that the full-length HA-SAP97 directly interacted with CRHR1 (Figure 9A, lane 3) but not with myc-GFP-CRHR1-STAVA (Figure 9A, lane 5). Furthermore, SAP97 mutants were studied to specify the PDZ domains relevant for the interaction with the CRHR1 PDZ binding motif. Co-IPs further revealed that the mutants HA-SAP97 PDZ1-3 (Figure 9B, lane 5) and HA-SAP97 PDZ1-2 (Figure 9B, lane 7) interacted with CRHR1. However, no interaction was detected with HA-SAP97 PDZ1 (Figure 9B, lane 9). This result indicates that CRHR1 interacts via its PDZ binding motif with PDZ2 and probably also with PDZ3 of SAP97.

As shown in these IPs, CRHR1 was detected in the immunoblot (IB) as HMWCs (*) and as a monomer (>). Consequently, the HMWCs are also displayed in the following IBs.
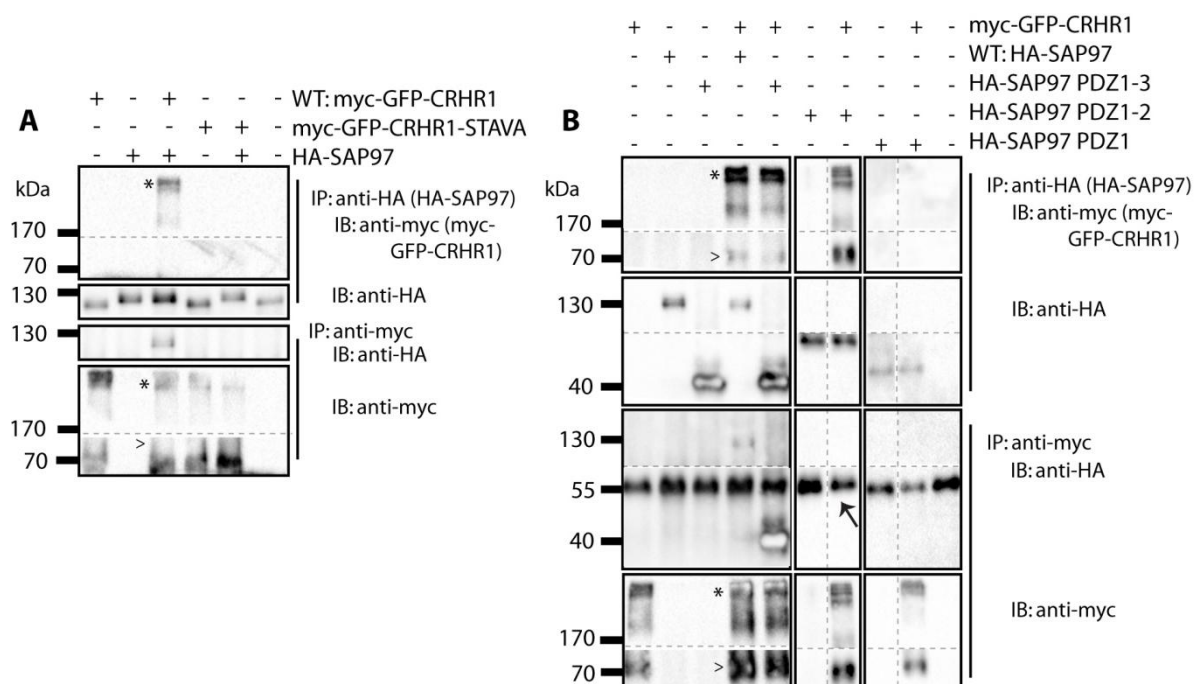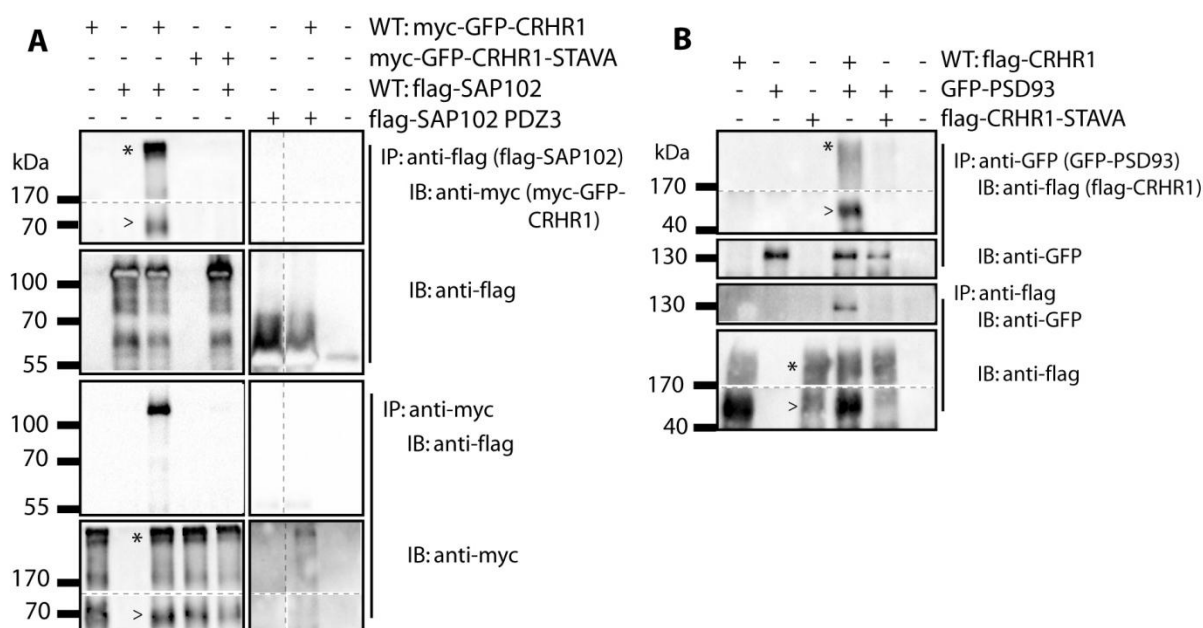
Figure 9: CRHR1 interacts with SAP97 via the PDZ binding motif.
Co-immunoprecipitations (Co-IPs) were performed using lysates of HEK293 cells transiently transfected as indicated. myc-GFP-CRHR1 was co-immunoprecipitated with HA-SAP97 (**A**) but not myc-GFP-CRHR1-STAVA, which has a functionally inactive PDZ binding motif, and similarly, HA-SAP97 was co-immunoprecipitated with myc-GFP-CRHR1 but not with myc-GFP-CRHR1-STAVA. The ~100 kDa band in lanes 1, 4 and 6 of the anti-HA IB is an unspecific band. (**B**) The receptor interacted with HA-SAP97 PDZ1-3, HA-SAP97 PDZ1-2, and accordingly, these SAP97 variants were co-immunoprecipitated with myc-GFP-CRHR1 using an anti-myc antibody in the Co-IP. No interaction was observed for HA-SAP97 PDZ1. The signal for the IP of HA-SAP97 PDZ1 after the IP with anti-myc is not distinguishable from the signal of the heavy chain of the anti-myc antibody, which has the same protein size of ~55 kDa (→). CRHR1 was detected as high molecular weight complexes (*) and as a monomer (>). Samples were separated by SDS-PAGE and immunoblotted (IB) with anti-myc or anti-HA antibodies. The IP and IB with the same antibody showed similar expression levels of the proteins. Dashed lines indicate that the samples were run on the same IB, however, not in adjacent lanes. Continuous lines separate different IBs from the same experiment. IP, immunoprecipitation.

4.1.5 CRHR1 interacts with SAP102 via the PDZ binding motif

Co-IPs against CRHR1 and SAP102 revealed an interaction in both directions proving SAP102 as an interaction partner (Figure 10A, lane 3). The interaction was mediated by the PDZ binding motif of CRHR1 (Figure 10A, lane 5). The mutant SAP102 PDZ3-flag did not interact with CRHR1 in any direction (Figure 10A, lane 7) confirming that at least one of the first two PDZ domains of SAP102 or both are important for the interaction with CRHR1.

Figure 10: CRHR1 interacts with SAP102 and with PSD93 via the PDZ binding motif.
Co-immunoprecipitations (Co-IPs) were performed using lysates of HEK293 cells transiently transfected as indicated. (**A**) myc-GFP-CRHR1 but not myc-GFP-CRHR1-STAVA, which has a disrupted PDZ binding motif, co-immunoprecipitated with flag-SAP102 but not with flag-SAP102 PDZ3. Complementary results were obtained when the Co-IP was executed against myc-GFP-CRHR1. (**B**) flag-CRHR1 but not flag-CRHR1-STAVA was co-immunoprecipitated with GFP-PSD93 and accordingly, GFP-PSD93 was co-immunoprecipitated with flag-CRHR1 but not with flag-CRHR1-STAVA. CRHR1 was detected as high molecular weight complexes (*) and as a monomer (>). Samples were separated by SDS-PAGE and immunoblotted (IB) with anti-myc, anti-GFP or anti-flag antibodies. The IP and IB with the same antibody showed similar expression levels of the proteins. Dashed lines indicate that the samples were run on the same IB, however, not in adjacent lanes. Continuous lines separate different IBs from the same experiment. The ~55 kDa band in the IB of anti-myc is the heavy chain of the antibody. IP, immunoprecipitation.

4.1.6   CRHR1 interacts with PSD93 via the PDZ binding motif

PSD93 was included in further studies because of its high homology to the other members of the PSD95 subfamily of MAGUKs identified in the Y2H screen. The candidate MAGUK PSD93 was successfully verified as interaction partner of CRHR1. CRHR1 was co-immunoprecipitated with PSD93 and similarly, PSD93 was co-immunoprecipitated with CRHR1 (Figure 10B, lane 4). Furthermore, the interaction depended on the PDZ binding motif because the mutant CRHR1-STAVA, which has a disrupted PDZ binding motif, did not interact with PSD93 and correspondingly, PSD93 did not interact with the mutant (Figure 10B, lane 5).

4.1.7 CRHR1 interacts with MAGI2 via the PDZ binding motif

The candidate interaction partner MAGI2 belongs to the MAGUKs but contains six PDZ domains. The verification of the interaction via Co-IP revealed that CRHR1 indeed co-immunoprecipitated with MAGI2 (Figure 11B, lane 4). Accordingly, MAGI2 was co-immunoprecipitated with CRHR1. The interaction depended on the PDZ binding motif of CRHR1 because CRHR1-STAVA did not interact with MAGI2 (Figure 11B, lane 5).
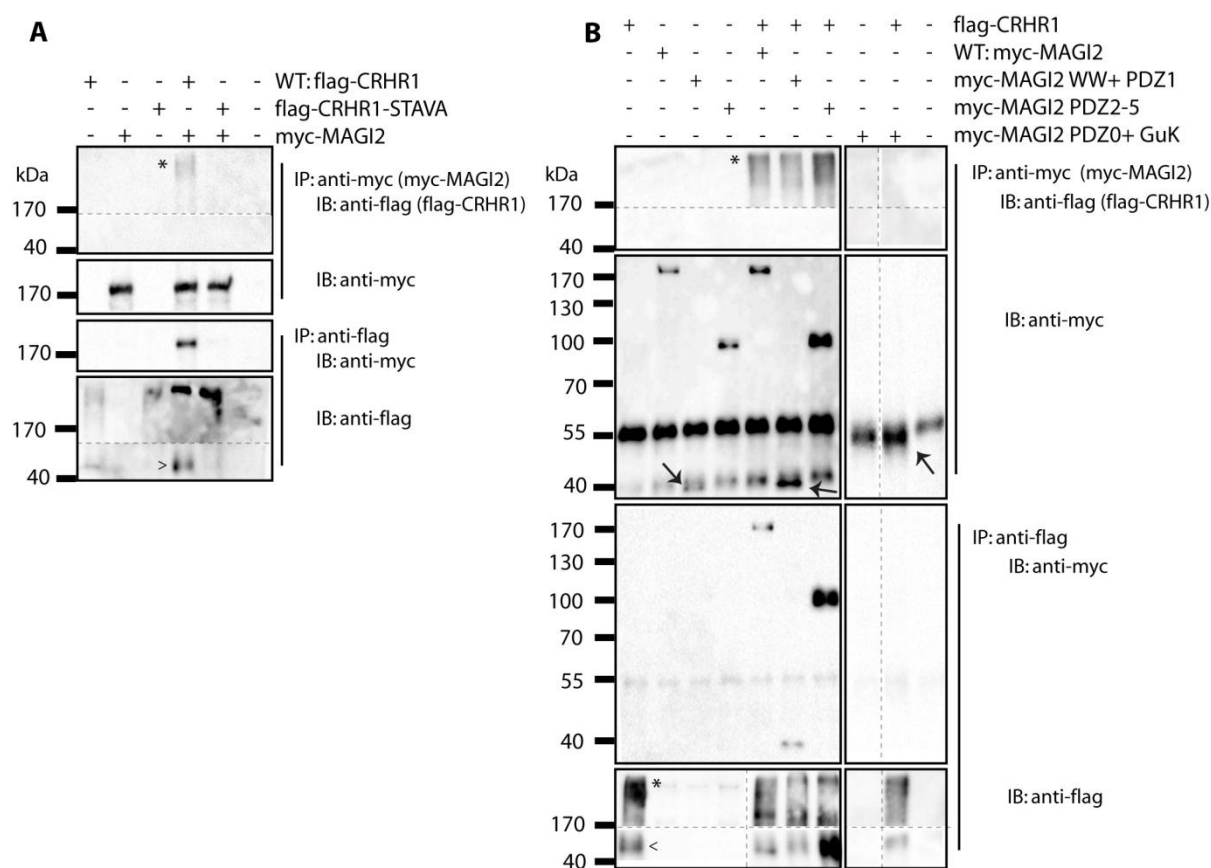
Figure 11: CRHR1 interacts with MAGI2 via the PDZ binding motif.
(**A**) flag-CRHR1 but not flag-CRHR1-STAVA interacted with myc-MAGI2, and myc-MAGI2 was co-immunoprecipitated with flag-CRHR1 but not with flag-CRHR1-STAVA. (**B**) flag-CRHR1 was co-immunoprecipitated with myc-MAGI2, myc-MAGI2 WW + PDZ1, and myc-MAGI2 PDZ2-5 but not with myc-MAGI2 PDZ0 + GuK. Co-IPs were also successful in the other direction. The bands for the mutants of MAGI2 in the control blot are highlighted when necessary (→). CRHR1 was detected as high molecular weight complexes (*) and as a monomer (>). Samples were separated by SDS-PAGE and immunoblotted (IB) with anti-myc or anti-flag antibodies. The IP and IB with the same antibody showed similar expression levels of the proteins. Dashed lines indicate that the samples were run on the same IB, however, not in adjacent lanes. Continuous lines separate different IBs from the same experiment. The ~55 kDa band in the IB of anti-myc is the heavy chain of the antibody. IP, immunoprecipitation.

To determine the important interaction domains of MAGI2, Co-IPs with different mutants of MAGI2 were conducted. The Co-IP of myc-MAGI2 WW + PDZ1 and myc-MAGI2 PDZ2-5 co-immunoprecipitated CRHR1 (Figure 11C, lane 6, 7) but CRHR1 was not co-immunoprecipitated with myc-MAGI2 PDZ0 + GuK (Figure 11C, lane 9). Complementary results were obtained when the Co-IP was performed against flag-CRHR1. These findings indicated that all or at least some of the PDZ 1-5 domains of MAGI2 are responsible for the interaction with CRHR1.

4.1.8 CRHR1 does not interact with Syntenin-1

Syntenin-1 contains two PDZ domains but did not co-immunoprecipitate with CRHR1 and similarly, CRHR1 did also not interact with Syntenin-1 (Figure 12). This result underscores the specificity of the detected interactions of CRHR1 with the MAGUKs. The interaction did also not occur when the cells were treated with the ligand corticotropin-releasing hormone (CRH) to stimulate CRHR1. Hence, this candidate partner was not further investigated.
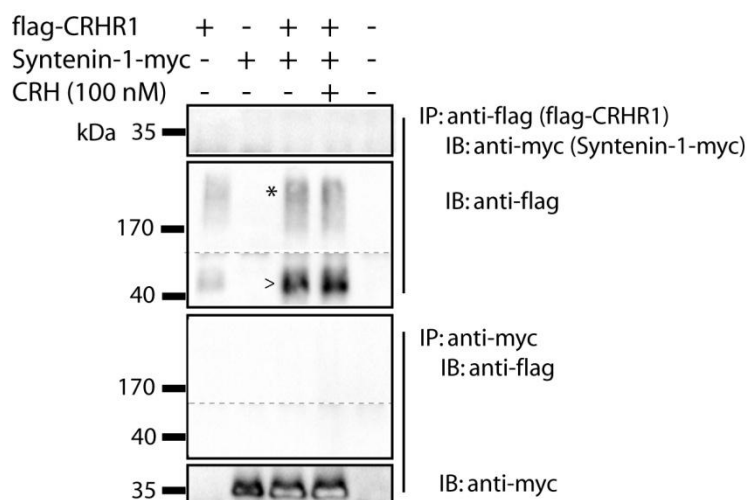
Figure 12: CRHR1 does not interact with Syntenin-1.
Co-immunoprecipitations (Co-IPs) were performed using lysates of HEK293 cells transiently transfected as indicated. flag-CRHR1 did not co-immunoprecipitate with Syntenin-1-myc and accordingly, Syntenin-1-myc did not co-immunoprecipitate with flag-CRHR1. Corticotropin-releasing hormone (CRH) treatment was conducted for 30 min. CRHR1 was detected as high molecular weight complexes (*) and as a monomer (>). Samples were separated by SDS-PAGE and immunoblotted (IB) with anti-myc or anti-flag antibodies. The IP and IB with the same antibody respectively showed similar expression levels of the proteins. Dashed lines indicate that the samples were run on the same IB, however, not in adjacent lanes. Continuous lines separate different IBs from the same experiment. IP, immunoprecipitation.

4.1.9 The interaction of CRHR1 with TMEM106B is unspecific

The candidate interaction partner TMEM106B was co-immunoprecipitated with CRHR1 (Figure 13A, lane 5). The CRHR1-STAVA mutant indicated an unspecific interaction because the Co-IP was also successful without a functional PDZ binding motif (data not shown).
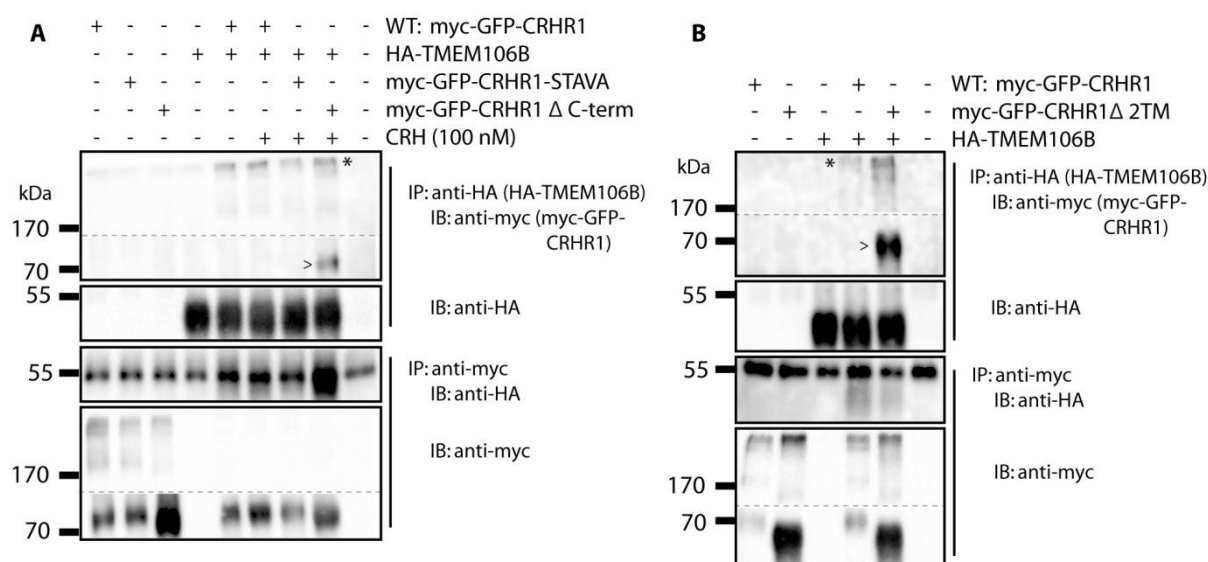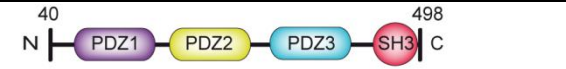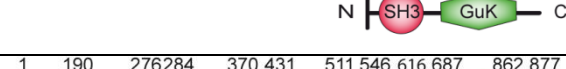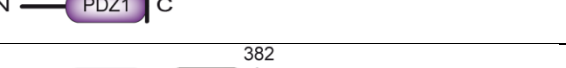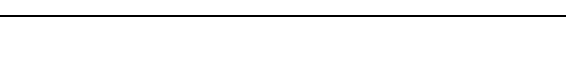

Figure 13: CRHR1 unspecifically interacts with TMEM106B.
Co-immunoprecipitations (Co-IPs) were performed using lysates of HEK293 cells transiently transfected as indicated. (**A**) myc-GFP-CRHR1, myc-GFP-CRHR1-STAVA and myc-GFP-CRHR1Δ C-term were co-immunoprecipitated with HA-TMEM106B after corticotropin-releasing hormone (CRH) treatment for 30 min. Co-IPs were also successful in the other direction. (**B**) HA-TMEM106B was co-immunoprecipitated with myc-GFP-CRHR1Δ 2TM. CRHR1 was detected as high molecular weight complexes (*) and as a monomer (>). Samples were separated by SDS-PAGE and immunoblotted (IB) with anti-myc or anti-flag antibodies. The IP and IB with the same antibody respectively showed similar expression levels of the proteins. Dashed lines indicate that the samples were run on the same IB, however, not in adjacent lanes. Continuous lines separate different IBs from the same experiment. The ~55 kDa band in the IB of anti-HA is the heavy chain of the antibody. IP, immunoprecipitation.

This experiment was repeated using CRH treatment but this did not change the fact that CRHR1-STAVA was co-immunoprecipitated with TMEM106B (Figure 13A, lane 7). Neither did the CRH activation affect the interaction of WT CRHR1 with TMEM106B (Figure 13A, lane 6). Furthermore, also the Co-IP of TMEM106B with the mutants CRHR1Δ C-term (Figure 13A, lane 8) and CRHR1Δ 2TM missing the C-terminal portion including the two last transmembrane domains were effective (Figure 13B, lane 5). This indicates that neither the PDZ binding motif nor the C-terminus of CRHR1 is important for the unspecific interaction with TMEM106B. This result suggests that TMEM106B does not interact specifically with CRHR1 but rather via unknown interacting regions, i.e. hydrophobic transmembrane regions of the proteins. Therefore, TMEM106B was not further investigated as a candidate protein.

4.1.10 Summary of co-immunoprecipitation experiments

Altogether, the co-immunoprecipitation experiments show that the C-terminal PDZ binding motif of CRHR1 is mediating the interaction with PDZ domain containing MAGUKs. In addition, different PDZ domains of the interacting MAGUKs are responsible for the interaction (Table 16). Moreover, the PDZ binding motif of CRHR1 interacts specifically with different PDZ domains of the examined MAGUKs, e.g. with the first PDZ domain of PSD95 but not with the PDZ domains of Syntenin-1.

Interacting protein	Structure	CRHR1	CRHR1-STAVA
PSD95		interaction	no interaction
PSD95 PDZ1-3		interaction	no interaction
PSD95 PDZ1		interaction	not analyzed
PSD95 PDZ2-3		interaction	not analyzed
PSD95 PDZ3		no interaction	not analyzed
PSD95 ΔPDZ1-3		no interaction	not analyzed
SAP97		interaction	no interaction
SAP97 PDZ1		no interaction	not analyzed
SAP97 PDZ1-2		interaction	not analyzed
SAP97 PDZ1-3		interaction	not analyzed
SAP102		interaction	no interaction
SAP102 PDZ3		no interaction	not analyzed
PSD93		interaction	no interaction
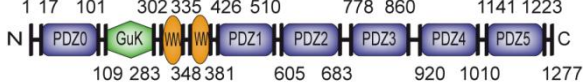
Interacting protein	Structure	CRHR1	CRHR1-STAVA
MAGI2	PDZ0 – GuK – WW – WW – PDZ1 – PDZ2 – PDZ3 – PDZ4 – PDZ5 (1 17 101 302 335 426 510 778 860 1141 1223 / 109 283 348 381 605 683 920 1010 1277)	interaction	no interaction
MAGI2 PDZ0+GuK	PDZ0 – GuK (283)	no interaction	not analyzed
MAGI2 WW+PDZ1	WW – WW – PDZ1 (295 578)	interaction	not analyzed
MAGI2 PDZ2-5	PDZ2 – PDZ3 – PDZ4 – PDZ5 (573)	interaction	not analyzed
Syntenin-1	PDZ1 – PDZ2 (1 115 194 199 273 299)	no interaction	no interaction
TMEM106B	TMD (1 98 118 275)	interaction	interaction

Table 16: Overview of co-immunoprecipitation experiments.

4.1.11 Clustering of CRHR1 with MAGUKs via the PDZ binding motif

MAGUKs are synaptic scaffolds proteins that are important to assemble receptors, adhesion proteins and intracellular signaling proteins (Kim and Sheng 2004). Along these lines, members of the PSD95 subfamily of the MAGUKs are known for their role in clustering of neuronal ion channels (Hsueh et al. 1997) what can be investigated in cell culture. After validation and characterization of the interaction with identified MAGUKs, the next step was to study the functional relevance of this interaction in terms of clustering activity. To examine the clustering activity of CRHR1 with the validated MAGUKs, HEK293 cells were co-transfected with CRHR1 and the MAGUKs. The localization of proteins was then determined by immunofluorescence microscopy.

When expressed alone, CRHR1 and the mutant CRHR1-STAVA showed a distribution at the cell membrane in HEK293 cells (Figure 14A, G). Transiently transfected PSD95, SAP97, SAP102 PSD93, and MAGI2 appeared with a diffuse cytosolic localization (Figure 14, first row). But when CRHR1 was co-expressed with respective MAGUKs, the proteins were redistributed and localized into clusters (Figure 14B-F). In contrast, when CRHR1-STAVA was co-expressed with respective MAGUKs, there was no altered distribution and the proteins were located as expressed individually (Figure 14H-L). This effect on the localization

of CRHR1 and interacting MGAUKs clearly depended on an intact PDZ binding motif what demonstrates the functional relevance of this motif.
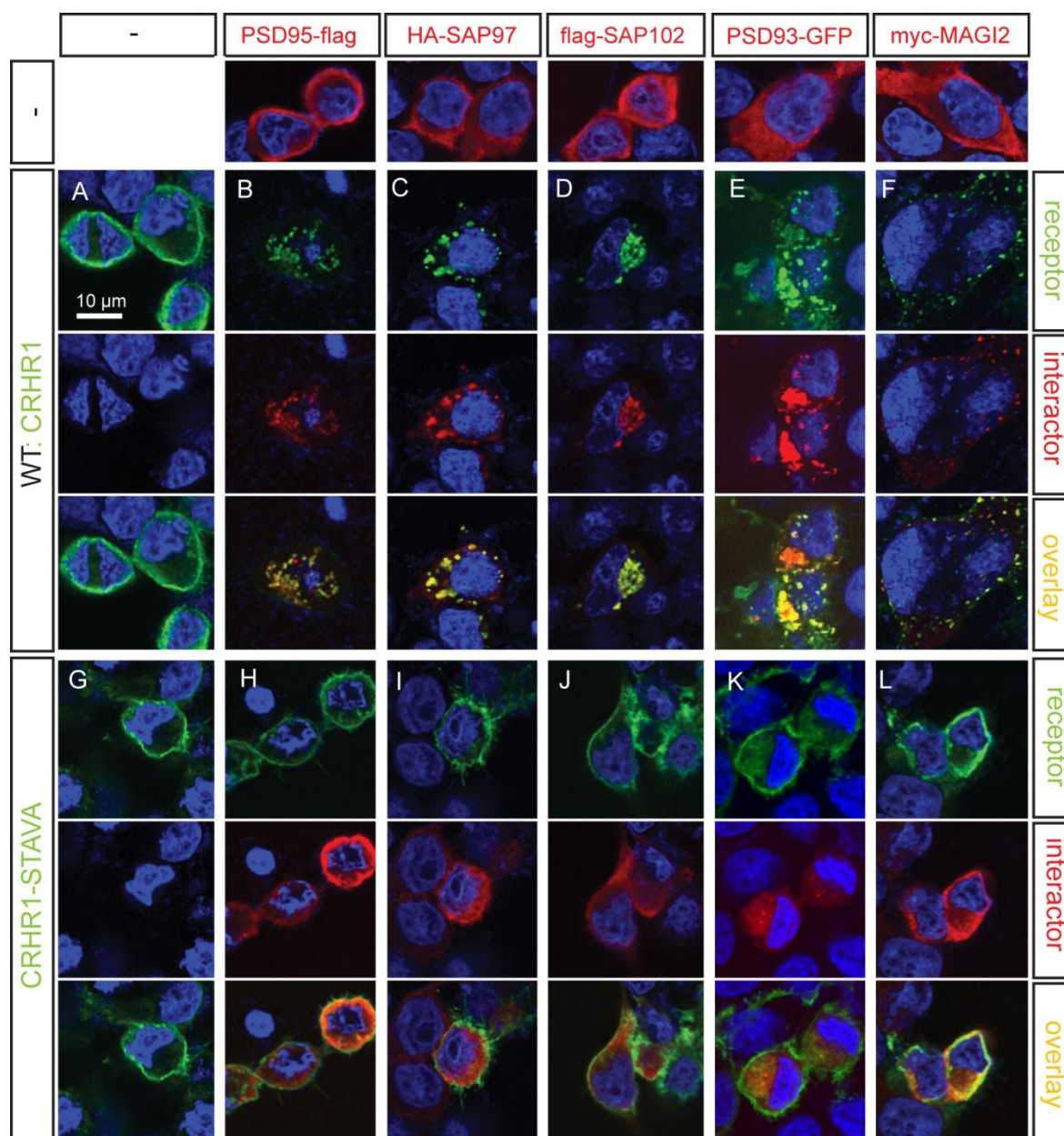

Figure 14: Clustering of CRHR1 with MAGUKs depends on the PDZ binding motif.
HEK293 cells were transiently transfected with expression vectors for WT CRHR1, CRHR1-STAVA or the interacting MAGUKs, respectively (**A, G, first row**). Co-transfection of WT (**B-F**) or mutant of CRHR1 (**H-L**) together with PSD95-flag (**B, H**), HA-SAP97 (**C, I**), flag-SAP102 (**D, J**) PSD93-GFP (**E, K**) or myc-MAGI2 (**F, L**) were performed. When CRHR1 was co-transfected with individual MAGUKs, they co-localized in clusters (**B-F**). But when the CRHR1-STAVA mutant was co-transfected with interacting MAGUKs, clustering was not observed (**H-L**), what underscores the importance of the PDZ binding motif STAV. Immunostaining was executed against the HA tag for HA-CRHR1 or HA-CRHR1-STAVA when co-transfected with PSD95-flag or flag-SAP102. Immunostaining against flag was performed when using flag-CRHR1 or flag-CRHR1-STAVA co-transfected with PSD93-GFP, HA-SAP97 or myc-MAGI2, respectively.

At higher magnification a cell surface and cytosolic clustering of CRHR1 with PSD95, SAP97 and MAGI2 (Figure 15A, B, E) was observed by confocal imaging on the nucleus and the cell surface level respectively (Figure 15F-K). For PSD93 and SAP102 there was only a cytosolic distribution of clusters when co-expressed with CRHR1 (Figure 15C, D). The clusters of CRHR1 co-expressed with the MAGUKs within one cell showed also differences in cluster-size of the related vesicles.

The clustering of CRHR1 with the MAGUKs via the PDZ binding motif *in vitro* independently confirmed the Co-IP experiments. The disruption of the PDZ binding motif of CRHR1 inhibited the interaction and clustering with the MAGUKs.

In summary, the *in vitro* investigation verified some of the candidate CRHR1 interaction partners, in particular the MAGUKs PSD95, SAP97, SAP102, PSD93 and MAGI2. For the interaction different PDZ domains interacted with the PDZ binding motif of CRHR1 resulting in an intracellular and partly membranous clustering.
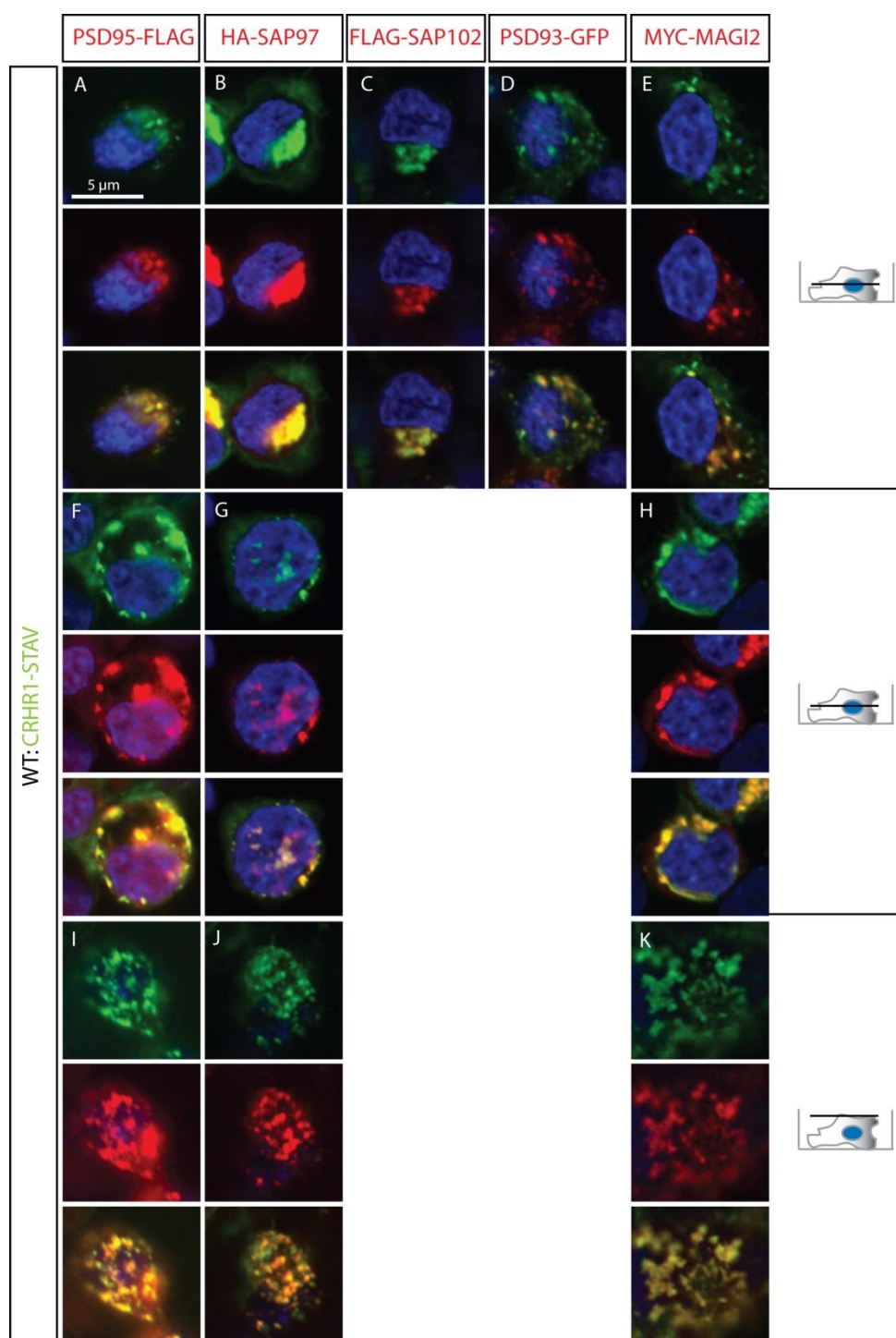
Figure 15: Cell surface and cytosolic clustering of CRHR1 with interacting partners *in vitro*.
CRHR1 was co-transfected with respective interacting partner in HEK293 cells and immunostained as described in Figure 14. CRHR1 clustered with PSD95-flag (**A**), HA-SAP97 (**B**), flag-SAP102 (**C**), PSD93-GFP (**D**), myc-MAGI2 (**E**) within the cytosol. PSD95-flag (**F, I**), HA-SAP97 (**G, J**), myc-MAGI2 (**H, K**) showed also a localization of clusters at the cell surface. The clusters for CRHR1 co-expressed with PSD95-flag (**A**), PSD93-GFP (**D**) and myc-MAGI2 (**E**) consisted of small vesicles whereas the clusters for CRHR1 co-expressed with HA-SAP97 (**B**) and flag-SAP102 (**C**) consisted of large vesicular structures, which often showed a perinuclear localization. At the top and in the middle part confocal images were taken at the level of the nucleus and at the bottom confocal images were taken at the cell surface level of transfected HEK293 cells.

78

4.2 Identification of a physiological relevance of the interaction of CRHR1 with identified MAGUKs

Since CRHR1 interacts with MAGUKs via the C-terminal PDZ binding motif, the next step was to figure out whether the interaction has any physiological implications besides the effect on receptor-MAGUK clustering. To investigate the possible physiological role of the interaction of CRHR1 with the MAGUKs, their expression was assessed by single and double *in situ* hybridization (ISH).

Primary neurons were analyzed with respect to the endogenous CRHR1/CRH system and with respect to their suitability as a primary cell culture system to study its physiology. Due to low endogenous expression of the receptor, it was necessary to overexpress the WT and mutant of myc-GFP-CRHR1. Therefore, different transfection methods were tested with respect to their suitability to overexpress CRHR1 in primary neurons.

4.2.1 CRHR1 is co-expressed with MAGUKs in the adult mouse brain

A prerequisite for the interaction of CRHR1 with identified MAGUKs is their physical co-localization within the same cell. Therefore, the expression of CRHR1 and the interaction partners was analyzed via ISH in the adult mouse brain (Figure 16). Radioactively-labeled riboprobes specifically detecting the murine CRHR1 mRNA and the interaction partners were generated and hybridized to mouse brain sections. In the single ISH the analysis of the mRNA expression of CRHR1 throughout the murine brain showed that CRHR1 was strongly expressed in the olfactory bulb, the cortex, the globus pallidus and the reticular thalamic nucleus (RTN) (Figure 16A). CRHR1 was also strongly expressed in the hippocampus, the magnocellular part of the red nucleus, in the pontine nucleus and the cerebellum. The candidate interaction partners showed also a strong expression in the olfactory bulb, cortex, hippocampus, cerebellum and other brain regions (Figure 16B-F). The comparison based on a false color display revealed a clear co-expression of CRHR1 and the candidate MAGUKs for instance in the olfactory bulb, cortex, hippocampus and the cerebellum (Figure 16B-F).
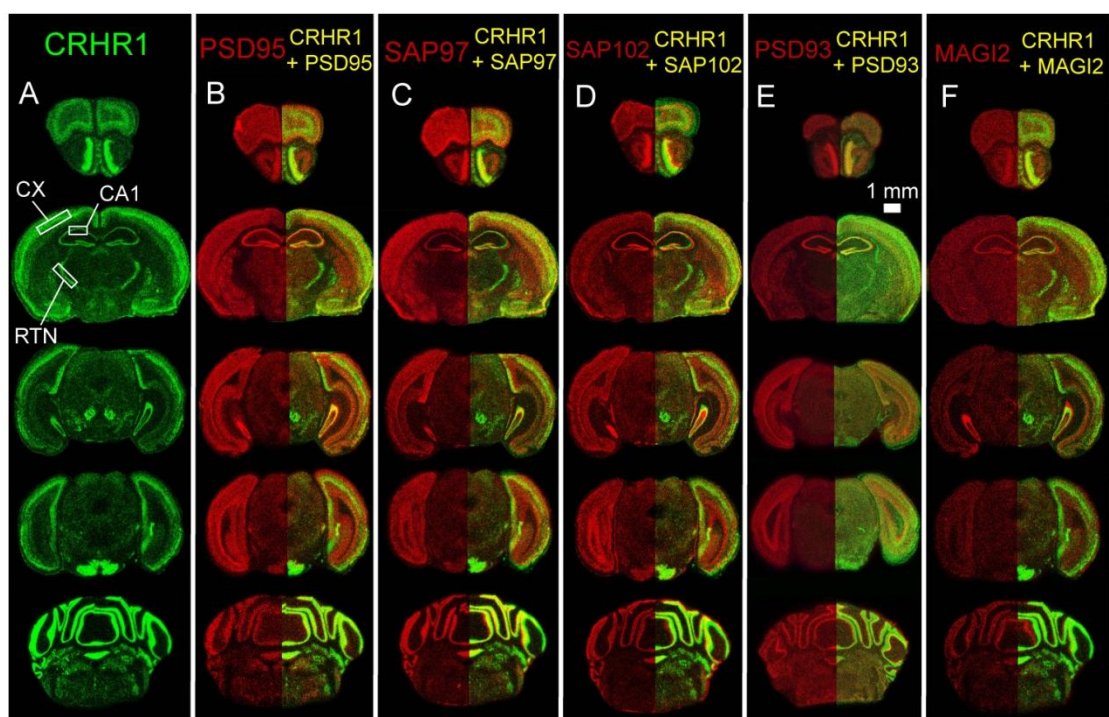
Figure 16: CRHR1 and candidate MAGUKs are co-expressed of the adult mouse brain.
Expression of CRHR1 and the candidate proteins was assessed by single *in situ* hybridization (**A-F**) in the adult mouse brain. (**A-F**) For comparison, representative photomicrographs of autoradiographs are shown in a false color display. CRHR1 expression is displayed in green and PSD95 (**B**), SAP97 (**C**), SAP102 (**D**), PSD93 (**E**) and MAGI2 (**F**) expression are displayed in red. In the overlay the yellow signal reveals overlapping expression of CRHR1 with the respective interaction partner. Depicted are representative photomicrographs of coronal brain sections of wild-type mice. CX, cortex; CA, cornu ammonis area; RTN, reticular thalamic nucleus.

To assess the co-expression also on the cellular level, the expression levels were analyzed by double ISH. The CRHR1 signal in the double ISH was enhanced by using a transgenic CRHR1-GFP mouse carrying a CRHR1-GFP BAC transgene. In this transgene the first exon of CRHR1 was replaced with the GFP sequence followed by a translation stop signal. In these mice GFP is transcribed from the CRHR1 promoter largely mimicking the endogenous expression of CRHR1 as recently described (Justice et al. 2008). The specific radiolabeled GFP riboprobe detected mRNA of GFP in cells endogenously expressing CRHR1 what provided a distinct and enhanced expression pattern of CRHR1 (Figure 17G-K). For example in the cortex the visualization of CRHR1 mRNA expression was strongest detectable in layer IV. The mRNA of CRHR1 and interaction partners was co-localized in pyramidal neurons of hippocampal CA1, in cells of the cortex and reticular thalamic nucleus (Figure 17G-K) demonstrating that CRHR1 is indeed co-expressed with the interacting partners on cellular level. This co-expression is a prerequisite for a physical interaction and thus supports the possible physiological relevance of the interaction between the receptor and the MAGUKs.
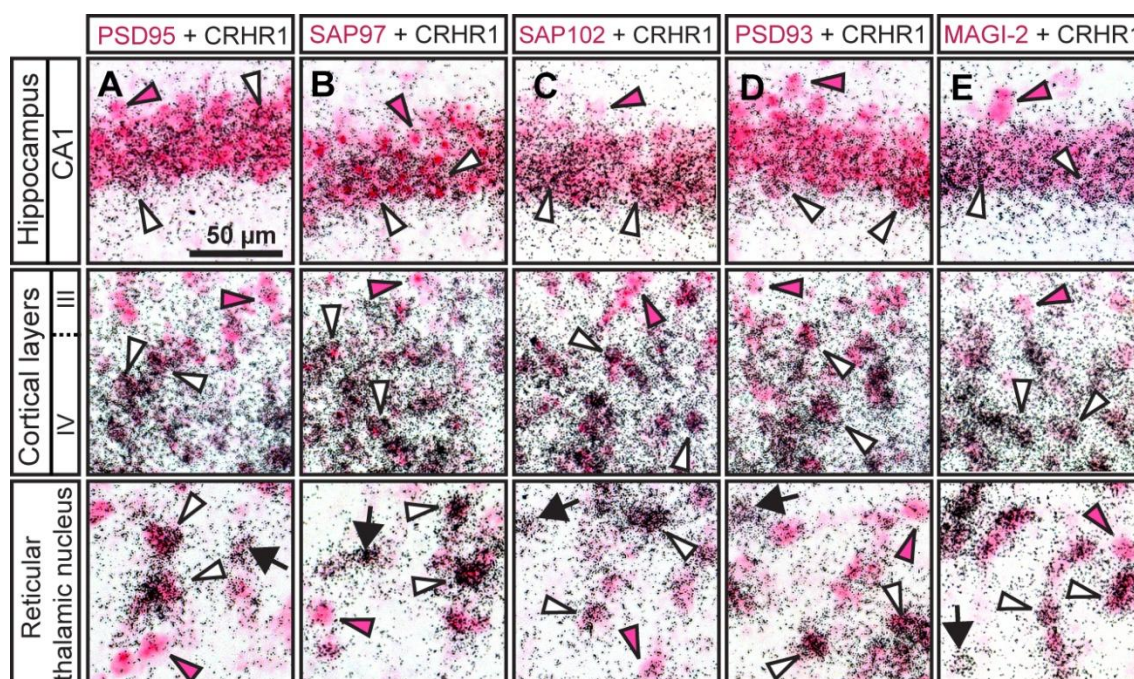
Figure 17: CRHR1 and candidate MAGUKs are co-expressed in neurons of the adult mouse brain.
Expression of CRHR1 and the candidate proteins was assessed by double *in situ* hybridization (**A-E**) in the adult mouse brain revealing co-expression of CRHR1 and the interacting partners on the cellular level. Depicted are representative photomicrographs of coronal brain sections transgenic derived from CRHR1-GFP reporter mice. Arrows indicate a single positive cell stained with silver grains for CRHR1 (→) and red arrowheads indicate cells expressing the candidate MAGUK only (▷). White arrowheads indicate double-positive cells co-expressing CRHR1 and its respective interaction partner (▷). CX, cortex; CA, cornu ammonis area; RTN, reticular thalamic nucleus.

4.2.2 Characterization of the CRHR1/CRH system in primary neurons

To address the role of the PDZ binding motif of CRHR1 with respect to its subcellular localization, primary hippocampal neurons were investigated in terms of the expression of MAGUKs, CRHR1 and its ligand CRH to elucidate the physiological relevance of this cell culture model.

4.2.2.1 Co-expression of CRHR1 and interaction proteins in primary neurons

The mRNA expression of CRHR1, CRHR2, CRH and urocortin 1-3 was determined in cultured primary hippocampal neurons by reverse transcriptase PCR. Of the entire system of CRH-related peptides and receptors only CRHR1 and CRH were detected (data not shown). The mRNA expression of CRHR1, CRH and of the MAGUKs was examined in primary hippocampal neurons also via quantitative real time PCR (qPCR) at 0 days *in vitro* (DIV) and

DIV 21 (Figure 18). The mRNA expression of CRHR1 and its ligand corticotropin-releasing hormone (CRH) was detectable whereas CRHR2 was again not detectable. The expression of the candidate partners PSD95, SAP97, SAP102, PSD93 and MAGI2 was also detectable. PSD95 showed a six fold upregulation at DIV 21 compared to DIV 0 (Figure 18). Similarly, PSD93 and SAP102 were also upregulated in the course of maturation of primary neurons.
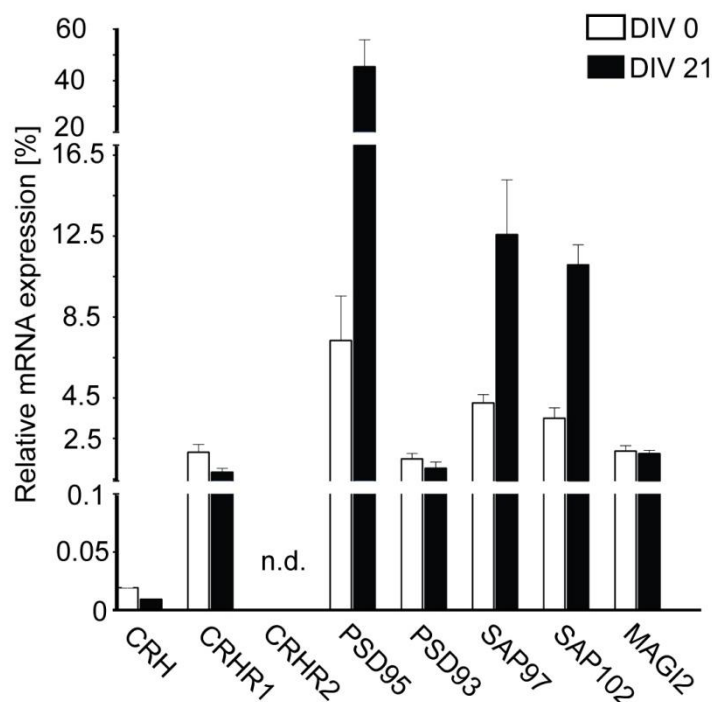

Figure 18: Expression levels of CRHR1 and candidate partners in primary hippocampal neurons at different time points in culture.
The mRNA levels of CRHR1, CRH, CRHR2 and the candidate partners PSD95, SAP97, SAP102, PSD93 and MAGI2 were determined by quantitative real time PCR and normalized to the expression of ribosomal protein L19 (RPL-19). The expression levels were analyzed at 0 days *in vitro* (DIV) and DIV 21. n.d. not detected.

The identified co-expression of CRHR1 with the interacting proteins in primary hippocampal neurons confirmed the co-expression in the adult mouse brain detected by *in situ* hybridization. Moreover, the co-expression supports the primary hippocampal culture as a cell culture model of physiological relevance for the CRHR1/CRH system. Furthermore, the low endogenous CRHR1 mRNA expression observed via qPCR is consistent with the fact that no antibody against CRHR1 was able to detect the endogenous CRHR1 neither in slices nor in primary cell culture as recently described by our laboratory (Refojo et al. 2011).

4.2.2.2 CRH is expressed in GABAergic neurons

In addition to the qPCR, to visualize the expression of CRH in primary neuronal, CRH-Cre mice were bred to Ai9 reporter mice. The CRH-Cre mouse line expresses Cre in CRH neurons as described (Taniguchi et al. 2011). In the Ai9 mouse line, a floxed stop cassette precedes of a tdTomato reporter gene (Madisen et al. 2010). In offspring from CRH-Cre x Ai9 breedings every CRH expressing neuron also expresses tdTomato due to the Cre-mediated activation of the reporter gene. At DIV 4 of primary cell culture ~1/10 000 cells in cortex and ~1/30 000 cells in hippocampus were tdTomato positive and, therefore, also expressing CRH (Figure 19). At DIV 14 there was no change in this ratio in cortical cultures but in hippocampal cultures the amount of positive cells duplicated to ~1/15 000 cells.
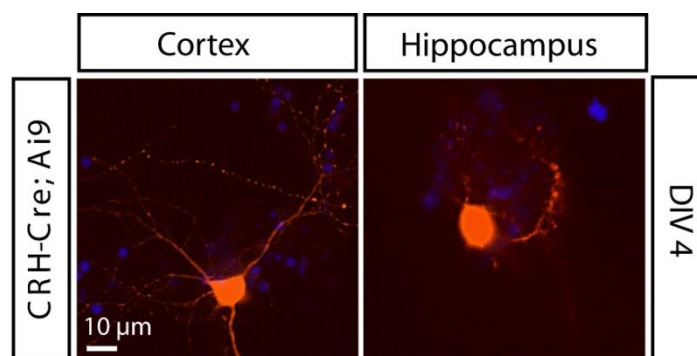

Figure 19: CRH is expressed in cultured neurons of the cortex and the hippocampus.
Neurons were prepared from CRH-Cre; Ai9 embryos at day 18 post coitum (dpc 18). Cells were fixed at DIV 4 and nuclei were counterstained with DAPI (4`,6-diamidino-2-phenylindole) (blue).

The identity of the CRH expressing neurons was determined using antibodies against GABAergic (gamma aminobutyric acid) markers Gad67, Gad65/67, calbindin D28-K and calretinin. Some of the tdTomato positive neurons were positive for Gad67, Gad65/67 or calbindin D28-K but there was no co-staining with calretinin (Figure 20). A similar analysis was conducted in cortical primary cell culture with comparable findings (data not shown). These results imply that CRH is expressed in GABAergic neurons in primary hippocampal and cortical cell cultures at different time points (DIV 0-14).
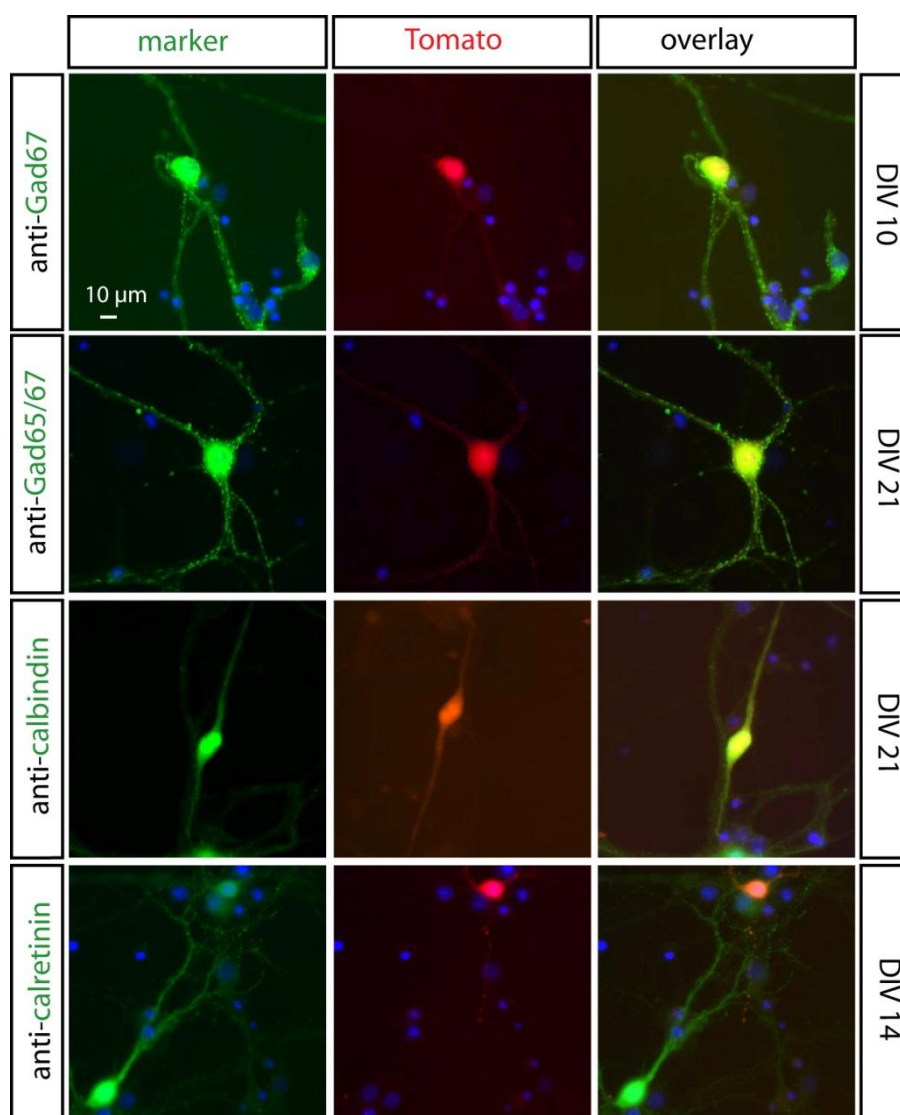
Figure 20: CRH is expressed in GABAergic neurons.
Neurons were prepared from CRH-Cre; Ai9 embryos (dpc 18). Cells were fixed at different time points of culture and nuclei were counterstained with DAPI (blue). Immunofluorescent stainings were performed against the GABAergic markers Gad67, Gad65/67, calbindin D28-K and calretinin.

4.2.2.3 CRHR1 is expressed in glutamatergic neurons

In order to visualize the CRHR1 expressing neurons in primary cell culture, primary hippocampal cell cultures were prepared from transgenic CRHR1-GFP reporter mice carrying a CRHR1-GFP BAC transgene. This mouse line was also used for the double *in situ* hybridization experiment (Figure 16). The identity of the CRHR1 expressing neurons was determined using antibodies against GFP to enhance the GFP expression in CRHR1 positive neurons and against pan-neuronal, glutamatergic and GABAergic markers (Figure 21). About 44 % of the neurons were CRHR1-GFP positive. In contrast, CRHR1 was not detectable in

primary neurons prepared from a mouse model, in which GFP is expressed from the endogenous CRHR1 promoter (data not shown). The staining with the glutamatergic marker VGluT1 (vesicular glutamate transporter 1) revealed that every CRHR1 positive neuron is glutamatergic confirming previous double ISH results by our group (Refojo et al. 2011). Simultaneously also most of the CRHR1 positive neurons, namely 90 %, were calbindin D28-K negative (Figure 21).
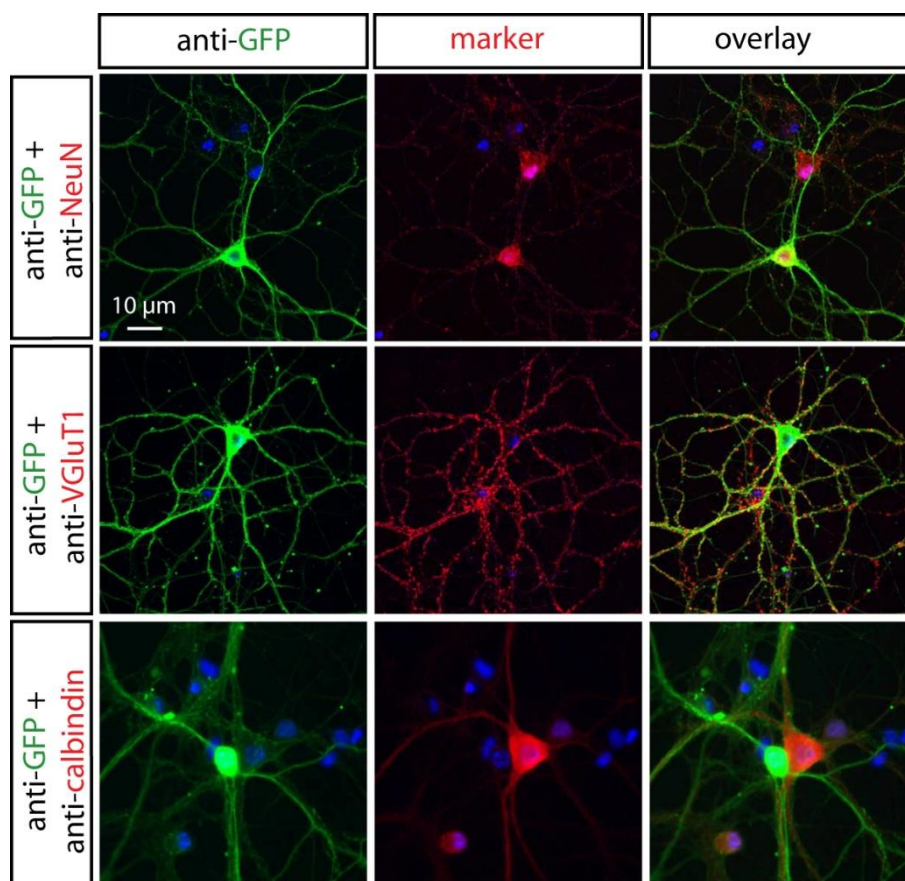

Figure 21: CRHR1 is predominantly expressed in glutamatergic neurons.
Neurons were prepared from transgenic CRHR1-GFP embryos (dpc 18). Cells were fixed at DIV 21 and nuclei were stained with DAPI (blue). Immunohistochemical stainings were performed against: GFP, the neuronal marker NeuN, the glutamatergic marker VGluT1 and the GABAergic marker calbindin D28-K. Representative confocal pictures are displayed.

4.2.3 Overexpression of CRHR1

The potential impact of the PDZ binding motif on the localization of the receptor was investigated in primary neurons by overexpression of CRHR1 variants. From previous studies in the lab it appeared that overexpression of any protein and especially of the CRH receptor type 1 at later time points of culture is challenging e.g. regarding transfection efficacy. Moreover, overexpression artifacts seemed to be toxic for primary neurons. To test

whether the observed toxicity is connected to CRHR1 signaling, different mutants of CRHR1 were designed (Figure 22): In myc-GFP-CRHR1-STAVA the PDZ binding motif is disrupted as described in Figure 8. The mutant myc-GFP-CRHR1-S301V contains an amino acid change at position 301 that is known to be important for cAMP production (Papadopoulou et al. 2004). myc-GFP-CRHR1Δ C-term and myc-GFP-CRHR1Δ 2TM were generated to delete the cytoplasmic C-terminus respectively the C-terminus, the third intracellular loop (IC3) and the last two transmembrane domains to disrupt amongst others the β-arrestin binding site and different phosphorylation sites relevant for receptor desensitization.

Figure 22: Schematic representation of designed CRHR1 variants.
myc-GFP-CRHR1 was used to construct the variants myc-GFP-CRHR1-STAVA, myc-GFP-CRHR1-S301V, myc-GFP-CRHR1Δ C-term (aa 1-375) and myc-GFP-CRHR1Δ 2TM (aa 1-298). CRHR1 variants were used to assess potential intrinsic receptor toxicity.

4.2.3.1 Overexpression of CRHR1 variants in HEK293 cells

First, the CRHR1 variants were tested by overexpression in HEK293 cells. The generated mutant CRHR1 variants showed a membranous distribution similar to the WT receptor, when transfected transiently in HEK293 cells with exception of myc-GFP-CRHR1Δ 2TM, which largely accumulated in intracellular vesicles (Figure 23). In general, the native GFP fluorescence of the tagged receptors was enhanced by immunofluorescence staining against GFP.
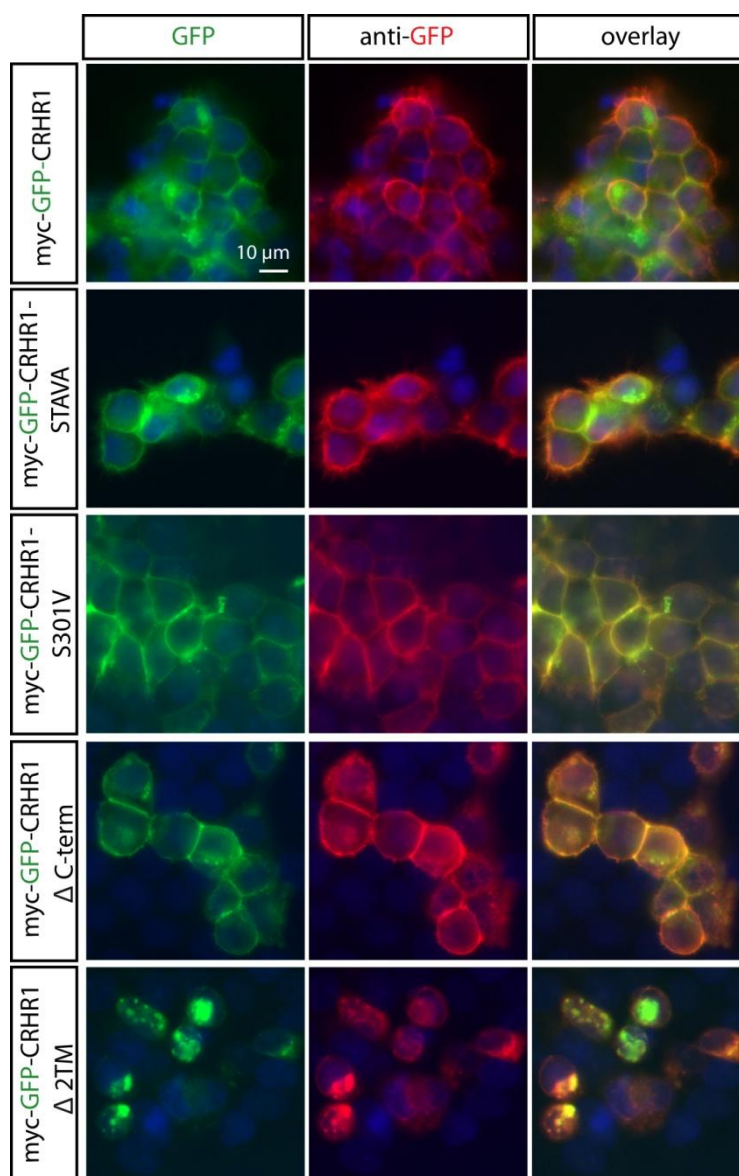

Figure 23: Expression of WT and mutant variants of CRHR1 in HEK293 cells.
HEK293 cells were transiently transfected with expression vectors for myc-GFP-CRHR1, myc-GFP-CRHR1-STAVA, myc-GFP-CRHR1-S301V, myc-GFP-CRHR1Δ C-term and myc-GFP-CRHR1Δ 2TM. Immunofluorescence staining was performed against GFP. As secondary antibody Alexa Fluor 594 was used.

The similar cellular distribution pattern revealed that the WT CRHR1 and its mutant variants are properly expressed in HEK293 cells. The aberrant vesicular distribution of the mutant receptor, which lacked the C-terminal portion including the two last transmembrane domains (myc-GFP-CRHR1Δ 2TM) demonstrated that the receptor trafficking is disturbed preventing correct membrane insertion.

4.2.3.2 Functional analysis of CRHR1 mutants

The functionality of mutant CRHR1 variants was tested by assessing their capacity to produce cyclic AMP (cAMP), a competitive immunoassay between native cAMP and cAMP labeled with the acceptor dye d2 was performed. Both cAMPs compete for a cryptate-labeled anti-cAMP antibody what is detected by fluorescence resonance energy transfer (FRET) that is inversely proportional to the concentration of cAMP in the sample.

The cAMP production was largely similar for all analyzed CRHR1 mutants except CRHR1Δ 2TM, which showed a clear impairment in cAMP production (Figure 24).
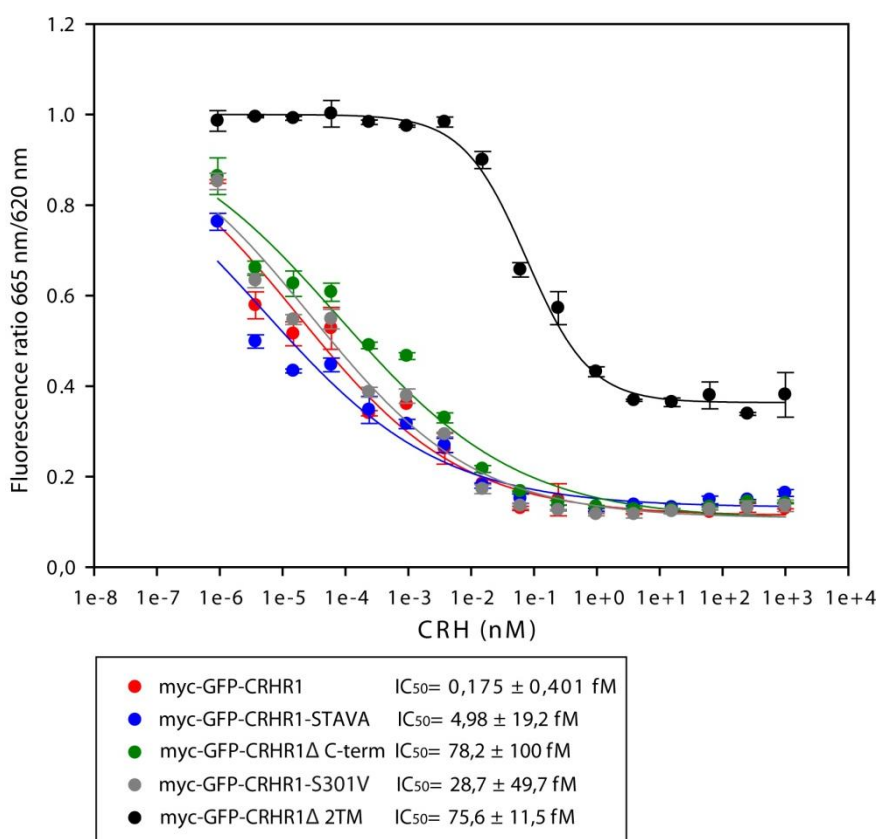

● myc-GFP-CRHR1	IC_{50}= 0,175 ± 0,401 fM
● myc-GFP-CRHR1-STAVA	IC_{50}= 4,98 ± 19,2 fM
● myc-GFP-CRHR1Δ C-term	IC_{50}= 78,2 ± 100 fM
● myc-GFP-CRHR1-S301V	IC_{50}= 28,7 ± 49,7 fM
● myc-GFP-CRHR1Δ 2TM	IC_{50}= 75,6 ± 11,5 fM

Figure 24: cAMP production of WT and mutant CRHR1 variants.
HEK293 cells were transiently transfected with indicated CRHR1 constructs. Cells were treated with different concentrations of CRH. cAMP was measured using a cell-based cyclic AMP assay kit. Untransfected HEK293 cells did not produce cAMP and showed a baseline of one (data not shown).

Surprisingly, myc-GFP-CRHR1-S301V, which was described to affect cAMP production, did not show a strong reduction of cAMP production. This is in contrast to the recently detected 50 % reduction of cAMP production of the same mutant following urocortin 1 stimulation which was also transfected transiently in HEK293 cells (Papadopoulou et al. 2004).

The analysis of cellular localization and cAMP production revealed that the mutant CRHR1 variants behaved as expected and did not provoke any toxicity in HEK293 cells. Only myc-GFP-CRHR1-S301V did not show the expected reduction in cAMP production. Next, WT and CRHR1 mutants were tested in primary neuronal cell culture.

4.2.3.3 Overexpression of WT and mutant CRHR1 variants *in vitro* and *in vivo*

To assess the subcellular localization of WT and CRHR1 mutants, primary hippocampal neurons were transfected with respective constructs using the calcium-phosphate protocol. Except for CRHR1Δ 2TM, the expression analysis by immunofluorescence revealed for WT and CRHR1 variants a typical localization to the plasma membrane and in perinuclear vesicles (Figure 25). In contrast, CRHR1Δ 2TM showed a strong accumulation in perinuclear vesicular structures and was not distributed into the neurites. This pattern was in accordance with the vesicular distribution observed in HEK293 cells.

At an early time point (DIV 6) it was possible to overexpress WT and CRHR1 mutants in primary neurons (Figure 25) but at later time points (e.g. DIV 14) the overexpression using the calcium-phosphate protocol was not successful in terms of efficacy and cell survival.

To analyze the cell survival in a more physiological context, WT and mutant CRHR1 variants were overexpressed *in vivo*. Therefore, gene delivery in mouse embryos was applied using *in utero* electroporation. In general, independent of the transfected CRHR1 variant the transfection efficacy was rather low and some cells showed equal distribution over the neuron while others showed only a vesicular distribution at the soma (Figure 26). Unfortunately, no successfully electroporated mouse embryo was obtained for CRHR1Δ 2TM.

The *in vivo* approach verified that an overexpression of CRHR1 was possible at least with a low efficacy resulting in overexpressing neurons that appeared largely healthy. To establish an overexpression in primary neurons at more mature time points different approaches were tested.

Overexpression was performed by using BacMAM technology, which is based on the use of a baculovirus, a double-stranded DNA insect virus, to deliver genes to mammalian cells. The transduction with baculoviruses has the advantage of reduced immune response due to the non-mammalian source (Luckow and Summers 1988, Torres-Vega et al. 2014). The

expression efficacy was very high also in matured neurons but unfortunately the neurons showed a pathological morphology (Figure 27). Neither the adjustment of the virus particle concentration, nor the incubation time solved this artifact. Therefore, this technology was not explored further.
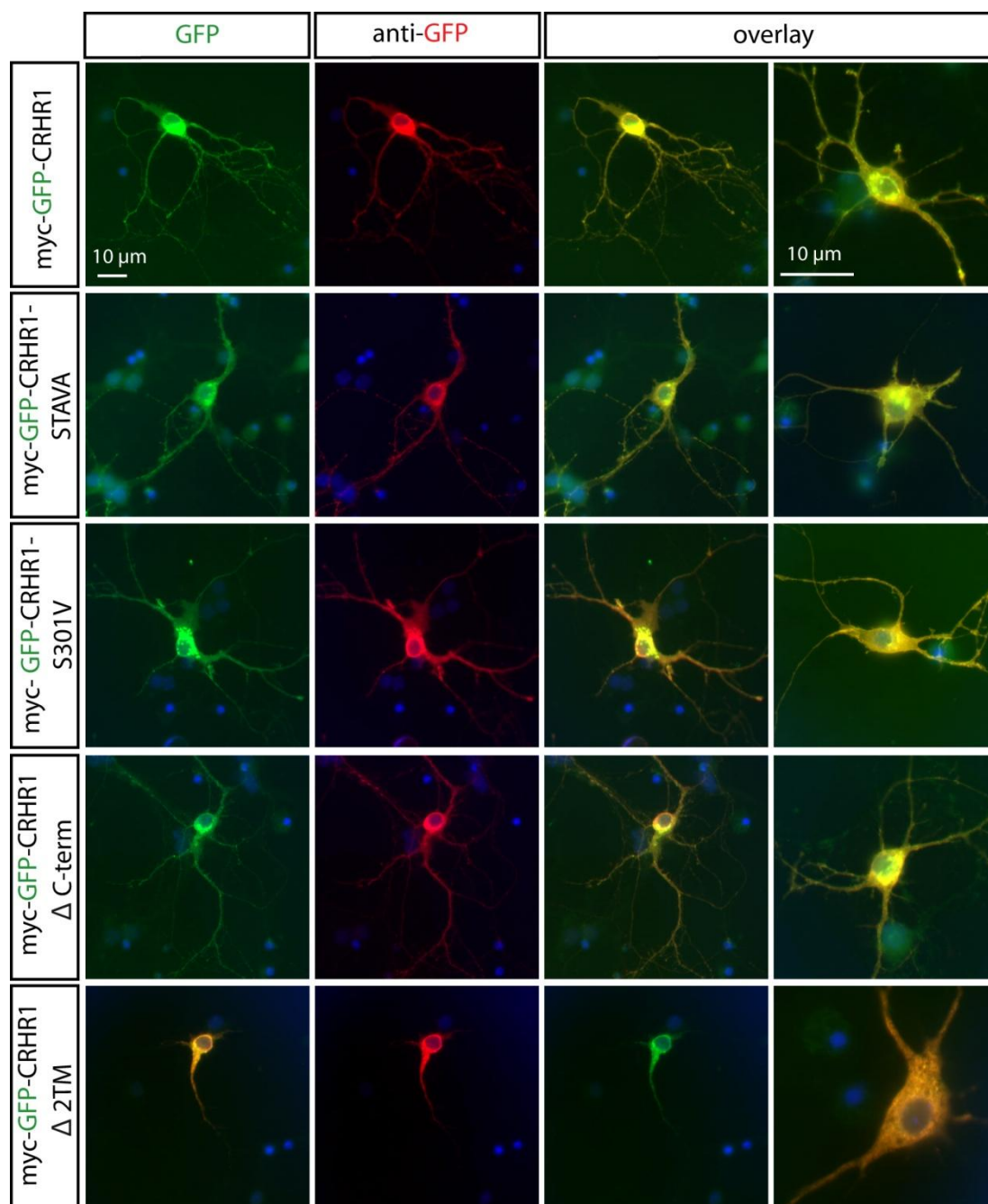

Figure 25: Expression of wild-type and mutant CRHR1 variants in immature primary neurons. Neurons were prepared from WT embryos (dpc 18). Primary hippocampal neurons were transfected with expression vectors for WT and mutant CRHR1 variants using the calcium-phosphate protocol at DIV 6. Cells were fixed at DIV 7 and immunofluorescent stainings were performed against GFP.
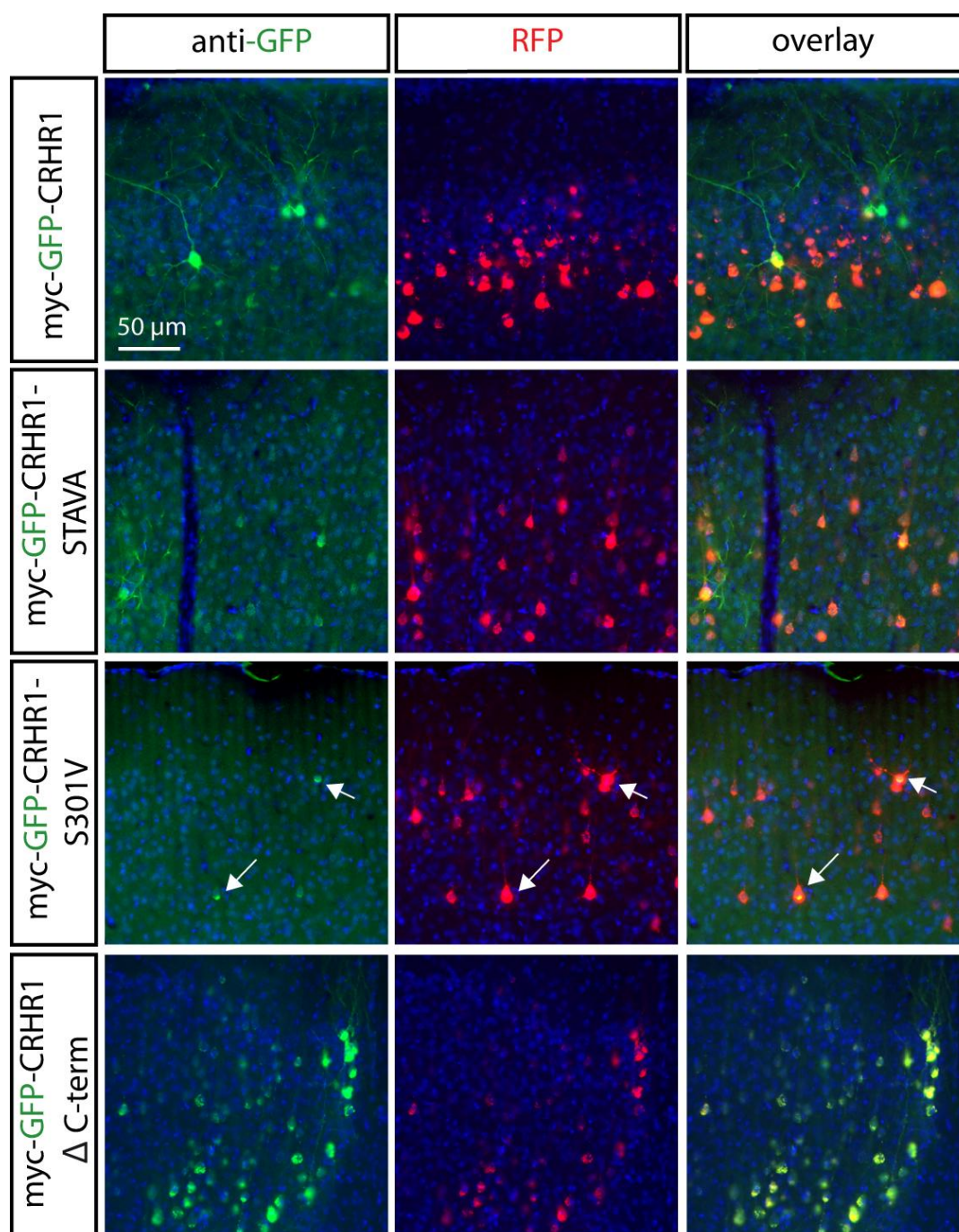
Figure 26: Expression of wild-type and mutant CRHR1 variants in the cortex following *in utero* electroporation.

Mouse embryos were *in utero* electroporated at embryonic day (E) 13.5-14.5 targeting the neocortex with expression vectors for WT and mutant CRHR1 variants. As a control an RFP (red fluorescent protein) expression vector was co-electroporated. Brains were fixed at postnatal day (pnd) 38-70 and were immunostained against GFP to enhance the GFP signal. For the myc-GFP-CRHR1-S301V only two positive cells were detected (→) in one out of six electroporated brains. Representative photomicrographs of the cortex taken by fluorescence microscopy are displayed.

To express proteins in HEK293 cells, lipofection is a well-working standard procedure as seen e.g. in Figure 14. However, in primary neurons Lipofectamine is toxic and results in cell

death (data not shown). Testing different conditions revealed that when the reduced serum medium Opti-MEM was used as the dilution medium it already damaged the cells by its own. The use of the Neurobasal A medium as the dilution medium, which is used as the growth medium, rescued the toxicity. Nevertheless, the transfection efficacy for the late time points was not sufficient for the planned investigations.
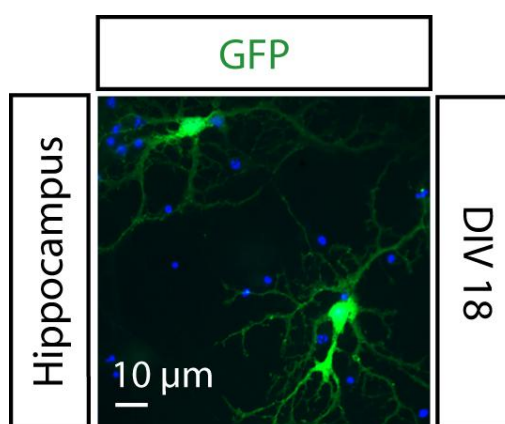

Figure 27: Primary neurons transduced with a baculovirus harboring a GFP expression cassette.
Neurons were prepared from wild-type embryos (dpc 18). Primary hippocampal neurons at DIV 14 were transduced with MOI (multiplicity of infection) of 10 using BacMAM technology. Cells were fixed at DIV 18 and counterstained with DAPI (blue).

Furthermore, two different electroporation protocols were tested to transfect primary neurons at a later time point by using electrodes for 24 well plates. None of the tested current modulations were able to improve the low transfection efficacy and cell viability (data not shown).

The transfection efficacy and cell survival of mature neurons (≥ DIV 14) was neither improved by the calcium-phosphate protocol using different incubation times, nor by the baculovirus based transduction, nor by a modified lipofection protocol, nor by two different ways of electroporation in the cell culture dish. To overcome these difficulties viral transduction of primary neurons was applied using lentiviruses and adeno-associated viruses, respectively.

4.2.3.3.1 Lentivirus-mediated overexpression of CRHR1 in primary neurons

Constructs for lentiviral overexpression were designed comprising the WT CRHR1 and the CRHR1-STAVA mutant, respectively, both tagged with myc and GFP (Figure 28).
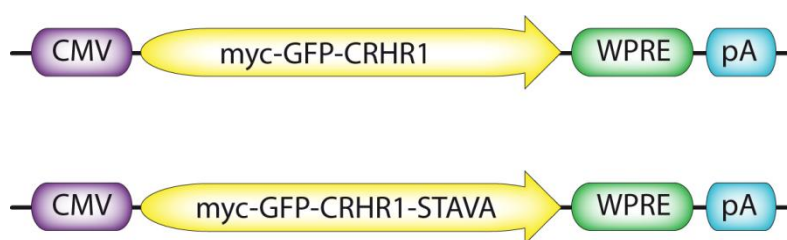
Figure 28: Constructs for lentiviral overexpression.
myc-GFP-CRHR1 or myc-GFP-CRHR1-STAVA was cloned into an expression vector under the control of the cytomegalovirus (CMV) promoter. WPRE, woodchuck hepatitis virus posttranscriptional regulatory element; pA, polyadenylation signal.

The lentiviral transduction of primary neurons resulted in successful overexpression of WT and mutant myc-GFP-CRHR1. The co-expression with a GFP control virus labeled fluorescently the entire primary neuron and thereby revealed the normal neuronal morphology despite overexpression of CRHR1 (Figure 29).
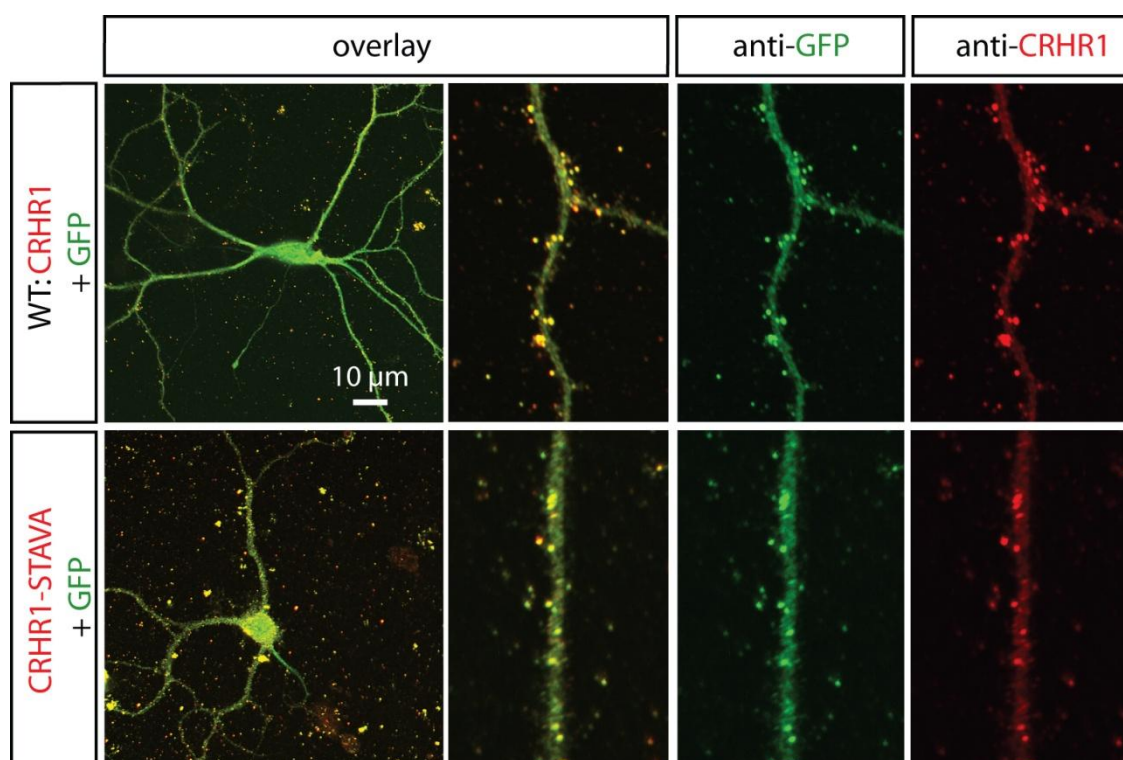
Figure 29: Lentiviral-mediated expression of CRHR1 reveals a punctuated distribution pattern along neurites of primary neurons.
Primary hippocampal neurons (DIV 18) were transduced with lentivirus harboring an expression unit for expression of WT and mutant of myc-GFP-CRHR1. To visualize the neuronal morphology, a GFP lentivirus was co-transduced. Neurons were fixed at DIV 20 and immunofluorescent stainings were performed against GFP and CRHR1. Representative confocal photomicrographs are displayed.

Immunostaining anti-GFP detected the receptor in a punctuated distribution pattern, which accumulated along the neuronal body and localized presumably in spines as visualized by co-expression of cytoplasmic GFP. To characterize the identity of GFP positive puncta immunostaining directly against CRHR1 was performed using an antibody that also worked in cells following overexpression of CRHR1.

To characterize the localization of the receptor, the pre-synapse, the inhibitory and excitatory post-synapse and the axons were specifically labeled by antibody staining. The immunostaining against the axonal marker SMI-312 showed that the receptor was also located as puncta close to the SMI-312 labeled axons (Figure 30).
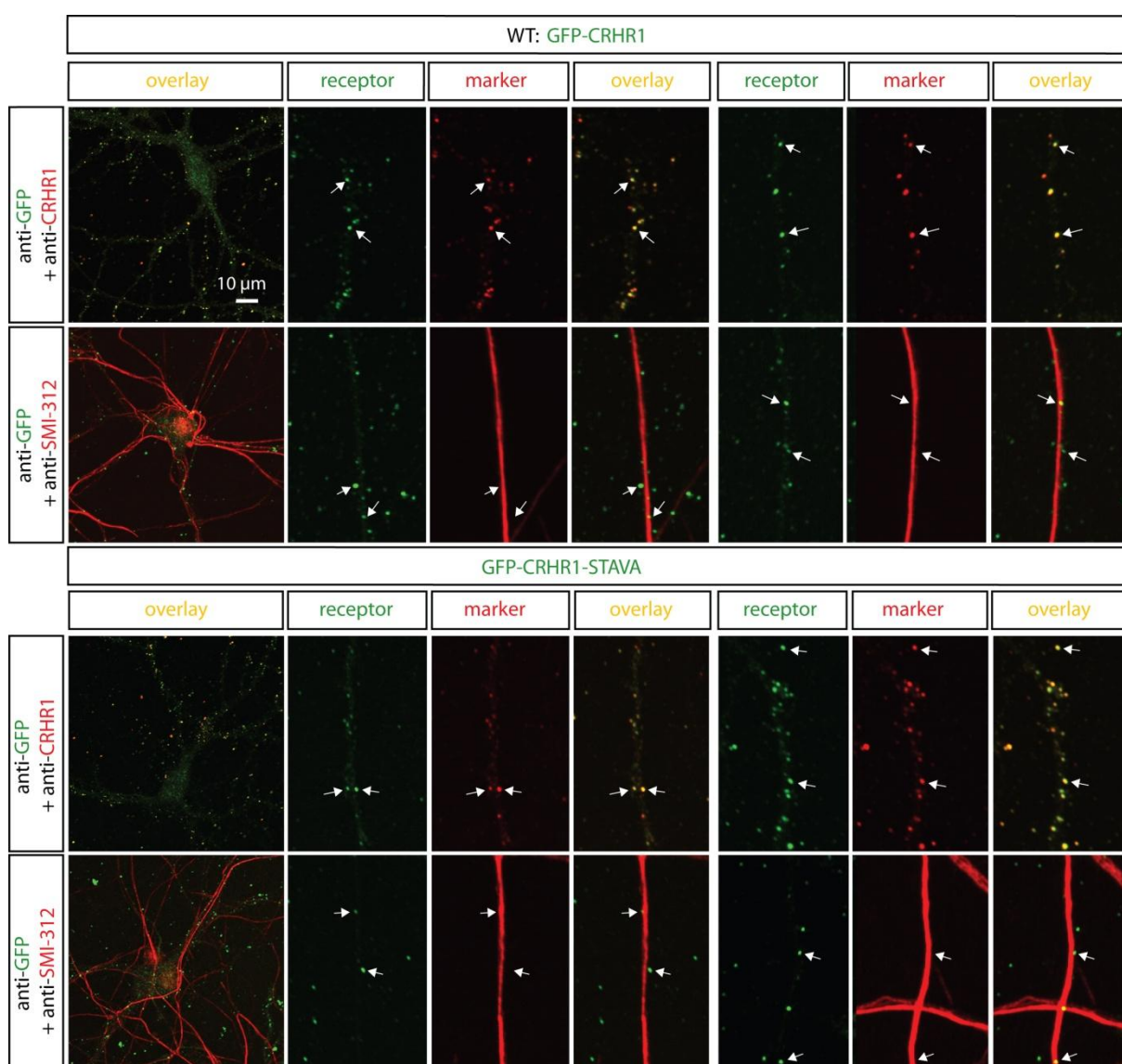

Figure 30: Axonal localization of WT and mutant CRHR1.
Neurons were prepared from wild-type embryos (dpc 18). Primary hippocampal neurons (DIV 18) were transduced with lentivirus harboring an expression unit for expression of WT and mutant myc-GFP-CRHR1 and fixed at DIV 20. Immunofluorescent stainings were performed against GFP and CRHR1

or the axonal marker SMI-312. Examples for adjacent puncta for anti-SMI-312 or overlapping puncta for anti-CRHR1 are highlighted (→). Two representative magnifications of confocal pictures are displayed.

Further characterization using the pre-synaptic marker synapsin resulted in a non-overlapping but adjacent distribution with the receptor independent of the PDZ binding motif (Figure 31). Also the inhibitory post-synaptic marker gephyrin did not overlap with the receptor.
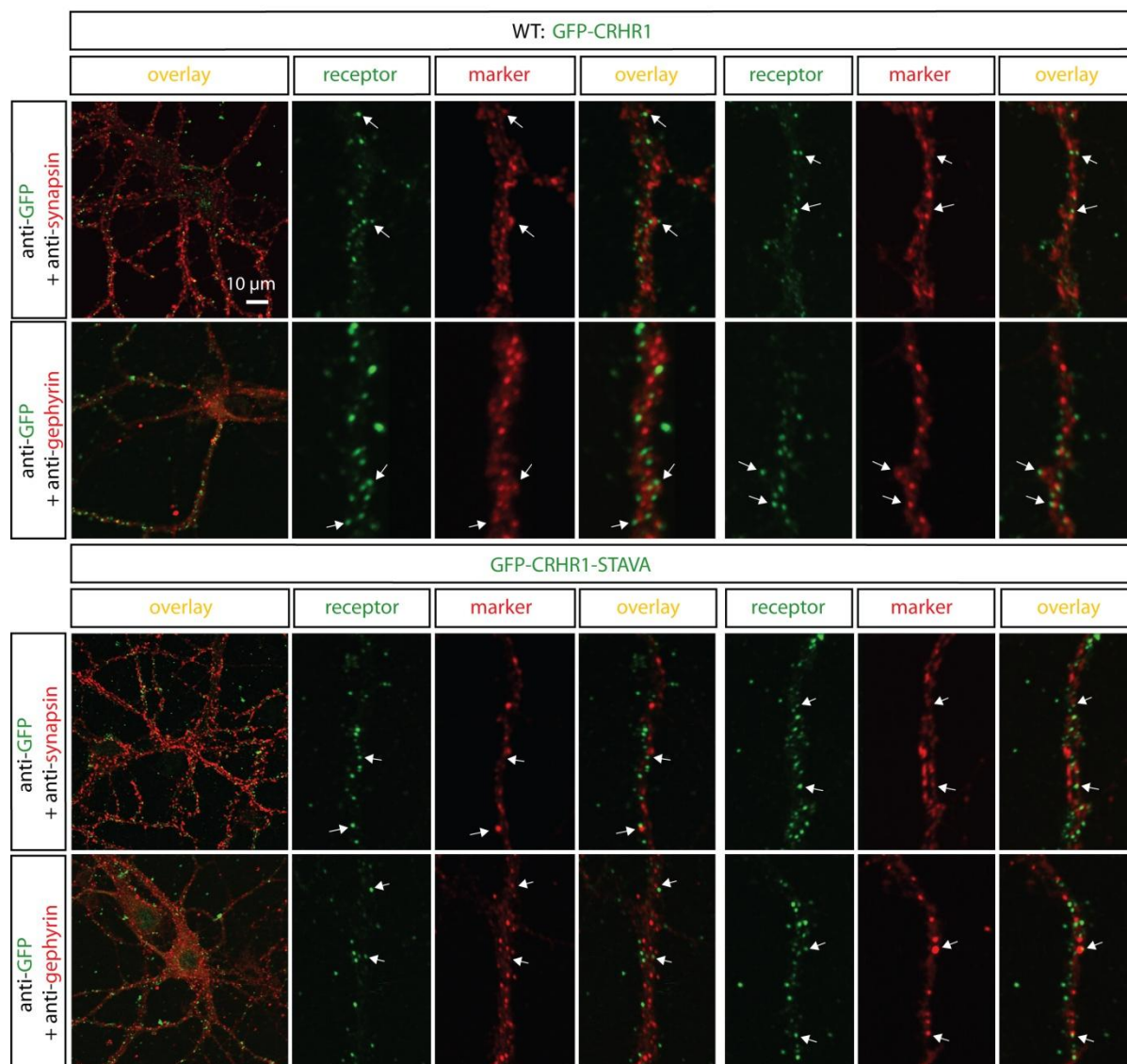
Figure 31: Overexpressed WT and mutant CRHR1 localize adjacent to pre- and post-synaptic markers in primary neurons.
Neurons were prepared from WT embryos (dpc 18). Primary hippocampal neurons were transduced with lentivirus harboring an expression unit for expression of WT and mutant myc-GFP-CRHR1 and fixed at DIV 20. Immunofluorescent stainings were performed against GFP and the pre-synaptic marker synapsin or the inhibitory post-synaptic marker gephyrin. Examples for adjacent puncta are highlighted (→). Two representative magnifications of confocal pictures are displayed.

In order to unravel the localization of the CRHR1 in relation to the interaction partners, immunolabeling of PSD95 and SAP97 revealed that the puncta stained for CRHR1 were localized adjacent but not overlapping with the pattern of the interacting proteins (Figure 32). PSD95 is also a marker for the excitatory post-synapse implying that the receptor was also not located at the excitatory post-synapse.
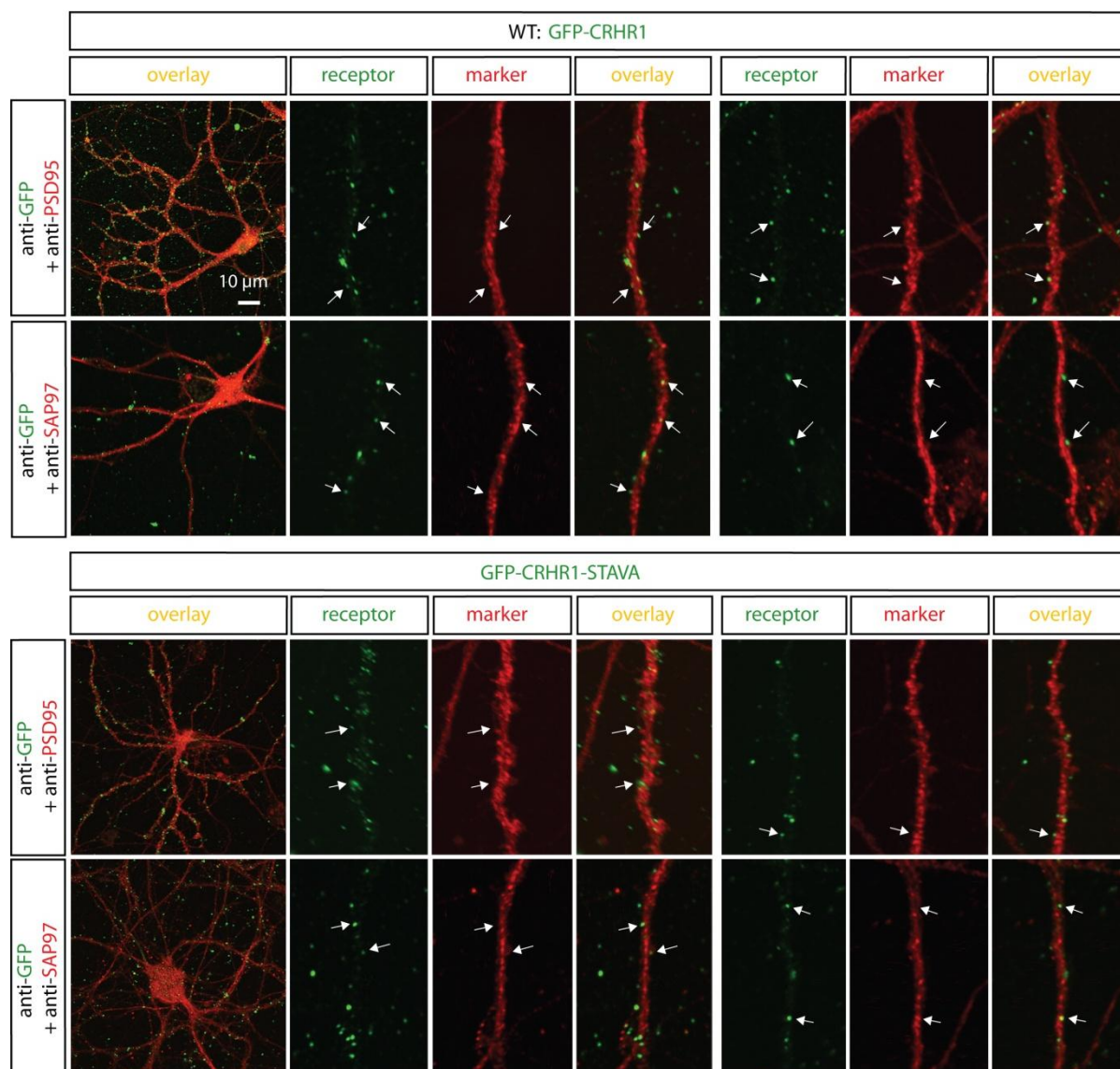
Figure 32: WT and mutant CRHR1 are localized adjacent to PSD95 and SAP97 in primary neurons.
Neurons were prepared from wild-type embryos (dpc 18). Primary hippocampal neurons were transduced with lentivirus harboring an expression unit for expression of WT and mutant myc-GFP-CRHR1 and fixed at DIV 20. Immunofluorescent stainings were performed against GFP and the interaction protein PSD95 or SAP97. Examples for adjacent puncta are highlighted (→). Two representative magnifications of confocal pictures are displayed.

4.2.3.3.2 Adeno-associated virus (AAV)-mediated overexpression of CRHR1 in primary neurons

Due to the lack of co-localization of CRHR1 positive puncta with any of the investigated markers another viral-mediated expression approach was used. To overexpress CRHR1 in primary neurons, adeno-associated viruses (serotype 8, AAV8) were used in a more restricted manner than the lentiviruses. In the attempt to overexpress CRHR1 more specifically in neurons endogenously expressing CRHR1, i.e. mainly excitatory neurons, primary neurons derived from Nex-Cre mice, which express Cre recombinase in excitatory glutamatergic neurons (Goebbels et al. 2006), were prepared. Transduction of these primary neurons with Cre-dependent AAVs, which are based on the DIO (double-floxed inverse open reading frame) expression system, restricted the overexpression of CRHR1 to glutamatergic neurons (Figure 33).
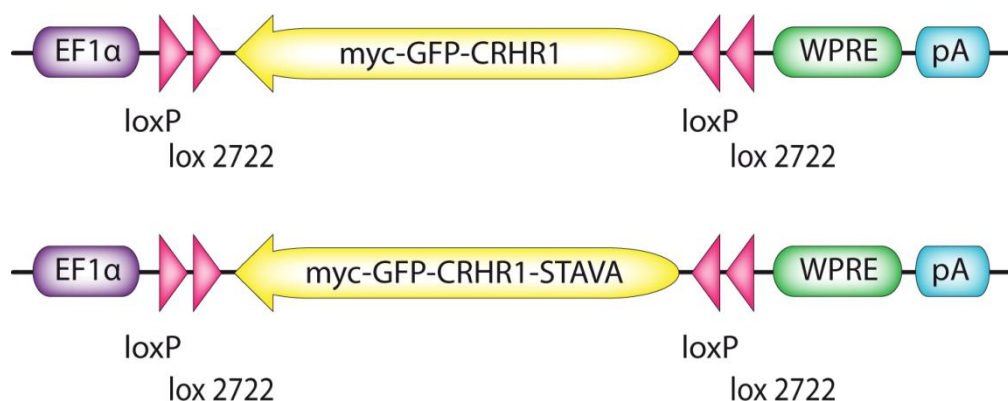
Figure 33: Constructs for adeno-associated virus-mediated overexpression.
myc-GFP-CRHR1 or myc-GFP-CRHR1-STAVA was cloned into an expression vector with a double-floxed inverse open reading frame under the control of the elongation factor-1α (EF1α) promoter. WPRE, woodchuck hepatitis virus posttranscriptional regulatory element; pA, polyadenylation signal.

Staining against GFP localized the WT and mutant receptor to the plasma membrane throughout the neuron (Figure 34). Immunostaining against CRHR1 confirmed that the GFP signal fully overlapped with the CRHR1 signal. The role of the PDZ binding motif in localization of the receptor was examined by co-staining of the receptor and markers specific for the neurites, the pre-synapse and the inhibitory and excitatory post-synapse. The WT and mutant myc-GFP-CRHR1 were localized in dendrites (Figure 34B) and axons (Figure 34C). CRHR1s were not present in the pre-synapse (Figure 34D) or in the inhibitory post-synapse (Figure 34E) but in the excitatory post-synapse (Figure 34F). Simultaneously the receptor co-

localized with the candidate interaction proteins PSD95 and SAP97 independent from the PDZ binding motif.

The co-localization in mature spines further supports a possible physiological relevance of the identified interaction between CRHR1 and PSD95 or SAP97. Whether there is any effect of the PDZ binding motif on CRHR1 localization following CRH treatment has to be further investigated. It is also possible that the endogenous CRHR1 is sufficient to rescue potential deficits of expressed CRHR1-STAVA via dimerization or oligomerization. Preliminary results did not show a PDZ binding motif-dependent localization of the receptor in CRHR1 lacking neurons (data not shown).

There are studies comparing expression by transduction with AAVs and lentivirus that find enormous differences in transduction efficacy depending on the cell type and virus compositions (Dishart et al. 2003, Shakhbazau et al. 2008, Kealy et al. 2009), but differences in localization of the virally expressed protein as observed in this study have not been described.

In summary, CRHR1 interacted with different PDZ domains of MAGUKs via its C-terminal PDZ binding motif, which also accounted for the clustering with MAGUKs. Moreover, the receptor was co-expressed with the MAGUKs on cellular level in the adult mouse brain. The primary hippocampal neurons were established as a suitable model for investigating the interactions of CRHR1. AAV-mediated overexpression of CRHR1 resulted in receptor localization throughout the neuronal plasma membrane. In primary neurons CRHR1 was localized in mature spines at the excitatory post-synapse and co-localized with the interacting partners PSD95 and SAP97.
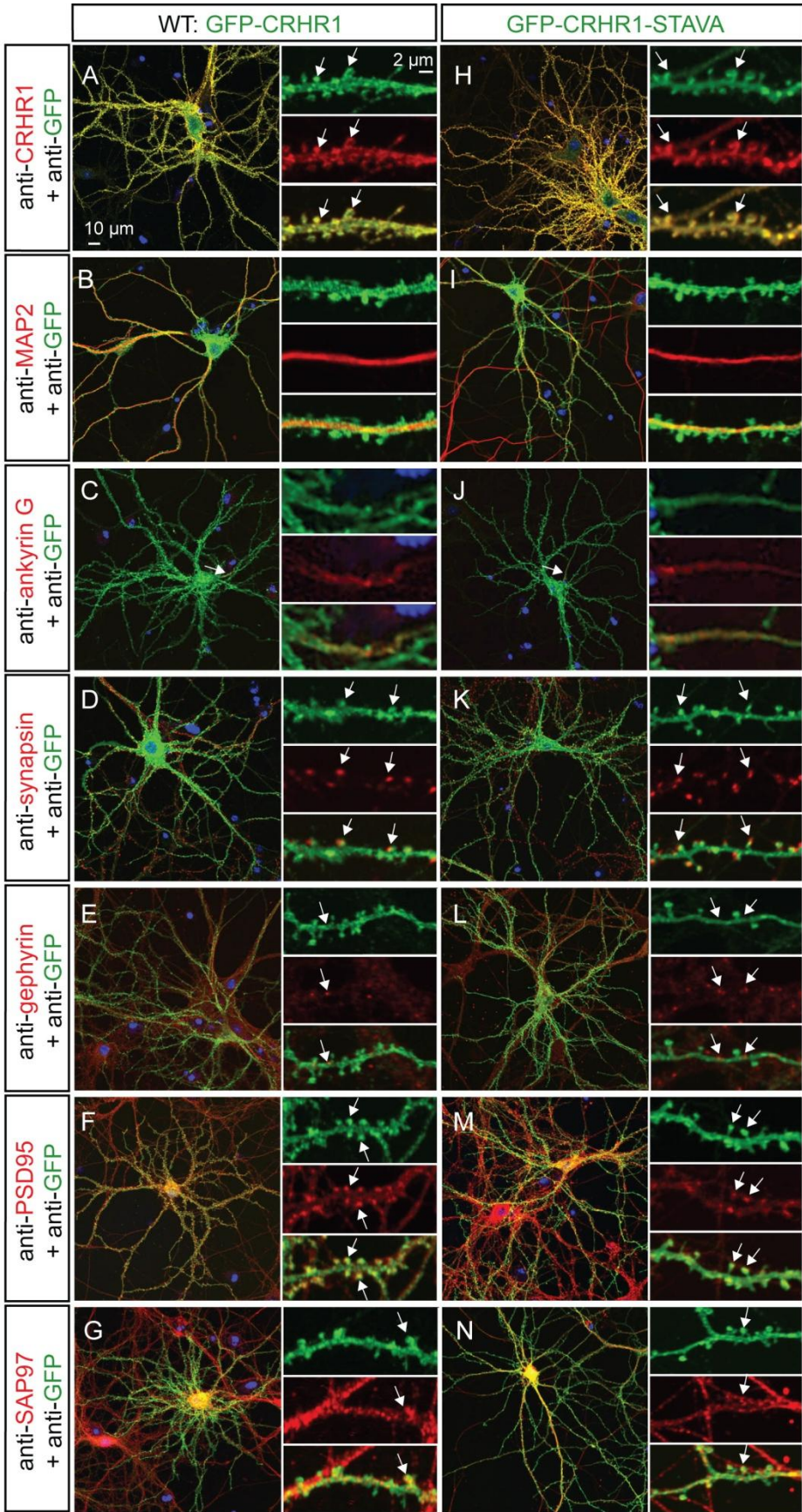
Figure 34: Localization of WT and mutant CRHR1 in primary neurons with PSD95 and SAP97 in the excitatory post-synapse.

Neurons were prepared from wild-type embryos (dpc 17). Primary hippocampal neurons (DIV 14) were transduced with AAV8 harboring an expression unit for overexpression of WT and mutant of myc-GFP-CRHR1. Neurons were fixed at DIV 20 and subjected to analysis by immunofluorescence. (**A**, **H**) the anti-GFP signal was confirmed by anti-CRHR1 staining. (**B**, **I**) Microtubule-associated protein 2 (MAP2) staining revealed the presence of the receptor in dendrites. (**C**, **J**) WT and mutant CRHR1 co-localize with the axon initial segment marker ankyrin G. The pre-synaptic marker synapsin stained the adjacent pre-synapse where the receptor was not detected (**D, K**). WT and mutant CRHR1 did not co-localize with the inhibitory post-synaptic marker gephyrin (**E, L**), but with the candidate partner and excitatory post-synaptic marker PSD95 in spines (**F, M**). (**G**, **N**) CRHR1 WT and mutant co-localize with the candidate partner SAP97. Immunofluorescence stainings were performed against GFP and the respective marker. Overlapping or non-overlapping signals are highlighted (→).

5 Discussion

The corticotropin-releasing hormone receptor type 1 (CRHR1) is a G protein-coupled receptor (GPCR) consisting of seven transmembrane domains. It is an important regulator of the neuroendocrine, behavioral, and autonomic response to stress. Dysregulation of CRHR1 and its ligand CRH has been causally linked to stress-related pathologies including mood and anxiety disorders. Until now only G proteins, G protein-coupled kinases (GRKs) and β-arrestins are familiar as intracellular interaction partners (Hauger et al. 2009). The starting point for this study was the previous identification of new interaction partners of CRHR1 in a yeast two-hybrid (Y2H) screen using the C-terminal cytoplasmic tail of CRHR1. Positive clones were among others the membrane-associated guanylate kinases (MAGUKs) postsynaptic density protein 95 (PSD95), synapse-associated protein 97 (SAP97), SAP102 and membrane-associated guanylate kinase, WW and PDZ domain containing 2 (MAGI2). In a parallel Y2H screen the transmembrane protein 106B (TMEM106B) and syndecan binding protein 1 (Syntenin-1) were identified as additional candidates. Furthermore, PSD93 was included into the study because of its affiliation to the PSD95 subfamily of MAGUKs and its high homology to the other members of this subfamily of PDZ scaffold proteins.

The specific aims of this study were: I) to verify the CRHR1 interaction partners and detect the protein domains essential for the interaction; II) to identify the functional relevance of the PDZ binding motif dependent interaction *in vitro*; III) to investigate the co-expression of CRHR1 with the candidate interaction partners *in vivo*; IV) to analyze whether primary neurons can serve as a cell culture model for investigating the CRHR1/CRH system and V) to examine the function of the CRHR1 PDZ binding motif with respect to receptor physiology in mature neurons.

5.1 High molecular weight complexes of CRHR1

In order to verify the candidate interaction partners, a co-immunoprecipitation (Co-IP) protocol followed by Western blot detection of precipitated proteins was established. In the Western blot (WB) CRHR1 appeared as two relatively distinct bands representing monomeric and oligomeric forms of the receptor as already shown before (Zmijewski and Slominski 2009). Recently, an equilibrium of CRHR1 monomers/dimers was demonstrated to be already established in the endoplasmatic reticulum (ER) (Teichmann et al. 2014). Also other GPCRs like the somatostatin receptor 1 (SSTR1) form detergent resistant complexes due to oligomerization (Cai et al. 2008). For the investigation of oligomerized GPCRs

different approaches with individual optimization are necessary (Harrison and van der Graaf 2006). For CRHR1 it is possible to detect monomers and to partly disrupt the oligomers with the protocol established in this study. The protocol implies to incubate the receptor at room temperature or maximally at 37°C. The deglycosylation verified the monomer weight of the CRHR1 fusion protein of ~75 kDa. A weight shift of ~15 kDa following deglycosylation was also seen in other studies (Alken et al. 2005).

5.2 Interaction of CRHR1 with the MAGUKs via the PDZ binding motif

The candidate interaction partners PSD95, SAP97, SAP102, PSD93, and MAGI2 were validated as interaction partners of CRHR1 by Co-IP. The interaction depended on the previously proposed PSD95/discs large 1/zona occludens 1 (PDZ) binding motif S^{412}-T^{413}-A^{414}-V^{415} of CRHR1 (Kornau et al. 1995) as confirmed by the CRHR1-STAVA mutant with its disrupted PDZ binding motif. The C-terminal amino acids S-T-A-V represent a typical class I PDZ binding motif (Kurakin et al. 2007, Lee and Zheng 2010), which is known to bind to PDZ domains e.g. of MAGUKs. Recently in the course of this study, it has been reported that disrupting the PDZ binding motif by deleting the motif or changing amino acids resulted in the abolishment of the indirect interaction of CRHR1 with 5-hydroxytryptamine receptor (5-HT2R), of the interaction of G protein-coupled estrogen receptor 1 (GPR30) with PSD95 and of the interaction of CRHR1 with SAP97 (Magalhaes et al. 2010, Akama et al. 2013, Dunn et al. 2013). Especially adding an alanine to the PDZ binding motif like in the studied CRHR1-STAVA most efficiently disrupted the interaction of CRHR1 with PSD95 PDZ1-3 and implies the advantage that it does not interfere with modifications of S^{412} and T^{413}, which are potential GRK or protein kinase C (PKC) phosphorylation sites (Hauger et al. 2009). The addition of an alanine to the PDZ binding motif of the dopamine transporter caused a dramatic loss of its expression in the striatum (Rickhag et al. 2012).

5.2.1 CRHR1 interacts via the PDZ binding motif with the N-terminal tandem PDZ domains of PSD95

CRHR1 interacted with the N-terminal tandem PDZ domains of PSD95 via its PDZ binding motif. PSD95 is the best studied and most abundant PDZ domain containing protein in the post-synaptic density (PSD) (Sheng and Sala 2001, Cheng et al. 2006). Therefore, it is not surprising that until now more than 25 interaction partners including membrane receptors and ion channels have been detected for PSD95, what is among the MAGUKs clearly the highest

number of known interaction partners. PSD95 interacts mainly via the N-terminal tandem PDZ domains with other proteins (Lim et al. 2002). These PDZ domains interact with the class I PDZ binding motif of the GPCRs SSTR1 and 4 (Christenn et al. 2007, Moller et al. 2013), GPR30 (Akama et al. 2013), brain-specific angiogenesis inhibitor 1 (Lim et al. 2002), of the cell surface neuregulin receptor ErbB-4 (Garcia et al. 2000) and of the ion channels subunits 2B (GluN2B) and 2A (Kornau et al. 1995, Niethammer et al. 1996, Lim et al. 2002, Stiffler et al. 2007) and subunit 2C of NMDA (N-methyl-d-aspartate) receptors (Chen et al. 2006). These findings make it highly reasonable that PSD95 interacts also with CRHR1 via the N-terminal tandem PDZ domains. Since PSD95 increased the amount of GPR30 residing at the cell surface through its interaction with the receptor (Akama et al. 2013), it is possible that the interaction of CRHR1 with PSD95 also influences the receptor amount at the membrane. In the course of this study another group also found that the N-terminal tandem PDZ domains of PSD95 interacted with the GST tagged C-terminus of CRHR1 in a PDZ blot overlay assay confirming the results of this study (Dunn et al. 2013).

5.2.2 Interaction of CRHR1 with SAP97 via the PDZ binding motif and the PDZ2 domain

The GPCR CRHR1 interacted via the PDZ binding motif with SAP97 involving its second PDZ domain but not the first PDZ domain. SAP97 was observed to interact with the class I PDZ binding motif of the 5-HT2AR (Dunn et al. 2014) similar to PSD95, which also interacts with serotonin receptors (Xia et al. 2003a). Since SAP97 overexpression decreased endocytosis of 5-HT2AR, it is possible that the endocytosis of CRHR1 is also influenced by the interaction with SAP97. Moreover, SAP97 is the only member of the PSD95 subfamily of the MAGUKs that directly links to GluA1 (Leonard et al. 1998), this interaction is also mediated via the second PDZ domain of SAP97 and the class I PDZ binding motif, but also via an additional tripeptide sequence SSG at position -9 to -11 at the C-terminus of GluA1 (Cai et al. 2002, von Ossowski et al. 2006a, von Ossowski et al. 2006b). Similar to PSD95, SAP97 interacts via the first and second PDZ domains with the class I PDZ binding motif containing GluN2A and GluN2B (Niethammer et al. 1996). However, in that publication the interaction was not investigated with a mutant with a single PDZ domain. Both proteins, PSD95 and SAP97, interact via their third PDZ domain with the β1-adrenergic receptor (β1AR) as demonstrated by a PDZ array overlay assay (He et al. 2006). These similar binding properties of PSD95 and SAP97 are in contrast to the finding that SAP97 was not able to interact with CRHR1 via the first PDZ domain while the PSD95 PDZ1 showed an

interaction. But as discussed above, SAP97 is the only PSD95-related MAGUK directly interacting with GluA1, underlining the diversity of PDZ domain binding capabilities and supporting the findings in this study. Nevertheless, it has to be examined whether the PDZ1 domain of SAP97 is relevant for the interaction with CRHR1 in the context of the complete protein in relationship with PDZ2 in terms of a supramodule. The N-terminal PDZ domains of PSD95 interact with themselves as a supramodule changing the binding affinity what can imply similar supramodules in other members of the PSD95 subfamily (Long et al. 2003, Feng and Zhang 2009). Whether the third PDZ domain can interact with CRHR1 has to be unraveled in the future with a SAP97 mutant specifically lacking the first two PDZ domains. Recently, in the course of this study, Dunn and colleagues reported also the interaction of SAP97 with CRHR1 (Dunn et al. 2013).

5.2.3 CRHR1 interacts with the MAGUK SAP102

The receptor CRHR1 interacted with the candidate partner SAP102 via one or both of the first two PDZ domains of SAP102 and the class I PDZ binding motif of CRHR1. Several studies reported that SAP102 interacts via the tandem N-terminal PDZ domains with GluN2B (Muller et al. 1996, Lim et al. 2002, Chung et al. 2004) and GluN2C (Chen et al. 2006). Moreover, SAP102 was observed to interact with the class I PDZ binding motif containing ErbB-4 (Garcia et al. 2000) like PSD95 and with 5-HT2CR like PSD95 and SAP97 (Becamel et al. 2004). These studies indicate that for the interaction of CRHR1 with SAP102, the PDZ1 and PDZ2 are probably important what has to be further dissected by corresponding mutants in future experiments. The interaction of GluN2B with SAP102 is disrupted via phosphorylation of a serine of the PDZ binding motif and thereby decreases the neuronal surface expression of GluN2B (Chung et al. 2004), that is why it could be that the S^{412} of the CRHR1 PDZ binding motif can be also phosphorylated disrupting the interaction of CRHR1 with SAP102.

5.2.4 CRHR1 interacts with the MAGUK PSD93

CRHR1 interacted with PSD93 via the PDZ binding motif. Previous studies demonstrated that PSD93 interacts via its N-terminal tandem PDZ domains with the class I PDZ binding motif containing GluN2B (Kim et al. 1996, Fiorentini et al. 2013), GluRδ1 and GluRδ2 (Roche et al. 1999). Furthermore, it was shown that PSD93 interacts via the first two PDZ domains with ErbB-4 (Garcia et al. 2000) and SSTR1 and 4 (Christenn et al. 2007) via the class I PDZ

binding motif interaction like PSD95. That is why it can be hypothesized that PSD93 interacts with CRHR1 also via the first two PDZ domains what has to be proven in the future.

5.2.5 CRHR1 interacts with a member of the MAGI subfamily

MAGI2 has six PDZ domains, which are in an inverted order in comparison to the other MAGUKs (Figure 4). In this study CRHR1 interacted with MAGI2 via the PDZ binding motif and some or all of the PDZ1-5 domains. MAGI2 is known to bind via its PDZ5 domain to class I PDZ binding motif containing GluN2A and C (Hirao et al. 1998) and GluRδ2 (Yap et al. 2003). Besides, MAGI2 interacts also with the cell surface receptor neuroligin 1 and 2 via the class I PDZ binding motif and the PDZ1 of MAGI2, which is functionally relevant for the synaptic maturation (Hirao et al. 1998, Iida et al. 2004, Sumita et al. 2007, Rosenberg et al. 2010). Like SAP97 and PSD95, MAGI2 interacts with its PDZ0 domain with β1AR via the class I PDZ binding motif (Xu et al. 2001, He et al. 2006). In accordance to these results, the interaction of CRHR1 with MAGI2 is highly likely. In the future the responsible PDZ domains have to be further restricted by corresponding mutants. Since the interaction of MAGI2 with GluRδ2 is regulated by PKC phosphorylation (Yap et al. 2003), it can be speculated that also the interaction of CRHR1 with MAGI2 is probably influenced by phosphorylation. In the course of the experiments for this study a PDZ blot overlay assay confirmed the interaction of MAGI2 with the C-terminus of CRHR1 via the PDZ1 domain (Dunn et al. 2013). In that assay the authors found that CRHR1 also interacted with MAGI1 and MAGI3 via their respective PDZ1 domain but the PDZ2-5 domains of these proteins including MAGI2 did not interact in opposite to the finding of the Co-IP in this study. Furthermore, Dunn and colleagues found that CRHR1 interacted with the PDZ3 of PSD95 but not with any PDZ domain of SAP102. This is in contrast to this study, most likely because the authors just used the very C-terminus of CRHR1 and a more artificial system, which does not fully recapitulate protein interactions in a living system.

5.2.6 CRHR1 does not specifically interact with Syntenin-1 and TMEM106B via the PDZ binding motif

Besides the interacting MAGUKs PSD95, SAP97, SAP102, PSD93 and MAGI2, also Syntenin-1 and TMEM106B were identified as potential candidate interacting partners for CRHR1 in a parallel Y2H screen.

CRHR1 did not interact with Syntenin-1, neither under unstimulated conditions, nor following CRH stimulation. Syntenin-1 possesses two PDZ domains and interacts via both domains

with the class II PDZ binding motif containing membrane proteoglycan NG2 (Chatterjee et al. 2008) as well as with the class I PDZ binding motif containing membrane glycoprotein CD6 respectively (Gimferrer et al. 2005). There is another GPCR GPR37, known also as the parkin-associated endothelin-like receptor (Pael-R), which interacts with Syntenin-1 via an atypical class I PDZ binding motif T-H-C resulting in a dramatic increase in the level of GPR37 surface expression in HEK-293 cells (Dunham et al. 2009). Also the glycine transporter subtype 2 (GlyT2) consisting of 12 transmembrane domains possesses an atypical class I PDZ binding motif T-Q-C and interacted with Syntenin-1 (Ohno et al. 2004). This indicates that PDZ domain depending interactions as discussed earlier are very specific and not arbitrary, because not every PDZ binding motif containing GPCR like CRHR1 interacts with any PDZ domain protein as e.g. Syntenin-1.

The interaction of CRHR1 with TMEM106B was initially confirmed. However, it appeared that this interaction was not specific since CRHR1 mutants lacking the PDZ binding motif or the C-terminal tail originally used in the Y2H screen were still co-immunoprecipitated with TMEM106B. Even the mutant of CRHR1 missing the C-terminal portion including the last two transmembrane domains still did interact. The Co-IP with this CRHR1 mutant was even more effective than with the wild-type what can maybe result from the later detected localization of both proteins in vesicles. TMEM106B was demonstrated to localize to late endosome and lysosomes (Lang et al. 2012), that is why it can lead to the assumption that also the CRHR1 mutant concentrated at these compartments. The interaction seemed to be based on an artificial interaction probably due to the fact that both proteins are transmembrane proteins. At least the interaction was clearly not PDZ binding motif dependent.

Taken together, the first aim of the study was accomplished, namely some of the candidate interactions proteins were verified by Co-IP and their interacting domains were successfully determined. These results using an additional and independent expression system (i.e. mammalian cells) underscore the importance of validating interaction partners at least with one additional method e.g. Co-IP. CRHR1 interacted with different MAGUKs via specific PDZ domains implying a possible functional relevance of individual interactions in terms of different functions e.g. internalization, de- and re-sensitization or scaffolding to particular signaling molecules in the synapse environment. That is especially important because the MAGUKs are to a certain extent functionally redundant but on the other hand many MAGUKs have their own specific function at a particular developmental stage (Zheng et al. 2011). Besides, there is clear spatial overlap but not every MAGUK is present in each spine including the possibility of a MAGUK dependent individual CRHR1 signaling. Meanwhile, it can be hypothesized that a single MAGUK can enhance the oligomerization of the receptor

since CRHR1 binds to different PDZ domains in one MAGUK as e.g. PSD95 or MAGI2. Oligomerized receptors could simultaneously bind to different MAGUKs at the same time in a given spine. Thus, these specific interactions between CRHR1 and a subset of MAGUKs could be essential for particular receptor functions in the neuron.

5.3   CRHR1 clusters with the MAGUKs depending on the PDZ binding motif

MAGUKs per se are known for multimer formation and are important for receptor clustering at the PSD (El-Husseini et al. 2000b, Rademacher et al. 2013), where they function as scaffolds organizing cellular signaling (Good et al. 2011). PSD95 supports 5-HT2A and 5-HT2C receptor sorting to apical dendritic spines and maintains receptor turnover *in vivo* (Xia et al. 2003b, Abbas et al. 2009). This sorting shows that PSD95 promotes the subcellular distribution of a GPCR through the interaction with its PDZ domains. In general, to assess PDZ domain dependent interactions in terms of effects on subcellular localization, clustering assays can be performed in which putative interaction partners are co-expressed in heterologous cell systems to examine co-clustering of interacting proteins. In COS-1 cells for example PSD95 promoted clustering of Shaker-type K+ channels (Kv1.4) via the second PDZ domain (Imamura et al. 2002). To assess the functional relevance of the PDZ binding motif dependent interaction, a clustering assay was executed in HEK293 cells. CRHR1 clustered with the MAGUKs PSD95, SAP97, SAP102, PSD93 and MAGI2 via the PDZ binding motif. When co-expressed CRHR1 showed a different cellular distribution than expressed alone: It was not localized equally at the membrane but in vesicles in the soma and partially at the membrane as patches together with respective interaction protein. This clustering pattern depended on the PDZ binding motif of CRHR1 because the mutant CRHR1 variant with a disrupted PDZ binding motif prevented the clustering. This altered protein localization can be due to an arrestment of the receptor in the secretory route because the interacting proteins inhibit the trafficking to the membrane after translation. On the other hand, it could be that MAGUKs enhance the oligomerization of the receptor and the internalization of CRHR1 patches from the membrane. Thus, it is likely that the interaction of CRHR1 with the MAGUKs influences the trafficking to distinct cellular compartments. Previous studies demonstrated that PSD95 promotes cell surface clustering with class I PDZ binding motif containing GluN2B in COS-7 cells (Kim et al. 1995, Kim et al. 1996). PSD93 showed also clustering activity in COS-7 cells with class I PDZ binding motif containing Kv1, GluN2B (Kim et al. 1996, Ogawa et al. 2008) and in HeLa cells with class I PDZ binding motif

containing iGluR δ2 (Roche et al. 1999). Similarly, MAGI2 clusters in COS-7 cells with the δ2 glutamate receptor containing a class I PDZ binding motif (Yap et al. 2003). Furthermore, the clustering activity of SAP97 was described in ER-derived intracellular vesicles for GluN2A in COS-7 cells (Mauceri et al. 2007) and for Kv channels in COS-1 and COS-7 cells (Tiffany et al. 2000, Murata et al. 2001). In contrast, SAP97 and PSD95 showed in this study cytosolic and membranous distribution patterns when co-expressed with CRHR1. For the clustering of Kv1.4 with PSD95 (El-Husseini et al. 2000b, Imamura et al. 2002) it was described that palmitoylation but not multimerization was necessary (Christopherson et al. 2003). Moreover, Chetkovich and colleagues found that the palmitoylated α-isoform of PSD95 clusters membranously and the non-palmitoylated β-isoform clusters perinuclearly with Kv1.4 (Chetkovich et al. 2002). PSD95 palmitoylation is a highly reversible process (el-Husseini Ael and Bredt 2002), therefore, it is reasonable that PSD95 clusters were found at the membrane and in the cytosol in this study because the palmitoylation site containing α-isoform was used. But for SAP97 the non-palmitoylated L27 containing β-isoform was used in the experiments, therefore, it has to be speculated that the palmitoylation was probably compensated by unknown mechanisms. For PSD93 the palmitoylation site containing b-isoform was used, therefore, it is unclear why only cytosolic clusters were found. This is also in contrast to another report which demonstrated that PSD93 mediates cell surface Kv ion channel clustering in COS-7 cells (El-Husseini et al. 2000b, Ogawa et al. 2008). SAP102 contains N-terminal cysteines, which normally represent palmitoylation sites, but no palmitoylation was observed (El-Husseini et al. 2000b, Funke et al. 2005). This is in line with the cytosolic distribution pattern of the clusters in this study and the previously reported intracellular pattern of clustering of Kv1.4 with SAP102 (El-Husseini et al. 2000b). MAGI2 has no palmitoylation site (Zheng et al. 2011), thus the detected membranous clustering of MAGI2 with CRHR1 must have other reasons. This finding is in line with previous studies, which found that MAGI2 was co-localized with GluN2A at the membrane in HEK293 cells (Hirao et al. 1998).

The second objective to identify the functional relevance of the PDZ binding motif dependent interaction *in vitro* was achieved. The clustering pattern, which depended on an intact PDZ binding motif, shows the functional relevance of the interaction between CRHR1 and the MAGUKs. Considering the localization of MAGUKs in the PSD, it can be speculated that the MAGUKs are responsible to cluster CRHR1 to the PSD and to bring them in close vicinity with specific signaling molecules.

5.4 Co-expression of CRHR1 with the MAGUKs *in vivo*

The Y2H screen can produce false positive interaction candidates in comparison to the endogenous situation since in this screen proteins can be joined that anatomically are not necessarily expressed in the same cell. Therefore, the third aim of the study was to investigate the co-expression of CRHR1 with the candidate interaction partners *in vivo.*

For this purpose, the mouse as a model organism is very helpful because the mouse is genetically similar to the human being (Venter et al. 2001) and wild-type (WT) and genetically modified mice give insights into brain functions and pathogenesis of diseases (Watase and Zoghbi 2003, Kalueff et al. 2007, Ito et al. 2012).

In this study the mRNA of CRHR1 and interaction partners was co-localized in brain regions like the olfactory bulb, cortex, hippocampus and the cerebellum of the adult mouse brain. This co-expression was also verified on the cellular level where CRHR1 mRNA co-localized with mRNA of interaction partners in pyramidal neurons of hippocampal CA1, in cells of the cortex and of the reticular thalamic nucleus. CRHR1 and MAGUKs were expressed throughout the murine brain resembling the previously reported broad expression for CRHR1 (Chen et al. 2000b, Van Pett et al. 2000, Refojo et al. 2011, Kuhne et al. 2012), PSD95 (Brenman et al. 1996, Fukaya and Watanabe 2000, Ohnuma et al. 2000), PSD93 (Brenman et al. 1996), SAP97 (Muller et al. 1995), SAP102 (Muller et al. 1996) and MAGI2 (Hirao et al. 2000, Yamada et al. 2003). These findings make it highly reasonable that a physical interaction of CRHR1 with MAGUKs is possible further supporting a physiological relevance of the identified interaction.

Alterations in the expression of MAGUKs in the brain were found in psychiatric illnesses (Kristiansen and Meador-Woodruff 2005), simultaneously CRHR1 is known to modulate emotionality including anxiety-related behavior. Recently, our laboratory also found that CRHR1 mediates anxiogenic and anxiolytic effects by neurotransmitter-specific neuronal expression (Refojo et al. 2011). Thus, it is possible that alterations of the CRHR1 interaction with MAGUKs are responsible for emotional disturbances in psychiatric diseases disclosing new opportunities for developing therapeutic treatments.

5.5 Characterization of dissociated primary neurons in culture

To address the role of the PDZ binding motif of CRHR1 with respect to its cellular localization in a more physiological model than HEK293 cells, primary hippocampal neurons were studied in terms of the expression of MAGUKs, CRHR1 and its ligand CRH to investigate the physiological relevance of this cell culture model.

In general, dissociated primary cell culture displays physiological events in a similar developing time course as neurons in an *in vivo* context regarding maturation (Mains and Patterson 1973, Bartlett and Banker 1984a, Ichikawa et al. 1993), synaptogenesis (Bornshein and Model 1972, Yavin and Yavin 1977, Bartlett and Banker 1984b, Kuroda et al. 1992), polarization (Dotti et al. 1988, Powell et al. 1997) and synaptic excitation (Habets et al. 1987, Ogura et al. 1987, Murphy et al. 1992). Primary neurons establish a functionally active network within they can communicate between pre-synaptic axon terminals and post-synaptic dendritic spines. Excitatory synapses harbor the PSD, which is composed of cytoskeletal and scaffold proteins adjacent to the postsynaptic membrane (Ziff 1997). That is why primary neuronal cultures are widely used to investigate the physiology of neurons (Giordano and Costa 2011).

5.5.1 Investigation of CRHR1/CRH system in primary neurons

Primary hippocampal neurons turned out to be a suitable cell culture model to study the interaction of CRHR1 with MAGUKs since the co-expression of the interacting proteins was verified on the mRNA level. Furthermore, primary neurons emerged to be specific for CRHR1 and CRH manipulations since the other components, CRHR2 and urocortin 1-3, of the CRHR1/CRH system were not detectable. The co-expression of CRHR1 and the interaction partners in primary hippocampal cell culture was supported by the co-expression in the adult mouse brain detected by *in situ* hybridization. These results are in agreement with previous studies describing the mRNA expression in primary neurons of CRHR1 (Bayatti et al. 2003), PSD95 (Tohda 2014), PSD93 (Zhang et al. 2010), SAP97 (Rumbaugh et al. 2003, Yokomaku et al. 2005) and SAP102 (Cui et al. 2007). For MAGI2, a broad protein expression was observed in the brain especially in the cortex, hippocampus and the cerebellum (Ohtsuka et al. 1999, Hirao et al. 2000, Yamada et al. 2003, Yap et al. 2003, Ihara et al. 2012), the mRNA expression was also detected in the brain but has been investigated only at embryonal stage of the whole mouse brain until now (Pfister et al. 2003). That is why this is the first study showing the mRNA expression of MAGI2 in primary hippocampal neurons. Besides, this study revealed a comprehensive overview of mRNA expression of PSD95 subfamily members of the MAGUK family including MAGI2 in young and mature primary hippocampal neurons. Except for SAP97 and MAGI2 the mRNA expression of investigated MAGUKs was upregulated in mature neurons resembling the upregulation of MAGUKs during maturation of neurons in the intact mouse brain (Oliva et al. 2011, Zheng et al. 2011). Primary neurons of the hippocampus resemble regarding the composition of neuron types the mature hippocampus with approximately 94 % excitatory glutamatergic pyramidal cells

and 6 % GABAergic (gamma aminobutyric acid) interneurons (Craig et al. 1993, Benson et al. 1994). The major cell types of the rat cortex are pyramidal, fusiform and multipolar neurons, which are also found in the primary cell culture (Huettner and Baughman 1986, McConnell 1995). These cells can be divided morphologically in 80 % excitatory glutamatergic pyramidal neurons and 20 % GABAergic interneurons (Kriegstein and Dichter 1983, Kawaguchi and Kondo 2002, Noback et al. 2005).

Primary dissociated neurons prepared from genetically modified mice can be used to investigate the specific absence or overexpression of a protein as well as the induced targeted protein expression via the Cre/loxP system (Goebbels et al. 2006, Justice et al. 2008, Taniguchi et al. 2011). The CRH expression in hippocampal and cortical primary neurons was verified and further specified by the usage of the CRH-Cre x Ai9 reporter mouse line, in which every CRH expressing neuron also expresses the tdTomato reporter due to Cre-mediated activation. The increase in CRH positive neurons in hippocampal neurons is in line with the results of the postnatal developing hippocampus (Chen et al. 2001). Immunocytochemistry stainings revealed that CRH is expressed in GABAergic neurons of primary hippocampal and cortical cultures at different time points (0-14 days *in vitro*, DIV). This is in line with the findings that CRH is expressed in GABAergic interneurons within the hippocampal pyramidal cell layer (Chen et al. 2004). Another report showed that CRH positive neurons did not co-express the GABAergic subtype marker calbindin D28-K in the hippocampus (Yan et al. 1998). This is in opposite to the CRH positive neurons, which were co-stained with calbindin D28-K in this study. This discrepancy can be a result of an altered differentiation of neurons in cell culture compared to the physiological environment of brain tissue.

The CRHR1 expression in hippocampal primary neurons was verified by the usage of the CRHR1-GFP reporter mouse line carrying a CRHR1-GFP BAC transgene. Remarkably, 44 % of the neurons were CRHR1-GFP positive. This is in agreement with the high proportion of CRHR1 positive neurons of cultured hippocampal cells detected recently (Sheng et al. 2008). However, it has to be considered that this and other studies (Chen et al. 2000b) used antibody staining to detect endogenous CRHR1. This in opposite to the experimental experience in our laboratory as discussed below. The staining with the glutamatergic marker VGluT1 (vesicular glutamate transporter 1) revealed that every CRHR1 positive neuron was glutamatergic what is in line with recent findings in our group (Refojo et al. 2011). Simultaneously also 11 % of the calbindin D28-K positive neurons were CRHR1 positive what is in accordance with publications demonstrating the co-expression of the glutamatergic marker VGluT1 with the GABAergic subtype marker calbindin D28-K in the rat nucleus accumbens (Hartig et al. 2003), in the pedunculopontine nucleus (Martinez-

Gonzalez et al. 2012) and in the mouse spinal dorsal horn (Punnakkal et al. 2014). Moreover, the calcium-binding protein calbindin D28-K is only partially co-localized with GABA in neurons of the hippocampus and the cortex (Rogers 1992). Therefore, it seems reasonable that CRHR1 was expressed in glutamatergic and partly simultaneously calbindin D28-K positive hippocampal neurons. In contrast to the CRHR1-GFP reporter line utilized in this study, CRHR1 expression was not detectable in primary cell cultures derived from a mouse model, which has the endogenous CRHR1 tagged with GFP or has the endogenous CRHR1 replaced by LacZ (β-galactosidase gene) transcribed under the CRHR1 promoter (data not shown) (Refojo et al. 2011, Kuhne et al. 2012). This discrepancy might be related to the GFP overexpression in BAC transgenic mice compared to the low endogenous expression levels in the GFP of LacZ knock-in mice.

In summary, the fourth objective was accomplished demonstrating that the CRHR1/CRH system could be investigated with respect of the interaction with MAGUKs in primary hippocampal neurons because the co-expression of the mRNA was validated by different techniques.

Furthermore, the low endogenous expression of CRHR1 mRNA found via qPCR and the fact that the two endogenous reporter mouse lines were not sensitive enough to detect CRHR1 expression in primary cultures, is consistent with the fact that no antibody against CRHR1 was able to detect the endogenous level of CRHR1 neither in slices nor in primary neurons (see also: (Refojo et al. 2011). This is in line with the general difficulty to raise antibodies against GPCRs, maybe because of the short length and compact conformation of the extracellular regions (Fredholm et al. 2007). Only after overexpression specific antibodies against CRHR1 are sensitive enough to detect tagged variants of CRHR1. Therefore, it was necessary to overexpress wild-type CRHR1 or the PDZ binding motif mutant in primary hippocampal neurons to assess the functional impact of the PDZ binding motif.

5.6 Overexpression of CRHR1 to functionally characterize the PDZ binding motif

Primary neurons are widely used because they are accessible by genetic manipulation in terms of overexpression and knockdown of a protein of interest. Nevertheless, they are not always easy to transfect and the efficacy is reduced with the age of the neurons (Huang and Richter 2007). There are different methods to transfect with distinct efficacy at specific time points like the Ca^{2+}-phosphate co-precipitate method, lipofection, electroporation and nucleofection (Martinez and Hollenbeck 2003, Jiang and Chen 2006, Zeitelhofer et al. 2007,

Karra and Dahm 2010). The challenge of transfecting neurons is based on the fact that neurons are non-dividing cells, but nevertheless the nucleotides have to pass the cell membrane and the nucleus membrane.

Especially CRHR1 showed a low transfection efficacy in preliminary experiments (data not shown) indicating that CRHR1 is might be toxic by itself after overexpression. Therefore, different mutants of CRHR1 in terms of function and structure were designed to evaluate the intrinsic toxicity of CRHR1 in primary neurons. The transfection in HEK293 cells showed that all mutant CRHR1 variants resided in the membrane except CRHR1Δ 2TM lacking the C-terminal portion including the last two transmembrane domains of the receptor, which was located in intracellular vesicles. Membrane proteins get sorted and transported to the membrane after translation by passing different membrane compartments after the ER (Balch et al. 1994, Barlowe 2003, Mellman and Nelson 2008). Many sorting signals within the membrane proteins have been identified in the C-terminus (Parmar et al. 2014) and rely on basic (Giraudo and Maccioni 2003) or acidic residues as for the angiotensin II receptors (Sevier et al. 2000, Stockklausner et al. 2001, Zhang et al. 2011). But recently it was also shown that a triple arginine motif in the third intracellular loop (IC3) functions as an ER export signal for α(2B)-AR (Dong et al. 2012). Since the CRHR1Δ C-term lacking the C-terminus was localized in the membrane and the IC3 of CRHR1 does not contain a triple arginine motif, the vesicular clustering of CRHR1Δ 2TM probably has other reasons. Many proteins get glycosylated at asparagine (N) residues at the motif N-X-S/T in the ER lumen during their translation (Duvernay et al. 2005, Mellman and Nelson 2008). Since CRHR1Δ 2TM lacks the last extracellular domain, which does not contain a motif for N-glycosylation, this is also not the reason. But it can be speculated that the truncated receptor was misfolded and stuck in the ER or lysosomes for subsequent degradation. This is in accordance to the more effective Co-IP with this CRHR1 mutant and TMEM106B which was demonstrated to localize to late endosome and lysosomes (Lang et al. 2012). This can lead to the assumption that CRHR1Δ 2TM was also concentrated at these compartments.

In conclusion, it was possible to overexpress the WT and most of the mutant variants of CRHR1 with the anticipated membranous subcellular localization. No signs of toxicity were detected after overexpression.

5.6.1 CRHR1 mutants show similar cAMP signaling properties in HEK293 cells

The functionality of CRHR1 constructs was investigated with regards to the receptors´ signal transduction pathways. CRHR1 preferentially signals via Gsα which couples to the IC3 resulting in adenylyl cyclase activation and cAMP production (Hauger et al. 2006, Hillhouse

and Grammatopoulos 2006, Hauger et al. 2009). To assess the CRHR1 signaling of CRHR1 WT and mutants in HEK293 cells, cAMP production was measured. Surprisingly, every mutant showed a cAMP production capacity largely comparable to the WT receptor with exception of CRHR1Δ 2TM. Papadopoulou and colleagues demonstrated a 50 % reduction of cAMP production in a mutant similar to myc-GFP-CRHR1-S301V following urocortin 1 stimulation (Papadopoulou et al. 2004). In agreement with these results the CRHR1Δ 2TM, which contains only aa 1-298, showed a strong reduction of cAMP production, probably due to the absence of the functional IC3 (aa 296-306), the G coupling site. In contrast, myc-GFP-CRHR1-S301V did not show a significant reduction of cAMP production although the experiments were conducted in the same cellular system: HEK293 cells. The only difference was the way of CRHR1 stimulation which was carried out in this study with CRH instead of urocortin 1. In human myometrium urocortin 1 but not CRH activates the mitogen-activated protein kinase (MAPK) signaling (Grammatopoulos et al. 2000). This might explain why CRH acts also in HEK293 cells differently regarding cAMP production compared to urocortin 1 as revealed in this study. Interestingly, the mutant CRHR1-STAVA, which has a disrupted PDZ binding motif, showed no reduction of cAMP production implying no relevance of the PDZ binding motif for this pathway, at least under the used experimental conditions.

5.6.2 Overexpression of mutant CRHR1 variants *in vitro* and *in vivo*

To identify the physiological role of the interaction in mature neurons, WT and mutant CRHR1 variants were first overexpressed in young neurons at DIV 6 with the calcium-phosphate protocol. As in HEK293 cells CRHR1 variants were similarly distributed throughout the neuronal membrane and in vesicular structures most likely representing the ER-Golgi network. Only CRHR1Δ 2TM showed a strong accumulation in perinuclear vesicles and was not distributed into the neurites. But at later time points - DIV 14 and thereafter - when primary neurons are terminally differentiated harboring dendritic spines (Barnes and Polleux 2009), the overexpression with the calcium-phosphate protocol was not successful in terms of efficacy and cell survival. In general, neurons are difficult to transfect because they are postmitotic and the transfected DNA has to gain access to the non-dividing nucleus (Craig 1998). At least in young neurons CRHR1 and its variants had no toxic effect when overexpressed, but it was not possible to transfect mature neurons in this way.

To analyze cell survival in a more physiological context, WT and mutant CRHR1 variants were overexpressed *in vivo* by *in utero* electroporation. Independent of the transfected CRHR1 variant the expression efficacy was very low, nevertheless, it was possible to overexpress CRHR1 also *in vivo* excluding a major intrinsic toxicity of CRHR1 on neurons.

To establish an overexpression in primary neurons at later time points, different approaches were tested. The transfection efficacy and cell survival of matured neurons was neither improved by the calcium-phosphate protocol with different incubation times, nor by baculovirus based transduction, nor by a modified lipofection protocol, nor by two different ways of electroporation.

Virus-based transfection methods have the advantages that viruses can infect non-dividing cells with a high efficiency resulting in stable expression of a gene of interest. Therefore, primary neurons can also be transduced with lentiviruses or adeno-associated viruses (Janas et al. 2006, Zhang et al. 2006, Buning et al. 2008, Royo et al. 2008). Consequently, viral transduction in primary neurons was performed using lentiviral vectors, since it was shown that they can efficiently and stably infect non-dividing cells (Naldini et al. 1996, Blomer et al. 1997). The lentiviral transduction of primary hippocampal neurons resulted in highly efficient overexpression of CRHR1 in healthy looking neurons what was confirmed by a control GFP virus and respective immunocytochemistry. Both CRHR1 WT and CRHR-STAVA appeared in a punctuated distribution pattern, accumulated along the neuronal body and located in spines. But surprisingly the fluorescent puncta did only co-localize adjacent to markers for the pre-synapse, the inhibitory and excitatory post-synapse and the interaction proteins PSD95 and SAP97 without any direct overlap. This distribution pattern was fully independent of the PDZ binding motif. The utilization of an antibody against CRHR1, which also worked in cell culture after CRHR1 overexpression, confirmed the CRHR1 identity of the puncta after virus transduction and GFP staining. Unusually, CRHR1 variants did not show any overlap with a synaptic marker indicating a potential artefact related to the overexpression. Recently a limited overlap of SAP102 with its interacting partner Neurobeachin in hippocampal neurons was shown (Lauks et al. 2012). The pattern of limited overlap is similar to the herein found adjacent distribution demonstrating that a complete overlap is not always necessary for interacting proteins as seen with PSD95 and SAP97. Furthermore, CRHR1 might be located extrasynaptically like NMDA receptors (Petralia et al. 2010) or probably co-localizes with the interactor proteins only after stimulation with CRH. Preliminary experiments with CRH treatment were not successful (data not shown) and have to be repeated.

However, due to the absence of a significant overlap of CRHR1-positive puncta with any tested marker and to confirm or falsify these unexpected results another viral expression system was used.

5.6.3 CRHR1 can be expressed in primary neurons and localizes to the plasma membrane

Adeno-associated viral (AAV) vectors transduce neurons *in vivo* with low toxicity even when they are entirely differentiated (Royo et al. 2008). It was not possible to reproduce the punctated pattern of WT and mutant CRHR1s in primary neurons after transduction with AAVs. Instead, WT and mutant CRHR1s were distributed throughout the plasma membrane within the somata, dendrites and axons. The staining was enhanced using an anti-GFP antibody and confirmed by anti-CRHR1 antibody staining. The receptor resided in the excitatory post-synapse independent of the PDZ binding motif but not in the inhibitory post-synapse or the pre-synapse. The lack of overlap with the inhibitory post-synaptic marker gephyrin indicates specifity for the localization of the receptor in the excitatory post-synapse. Studies using antibodies against endogenous CRHR1 also demonstrated that CRHR1 is localized within dendritic spine heads of excitatory synapses of the stratum oriens in the hippocampus (Chen et al. 2004, Chen et al. 2010) although in our laboratory CRHR1 antibodies did not work as already discussed. In contrast to CRHR1 localization, CRH is released from vesicles of axon terminals surrounding the cell somata and axon initial segments (AIS) of pyramidal cells of the pyramidal cell layer (Chen et al. 2004). This release site is > 100 µm away from the localization of CRHR1. Another consideration is that CRH is probably released at inhibitory synapses since it is expressed in GABAergic interneurons but CRHR1 did not reside in the inhibitory post-synapse. This fact and the distant releasing site make it highly reasonable that volume transmission takes place including diffusion of CRH over a relatively wide distance (Chen et al. 2012a).

The identical distribution of WT and mutant CRHR1s could be related to the overexpression or to the non-activated state of the neurons. Moreover, it could be that the low expressed endogenous CRHR1 in the cultured neurons was sufficient to cluster with the overexpressed CRHR1-STAVA mutant as with the CRHR1 WT, thereby determining the localization of exogenously expressed receptors. This problem was also disturbing Co-IP experiments between CRHR1-STAVA and PSD95 in Neuro2A cells, which endogenously express CRHR1 (data not shown). Preliminary results did not show a PDZ binding motif-dependent localization of the receptor in CRHR1 lacking neurons. However, this has to be investigated in more detail in additional experiments. Furthermore, CRHR1 directly was co-localized with the interacting partners PSD95 and SAP97 in spines, however, also independently of the PDZ binding motif. Others also found CRHR1 co-localized with PSD95 on dendritic spine heads using murine brain sections (Chen et al. 2004, Chen et al. 2010). But it has to be considered that these studies used an antibody against the endogenous CRHR1 which was

not working in our laboratory as discussed in paragraph 5.5.1. Similarly, we could recently show that PSD95 also interacted with the PDZ binding motif containing GPCR SSTR1 and co-localized with SSTR1 in dendritic spines (Moller et al. 2013). This study demonstrates that CRHR1 is localized at the excitatory PSD where the interacting MAGUKs can act as scaffolds for the receptor.

The co-localization in mature spines indicates a possible physiological role of the interaction between CRHR1 and PSD95 and SAP97. Together with the clustering assay our results make it highly reasonable that the MAGUKs have the potential to promote clustering of CRHR1 in the PSD via the PDZ binding motif. MAGUKs can perhaps anchor CRHR1 in clusters to the cell surface and possibly serve also as downstream signaling molecules and inhibit for example the internalization as it was revealed for PSD95 and 5-HT2A receptors (Xia et al. 2003a). But until now the PDZ binding motif of CRHR1 did not determine the localization of the receptor in primary neurons after overexpression including that the fifth aim was not fully fulfilled. The same controversial situation was observed for NMDARs, which were found to cluster at synapses independently of PDZ interactions via PSD95 (Migaud et al. 1998, Passafaro et al. 1999), but simultaneously the functional localization of NMDARs in synapses was dependent on PSD95 in terms of synaptic activity, entry to the synapse and internalization (Steigerwald et al. 2000, Roche et al. 2001, Prybylowski et al. 2002). These differences can be explained by the redundancy of the PSD95 subfamily and compensations through other members in knockout situations. Nevertheless, in comparison to NMDARs, it can be can lead to the assumption that only the functional localization of CRHR1 dependents on PDZ interactions via the MAGUKs. To further decipher this issue a CRHR1-STAVA mouse line could help to avoid the artificial viral overexpression used in this study and to investigate changes of CRHR1 localization and function in the synapse in a physiological context.

5.7 Hypothesis of CRHR1 interaction pathways and outlook

The co-localization of CRHR1 with MAGUKs in the PSD could be a connection of CRH-related phenomena described in the literature like spine dynamics what will be discussed in the following.

CRHR1 has been demonstrated to play a role in spine dynamics. Following CRH treatment or stress, spine loss is induced, an effect that can be abolished by blocking CRHR1. For this process destabilization of spine actin is necessary what is triggered by CRH-mediated RhoA (Ras homolog gene family member A) activation (Chen et al. 2008, Chen et al. 2012b). In

this context, it has been shown that the SH3/GuK domains of the MAGUKs are indirectly linked to actin through proteins of the PSD including guanylate kinase-associated protein (GKAP) and SPAR (spine-associated Rap guanosine triphosphatase-activating protein) (Naisbitt et al. 2000, Pak et al. 2001, Gerrow et al. 2006). It can be hypothesized that CRHR1 is able to induce destabilization of spine actin because of its interaction with MAGUKs that link the receptor to actin and organize the CRHR1 signaling to the appropriate compartment what needs to be investigated in the future.

The calcium-independent cell adhesion molecule Nectin-3 was also found to link CRHR1 signaling to stress-induced memory deficits and spine loss (Wang et al. 2013). Accordingly, CRH treatment reduced Nectin-3 levels what resulted in a decreased number of dendritic spines. Nectin-3, which contains a class II PDZ binding motif, mediated the effect via the actin binding protein afadin, to which it was shown to bind via the PDZ domain (Takahashi et al. 1999, Giagtzoglou et al. 2009). As discussed above, CRHR1 could be coordinated to actin via MAGUKs as Nectin-3 is linked to actin via afadin and this spatial arrangement could be required for the induced spine loss.

On the other hand, there is evidence that the CRHR1-CRH-mediated spine loss needs network activity and the activation of NMDA receptors results in activation of the calcium-dependent enzyme calpain, which leads to the breakdown of the spine cytoskeleton (Andres et al. 2013). Additionally CRH depresses NMDA-mediated current via the CRHR1 (Sheng et al. 2008). Since every identified MAGUK interacts with NMDA receptors (Kornau et al. 1995, Kim et al. 1996, Muller et al. 1996, Niethammer et al. 1996, Hirao et al. 2000, Lim et al. 2002, Fiorentini et al. 2013), it can be speculated that CRHR1 is connected to NMDA receptors via MAGUKs what is maybe important to convey the effect of spine loss and current depression. Obviously many signaling molecules are involved in the CRHR1-CRH-mediated spine loss, but it is reasonable that the signaling is divergent due to different temporal and spatial signal compositions. The described mechanisms are either calcium-dependent or -independent and probably not the only mechanisms. This will require further investigation in the future.

Another report showed that CRHR1 regulates anxiety behavior via the sensitization of 5-HT receptor signaling which requires intact PDZ binding motifs of both receptors (Magalhaes et al. 2010). It was found that SAP97 is not responsible for this effect (Dunn et al. 2014), but it is possible that the sensitization of 5-HT receptors depends on another identified MAGUK which could be responsible for connecting both receptors via different PDZ domains. PSD95 is a good candidate, which has been shown to interact with 5-HT receptors (Xia et al. 2003a). Similarly it has been revealed that PSD95 mediates the interaction of the β1AR with NMDARs (Hu et al. 2000).

CRHR1 is a GPCR of the B1 family and preferentially signals via Gsα resulting in the activation of the adenylyl cyclase/protein kinase A (AC-PKA) pathway (Grammatopoulos et al. 1996, Hauger et al. 2009). However, depending on its cellular localization and context, CRHR1 can activate multiple G proteins triggering a plethora of different second messengers (Grammatopoulos and Chrousos 2002). For example the coupling to Gsα can result in the activation of the ERK1/2 signaling pathway, which can also be provoked by Gqα (Kovalovsky et al. 2002, Papadopoulou et al. 2004). Coupling to Gsα can also result into intracellular calcium mobilization via the activation of AC which activates the ε isoform of phospholipase C (PLCε) (Gutknecht et al. 2009). Until now it is not clear what determines whether CRHR1 signals after G protein coupling via the phospholipase C-protein kinase C (PLC-PKC) pathway or via the AC-PKA cascade (Hauger et al. 2009) but it is known that PSD95 and SAP97 can interact with A-kinase anchoring protein 79/150 (AKAP79/150) (Colledge et al. 2000), which couples PKC and PKA (Klauck et al. 1996, Colledge and Scott 1999). Therefore, it can be speculated that the CRHR1 signaling is influenced by the presence of MAGUKs that aggregate CRHR1 with particular signaling molecules and bring them into proximity of CRHR1.

Furthermore, the effect of the PDZ binding motif on neuronal excitability could be examined *in vivo* in slices of a respective mutant mouse line or after viral mediated re-expression of WT and mutant receptors in a CRHR1 negative background. Recently, it has been shown that the activation of CRHR1 expressed on glutamatergic neurons increases the excitability of CA1 pyramidal neurons by the modulation of voltage-gated ion channels (Kratzer et al. 2013) which could depend on an interaction of CRHR1 with identified MAGUKs.

In summary, CRHR1 interacted with different PDZ domains of MAGUKs via the receptors´ PDZ binding motif. This motif also accounted for the clustering with MAGUKs. Moreover, the receptor was co-expressed with the MAGUKs on cellular level in the adult mouse brain. Hippocampal primary neurons were established as a suitable model for investigating the interactions of CRHR1. In these primary neurons CRHR1 was localized independent of the PDZ binding motif throughout the neuronal plasma membrane including the excitatory post-synapse where it co-localized with the interacting partners PSD95 and SAP97.

6 Appendix

6.1 Index of Figures

6.2 Index of Tables

6.3 List of abbreviations

A	adenine
A	asparagine
AAV	adeno-associated virus
β2AR	β2-adrenergic receptor
5-HTR	5-hydroxytryptamine receptor
AC-PKA	adenylyl cyclase/protein kinase A
ACTH	adrenocorticotropic hormone
AKAP79/150	A-kinase anchoring protein 79/150
AMPA	α-amino-3-hydroxy-5-methyl-4-isoxazole propionic acid
ARIP1	activin receptor-interacting protein 1
AT1R	angiotensin II type 1 receptors
ATP	adenosine triphosphate
Bai1	Brain-specific angiogenesis inhibitor 1
Bp	base pair
BRET	bioluminescence RET
BSA	bovine serum albumin
CA	cornu ammonis area
$CaCl_2$	calcium chloride
CaMKII	calcium/calmodulin-dependent protein kinase II
cAMP	cylic adenosine monophosphate
CaSR	calcium sensing receptor
cDNA	complementary DNA
CMV	cytomegalovirus
CNS	central nervous system
CO_2	carbon dioxide
Co-IP	co-immunoprecipitation
cpm	counts per minute
CREB	cAMP response element-binding protein
CRH	corticotropin-releasing hormone
CRHR1	corticotropin-releasing hormone receptor type 1
CRIPT	cysteine-rich PDZ-binding protein

CRLR	calcitonin receptor-like receptor
CT	calcitonin
C-terminus	carboxyl terminus
CX	cortex
CXCR2	C-X-C chemokine receptor type 2
Da	Dalton
DAPI	4`,6-diamidino-2-phenylindole
Dasm1	Dendrite arborization and synapse maturation 1
DEPC	diethyl pyrocarbonate
DH5α	*E. coli* strain DH5α
DIG	Digoxigenin
DISH	double *in situ* hybridization
DIO	<u>d</u>ouble-floxed <u>i</u>nverse <u>o</u>pen reading frame
DIV	day/dies *in vitro*
DMEM	Dulbecco's Modified Eagle's Medium
DMSO	dimethylsulfoxide
DNA	desoxyribonucleic acid
dNTP	desoxyribonucleotide triphosphate
dpc	day/dies post coitum
DTT	dithiothreitol
EDTA	ethylenediaminetetraacetic acid
E	embryonic day´
E.coli	*Escherichia coli*
EF1α	elongation factor-1α
e.g.	exempli gratia, for example
eGFP	enhanced green fluorescent protein
EPSCs	excitatory post-synaptic currents
ER	endoplasmatic reticulum
ERK	extracellular signal-regulated kinase
EtOH	ethanol
EVH domain	enabled/VASP homology domain
FRET	fluorescent molecules energy transfer
FCS	fetal calf serum
GABA	gamma aminobutyric acid
GASPs	GPCR-associated sorting proteins
GAPs	GTPase activating proteins

GC	glucocorticoid
gc	genome copies
GDP	guanosine diphosphate
GEFs	GTP exchange factors
GIP	GPCR interacting proteins
GluA	AMPA receptor subunit
GluK5	glutamate kainate receptor 5
GluN	NMDA receptor subunit
GluRδ2	glutamate receptor ionotropic, delta
GlyT2	glycine transporter subtype 2
GKAP	guanylate kinase-associated protein
GPR30	G protein-coupled estrogen receptor 1
GPCR	G protein-coupled receptors
G proteins	GTP-binding proteins
GRKs	G protein-coupled kinases
GTP	guanosine triphosphate
GuK	guanylate kinase like domain
HBSS	Hanks´s balanced salt solution
HCl	hydrochloric acid
HEK293	Human embryonic kidney cell line
HEPES	4-(2-Hydroxyethyl)piperazine-1-ethanesulfonic acid
HMWCs	high molecular weight complexes
HP	hippocampus
HPA	hypothalamic-pituitary-adrenal
hybmix	hybridization-mix
IC3	third intracellular loop
i.p.	intraperitoneal
IB	immunoblot
IF	immunofluorescence
IP	immunoprecipitation
IP3	inositol-triphosphate
IRES	internal ribosome entry site
ISH	*in situ* hybridization
Kb	kilobase pairs
Kir2.2	ATP-sensitive inward rectifier potassium channel 12
Kv	Shaker-type K+ channel

kDa	kilodalton
KO	knockout
L27	MAGUK Lin-2 + Lin-7
LacZ	β-galactosidase gene
LB	lysogeny broth
LCP3	larval cuticle protein 3
LRP4	LDL receptor-related protein 4
LTD	long-term depression
LTP	Long-term potentiation
M71OR	mouse 71 olfactory receptor
MAGI	membrane-associated guanylate kinase inverted
MAGI2	membrane-associated guanylate kinase, WW and PDZ domain containing 2
MAGUKs	membrane-associated guanylate kinases
MAP	microtubule-associated protein
MAPK	mitogen-activated protein kinase
MEM	Minimal Essential Medium
MEK	mitogen-activated protein kinase kinase
$MgCl_2$	magnesium chloride
mGluRs	metabotropic glutamate receptors
MOI	multiplicity of infection
mRNA	messenger ribonucleic acid
NaCl	sodium chloride
NBT/BCIP	nitroblue tetrazolium /5-bromo-4-chloro-3-indolyl-phosphate
NH_4OAc	Ammonium acetate
nNOS	neuronal nitric oxide synthase
NMDA	N-methyl-d-aspartate
NPY2-R	Neuropeptide Y receptor type 2
o.n.	overnight
OD	optical density
pA	polyadenylation signal
Pael-R	endothelin-like receptor
PBS	phosphate buffered saline
PCR	polymerase chain reaction
PDZ	PSD95/discs large/zona occludens 1
PFA	paraformaldehyde

PLC-PKC	phospholipase C- protein kinase C
PMCA	plasma membrane calcium ATPase isoform
pnd	postnatal day
PP2A	protein phosphatase 2A
PS	population spikes
PSD	post-synaptic density
PSD95	postsynaptic density protein 95
PVDF	polyvinylidene difluoride
PVP40	polyvinylpyrrolidone 40
qPCR	quantitative real time PCR
RAMPs	receptor activity-modifying proteins
RET	resonance energy transfer
RFP	red fluorescent protein
RGS	regulators of G protein signaling
RhoA	Ras homolog gene family member A
RNA	ribonucleic acid
RNasin	RNAse-inhibitor
RPL-19	ribosomal protein L19
RT	room temperature
RTN	reticular thalamic nucleus
SALM	Synaptic adhesion-like molecules
SAP	synapse-associated protein
SDS	sodium dodecyl sulfate
SH3	SRC homology 3
SPAR	spine-associated Rap guanosine triphosphatase-activating protein
S-SCAM	synaptic scaffolding molecule
SSTR	somatostatin receptor
SSC	standard saline citrate
Syntenin-1	syndecan binding protein 1, SDCBP
TAE	Tris acetate EDTA
TBS	Tris buffered saline
TBS-T	Tris buffered saline with Tween
TEA	triethanolamine
TMEM106B	transmembrane protein 106B
Tris	tris(hydroxylmethyl)-aminomethan
TSA mix	tyramide-biotin

UCN1	Urocortin 1
V1bR	vasopressin V1b receptor
VGluT1	vesicular glutamate transporter 1
VIP	vasoactive intestinal peptide
VPAC1	Vasoactive intestinal polypeptide type-1 receptor
vsvg	vesicular stomatitis virus
WB	Western blot
WPRE	woodchuck hepatitis virus posttranscriptional regulatory element
WW	two tryptophan residues
WT	wild-type
x	symbol for crosses between mouse lines
Y2H	yeast two-hybrid
ZO-1	zona occludens 1

Please note that all units defined by the International System of unis (SI) are not considered in the list of abbreviations.

7   References

Abbas, A. I., P. N. Yadav, W. D. Yao, M. I. Arbuckle, S. G. Grant, M. G. Caron and B. L. Roth (2009). "PSD-95 is essential for hallucinogen and atypical antipsychotic drug actions at serotonin receptors." J Neurosci **29**(22): 7124-7136.

Abraham, W. C., B. Logan, J. M. Greenwood and M. Dragunow (2002). "Induction and Experience-Dependent Consolidation of Stable Long-Term Potentiation Lasting Months in the Hippocampus." The Journal of Neuroscience **22**(21): 9626-9634.

Agnati, L. F., K. Fuxe and S. Ferre (2005). "How receptor mosaics decode transmitter signals. Possible relevance of cooperativity." Trends Biochem Sci **30**(4): 188-193.

Akama, K. T., L. I. Thompson, T. A. Milner and B. S. McEwen (2013). "Post-synaptic density-95 (PSD-95) binding capacity of G-protein-coupled receptor 30 (GPR30), an estrogen receptor that can be identified in hippocampal dendritic spines." J Biol Chem **288**(9): 6438-6450.

Akum, B. F., M. Chen, S. I. Gunderson, G. M. Riefler, M. M. Scerri-Hansen and B. L. Firestein (2004). "Cypin regulates dendrite patterning in hippocampal neurons by promoting microtubule assembly." Nat Neurosci **7**(2): 145-152.

Alberts, B. A. J., Peter Walter, Julian Lewis, Martin Raff, Keith Roberts, Nigel Orme (2007). "Molecular Biology of the Cell." Taylor & Francis Ltd **5th Revised edition**.

Aldenhoff, J. B., D. L. Gruol, J. Rivier, W. Vale and G. R. Siggins (1983). "Corticotropin releasing factor decreases postburst hyperpolarizations and excites hippocampal neurons." Science **221**(4613): 875-877.

Alken, M., C. Rutz, R. Kochl, U. Donalies, M. Oueslati, J. Furkert, D. Wietfeld, R. Hermosilla, A. Scholz, M. Beyermann, W. Rosenthal and R. Schulein (2005). "The signal peptide of the rat corticotropin-releasing factor receptor 1 promotes receptor expression but is not essential for establishing a functional receptor." Biochem J **390**(Pt 2): 455-464.

Andres, A. L., L. Regev, L. Phi, R. R. Seese, Y. Chen, C. M. Gall and T. Z. Baram (2013). "NMDA receptor activation and calpain contribute to disruption of dendritic spines by the stress neuropeptide CRH." J Neurosci **33**(43): 16945-16960.

Angers, S., A. Salahpour and M. Bouvier (2001). "Biochemical and biophysical demonstration of GPCR oligomerization in mammalian cells." Life Sci **68**(19-20): 2243-2250.

Arborelius, L., M. J. Owens, P. M. Plotsky and C. B. Nemeroff (1999). "The role of corticotropin-releasing factor in depression and anxiety disorders." J Endocrinol **160**(1): 1-12.

Balbas, M. D., M. R. Burgess, R. Murali, J. Wongvipat, B. J. Skaggs, P. Mundel, A. Weins and C. L. Sawyers (2014). "MAGI-2 scaffold protein is critical for kidney barrier function." Proc Natl Acad Sci U S A **111**(41): 14876-14881.

Balch, W. E., J. M. McCaffery, H. Plutner and M. G. Farquhar (1994). "Vesicular stomatitis virus glycoprotein is sorted and concentrated during export from the endoplasmic reticulum." Cell **76**(5): 841-852.

Barki-Harrington, L., L. M. Luttrell and H. A. Rockman (2003). "Dual inhibition of beta-adrenergic and angiotensin II receptors by a single antagonist: a functional role for receptor-receptor interaction in vivo." Circulation **108**(13): 1611-1618.

Barlowe, C. (2003). "Signals for COPII-dependent export from the ER: what's the ticket out?" Trends Cell Biol **13**(6): 295-300.

Barnes, A. P. and F. Polleux (2009). "Establishment of axon-dendrite polarity in developing neurons." Annu Rev Neurosci **32**: 347-381.

Bartlett, S. E., J. Enquist, F. W. Hopf, J. H. Lee, F. Gladher, V. Kharazia, M. Waldhoer, W. S. Mailliard, R. Armstrong, A. Bonci and J. L. Whistler (2005). "Dopamine responsiveness is regulated by targeted sorting of D2 receptors." Proc Natl Acad Sci U S A **102**(32): 11521-11526.

Bartlett, W. P. and G. A. Banker (1984a). "An electron microscopic study of the development of axons and dendrites by hippocampal neurons in culture. I. Cells which develop without intercellular contacts." J Neurosci **4**(8): 1944-1953.

Bartlett, W. P. and G. A. Banker (1984b). "An electron microscopic study of the development of axons and dendrites by hippocampal neurons in culture. II. Synaptic relationships." J Neurosci **4**(8): 1954-1965.

Bayatti, N., J. Zschocke and C. Behl (2003). "Brain region-specific neuroprotective action and signaling of corticotropin-releasing hormone in primary neurons." Endocrinology **144**(9): 4051-4060.

Becamel, C., S. Gavarini, B. Chanrion, G. Alonso, N. Galeotti, A. Dumuis, J. Bockaert and P. Marin (2004). "The serotonin 5-HT2A and 5-HT2C receptors interact with specific sets of PDZ proteins." J Biol Chem **279**(19): 20257-20266.

Beique, J. C. and R. Andrade (2003). "PSD-95 regulates synaptic transmission and plasticity in rat cerebral cortex." J Physiol **546**(Pt 3): 859-867.

Benson, D. L., F. H. Watkins, O. Steward and G. Banker (1994). "Characterization of GABAergic neurons in hippocampal cell cultures." J Neurocytol **23**(5): 279-295.

Bilder, D. (2001). "PDZ proteins and polarity: functions from the fly." Trends in Genetics **17**(9): 511-519.

Binneman, B., D. Feltner, S. Kolluri, Y. Shi, R. Qiu and T. Stiger (2008). "A 6-week randomized, placebo-controlled trial of CP-316,311 (a selective CRH1 antagonist) in the treatment of major depression." Am J Psychiatry **165**(5): 617-620.

Blank, T., I. Nijholt, K. Eckart and J. Spiess (2002). "Priming of long-term potentiation in mouse hippocampus by corticotropin-releasing factor and acute stress: implications for hippocampus-dependent learning." J Neurosci **22**(9): 3788-3794.

Bliss, T. V. P. and A. R. Gardner-Medwin (1973). "Long-lasting potentiation of synaptic transmission in the dentate area of the unanaesthetized rabbit following stimulation of the perforant path." The Journal of Physiology **232**(2): 357-374.

Blomer, U., L. Naldini, T. Kafri, D. Trono, I. M. Verma and F. H. Gage (1997). "Highly efficient and sustained gene transfer in adult neurons with a lentivirus vector." J Virol **71**(9): 6641-6649.

Bockaert, J., L. Fagni, A. Dumuis and P. Marin (2004). "GPCR interacting proteins (GIP)." Pharmacol Ther **103**(3): 203-221.

Bofill-Cardona, E., O. Kudlacek, Q. Yang, H. Ahorn, M. Freissmuth and C. Nanoff (2000). "Binding of Calmodulin to the D2-Dopamine Receptor Reduces Receptor Signaling by Arresting the G Protein Activation Switch." Journal of Biological Chemistry **275**(42): 32672-32680.

Bond, R. A. and A. P. Ijzerman (2006). "Recent developments in constitutive receptor activity and inverse agonism, and their potential for GPCR drug discovery." Trends in Pharmacological Sciences **27**(2): 92-96.

Bonfiglio, J. J., C. Inda, D. Refojo, F. Holsboer, E. Arzt and S. Silberstein (2011). "The Corticotropin-Releasing Hormone Network and the Hypothalamic-Pituitary-Adrenal Axis: Molecular and Cellular Mechanisms Involved." Neuroendocrinology **94**(1): 12-20.

Bornshein, M. B. and P. G. Model (1972). "Development of synapses and myelin in cultures of dissociated embryonic mouse spinal cord, medulla and cerebrum." Brain Res **37**(2): 287-293.

Bouschet, T., S. Martin and J. M. Henley (2005). "Receptor-activity-modifying proteins are required for forward trafficking of the calcium-sensing receptor to the plasma membrane." J Cell Sci **118**(Pt 20): 4709-4720.

Brenman, J. E., D. S. Chao, S. H. Gee, A. W. McGee, S. E. Craven, D. R. Santillano, Z. Wu, F. Huang, H. Xia, M. F. Peters, S. C. Froehner and D. S. Bredt (1996). "Interaction of nitric oxide synthase with the postsynaptic density protein PSD-95 and alpha1-syntrophin mediated by PDZ domains." Cell **84**(5): 757-767.

Brenman, J. E., J. R. Topinka, E. C. Cooper, A. W. McGee, J. Rosen, T. Milroy, H. J. Ralston and D. S. Bredt (1998). "Localization of postsynaptic density-93 to dendritic microtubules and interaction with microtubule-associated protein 1A." J Neurosci **18**(21): 8805-8813.

Buning, H., L. Perabo, O. Coutelle, S. Quadt-Humme and M. Hallek (2008). "Recent developments in adeno-associated virus vector technology." J Gene Med **10**(7): 717-733.

Bustos, F. J., L. Varela-Nallar, M. Campos, B. Henriquez, M. Phillips, C. Opazo, L. G. Aguayo, M. Montecino, M. Constantine-Paton, N. C. Inestrosa and B. van Zundert (2014). "PSD95 suppresses dendritic arbor development in mature hippocampal neurons by occluding the clustering of NR2B-NMDA receptors." PLoS One **9**(4): e94037.

Cai, C., S. K. Coleman, K. Niemi and K. Keinanen (2002). "Selective binding of synapse-associated protein 97 to GluR-A alpha-amino-5-hydroxy-3-methyl-4-isoxazole propionate receptor subunit is determined by a novel sequence motif." J Biol Chem **277**(35): 31484-31490.

Cai, C., H. Li, A. Kangasniemi, T. Pihlajamaa, L. Von Ossowski, K. Kerkela, S. Schulz, C. Rivera and K. Keinanen (2008). "Somatostatin receptor subtype 1 is a PDZ ligand for synapse-associated protein 97 and a potential regulator of growth cone dynamics." Neuroscience **157**(4): 833-843.

Chatterjee, N., J. Stegmuller, P. Schatzle, K. Karram, M. Koroll, H. B. Werner, K. A. Nave and J. Trotter (2008). "Interaction of syntenin-1 and the NG2 proteoglycan in migratory oligodendrocyte precursor cells." J Biol Chem **283**(13): 8310-8317.

Chen, B. S., S. Braud, J. D. Badger, 2nd, J. T. Isaac and K. W. Roche (2006). "Regulation of NR1/NR2C N-methyl-D-aspartate (NMDA) receptors by phosphorylation." J Biol Chem **281**(24): 16583-16590.

Chen, L., D. M. Chetkovich, R. S. Petralia, N. T. Sweeney, Y. Kawasaki, R. J. Wenthold, D. S. Bredt and R. A. Nicoll (2000a). "Stargazin regulates synaptic targeting of AMPA receptors by two distinct mechanisms." Nature **408**(6815): 936-943.

Chen, R., K. A. Lewis, M. H. Perrin and W. W. Vale (1993). "Expression cloning of a human corticotropin-releasing-factor receptor." Proceedings of the National Academy of Sciences of the United States of America **90**(19): 8967-8971.

Chen, Y., A. L. Andres, M. Frotscher and T. Z. Baram (2012a). "Tuning synaptic transmission in the hippocampus by stress: the CRH system." Frontiers in Cellular Neuroscience **6**: 13.

Chen, Y., R. A. Bender, M. Frotscher and T. Z. Baram (2001). "Novel and transient populations of corticotropin-releasing hormone-expressing neurons in developing hippocampus suggest unique functional roles: a quantitative spatiotemporal analysis." J Neurosci **21**(18): 7171-7181.

Chen, Y., K. L. Brunson, G. Adelmann, R. A. Bender, M. Frotscher and T. Z. Baram (2004). "Hippocampal corticotropin releasing hormone: pre- and postsynaptic location and release by stress." Neuroscience **126**(3): 533-540.

Chen, Y., K. L. Brunson, M. B. Muller, W. Cariaga and T. Z. Baram (2000b). "Immunocytochemical distribution of corticotropin-releasing hormone receptor type-1 (CRF(1))-like immunoreactivity in the mouse brain: light microscopy analysis using an antibody directed against the C-terminus." J Comp Neurol **420**(3): 305-323.

Chen, Y., C. M. Dube, C. J. Rice and T. Z. Baram (2008). "Rapid loss of dendritic spines after stress involves derangement of spine dynamics by corticotropin-releasing hormone." J Neurosci **28**(11): 2903-2911.

Chen, Y., E. A. Kramar, L. Y. Chen, A. H. Babayan, A. L. Andres, C. M. Gall, G. Lynch and T. Z. Baram (2012b). "Impairment of synaptic plasticity by the stress mediator CRH involves selective destruction of thin dendritic spines via RhoA signaling." Mol Psychiatry **18**(4): 485-496.

Chen, Y., C. S. Rex, C. J. Rice, C. M. Dube, C. M. Gall, G. Lynch and T. Z. Baram (2010). "Correlated memory defects and hippocampal dendritic spine loss after acute stress involve corticotropin-releasing hormone signaling." Proc Natl Acad Sci U S A **107**(29): 13123-13128.

Cheng, D., C. C. Hoogenraad, J. Rush, E. Ramm, M. A. Schlager, D. M. Duong, P. Xu, S. R. Wijayawardana, J. Hanfelt, T. Nakagawa, M. Sheng and J. Peng (2006). "Relative and absolute quantification of postsynaptic density proteome isolated from rat forebrain and cerebellum." Mol Cell Proteomics **5**(6): 1158-1170.

Chetkovich, D. M., R. C. Bunn, S. H. Kuo, Y. Kawasaki, M. Kohwi and D. S. Bredt (2002). "Postsynaptic targeting of alternative postsynaptic density-95 isoforms by distinct mechanisms." J Neurosci **22**(15): 6415-6425.

Chi, C. N., A. Bach, K. Stromgaard, S. Gianni and P. Jemth (2012). "Ligand binding by PDZ domains." Biofactors **38**(5): 338-348.

Christenn, M., S. Kindler, S. Schulz, F. Buck, D. Richter and H. J. Kreienkamp (2007). "Interaction of brain somatostatin receptors with the PDZ domains of PSD-95." FEBS Lett **581**(27): 5173-5177.

Christopherson, K. S., N. T. Sweeney, S. E. Craven, R. Kang, D. El-Husseini Ael and D. S. Bredt (2003). "Lipid- and protein-mediated multimerization of PSD-95: implications for receptor clustering and assembly of synaptic protein networks." J Cell Sci **116**(Pt 15): 3213-3219.

Chung, H. J., Y. H. Huang, L. F. Lau and R. L. Huganir (2004). "Regulation of the NMDA receptor complex and trafficking by activity-dependent phosphorylation of the NR2B subunit PDZ ligand." J Neurosci **24**(45): 10248-10259.

Cohen, N. A., J. E. Brenman, S. H. Snyder and D. S. Bredt (1996). "Binding of the inward rectifier K+ channel Kir 2.3 to PSD-95 is regulated by protein kinase A phosphorylation." Neuron **17**(4): 759-767.

Colledge, M., R. A. Dean, G. K. Scott, L. K. Langeberg, R. L. Huganir and J. D. Scott (2000). "Targeting of PKA to glutamate receptors through a MAGUK-AKAP complex." Neuron **27**(1): 107-119.

Colledge, M. and J. D. Scott (1999). "AKAPs: from structure to function." Trends Cell Biol **9**(6): 216-221.

Cooke, S. F. and T. V. Bliss (2006). "Plasticity in the human central nervous system." Brain **129**(Pt 7): 1659-1673.

Cornea-Hebert, V., K. C. Watkins, B. L. Roth, W. K. Kroeze, P. Gaudreau, N. Leclerc and L. Descarries (2002). "Similar ultrastructural distribution of the 5-HT(2A) serotonin receptor and microtubule-associated protein MAP1A in cortical dendrites of adult rat." Neuroscience **113**(1): 23-35.

Cottet, M., L. Albizu, L. Comps-Agrar, E. Trinquet, J. P. Pin, B. Mouillac and T. Durroux (2011). "Time resolved FRET strategy with fluorescent ligands to analyze receptor interactions in native tissues: application to GPCR oligomerization." Methods Mol Biol **746**: 373-387.

Craig, A. (1998). "Transfecting cultured neurons." Culturing nerve cells: 79-111.

Craig, A. M., C. D. Blackstone, R. L. Huganir and G. Banker (1993). "The distribution of glutamate receptors in cultured rat hippocampal neurons: postsynaptic clustering of AMPA-selective subunits." Neuron **10**(6): 1055-1068.

Craven, S. E. and D. S. Bredt (1998). "PDZ proteins organize synaptic signaling pathways." Cell **93**(4): 495-498.

Cui, H., A. Hayashi, H. S. Sun, M. P. Belmares, C. Cobey, T. Phan, J. Schweizer, M. W. Salter, Y. T. Wang, R. A. Tasker, D. Garman, J. Rabinowitz, P. S. Lu and M. Tymianski (2007). "PDZ protein interactions underlying NMDA receptor-mediated excitotoxicity and neuroprotection by PSD-95 inhibitors." J Neurosci **27**(37): 9901-9915.

Cuthbert, P. C., L. E. Stanford, M. P. Coba, J. A. Ainge, A. E. Fink, P. Opazo, J. Y. Delgado, N. H. Komiyama, T. J. O'Dell and S. G. N. Grant (2007). "Synapse-Associated Protein 102/dlgh3 Couples the NMDA Receptor to Specific Plasticity Pathways and Learning Strategies." The Journal of Neuroscience **27**(10): 2673-2682.

Cvejic, S. and L. A. Devi (1997). "Dimerization of the delta opioid receptor: implication for a role in receptor internalization." J Biol Chem **272**(43): 26959-26964.

Dakoji, S., S. Tomita, S. Karimzadegan, R. A. Nicoll and D. S. Bredt (2003). "Interaction of transmembrane AMPA receptor regulatory proteins with multiple membrane associated guanylate kinases." Neuropharmacology **45**(6): 849-856.

de Kloet, E. R., M. Joels and F. Holsboer (2005). "Stress and the brain: from adaptation to disease." Nat Rev Neurosci **6**(6): 463-475.

Dean, C., F. G. Scholl, J. Choih, S. DeMaria, J. Berger, E. Isacoff and P. Scheiffele (2003). "Neurexin mediates the assembly of presynaptic terminals." Nat Neurosci **6**(7): 708-716.

DeMarco, S. J. and E. E. Strehler (2001). "Plasma membrane Ca2+-atpase isoforms 2b and 4b interact promiscuously and selectively with members of the membrane-associated guanylate kinase family of PDZ (PSD95/Dlg/ZO-1) domain-containing proteins." J Biol Chem **276**(24): 21594-21600.

Dishart, K. L., L. Denby, S. J. George, S. A. Nicklin, S. Yendluri, M. J. Tuerk, M. P. Kelley, B. A. Donahue, A. C. Newby, T. Harding and A. H. Baker (2003). "Third-generation lentivirus vectors efficiently transduce and phenotypically modify vascular cells: implications for gene therapy." Journal of Molecular and Cellular Cardiology **35**(7): 739-748.

Dong, C., C. D. Nichols, J. Guo, W. Huang, N. A. Lambert and G. Wu (2012). "A triple arg motif mediates alpha(2B)-adrenergic receptor interaction with Sec24C/D and export." Traffic **13**(6): 857-868.

Dotti, C. G., C. A. Sullivan and G. A. Banker (1988). "The establishment of polarity by hippocampal neurons in culture." J Neurosci **8**(4): 1454-1468.

Dunham, J. H., R. C. Meyer, E. L. Garcia and R. A. Hall (2009). "GPR37 surface expression enhancement via N-terminal truncation or protein-protein interactions." Biochemistry **48**(43): 10286-10297.

Dunn, H. A., C. Walther, C. M. Godin, R. A. Hall and S. S. Ferguson (2013). "Role of SAP97 protein in the regulation of corticotropin-releasing factor receptor 1 endocytosis and extracellular signal-regulated kinase 1/2 signaling." J Biol Chem **288**(21): 15023-15034.

Dunn, H. A., C. Walther, G. Y. Yuan, F. A. Caetano, C. M. Godin and S. S. Ferguson (2014). "Role of SAP97 in the regulation of 5-HT2AR endocytosis and signaling." Mol Pharmacol **86**(3): 275-283.

Duvernay, M. T., C. M. Filipeanu and G. Wu (2005). "The regulatory mechanisms of export trafficking of G protein-coupled receptors." Cellular Signalling **17**(12): 1457-1465.

Ehrlich, I. and R. Malinow (2004). "Postsynaptic density 95 controls AMPA receptor incorporation during long-term potentiation and experience-driven synaptic plasticity." J Neurosci **24**(4): 916-927.

El-Husseini, A. E.-D., E. Schnell, D. M. Chetkovich, R. A. Nicoll and D. S. Bredt (2000a). "PSD-95 Involvement in Maturation of Excitatory Synapses." Science **290**(5495): 1364-1368.

El-Husseini, A. E., J. R. Topinka, J. E. Lehrer-Graiwer, B. L. Firestein, S. E. Craven, C. Aoki and D. S. Bredt (2000b). "Ion channel clustering by membrane-associated guanylate kinases. Differential regulation by N-terminal lipid and metal binding motifs." J Biol Chem **275**(31): 23904-23910.

el-Husseini Ael, D. and D. S. Bredt (2002). "Protein palmitoylation: a regulator of neuronal development and function." Nat Rev Neurosci **3**(10): 791-802.

Elias, G. M., L. Funke, V. Stein, S. G. Grant, D. S. Bredt and R. A. Nicoll (2006). "Synapse-specific and developmentally regulated targeting of AMPA receptors by a family of MAGUK scaffolding proteins." Neuron **52**(2): 307-320.

Engeholm, M. (2004). Identifizierung von Proteinen, die an die carboxyterminale zytoplasmatische Domäne des CRF1-Rezeptors binden, und biochemische Charakterisierung der Wechselwirkung zwischen dem CRF1-Rezeptor und PSD-95. Ph.D. thesis, Ludwig-Maximilians-Universität zu München.

Esseltine, J. L., L. B. Dale and S. S. Ferguson (2011). "Rab GTPases bind at a common site within the angiotensin II type I receptor carboxyl-terminal tail: evidence that Rab4 regulates receptor phosphorylation, desensitization, and resensitization." Mol Pharmacol **79**(1): 175-184.

Fagni, L., F. Ango, J. Perroy and J. Bockaert (2004). "Identification and functional roles of metabotropic glutamate receptor-interacting proteins." Semin Cell Dev Biol **15**(3): 289-298.

Fanning, A. S. and J. M. Anderson (1996). "Protein-protein interactions: PDZ domain networks." Curr Biol **6**(11): 1385-1388.

Feng, W., J. F. Long, J. S. Fan, T. Suetake and M. Zhang (2004). "The tetrameric L27 domain complex as an organization platform for supramolecular assemblies." Nat Struct Mol Biol **11**(5): 475-480.

Feng, W. and M. Zhang (2009). "Organization and dynamics of PDZ-domain-related supramodules in the postsynaptic density." Nat Rev Neurosci **10**(2): 87-99.

Ferre, S., V. Casado, L. A. Devi, M. Filizola, R. Jockers, M. J. Lohse, G. Milligan, J. P. Pin and X. Guitart (2014). "G protein-coupled receptor oligomerization revisited: functional and pharmacological perspectives." Pharmacol Rev **66**(2): 413-434.

Fiorentini, M., A. Bach, K. Stromgaard, J. S. Kastrup and M. Gajhede (2013). "Interaction partners of PSD-93 studied by X-ray crystallography and fluorescence polarization spectroscopy." Acta Crystallogr D Biol Crystallogr **69**(Pt 4): 587-594.

Firestein, B. L., B. L. Firestein, J. E. Brenman, C. Aoki, A. M. Sanchez-Perez, A. E. El-Husseini and D. S. Bredt (1999). "Cypin: a cytosolic regulator of PSD-95 postsynaptic targeting." Neuron **24**(3): 659-672.

Fredholm, B. B., T. Hokfelt and G. Milligan (2007). "G-protein-coupled receptors: an update." Acta Physiol (Oxf) **190**(1): 3-7.

Fukaya, M. and M. Watanabe (2000). "Improved immunohistochemical detection of postsynaptically located PSD-95/SAP90 protein family by protease section pretreatment: a study in the adult mouse brain." J Comp Neurol **426**(4): 572-586.

Fung, J. J., X. Deupi, L. Pardo, X. J. Yao, G. A. Velez-Ruiz, B. T. Devree, R. K. Sunahara and B. K. Kobilka (2009). "Ligand-regulated oligomerization of beta(2)-adrenoceptors in a model lipid bilayer." Embo J **28**(21): 3315-3328.

Funke, L., S. Dakoji and D. S. Bredt (2005). "Membrane-associated guanylate kinases regulate adhesion and plasticity at cell junctions." Annu Rev Biochem **74**: 219-245.

Gallagher, J. P., L. F. Orozco-Cabal, J. Liu and P. Shinnick-Gallagher (2008). "Synaptic physiology of central CRH system." Eur J Pharmacol **583**(2-3): 215-225.

Garcia, E. P., S. Mehta, L. A. Blair, D. G. Wells, J. Shang, T. Fukushima, J. R. Fallon, C. C. Garner and J. Marshall (1998). "SAP90 binds and clusters kainate receptors causing incomplete desensitization." Neuron **21**(4): 727-739.

Garcia, R. A., K. Vasudevan and A. Buonanno (2000). "The neuregulin receptor ErbB-4 interacts with PDZ-containing proteins at neuronal synapses." Proc Natl Acad Sci U S A **97**(7): 3596-3601.

Gee, H. Y., Y. W. Kim, M. J. Jo, W. Namkung, J. Y. Kim, H. W. Park, K. S. Kim, H. Kim, A. Baba, J. Yang, E. Kim, K. H. Kim and M. G. Lee (2009). "Synaptic scaffolding molecule binds to and regulates vasoactive intestinal polypeptide type-1 receptor in epithelial cells." Gastroenterology **137**(2): 607-617, 617 e601-604.

Gerrow, K., S. Romorini, S. M. Nabi, M. A. Colicos, C. Sala and A. El-Husseini (2006). "A preformed complex of postsynaptic proteins is involved in excitatory synapse development." Neuron **49**(4): 547-562.

Giagtzoglou, N., C. V. Ly and H. J. Bellen (2009). "Cell adhesion, the backbone of the synapse: "vertebrate" and "invertebrate" perspectives." Cold Spring Harb Perspect Biol **1**(4): a003079.

Gimferrer, I., A. Ibanez, M. Farnos, M. R. Sarrias, R. Fenutria, S. Rosello, P. Zimmermann, G. David, J. Vives, C. Serra-Pages and F. Lozano (2005). "The lymphocyte receptor CD6 interacts with syntenin-1, a scaffolding protein containing PDZ domains." J Immunol **175**(3): 1406-1414.

Gines, S., J. Hillion, M. Torvinen, S. Le Crom, V. Casado, E. I. Canela, S. Rondin, J. Y. Lew, S. Watson, M. Zoli, L. F. Agnati, P. Verniera, C. Lluis, S. Ferre, K. Fuxe and R. Franco (2000). "Dopamine D1 and adenosine A1 receptors form functionally interacting heteromeric complexes." Proc Natl Acad Sci U S A **97**(15): 8606-8611.

Giordano, G. and L. G. Costa (2011). "Primary neurons in culture and neuronal cell lines for in vitro neurotoxicological studies." Methods Mol Biol **758**: 13-27.

Giraudo, C. G. and H. J. Maccioni (2003). "Endoplasmic reticulum export of glycosyltransferases depends on interaction of a cytoplasmic dibasic motif with Sar1." Mol Biol Cell **14**(9): 3753-3766.

Glasl, L., K. Kloos, F. Giesert, A. Roethig, B. Di Benedetto, R. Kühn, J. Zhang, U. Hafen, J. Zerle, A. Hofmann, M. Hrabé de Angelis, K. F. Winklhofer, S. M. Hölter, D. M. Vogt Weisenhorn and W. Wurst (2012). "Pink1-deficiency in mice impairs gait, olfaction and serotonergic innervation of the olfactory bulb." Experimental Neurology **235**(1): 214-227.

Goebbels, S., I. Bormuth, U. Bode, O. Hermanson, M. H. Schwab and K. A. Nave (2006). "Genetic targeting of principal neurons in neocortex and hippocampus of NEX-Cre mice." Genesis **44**(12): 611-621.

Gonzalez-Maeso, J. (2011). "GPCR oligomers in pharmacology and signaling." Molecular Brain **4**(1): 20.

Gonzalez-Maeso, J., R. L. Ang, T. Yuen, P. Chan, N. V. Weisstaub, J. F. Lopez-Gimenez, M. Zhou, Y. Okawa, L. F. Callado, G. Milligan, J. A. Gingrich, M. Filizola, J. J. Meana and S. C. Sealfon (2008). "Identification of a serotonin/glutamate receptor complex implicated in psychosis." Nature **452**(7183): 93-97.

Good, M. C., J. G. Zalatan and W. A. Lim (2011). "Scaffold proteins: hubs for controlling the flow of cellular information." Science **332**(6030): 680-686.

Goodman, O. B., Jr., J. G. Krupnick, F. Santini, V. V. Gurevich, R. B. Penn, A. W. Gagnon, J. H. Keen and J. L. Benovic (1996). "Beta-arrestin acts as a clathrin adaptor in endocytosis of the beta2-adrenergic receptor." Nature **383**(6599): 447-450.

Graf, C., C. Kuehne, M. Panhuysen, B. Puetz, P. Weber, F. Holsboer, W. Wurst and J. M. Deussing (2012). "Corticotropin-releasing hormone regulates common target genes with divergent functions in corticotrope and neuronal cells." Mol Cell Endocrinol **362**(1-2): 29-38.

Grammatopoulos, D., G. M. Stirrat, S. A. Williams and E. W. Hillhouse (1996). "The biological activity of the corticotropin-releasing hormone receptor-adenylate cyclase complex in human myometrium is reduced at the end of pregnancy." J Clin Endocrinol Metab **81**(2): 745-751.

Grammatopoulos, D. K. and G. P. Chrousos (2002). "Functional characteristics of CRH receptors and potential clinical applications of CRH-receptor antagonists." Trends Endocrinol Metab **13**(10): 436-444.

Grammatopoulos, D. K., H. S. Randeva, M. A. Levine, E. S. Katsanou and E. W. Hillhouse (2000). "Urocortin, but not corticotropin-releasing hormone (CRH), activates the mitogen-activated protein kinase signal transduction pathway in human pregnant myometrium: an effect mediated via R1alpha and R2beta CRH receptor subtypes and stimulation of Gq-proteins." Mol Endocrinol **14**(12): 2076-2091.

Gutknecht, E., I. Van der Linden, K. Van Kolen, K. F. Verhoeven, G. Vauquelin and F. M. Dautzenberg (2009). "Molecular mechanisms of corticotropin-releasing factor receptor-induced calcium signaling." Mol Pharmacol **75**(3): 648-657.

Habets, A. M., A. M. Van Dongen, F. Van Huizen and M. A. Corner (1987). "Spontaneous neuronal firing patterns in fetal rat cortical networks during development in vitro: a quantitative analysis." Exp Brain Res **69**(1): 43-52.

Hague, C., M. A. Uberti, Z. Chen, C. F. Bush, S. V. Jones, K. J. Ressler, R. A. Hall and K. P. Minneman (2004). "Olfactory receptor surface expression is driven by association with the beta2-adrenergic receptor." Proc Natl Acad Sci U S A **101**(37): 13672-13676.

Hanson, S. M. and V. V. Gurevich (2006). "The differential engagement of arrestin surface charges by the various functional forms of the receptor." J Biol Chem **281**(6): 3458-3462.

Harrison, C. and P. H. van der Graaf (2006). "Current methods used to investigate G protein coupled receptor oligomerisation." J Pharmacol Toxicol Methods **54**(1): 26-35.

Hartig, W., A. Riedel, J. Grosche, R. H. Edwards, R. T. Fremeau, Jr., T. Harkany, K. Brauer and T. Arendt (2003). "Complementary distribution of vesicular glutamate transporters 1 and 2 in the nucleus accumbens of rat: Relationship to calretinin-containing extrinsic innervation and calbindin-immunoreactive neurons." J Comp Neurol **465**(1): 1-10.

Hauger, R. L., V. Risbrough, O. Brauns and F. M. Dautzenberg (2006). "Corticotropin releasing factor (CRF) receptor signaling in the central nervous system: new molecular targets." CNS Neurol Disord Drug Targets **5**(4): 453-479.

Hauger, R. L., V. Risbrough, R. H. Oakley, J. A. Olivares-Reyes and F. M. Dautzenberg (2009). "Role of CRF receptor signaling in stress vulnerability, anxiety, and depression." Ann N Y Acad Sci **1179**: 120-143.

Hayashi, M. K., H. M. Ames and Y. Hayashi (2006). "Tetrameric hub structure of postsynaptic scaffolding protein homer." J Neurosci **26**(33): 8492-8501.

He, J., M. Bellini, H. Inuzuka, J. Xu, Y. Xiong, X. Yang, A. M. Castleberry and R. A. Hall (2006). "Proteomic analysis of beta1-adrenergic receptor interactions with PDZ scaffold proteins." J Biol Chem **281**(5): 2820-2827.

Hebert, T. E., S. Moffett, J. P. Morello, T. P. Loisel, D. G. Bichet, C. Barret and M. Bouvier (1996). "A peptide derived from a beta2-adrenergic receptor transmembrane domain inhibits both receptor dimerization and activation." J Biol Chem **271**(27): 16384-16392.

Heo, K., S. H. Ha, Y. C. Chae, S. Lee, Y. S. Oh, Y. H. Kim, S. H. Kim, J. H. Kim, A. Mizoguchi, T. J. Itoh, H. M. Kwon, S. H. Ryu and P. G. Suh (2006). "RGS2 promotes formation of neurites by stimulating microtubule polymerization." Cell Signal **18**(12): 2182-2192.

Herman, J. P. and W. E. Cullinan (1997). "Neurocircuitry of stress: central control of the hypothalamo-pituitary-adrenocortical axis." Trends Neurosci **20**(2): 78-84.

Hillhouse, E. W. and D. K. Grammatopoulos (2006). "The molecular mechanisms underlying the regulation of the biological activity of corticotropin-releasing hormone receptors: implications for physiology and pathophysiology." Endocr Rev **27**(3): 260-286.

Hirao, K., Y. Hata, N. Ide, M. Takeuchi, M. Irie, I. Yao, M. Deguchi, A. Toyoda, T. C. Sudhof and Y. Takai (1998). "A novel multiple PDZ domain-containing molecule interacting with N-methyl-D-aspartate receptors and neuronal cell adhesion proteins." J Biol Chem **273**(33): 21105-21110.

Hirao, K., Y. Hata, I. Yao, M. Deguchi, H. Kawabe, A. Mizoguchi and Y. Takai (2000). "Three isoforms of synaptic scaffolding molecule and their characterization. Multimerization between the isoforms and their interaction with N-methyl-D-aspartate receptors and SAP90/PSD-95-associated protein." J Biol Chem **275**(4): 2966-2972.

Hock, B., B. Bohme, T. Karn, T. Yamamoto, K. Kaibuchi, U. Holtrich, S. Holland, T. Pawson, H. Rubsamen-Waigmann and K. Strebhardt (1998). "PDZ-domain-mediated interaction of the Eph-related receptor tyrosine kinase EphB3 and the ras-binding protein AF6 depends on the kinase activity of the receptor." Proc Natl Acad Sci U S A **95**(17): 9779-9784.

Holsboer, F. (2000). "The corticosteroid receptor hypothesis of depression." Neuropsychopharmacology **23**(5): 477-501.

Holsboer, F. (2014). "Redesigning antidepressant drug discovery." Dialogues Clin Neurosci **16**(1): 5-7.

Holsboer, F. and M. Ising (2008). "Central CRH system in depression and anxiety--evidence from clinical studies with CRH1 receptor antagonists." Eur J Pharmacol **583**(2-3): 350-357.

Howard, M. A., G. M. Elias, L. A. Elias, W. Swat and R. A. Nicoll (2010). "The role of SAP97 in synaptic glutamate receptor dynamics." Proc Natl Acad Sci U S A **107**(8): 3805-3810.

Hsueh, Y. P., E. Kim and M. Sheng (1997). "Disulfide-linked head-to-head multimerization in the mechanism of ion channel clustering by PSD-95." Neuron **18**(5): 803-814.

Hu, L. A., Y. Tang, W. E. Miller, M. Cong, A. G. Lau, R. J. Lefkowitz and R. A. Hall (2000). "beta 1-adrenergic receptor association with PSD-95. Inhibition of receptor internalization and facilitation of beta 1-adrenergic receptor interaction with N-methyl-D-aspartate receptors." J Biol Chem **275**(49): 38659-38666.

Huang, Y. S. and J. D. Richter (2007). "Analysis of mRNA translation in cultured hippocampal neurons." Methods Enzymol **431**: 143-162.

Huettner, J. E. and R. W. Baughman (1986). "Primary culture of identified neurons from the visual cortex of postnatal rats." J Neurosci **6**(10): 3044-3060.

Huganir, R. L. and R. A. Nicoll (2013). "AMPARs and synaptic plasticity: the last 25 years." Neuron **80**(3): 704-717.

Ichikawa, M., K. Muramoto, K. Kobayashi, M. Kawahara and Y. Kuroda (1993). "Formation and maturation of synapses in primary cultures of rat cerebral cortical cells: an electron microscopic study." Neurosci Res **16**(2): 95-103.

Ide, N., Y. Hata, H. Nishioka, K. Hirao, I. Yao, M. Deguchi, A. Mizoguchi, H. Nishimori, T. Tokino, Y. Nakamura and Y. Takai (1999). "Localization of membrane-associated guanylate kinase (MAGI)-1/BAI-associated protein (BAP) 1 at tight junctions of epithelial cells." Oncogene **18**(54): 7810-7815.

Ihara, K.-i., T. Nishimura, T. Fukuda, T. Ookura and K. Nishimori (2012). "Generation of Venus reporter knock-in mice revealed MAGI-2 expression patterns in adult mice." Gene Expression Patterns **12**(3â€"4): 95-101.

Iida, J., S. Hirabayashi, Y. Sato and Y. Hata (2004). "Synaptic scaffolding molecule is involved in the synaptic clustering of neuroligin." Mol Cell Neurosci **27**(4): 497-508.

Imamura, F., S. Maeda, T. Doi and Y. Fujiyoshi (2002). "Ligand binding of the second PDZ domain regulates clustering of PSD-95 with the Kv1.4 potassium channel." J Biol Chem **277**(5): 3640-3646.

Irie, M., Y. Hata, M. Takeuchi, K. Ichtchenko, A. Toyoda, K. Hirao, Y. Takai, T. W. Rosahl and T. C. Sudhof (1997). "Binding of neuroligins to PSD-95." Science **277**(5331): 1511-1515.

Ito, R., T. Takahashi, I. Katano and M. Ito (2012). "Current advances in humanized mouse models." Cell Mol Immunol **9**(3): 208-214.

Janas, J., J. Skowronski and L. Van Aelst (2006). "Lentiviral delivery of RNAi in hippocampal neurons." Methods Enzymol **406**: 593-605.

Jiang, M. and G. Chen (2006). "High Ca2+-phosphate transfection efficiency in low-density neuronal cultures." Nat Protoc **1**(2): 695-700.

Jugloff, D. G., R. Khanna, L. C. Schlichter and O. T. Jones (2000). "Internalization of the Kv1.4 potassium channel is suppressed by clustering interactions with PSD-95." J Biol Chem **275**(2): 1357-1364.

Justice, N. J., Z. F. Yuan, P. E. Sawchenko and W. Vale (2008). "Type 1 corticotropin-releasing factor receptor expression reported in BAC transgenic mice: implications for reconciling ligand-receptor mismatch in the central corticotropin-releasing factor system." J Comp Neurol **511**(4): 479-496.

Kalueff, A. V., M. Wheaton and D. L. Murphy (2007). "What's wrong with my mouse model? Advances and strategies in animal modeling of anxiety and depression." <u>Behav Brain Res</u> **179**(1): 1-18.

Kammermeier, P. J. and P. F. Worley (2007). "Homer 1a uncouples metabotropic glutamate receptor 5 from postsynaptic effectors." <u>Proc Natl Acad Sci U S A</u> **104**(14): 6055-6060.

Kaplan, N. A., X. Liu and N. S. Tolwinski (2009). "Epithelial polarity: interactions between junctions and apical-basal machinery." <u>Genetics</u> **183**(3): 897-904.

Karra, D. and R. Dahm (2010). "Transfection techniques for neuronal cells." <u>The Journal of Neuroscience</u> **30**(18): 6171-6177.

Kawaguchi, Y. and S. Kondo (2002). "Parvalbumin, somatostatin and cholecystokinin as chemical markers for specific GABAergic interneuron types in the rat frontal cortex." <u>Journal of Neurocytology</u> **31**(3-5): 277-287.

Kealy, B., A. Liew, J. M. McMahon, T. Ritter, A. O'Doherty, M. Hoare, U. Greiser, E. E. Vaughan, M. Maenz, C. O'Shea, F. Barry and T. O'Brien (2009). "Comparison of Viral and Nonviral Vectors for Gene Transfer to Human Endothelial Progenitor Cells." <u>Tissue Engineering Part C: Methods</u> **15**(2): 223-231.

Kevany, B. M. and K. Palczewski (2010). "Phagocytosis of retinal rod and cone photoreceptors." <u>Physiology (Bethesda)</u> **25**(1): 8-15.

Kim, E., K. O. Cho, A. Rothschild and M. Sheng (1996). "Heteromultimerization and NMDA receptor-clustering activity of Chapsyn-110, a member of the PSD-95 family of proteins." <u>Neuron</u> **17**(1): 103-113.

Kim, E., S. J. DeMarco, S. M. Marfatia, A. H. Chishti, M. Sheng and E. E. Strehler (1998). "Plasma membrane Ca2+ ATPase isoform 4b binds to membrane-associated guanylate kinase (MAGUK) proteins via their PDZ (PSD-95/Dlg/ZO-1) domains." <u>J Biol Chem</u> **273**(3): 1591-1595.

Kim, E., S. Naisbitt, Y.-P. Hsueh, A. Rao, A. Rothschild, A. M. Craig and M. Sheng (1997). "GKAP, a Novel Synaptic Protein That Interacts with the Guanylate Kinase-like Domain of the PSD-95/SAP90 Family of Channel Clustering Molecules." <u>The Journal of Cell Biology</u> **136**(3): 669-678.

Kim, E., M. Niethammer, A. Rothschild, Y. N. Jan and M. Sheng (1995). "Clustering of Shaker-type K+ channels by interaction with a family of membrane-associated guanylate kinases." <u>Nature</u> **378**(6552): 85-88.

Kim, E. and M. Sheng (2004). "PDZ domain proteins of synapses." <u>Nat Rev Neurosci</u> **5**(10): 771-781.

Klauck, T. M., M. C. Faux, K. Labudda, L. K. Langeberg, S. Jaken and J. D. Scott (1996). "Coordination of three signaling enzymes by AKAP79, a mammalian scaffold protein." <u>Science</u> **271**(5255): 1589-1592.

Koch, S., V. Sothilingam, M. Garcia Garrido, N. Tanimoto, E. Becirovic, F. Koch, C. Seide, S. C. Beck, M. W. Seeliger, M. Biel, R. Muhlfriedel and S. Michalakis (2012). "Gene therapy restores vision and delays degeneration in the CNGB1(-/-) mouse model of retinitis pigmentosa." <u>Hum Mol Genet</u> **21**(20): 4486-4496.

Kornau, H. C., L. T. Schenker, M. B. Kennedy and P. H. Seeburg (1995). "Domain interaction between NMDA receptor subunits and the postsynaptic density protein PSD-95." <u>Science</u> **269**(5231): 1737-1740.

Kovalovsky, D., D. Refojo, A. C. Liberman, D. Hochbaum, M. P. Pereda, O. A. Coso, G. K. Stalla, F. Holsboer and E. Arzt (2002). "Activation and induction of NUR77/NURR1 in corticotrophs by CRH/cAMP: involvement of calcium, protein kinase A, and MAPK pathways." Mol Endocrinol **16**(7): 1638-1651.

Kraetke, O., B. Wiesner, J. Eichhorst, J. Furkert, M. Bienert and M. Beyermann (2005). "Dimerization of corticotropin-releasing factor receptor type 1 is not coupled to ligand binding." J Recept Signal Transduct Res **25**(4-6): 251-276.

Kratzer, S., C. Mattusch, M. W. Metzger, N. Dedic, M. Noll-Hussong, K. W. Kafitz, M. Eder, J. M. Deussing, F. Holsboer, E. Kochs and G. Rammes (2013). "Activation of CRH receptor type 1 expressed on glutamatergic neurons increases excitability of CA1 pyramidal neurons by the modulation of voltage-gated ion channels." Front Cell Neurosci **7**: 91.

Kriegstein, A. R. and M. A. Dichter (1983). "Morphological classification of rat cortical neurons in cell culture." The Journal of Neuroscience **3**(8): 1634-1647.

Kristiansen, L. V. and J. H. Meador-Woodruff (2005). "Abnormal striatal expression of transcripts encoding NMDA interacting PSD proteins in schizophrenia, bipolar disorder and major depression." Schizophr Res **78**(1): 87-93.

Krueger, K. M., Y. Daaka, J. A. Pitcher and R. J. Lefkowitz (1997). "The role of sequestration in G protein-coupled receptor resensitization. Regulation of beta2-adrenergic receptor dephosphorylation by vesicular acidification." J Biol Chem **272**(1): 5-8.

Kuhne, C., O. Puk, J. Graw, M. Hrabe de Angelis, G. Schutz, W. Wurst and J. M. Deussing (2012). "Visualizing corticotropin-releasing hormone receptor type 1 expression and neuronal connectivities in the mouse using a novel multifunctional allele." J Comp Neurol **520**(14): 3150-3180.

Kurakin, A., A. Swistowski, S. C. Wu and D. E. Bredesen (2007). "The PDZ domain as a complex adaptive system." PLoS One **2**(9): e953.

Kuroda, Y., M. Ichikawa, K. Muramoto, K. Kobayashi, Y. Matsuda, A. Ogura and Y. Kudo (1992). "Block of synapse formation between cerebral cortical neurons by a protein kinase inhibitor." Neurosci Lett **135**(2): 255-258.

Lang, C. M., K. Fellerer, B. M. Schwenk, P. H. Kuhn, E. Kremmer, D. Edbauer, A. Capell and C. Haass (2012). "Membrane orientation and subcellular localization of transmembrane protein 106B (TMEM106B), a major risk factor for frontotemporal lobar degeneration." J Biol Chem **287**(23): 19355-19365.

Lauks, J., P. Klemmer, F. Farzana, R. Karupothula, R. Zalm, N. E. Cooke, K. W. Li, A. B. Smit, R. Toonen and M. Verhage (2012). "Synapse associated protein 102 (SAP102) binds the C-terminal part of the scaffolding protein neurobeachin." PLoS One **7**(6): e39420.

Laura, R. P., S. Ross, H. Koeppen and L. A. Lasky (2002). "MAGI-1: a widely expressed, alternatively spliced tight junction protein." Exp Cell Res **275**(2): 155-170.

Lee, H. J. and J. J. Zheng (2010). "PDZ domains and their binding partners: structure, specificity, and modification." Cell Commun Signal **8**: 8.

Lee, S. P., B. F. O'Dowd and S. R. George (2003). "Homo- and hetero-oligomerization of G protein-coupled receptors." Life Sci **74**(2-3): 173-180.

Lefkowitz, R. J. (1998). "G Protein-coupled Receptors: III. NEW ROLES FOR RECEPTOR KINASES AND Î²-ARRESTINS IN RECEPTOR SIGNALING AND DESENSITIZATION." Journal of Biological Chemistry **273**(30): 18677-18680.

Lehtonen, S., J. J. Ryan, K. Kudlicka, N. Iino, H. Zhou and M. G. Farquhar (2005). "Cell junction-associated proteins IQGAP1, MAGI-2, CASK, spectrins, and alpha-actinin are components of the nephrin multiprotein complex." Proc Natl Acad Sci U S A **102**(28): 9814-9819.

Leonard, A. S., M. A. Davare, M. C. Horne, C. C. Garner and J. W. Hell (1998). "SAP97 is associated with the alpha-amino-3-hydroxy-5-methylisoxazole-4-propionic acid receptor GluR1 subunit." J Biol Chem **273**(31): 19518-19524.

Leonoudakis, D., W. Mailliard, K. Wingerd, D. Clegg and C. Vandenberg (2001). "Inward rectifier potassium channel Kir2.2 is associated with synapse-associated protein SAP97." J Cell Sci **114**(Pt 5): 987-998.

Li, M., J. C. Bermak, Z. W. Wang and Q. Y. Zhou (2000). "Modulation of dopamine D(2) receptor signaling by actin-binding protein (ABP-280)." Mol Pharmacol **57**(3): 446-452.

Li, Z. and M. Sheng (2003). "Some assembly required: the development of neuronal synapses." Nat Rev Mol Cell Biol **4**(11): 833-841.

Lim, I. A., D. D. Hall and J. W. Hell (2002). "Selectivity and promiscuity of the first and second PDZ domains of PSD-95 and synapse-associated protein 102." J Biol Chem **277**(24): 21697-21711.

Lin, R., K. Karpa, N. Kabbani, P. Goldman-Rakic and R. Levenson (2001). "Dopamine D2 and D3 receptors are linked to the actin cytoskeleton via interaction with filamin A." Proc Natl Acad Sci U S A **98**(9): 5258-5263.

Long, J. F., H. Tochio, P. Wang, J. S. Fan, C. Sala, M. Niethammer, M. Sheng and M. Zhang (2003). "Supramodular structure and synergistic target binding of the N-terminal tandem PDZ domains of PSD-95." J Mol Biol **327**(1): 203-214.

Lopez-Munoz, F. and C. Alamo (2009). "Historical evolution of the neurotransmission concept." J Neural Transm **116**(5): 515-533.

Lu, A., M. A. Steiner, N. Whittle, A. M. Vogl, S. M. Walser, M. Ableitner, D. Refojo, M. Ekker, J. L. Rubenstein, G. K. Stalla, N. Singewald, F. Holsboer, C. T. Wotjak, W. Wurst and J. M. Deussing (2008). "Conditional mouse mutants highlight mechanisms of corticotropin-releasing hormone effects on stress-coping behavior." Mol Psychiatry **13**(11): 1028-1042.

Luckow, V. A. and M. D. Summers (1988). "Trends in the Development of Baculovirus Expression Vectors." Nat Biotech **6**(1): 47-55.

Luttrell, L. M. (2008). "Reviews in molecular biology and biotechnology: transmembrane signaling by G protein-coupled receptors." Mol Biotechnol **39**(3): 239-264.

Madisen, L., T. A. Zwingman, S. M. Sunkin, S. W. Oh, H. A. Zariwala, H. Gu, L. L. Ng, R. D. Palmiter, M. J. Hawrylycz, A. R. Jones, E. S. Lein and H. Zeng (2010). "A robust and high-throughput Cre reporting and characterization system for the whole mouse brain." Nat Neurosci **13**(1): 133-140.

Magalhaes, A. C., H. Dunn and S. S. Ferguson (2011). "Regulation of GPCR activity, trafficking and localization by GPCR-interacting proteins." Br J Pharmacol **165**(6): 1717-1736.

Magalhaes, A. C., K. D. Holmes, L. B. Dale, L. Comps-Agrar, D. Lee, P. N. Yadav, L. Drysdale, M. O. Poulter, B. L. Roth, J. P. Pin, H. Anisman and S. S. Ferguson (2010). "CRF receptor 1 regulates anxiety behavior via sensitization of 5-HT2 receptor signaling." Nat Neurosci **13**(5): 622-629.

Mah, W., J. Ko, J. Nam, K. Han, W. S. Chung and E. Kim (2010). "Selected SALM (synaptic adhesion-like molecule) family proteins regulate synapse formation." J Neurosci **30**(16): 5559-5568.

Mains, R. E. and P. H. Patterson (1973). "Primary cultures of dissociated sympathetic neurons. I. Establishment of long-term growth in culture and studies of differentiated properties." J Cell Biol **59**(2 Pt 1): 329-345.

Malenka, R. C. and M. F. Bear (2004). "LTP and LTD: an embarrassment of riches." Neuron **44**(1): 5-21.

Martinez-Gonzalez, C., H. L. Wang, B. R. Micklem, J. P. Bolam and J. Mena-Segovia (2012). "Subpopulations of cholinergic, GABAergic and glutamatergic neurons in the pedunculopontine nucleus contain calcium-binding proteins and are heterogeneously distributed." Eur J Neurosci **35**(5): 723-734.

Martinez, C. Y. and P. J. Hollenbeck (2003). "Transfection of primary central and peripheral nervous system neurons by electroporation." Methods Cell Biol **71**: 339-351.

Mauceri, D., F. Gardoni, E. Marcello and M. Di Luca (2007). "Dual role of CaMKII-dependent SAP97 phosphorylation in mediating trafficking and insertion of NMDA receptor subunit NR2A." J Neurochem **100**(4): 1032-1046.

Maurel, D., L. Comps-Agrar, C. Brock, M.-L. Rives, E. Bourrier, M. A. Ayoub, H. Bazin, N. Tinel, T. Durroux, L. Prezeau, E. Trinquet and J.-P. Pin (2008). "Cell-surface protein-protein interaction analysis with time-resolved FRET and snap-tag technologies: application to GPCR oligomerization." Nat Meth **5**(6): 561-567.

Maximov, A., T. C. Südhof and I. Bezprozvanny (1999). "Association of Neuronal Calcium Channels with Modular Adaptor Proteins." Journal of Biological Chemistry **274**(35): 24453-24456.

May, L. T., L. J. Bridge, L. A. Stoddart, S. J. Briddon and S. J. Hill (2011). "Allosteric interactions across native adenosine-A3 receptor homodimers: quantification using single-cell ligand-binding kinetics." Faseb J **25**(10): 3465-3476.

McConnell, S. K. (1995). "Constructing the cerebral cortex: neurogenesis and fate determination." Neuron **15**(4): 761-768.

McDowell, E. N., A. E. Kisielewski, J. W. Pike, H. L. Franco, H. H. Yao and K. J. Johnson (2012). "A transcriptome-wide screen for mRNAs enriched in fetal Leydig cells: CRHR1 agonism stimulates rat and mouse fetal testis steroidogenesis." PLoS One **7**(10): e47359.

McLatchie, L. M., N. J. Fraser, M. J. Main, A. Wise, J. Brown, N. Thompson, R. Solari, M. G. Lee and S. M. Foord (1998). "RAMPs regulate the transport and ligand specificity of the calcitonin-receptor-like receptor." Nature **393**(6683): 333-339.

Mellman, I. and W. J. Nelson (2008). "Coordinated protein sorting, targeting and distribution in polarized cells." Nat Rev Mol Cell Biol **9**(11): 833-845.

Meyer, D., T. Bonhoeffer and V. Scheuss (2014). "Balance and stability of synaptic structures during synaptic plasticity." Neuron **82**(2): 430-443.

Migaud, M., P. Charlesworth, M. Dempster, L. C. Webster, A. M. Watabe, M. Makhinson, Y. He, M. F. Ramsay, R. G. Morris, J. H. Morrison, T. J. O'Dell and S. G. Grant (1998). "Enhanced long-term potentiation and impaired learning in mice with mutant postsynaptic density-95 protein." Nature **396**(6710): 433-439.

Milligan, G. (2010). "The role of dimerisation in the cellular trafficking of G-protein-coupled receptors." Curr Opin Pharmacol **10**(1): 23-29.

Moller, T. C., V. F. Wirth, N. I. Roberts, J. Bender, A. Bach, B. P. Jacky, K. Stromgaard, J. M. Deussing, T. W. Schwartz and K. L. Martinez (2013). "PDZ domain-mediated interactions of G protein-coupled receptors with postsynaptic density protein 95: quantitative characterization of interactions." PLoS One **8**(5): e63352.

Montgomery, J. M., P. L. Zamorano and C. C. Garner (2004). "MAGUKs in synapse assembly and function: an emerging view." Cell Mol Life Sci **61**(7-8): 911-929.

Moore, C. A., S. K. Milano and J. L. Benovic (2007). "Regulation of receptor trafficking by GRKs and arrestins." Annu Rev Physiol **69**: 451-482.

Muller, B. M., U. Kistner, S. Kindler, W. J. Chung, S. Kuhlendahl, S. D. Fenster, L. F. Lau, R. W. Veh, R. L. Huganir, E. D. Gundelfinger and C. C. Garner (1996). "SAP102, a novel postsynaptic protein that interacts with NMDA receptor complexes in vivo." Neuron **17**(2): 255-265.

Muller, B. M., U. Kistner, R. W. Veh, C. Cases-Langhoff, B. Becker, E. D. Gundelfinger and C. C. Garner (1995). "Molecular characterization and spatial distribution of SAP97, a novel presynaptic protein homologous to SAP90 and the Drosophila discs-large tumor suppressor protein." J Neurosci **15**(3 Pt 2): 2354-2366.

Muller, M. B., J. Preil, U. Renner, S. Zimmermann, A. E. Kresse, G. K. Stalla, M. E. Keck, F. Holsboer and W. Wurst (2001). "Expression of CRHR1 and CRHR2 in mouse pituitary and adrenal gland: implications for HPA system regulation." Endocrinology **142**(9): 4150-4153.

Muller, M. B., S. Zimmermann, I. Sillaber, T. P. Hagemeyer, J. M. Deussing, P. Timpl, M. S. Kormann, S. K. Droste, R. Kuhn, J. M. Reul, F. Holsboer and W. Wurst (2003). "Limbic corticotropin-releasing hormone receptor 1 mediates anxiety-related behavior and hormonal adaptation to stress." Nat Neurosci **6**(10): 1100-1107.

Murata, M., P. D. Buckett, J. Zhou, M. Brunner, E. Folco and G. Koren (2001). "SAP97 interacts with Kv1.5 in heterologous expression systems." Am J Physiol Heart Circ Physiol **281**(6): H2575-2584.

Murata, Y. and M. Constantine-Paton (2013). "Postsynaptic density scaffold SAP102 regulates cortical synapse development through EphB and PAK signaling pathway." J Neurosci **33**(11): 5040-5052.

Murphy, T. H., L. A. Blatter, W. G. Wier and J. M. Baraban (1992). "Spontaneous synchronous synaptic calcium transients in cultured cortical neurons." J Neurosci **12**(12): 4834-4845.

Mushynski, W. E., S. Glen and H. M. Therien (1978). "Actin-like and tubulin-like proteins in synaptic junctional complexes." Can J Biochem **56**(8): 820-830.

Naisbitt, S., J. Valtschanoff, D. W. Allison, C. Sala, E. Kim, A. M. Craig, R. J. Weinberg and M. Sheng (2000). "Interaction of the postsynaptic density-95/guanylate kinase domain-associated protein complex with a light chain of myosin-V and dynein." J Neurosci **20**(12): 4524-4534.

Nakahira, E. and S. Yuasa (2005). "Neuronal generation, migration, and differentiation in the mouse hippocampal primoridium as revealed by enhanced green fluorescent protein gene transfer by means of in utero electroporation." J Comp Neurol **483**(3): 329-340.

Naldini, L., U. Blomer, P. Gallay, D. Ory, R. Mulligan, F. H. Gage, I. M. Verma and D. Trono (1996). "In vivo gene delivery and stable transduction of nondividing cells by a lentiviral vector." Science **272**(5259): 263-267.

Neer, E. J. (1995). "Heterotrimeric G proteins: organizers of transmembrane signals." Cell **80**(2): 249-257.

Nehring, R. B., E. Wischmeyer, F. Döring, R. d. W. Veh, M. Sheng and A. Karschin (2000a). "Neuronal Inwardly Rectifying K+ Channels Differentially Couple to PDZ Proteins of the PSD-95/SAP90 Family." The Journal of Neuroscience **20**(1): 156-162.

Nehring, R. B., E. Wischmeyer, F. Doring, R. W. Veh, M. Sheng and A. Karschin (2000b). "Neuronal inwardly rectifying K(+) channels differentially couple to PDZ proteins of the PSD-95/SAP90 family." J Neurosci **20**(1): 156-162.

Nemeroff, C. B., M. J. Owens, G. Bissette, A. C. Andorn and M. Stanley (1988). "Reduced corticotropin releasing factor binding sites in the frontal cortex of suicide victims." Arch Gen Psychiatry **45**(6): 577-579.

Nemeroff, C. B., E. Widerlov, G. Bissette, H. Walleus, I. Karlsson, K. Eklund, C. D. Kilts, P. T. Loosen and W. Vale (1984). "Elevated concentrations of CSF corticotropin-releasing factor-like immunoreactivity in depressed patients." Science **226**(4680): 1342-1344.

Niethammer, M., E. Kim and M. Sheng (1996). "Interaction between the C terminus of NMDA receptor subunits and multiple members of the PSD-95 family of membrane-associated guanylate kinases." J Neurosci **16**(7): 2157-2163.

Nishiyama, M., K. Hong, K. Mikoshiba, M. M. Poo and K. Kato (2000). "Calcium stores regulate the polarity and input specificity of synaptic modification." Nature **408**(6812): 584-588.

Noback, C. R., N. L. Strominger, R. J. Demarest and D. A. Ruggiero (2005). The human nervous system: structure and function, Springer.

Noctor, S. C., A. C. Flint, T. A. Weissman, R. S. Dammerman and A. R. Kriegstein (2001). "Neurons derived from radial glial cells establish radial units in neocortex." Nature **409**(6821): 714-720.

Oakley, R. H., S. A. Laporte, J. A. Holt, M. G. Caron and L. S. Barak (2000). "Differential affinities of visual arrestin, beta arrestin1, and beta arrestin2 for G protein-coupled receptors delineate two major classes of receptors." J Biol Chem **275**(22): 17201-17210.

Oakley, R. H., J. A. Olivares-Reyes, C. C. Hudson, F. Flores-Vega, F. M. Dautzenberg and R. L. Hauger (2007). "Carboxyl-terminal and intracellular loop sites for CRF1 receptor phosphorylation and beta-

arrestin-2 recruitment: a mechanism regulating stress and anxiety responses." Am J Physiol Regul Integr Comp Physiol **293**(1): R209-222.

Ogawa, Y., I. Horresh, J. S. Trimmer, D. S. Bredt, E. Peles and M. N. Rasband (2008). "Postsynaptic density-93 clusters Kv1 channels at axon initial segments independently of Caspr2." J Neurosci **28**(22): 5731-5739.

Ogura, A., T. Iijima, T. Amano and Y. Kudo (1987). "Optical monitoring of excitatory synaptic activity between cultured hippocampal neurons by a multi-site Ca2+ fluorometry." Neurosci Lett **78**(1): 69-74.

Ohno, K., M. Koroll, O. El Far, P. Scholze, J. Gomeza and H. Betz (2004). "The neuronal glycine transporter 2 interacts with the PDZ domain protein syntenin-1." Mol Cell Neurosci **26**(4): 518-529.

Ohnuma, T., H. Kato, H. Arai, R. L. Faull, P. J. McKenna and P. C. Emson (2000). "Gene expression of PSD95 in prefrontal cortex and hippocampus in schizophrenia." Neuroreport **11**(14): 3133-3137.

Ohtsuka, T., Y. Hata, N. Ide, T. Yasuda, E. Inoue, T. Inoue, A. Mizoguchi and Y. Takai (1999). "nRap GEP: A Novel Neural GDP/GTP Exchange Protein for Rap1 Small G Protein That Interacts with Synaptic Scaffolding Molecule (S-SCAM)." Biochemical and Biophysical Research Communications **265**(1): 38-44.

Oliva, C., P. Escobedo, C. Astorga, C. Molina and J. Sierralta (2011). "Role of the MAGUK protein family in synapse formation and function." Dev Neurobiol **72**(1): 57-72.

Opazo, P., A. M. Watabe, S. G. Grant and T. J. O'Dell (2003). "Phosphatidylinositol 3-kinase regulates the induction of long-term potentiation through extracellular signal-related kinase-independent mechanisms." J Neurosci **23**(9): 3679-3688.

Orru, M., J. Bakesova, M. Brugarolas, C. Quiroz, V. Beaumont, S. R. Goldberg, C. Lluis, A. Cortes, R. Franco, V. Casado, E. I. Canela and S. Ferre (2011). "Striatal pre- and postsynaptic profile of adenosine A(2A) receptor antagonists." PLoS One **6**(1): e16088.

Pak, D. T., S. Yang, S. Rudolph-Correia, E. Kim and M. Sheng (2001). "Regulation of dendritic spine morphology by SPAR, a PSD-95-associated RapGAP." Neuron **31**(2): 289-303.

Pan, L., J. Chen, J. Yu, H. Yu and M. Zhang (2011). "The structure of the PDZ3-SH3-GuK tandem of ZO-1 protein suggests a supramodular organization of the membrane-associated guanylate kinase (MAGUK) family scaffold protein core." J Biol Chem **286**(46): 40069-40074.

Papadopoulou, N., J. Chen, H. S. Randeva, M. A. Levine, E. W. Hillhouse and D. K. Grammatopoulos (2004). "Protein kinase A-induced negative regulation of the corticotropin-releasing hormone R1alpha receptor-extracellularly regulated kinase signal transduction pathway: the critical role of Ser301 for signaling switch and selectivity." Mol Endocrinol **18**(3): 624-639.

Parmar, H. B., C. Barry and R. Duncan (2014). "Polybasic trafficking signal mediates golgi export, ER retention or ER export and retrieval based on membrane-proximity." PLoS One **9**(4): e94194.

Passafaro, M., C. Sala, M. Niethammer and M. Sheng (1999). "Microtubule binding by CRIPT and its potential role in the synaptic clustering of PSD-95." Nat Neurosci **2**(12): 1063-1069.

Penzes, P., R. C. Johnson, R. Sattler, X. Zhang, R. L. Huganir, V. Kambampati, R. E. Mains and B. A. Eipper (2001). "The neuronal Rho-GEF Kalirin-7 interacts with PDZ domain-containing proteins and regulates dendritic morphogenesis." Neuron **29**(1): 229-242.

Peralta, E. G., A. Ashkenazi, J. W. Winslow, J. Ramachandran and D. J. Capon (1988). "Differential regulation of PI hydrolysis and adenylyl cyclase by muscarinic receptor subtypes." Nature **334**(6181): 434-437.

Perez-Perez, J. M., H. Candela and J. L. Micol (2009). "Understanding synergy in genetic interactions." Trends Genet **25**(8): 368-376.

Petralia, R. S., Y. X. Wang, F. Hua, Z. Yi, A. Zhou, L. Ge, F. A. Stephenson and R. J. Wenthold (2010). "Organization of NMDA receptors at extrasynaptic locations." Neuroscience **167**(1): 68-87.

Pfister, S., G. K. Przemeck, J. K. Gerber, J. Beckers, J. Adamski and M. Hrabe de Angelis (2003). "Interaction of the MAGUK family member Acvrinp1 and the cytoplasmic domain of the Notch ligand Delta1." J Mol Biol **333**(2): 229-235.

Powell, S. K., R. J. Rivas, E. Rodriguez-Boulan and M. E. Hatten (1997). "Development of polarity in cerebellar granule neurons." J Neurobiol **32**(2): 223-236.

Prybylowski, K., Z. Fu, G. Losi, L. M. Hawkins, J. Luo, K. Chang, R. J. Wenthold and S. Vicini (2002). "Relationship between availability of NMDA receptor subunits and their expression at the synapse." J Neurosci **22**(20): 8902-8910.

Punn, A., J. Chen, M. Delidaki, J. Tang, G. Liapakis, H. Lehnert, M. A. Levine and D. K. Grammatopoulos (2012). "Mapping structural determinants within third intracellular loop that direct signaling specificity of type 1 corticotropin-releasing hormone receptor." J Biol Chem **287**(12): 8974-8985.

Punnakkal, P., C. von Schoultz, K. Haenraets, H. Wildner and H. U. Zeilhofer (2014). "Morphological, biophysical and synaptic properties of glutamatergic neurons of the mouse spinal dorsal horn." J Physiol **592**(Pt 4): 759-776.

Raadsheer, F. C., W. J. Hoogendijk, F. C. Stam, F. J. Tilders and D. F. Swaab (1994). "Increased numbers of corticotropin-releasing hormone expressing neurons in the hypothalamic paraventricular nucleus of depressed patients." Neuroendocrinology **60**(4): 436-444.

Rademacher, N., S. A. Kunde, V. M. Kalscheuer and S. A. Shoichet (2013). "Synaptic MAGUK multimer formation is mediated by PDZ domains and promoted by ligand binding." Chem Biol **20**(8): 1044-1054.

Refojo, D., M. Schweizer, C. Kuehne, S. Ehrenberg, C. Thoeringer, A. M. Vogl, N. Dedic, M. Schumacher, G. von Wolff, C. Avrabos, C. Touma, D. Engblom, G. Schutz, K. A. Nave, M. Eder, C. T. Wotjak, I. Sillaber, F. Holsboer, W. Wurst and J. M. Deussing (2011). "Glutamatergic and dopaminergic neurons mediate anxiogenic and anxiolytic effects of CRHR1." Science **333**(6051): 1903-1907.

Reul, J. M. and F. Holsboer (2002). "On the role of corticotropin-releasing hormone receptors in anxiety and depression." Dialogues Clin Neurosci **4**(1): 31-46.

Rickhag, M., F. H. Hansen, G. Sorensen, K. N. Strandfelt, B. Andresen, K. Gotfryd, K. L. Madsen, I. Vestergaard-Klewe, I. Ammendrup-Johnsen, J. Eriksen, A. H. Newman, E. M. Fuchtbauer, J. Gomeza, D. P. Woldbye, G. Wortwein and U. Gether (2012). "A C-terminal PDZ domain-binding sequence is required for striatal distribution of the dopamine transporter." <u>Nat Commun</u> **4**: 1580.

Rizzoli, S. O. and W. J. Betz (2005). "Synaptic vesicle pools." <u>Nat Rev Neurosci</u> **6**(1): 57-69.

Roberts, S., C. Delury and E. Marsh (2012). "The PDZ protein discs-large (DLG): the 'Jekyll and Hyde' of the epithelial polarity proteins." <u>Febs J</u> **279**(19): 3549-3558.

Roche, K. W., C. D. Ly, R. S. Petralia, Y. X. Wang, A. W. McGee, D. S. Bredt and R. J. Wenthold (1999). "Postsynaptic density-93 interacts with the delta2 glutamate receptor subunit at parallel fiber synapses." <u>J Neurosci</u> **19**(10): 3926-3934.

Roche, K. W., S. Standley, J. McCallum, C. Dune Ly, M. D. Ehlers and R. J. Wenthold (2001). "Molecular determinants of NMDA receptor internalization." <u>Nat Neurosci</u> **4**(8): 794-802.

Rockman, H. A., W. J. Koch and R. J. Lefkowitz (2002). "Seven-transmembrane-spanning receptors and heart function." <u>Nature</u> **415**(6868): 206-212.

Rogers, J. H. (1992). "Immunohistochemical markers in rat cortex: co-localization of calretinin and calbindin-D28k with neuropeptides and GABA." <u>Brain Res</u> **587**(1): 147-157.

Rong, R., J. Y. Ahn, H. Huang, E. Nagata, D. Kalman, J. A. Kapp, J. Tu, P. F. Worley, S. H. Snyder and K. Ye (2003). "PI3 kinase enhancer-Homer complex couples mGluRI to PI3 kinase, preventing neuronal apoptosis." <u>Nat Neurosci</u> **6**(11): 1153-1161.

Rosenberg, M. M., F. Yang, J. L. Mohn, E. K. Storer and M. H. Jacob (2010). "The postsynaptic adenomatous polyposis coli (APC) multiprotein complex is required for localizing neuroligin and neurexin to neuronal nicotinic synapses in vivo." <u>J Neurosci</u> **30**(33): 11073-11085.

Royo, N. C., L. H. Vandenberghe, J. Y. Ma, A. Hauspurg, L. Yu, M. Maronski, J. Johnston, M. A. Dichter, J. M. Wilson and D. J. Watson (2008). "Specific AAV serotypes stably transduce primary hippocampal and cortical cultures with high efficiency and low toxicity." <u>Brain Res</u> **1190**: 15-22.

Rubin, R. T., R. E. Poland, I. M. Lesser, R. A. Winston and A. L. Blodgett (1987). "Neuroendocrine aspects of primary endogenous depression. I. Cortisol secretory dynamics in patients and matched controls." <u>Arch Gen Psychiatry</u> **44**(4): 328-336.

Rumbaugh, G., G. M. Sia, C. C. Garner and R. L. Huganir (2003). "Synapse-associated protein-97 isoform-specific regulation of surface AMPA receptors and synaptic function in cultured neurons." <u>J Neurosci</u> **23**(11): 4567-4576.

Saito, T. and N. Nakatsuji (2001). "Efficient gene transfer into the embryonic mouse brain using in vivo electroporation." <u>Dev Biol</u> **240**(1): 237-246.

Salaun, C., J. Greaves and L. H. Chamberlain (2010). "The intracellular dynamic of protein palmitoylation." <u>J Cell Biol</u> **191**(7): 1229-1238.

Sans, N., R. S. Petralia, Y. X. Wang, J. Blahos, 2nd, J. W. Hell and R. J. Wenthold (2000). "A developmental change in NMDA receptor-associated proteins at hippocampal synapses." <u>J Neurosci</u> **20**(3): 1260-1271.

Seachrist, J. L., S. A. Laporte, L. B. Dale, A. V. Babwah, M. G. Caron, P. H. Anborgh and S. S. Ferguson (2002). "Rab5 association with the angiotensin II type 1A receptor promotes Rab5 GTP binding and vesicular fusion." J Biol Chem **277**(1): 679-685.

Sethakorn, N., D. M. Yau and N. O. Dulin (2010). "Non-canonical functions of RGS proteins." Cell Signal **22**(9): 1274-1281.

Sevier, C. S., O. A. Weisz, M. Davis and C. E. Machamer (2000). "Efficient export of the vesicular stomatitis virus G protein from the endoplasmic reticulum requires a signal in the cytoplasmic tail that includes both tyrosine-based and di-acidic motifs." Mol Biol Cell **11**(1): 13-22.

Sexton, P. M., M. Morfis, N. Tilakaratne, D. L. Hay, M. Udawela, G. Christopoulos and A. Christopoulos (2006). "Complexing Receptor Pharmacology." Annals of the New York Academy of Sciences **1070**(1): 90-104.

Shakhbazau, A. V., I. N. Sevyaryn, N. V. Goncharova, V. V. Grinev, S. M. Kosmacheva and M. P. Potapnev (2008). "Viral vectors for stable transduction of human mesenchymal stem cells: systems based on adeno-associated viruses and lentiviruses." Bull Exp Biol Med **146**(4): 531-533.

Sheng, H., Y. Zhang, J. Sun, L. Gao, B. Ma, J. Lu and X. Ni (2008). "Corticotropin-releasing hormone (CRH) depresses n-methyl-D-aspartate receptor-mediated current in cultured rat hippocampal neurons via CRH receptor type 1." Endocrinology **149**(3): 1389-1398.

Sheng, M. and C. Sala (2001). "PDZ domains and the organization of supramolecular complexes." Annu Rev Neurosci **24**: 1-29.

Shenoy, S. K., P. H. McDonald, T. A. Kohout and R. J. Lefkowitz (2001). "Regulation of receptor fate by ubiquitination of activated beta 2-adrenergic receptor and beta-arrestin." Science **294**(5545): 1307-1313.

Shi, S. H., T. Cheng, L. Y. Jan and Y. N. Jan (2004). "The immunoglobulin family member dendrite arborization and synapse maturation 1 (Dasm1) controls excitatory synapse maturation." Proc Natl Acad Sci U S A **101**(36): 13346-13351.

Shoji, H., K. Tsuchida, H. Kishi, N. Yamakawa, T. Matsuzaki, Z. Liu, T. Nakamura and H. Sugino (2000). "Identification and characterization of a PDZ protein that interacts with activin type II receptors." J Biol Chem **275**(8): 5485-5492.

Sillaber, I., G. Rammes, S. Zimmermann, B. Mahal, W. Zieglgänsberger, W. Wurst, F. Holsboer and R. Spanagel (2002). "Enhanced and Delayed Stress-Induced Alcohol Drinking in Mice Lacking Functional CRH1 Receptors." Science **296**(5569): 931-933.

Sjogren, B. and R. R. Neubig (2010). "Thinking outside of the "RGS box": new approaches to therapeutic targeting of regulators of G protein signaling." Mol Pharmacol **78**(4): 550-557.

Skelton, N. J., M. F. Koehler, K. Zobel, W. L. Wong, S. Yeh, M. T. Pisabarro, J. P. Yin, L. A. Lasky and S. S. Sidhu (2003). "Origins of PDZ domain ligand specificity. Structure determination and mutagenesis of the Erbin PDZ domain." J Biol Chem **278**(9): 7645-7654.

Skieterska, K., J. Duchou, B. Lintermans and K. Van Craenenbroeck (2013). "Detection of G protein-coupled receptor (GPCR) dimerization by coimmunoprecipitation." Methods Cell Biol **117**: 323-340.

Smith, F. D., G. S. Oxford and S. L. Milgram (1999). "Association of the D2 dopamine receptor third cytoplasmic loop with spinophilin, a protein phosphatase-1-interacting protein." J Biol Chem **274**(28): 19894-19900.

Smith, G. W., J. M. Aubry, F. Dellu, A. Contarino, L. M. Bilezikjian, L. H. Gold, R. Chen, Y. Marchuk, C. Hauser, C. A. Bentley, P. E. Sawchenko, G. F. Koob, W. Vale and K. F. Lee (1998). "Corticotropin releasing factor receptor 1-deficient mice display decreased anxiety, impaired stress response, and aberrant neuroendocrine development." Neuron **20**(6): 1093-1102.

Smotrys, J. E. and M. E. Linder (2004). "Palmitoylation of intracellular signaling proteins: regulation and function." Annu Rev Biochem **73**: 559-587.

Standley, S., K. W. Roche, J. McCallum, N. Sans and R. J. Wenthold (2000). "PDZ domain suppression of an ER retention signal in NMDA receptor NR1 splice variants." Neuron **28**(3): 887-898.

Steigerwald, F., T. W. Schulz, L. T. Schenker, M. B. Kennedy, P. H. Seeburg and G. Kohr (2000). "C-Terminal truncation of NR2A subunits impairs synaptic but not extrasynaptic localization of NMDA receptors." J Neurosci **20**(12): 4573-4581.

Stein, V., D. R. House, D. S. Bredt and R. A. Nicoll (2003). "Postsynaptic density-95 mimics and occludes hippocampal long-term potentiation and enhances long-term depression." J Neurosci **23**(13): 5503-5506.

Steiner, P., M. J. Higley, W. Xu, B. L. Czervionke, R. C. Malenka and B. L. Sabatini (2008). "Destabilization of the postsynaptic density by PSD-95 serine 73 phosphorylation inhibits spine growth and synaptic plasticity." Neuron **60**(5): 788-802.

Stiffler, M. A., J. R. Chen, V. P. Grantcharova, Y. Lei, D. Fuchs, J. E. Allen, L. A. Zaslavskaia and G. MacBeath (2007). "PDZ domain binding selectivity is optimized across the mouse proteome." Science **317**(5836): 364-369.

Stockklausner, C., J. Ludwig, J. P. Ruppersberg and N. Klocker (2001). "A sequence motif responsible for ER export and surface expression of Kir2.0 inward rectifier K(+) channels." FEBS Lett **493**(2-3): 129-133.

Sumita, K., Y. Sato, J. Iida, A. Kawata, M. Hamano, S. Hirabayashi, K. Ohno, E. Peles and Y. Hata (2007). "Synaptic scaffolding molecule (S-SCAM) membrane-associated guanylate kinase with inverted organization (MAGI)-2 is associated with cell adhesion molecules at inhibitory synapses in rat hippocampal neurons." J Neurochem **100**(1): 154-166.

Sun, Y., D. McGarrigle and X. Y. Huang (2007). "When a G protein-coupled receptor does not couple to a G protein." Mol Biosyst **3**(12): 849-854.

Szafran, K., A. Faron-Gorecka, M. Kolasa, M. Kusmider, J. Solich, D. Zurawek and M. Dziedzicka-Wasylewska (2013). "Potential role of G protein-coupled receptor (GPCR) heterodimerization in neuropsychiatric disorders: a focus on depression." Pharmacol Rep **65**(6): 1498-1505.

Szidonya, L., M. Cserzo and L. Hunyady (2008). "Dimerization and oligomerization of G-protein-coupled receptors: debated structures with established and emerging functions." J Endocrinol **196**(3): 435-453.

Tabata, H. and K. Nakajima (2001). "Efficient in utero gene transfer system to the developing mouse brain using electroporation: visualization of neuronal migration in the developing cortex." Neuroscience **103**(4): 865-872.

Tada, T. and M. Sheng (2006). "Molecular mechanisms of dendritic spine morphogenesis." Curr Opin Neurobiol **16**(1): 95-101.

Takahashi, K., H. Nakanishi, M. Miyahara, K. Mandai, K. Satoh, A. Satoh, H. Nishioka, J. Aoki, A. Nomoto, A. Mizoguchi and Y. Takai (1999). "Nectin/PRR: an immunoglobulin-like cell adhesion molecule recruited to cadherin-based adherens junctions through interaction with Afadin, a PDZ domain-containing protein." J Cell Biol **145**(3): 539-549.

Takai, Y., T. Sasaki and T. Matozaki (2001). "Small GTP-binding proteins." Physiol Rev **81**(1): 153-208.

Takeuchi, M., Y. Hata, K. Hirao, A. Toyoda, M. Irie and Y. Takai (1997). "SAPAPs: A FAMILY OF PSD-95/SAP90-ASSOCIATED PROTEINS LOCALIZED AT POSTSYNAPTIC DENSITY." Journal of Biological Chemistry **272**(18): 11943-11951.

Tang, W. J. and A. G. Gilman (1991). "Type-specific regulation of adenylyl cyclase by G protein beta gamma subunits." Science **254**(5037): 1500-1503.

Taniguchi, H., M. He, P. Wu, S. Kim, R. Paik, K. Sugino, D. Kvitsiani, Y. Fu, J. Lu, Y. Lin, G. Miyoshi, Y. Shima, G. Fishell, S. B. Nelson and Z. J. Huang (2011). "A resource of Cre driver lines for genetic targeting of GABAergic neurons in cerebral cortex." Neuron **71**(6): 995-1013.

Tao, Y.-X. (2008). "Constitutive Activation of G Protein-Coupled Receptors and Diseases: Insights into Mechanisms of Activation and Therapeutics." Pharmacology & therapeutics **120**(2): 129-148.

Teichmann, A., A. Gibert, A. Lampe, P. Grzesik, C. Rutz, J. Furkert, J. Schmoranzer, G. Krause, B. Wiesner and R. Schülein (2014). "The Specific Monomer/Dimer Equilibrium of the Corticotropin-releasing Factor Receptor Type 1 Is Established in the Endoplasmic Reticulum." Journal of Biological Chemistry **289**(35): 24250-24262.

Thevenin, D., T. Lazarova, M. F. Roberts and C. R. Robinson (2005). "Oligomerization of the fifth transmembrane domain from the adenosine A2A receptor." Protein Sci **14**(8): 2177-2186.

Tian, Q. B., T. Suzuki, T. Yamauchi, H. Sakagami, Y. Yoshimura, S. Miyazawa, K. Nakayama, F. Saitoh, J. P. Zhang, Y. Lu, H. Kondo and S. Endo (2006). "Interaction of LDL receptor-related protein 4 (LRP4) with postsynaptic scaffold proteins via its C-terminal PDZ domain-binding motif, and its regulation by Ca/calmodulin-dependent protein kinase II." Eur J Neurosci **23**(11): 2864-2876.

Tiffany, A. M., L. N. Manganas, E. Kim, Y. P. Hsueh, M. Sheng and J. S. Trimmer (2000). "PSD-95 and SAP97 exhibit distinct mechanisms for regulating K(+) channel surface expression and clustering." J Cell Biol **148**(1): 147-158.

Timpl, P., R. Spanagel, I. Sillaber, A. Kresse, J. M. Reul, G. K. Stalla, V. Blanquet, T. Steckler, F. Holsboer and W. Wurst (1998). "Impaired stress response and reduced anxiety in mice lacking a functional corticotropin-releasing hormone receptor 1." Nat Genet **19**(2): 162-166.

Tohda, M. (2014). "Changes in the expression of BNIP-3 and other neuronal factors during the cultivation period of primary cultured rat cerebral cortical neurons and an assessment of each factor's functions." Cell signalling and Trafficking **2**.

Tonikian, R., Y. Zhang, S. L. Sazinsky, B. Currell, J. H. Yeh, B. Reva, H. A. Held, B. A. Appleton, M. Evangelista, Y. Wu, X. Xin, A. C. Chan, S. Seshagiri, L. A. Lasky, C. Sander, C. Boone, G. D. Bader and S. S. Sidhu (2008). "A specificity map for the PDZ domain family." PLoS Biol **6**(9): e239.

Tonon, M. C., P. Cuet, M. Lamacz, S. Jegou, J. Cote, L. Gouteaux, N. Ling, G. Pelletier and H. Vaudry (1986). "Comparative effects of corticotropin-releasing factor, arginine vasopressin, and related neuropeptides on the secretion of ACTH and alpha-MSH by frog anterior pituitary cells and neurointermediate lobes in vitro." Gen Comp Endocrinol **61**(3): 438-445.

Torres-Vega, M. A., R. Y. Vargas-Jeronimo, A. G. Montiel-Martinez, R. M. Munoz-Fuentes, A. Zamorano-Carrillo, A. R. Pastor and L. A. Palomares (2014). "Delivery of glutamine synthetase gene by baculovirus vectors: a proof of concept for the treatment of acute hyperammonemia." Gene Ther.

Tu, J. C., B. Xiao, J. P. Yuan, A. A. Lanahan, K. Leoffert, M. Li, D. J. Linden and P. F. Worley (1998). "Homer binds a novel proline-rich motif and links group 1 metabotropic glutamate receptors with IP3 receptors." Neuron **21**(4): 717-726.

Valdez, G. R. (2006). "Development of CRF1 receptor antagonists as antidepressants and anxiolytics: progress to date." CNS Drugs **20**(11): 887-896.

Valtschanoff, J. G., A. Burette, M. A. Davare, A. S. Leonard, J. W. Hell and R. J. Weinberg (2000). "SAP97 concentrates at the postsynaptic density in cerebral cortex." Eur J Neurosci **12**(10): 3605-3614.

Van Pett, K., V. Viau, J. C. Bittencourt, R. K. Chan, H. Y. Li, C. Arias, G. S. Prins, M. Perrin, W. Vale and P. E. Sawchenko (2000). "Distribution of mRNAs encoding CRF receptors in brain and pituitary of rat and mouse." J Comp Neurol **428**(2): 191-212.

Vargas, A., M. Lopez, C. Lillo and M. J. Vargas (2012). "[The Edwin Smith papyrus in the history of medicine]." Rev Med Chil **140**(10): 1357-1362.

Venkatakrishnan, A. J., X. Deupi, G. Lebon, C. G. Tate, G. F. Schertler and M. M. Babu (2013). "Molecular signatures of G-protein-coupled receptors." Nature **494**(7436): 185-194.

Venter, J. C., M. D. Adams, E. W. Myers, P. W. Li, R. J. Mural, G. G. Sutton, H. O. Smith, M. Yandell, C. A. Evans, R. A. Holt, J. D. Gocayne, P. Amanatides, R. M. Ballew, D. H. Huson, J. R. Wortman, Q. Zhang, C. D. Kodira, X. H. Zheng, L. Chen, M. Skupski, G. Subramanian, P. D. Thomas, J. Zhang, G. L. Gabor Miklos, C. Nelson, S. Broder, A. G. Clark, J. Nadeau, V. A. McKusick, N. Zinder, A. J. Levine, R. J. Roberts, M. Simon, C. Slayman, M. Hunkapiller, R. Bolanos, A. Delcher, I. Dew, D. Fasulo, M. Flanigan, L. Florea, A. Halpern, S. Hannenhalli, S. Kravitz, S. Levy, C. Mobarry, K. Reinert, K. Remington, J. Abu-Threideh, E. Beasley, K. Biddick, V. Bonazzi, R. Brandon, M. Cargill, I. Chandramouliswaran, R. Charlab, K. Chaturvedi, Z. Deng, V. Di Francesco, P. Dunn, K. Eilbeck, C. Evangelista, A. E. Gabrielian, W. Gan, W. Ge, F. Gong, Z. Gu, P. Guan, T. J. Heiman, M. E. Higgins, R. R. Ji, Z. Ke, K. A. Ketchum, Z. Lai, Y. Lei, Z. Li, J. Li, Y. Liang, X. Lin, F. Lu, G. V. Merkulov, N. Milshina, H. M. Moore, A. K. Naik, V. A. Narayan, B. Neelam, D. Nusskern, D. B. Rusch, S. Salzberg, W. Shao, B. Shue, J. Sun, Z. Wang, A. Wang, X. Wang, J. Wang, M. Wei, R. Wides, C. Xiao, C. Yan, A. Yao, J. Ye, M. Zhan, W. Zhang, H. Zhang, Q. Zhao, L. Zheng, F. Zhong, W. Zhong, S. Zhu, S. Zhao, D. Gilbert, S. Baumhueter, G. Spier, C. Carter, A. Cravchik, T. Woodage, F. Ali, H. An, A. Awe, D. Baldwin, H. Baden, M. Barnstead, I. Barrow, K. Beeson, D. Busam, A. Carver, A. Center, M. L. Cheng, L. Curry, S. Danaher, L. Davenport, R. Desilets, S. Dietz, K. Dodson, L. Doup, S. Ferriera, N. Garg, A. Gluecksmann, B. Hart, J. Haynes, C. Haynes, C. Heiner, S. Hladun, D. Hostin, J. Houck, T. Howland, C. Ibegwam, J. Johnson, F. Kalush, L. Kline, S. Koduru, A. Love, F. Mann, D. May, S. McCawley, T. McIntosh, I. McMullen, M. Moy, L. Moy, B. Murphy, K. Nelson, C. Pfannkoch,

E. Pratts, V. Puri, H. Qureshi, M. Reardon, R. Rodriguez, Y. H. Rogers, D. Romblad, B. Ruhfel, R. Scott, C. Sitter, M. Smallwood, E. Stewart, R. Strong, E. Suh, R. Thomas, N. N. Tint, S. Tse, C. Vech, G. Wang, J. Wetter, S. Williams, M. Williams, S. Windsor, E. Winn-Deen, K. Wolfe, J. Zaveri, K. Zaveri, J. F. Abril, R. Guigo, M. J. Campbell, K. V. Sjolander, B. Karlak, A. Kejariwal, H. Mi, B. Lazareva, T. Hatton, A. Narechania, K. Diemer, A. Muruganujan, N. Guo, S. Sato, V. Bafna, S. Istrail, R. Lippert, R. Schwartz, B. Walenz, S. Yooseph, D. Allen, A. Basu, J. Baxendale, L. Blick, M. Caminha, J. Carnes-Stine, P. Caulk, Y. H. Chiang, M. Coyne, C. Dahlke, A. Mays, M. Dombroski, M. Donnelly, D. Ely, S. Esparham, C. Fosler, H. Gire, S. Glanowski, K. Glasser, A. Glodek, M. Gorokhov, K. Graham, B. Gropman, M. Harris, J. Heil, S. Henderson, J. Hoover, D. Jennings, C. Jordan, J. Jordan, J. Kasha, L. Kagan, C. Kraft, A. Levitsky, M. Lewis, X. Liu, J. Lopez, D. Ma, W. Majoros, J. McDaniel, S. Murphy, M. Newman, T. Nguyen, N. Nguyen, M. Nodell, S. Pan, J. Peck, M. Peterson, W. Rowe, R. Sanders, J. Scott, M. Simpson, T. Smith, A. Sprague, T. Stockwell, R. Turner, E. Venter, M. Wang, M. Wen, D. Wu, M. Wu, A. Xia, A. Zandieh and X. Zhu (2001). "The sequence of the human genome." Science **291**(5507): 1304-1351.

Vidi, P. A. and V. J. Watts (2009). "Fluorescent and bioluminescent protein-fragment complementation assays in the study of G protein-coupled receptor oligomerization and signaling." Mol Pharmacol **75**(4): 733-739.

Violin, J. D. and R. J. Lefkowitz (2007). "Beta-arrestin-biased ligands at seven-transmembrane receptors." Trends Pharmacol Sci **28**(8): 416-422.

von Ossowski, I., E. Oksanen, L. von Ossowski, C. Cai, M. Sundberg, A. Goldman and K. Keinanen (2006a). "Crystal structure of the second PDZ domain of SAP97 in complex with a GluR-A C-terminal peptide." Febs J **273**(22): 5219-5229.

von Ossowski, L., H. Tossavainen, I. von Ossowski, C. Cai, O. Aitio, K. Fredriksson, P. Permi, A. Annila and K. Keinanen (2006b). "Peptide binding and NMR analysis of the interaction between SAP97 PDZ2 and GluR-A: potential involvement of a disulfide bond." Biochemistry **45**(17): 5567-5575.

Waites, C. L., C. G. Specht, K. Hartel, S. Leal-Ortiz, D. Genoux, D. Li, R. C. Drisdel, O. Jeyifous, J. E. Cheyne, W. N. Green, J. M. Montgomery and C. C. Garner (2009). "Synaptic SAP97 isoforms regulate AMPA receptor dynamics and access to presynaptic glutamate." J Neurosci **29**(14): 4332-4345.

Wallerath, T., K. Witte, S. C. Schäfer, P. M. Schwarz, W. Prellwitz, P. Wohlfart, H. Kleinert, H.-A. Lehr, B. r. Lemmer and U. Förstermann (1999). "Down-regulation of the expression of endothelial NO synthase is likely to contribute to glucocorticoid-mediated hypertension." Proceedings of the National Academy of Sciences of the United States of America **96**(23): 13357-13362.

Wang, X. D., Y. A. Su, K. V. Wagner, C. Avrabos, S. H. Scharf, J. Hartmann, M. Wolf, C. Liebl, C. Kuhne, W. Wurst, F. Holsboer, M. Eder, J. M. Deussing, M. B. Muller and M. V. Schmidt (2013). "Nectin-3 links CRHR1 signaling to stress-induced memory deficits and spine loss." Nat Neurosci **16**(6): 706-713.

Watase, K. and H. Y. Zoghbi (2003). "Modelling brain diseases in mice: the challenges of design and analysis." Nat Rev Genet **4**(4): 296-307.

Whistler, J. L., J. Enquist, A. Marley, J. Fong, F. Gladher, P. Tsuruda, S. R. Murray and M. Von Zastrow (2002). "Modulation of postendocytic sorting of G protein-coupled receptors." Science **297**(5581): 615-620.

Whorton, M. R., M. P. Bokoch, S. G. Rasmussen, B. Huang, R. N. Zare, B. Kobilka and R. K. Sunahara (2007). "A monomeric G protein-coupled receptor isolated in a high-density lipoprotein particle efficiently activates its G protein." Proc Natl Acad Sci U S A **104**(18): 7682-7687.

Woods, D. F. and P. J. Bryant (1989). "Molecular cloning of the lethal(1)discs large-1 oncogene of Drosophila." Dev Biol **134**(1): 222-235.

Woods, D. F. and P. J. Bryant (1991). "The discs-large tumor suppressor gene of Drosophila encodes a guanylate kinase homolog localized at septate junctions." Cell **66**(3): 451-464.

Woods, D. F., C. Hough, D. Peel, G. Callaini and P. J. Bryant (1996). "Dlg protein is required for junction structure, cell polarity, and proliferation control in Drosophila epithelia." J Cell Biol **134**(6): 1469-1482.

Xia, Z., J. A. Gray, B. A. Compton-Toth and B. L. Roth (2003a). "A direct interaction of PSD-95 with 5-HT2A serotonin receptors regulates receptor trafficking and signal transduction." J Biol Chem **278**(24): 21901-21908.

Xia, Z., S. J. Hufeisen, J. A. Gray and B. L. Roth (2003b). "The PDZ-binding domain is essential for the dendritic targeting of 5-HT2A serotonin receptors in cortical pyramidal neurons in vitro." Neuroscience **122**(4): 907-920.

Xu, J., J. D. Hennebold and R. L. Stouffer (2006). "Dynamic Expression and Regulation of the Corticotropin-Releasing Hormone/Urocortin-Receptor-Binding Protein System in the Primate Ovary during the Menstrual Cycle." The Journal of Clinical Endocrinology & Metabolism **91**(4): 1544-1553.

Xu, J., M. Paquet, A. G. Lau, J. D. Wood, C. A. Ross and R. A. Hall (2001). "beta 1-adrenergic receptor association with the synaptic scaffolding protein membrane-associated guanylate kinase inverted-2 (MAGI-2). Differential regulation of receptor internalization by MAGI-2 and PSD-95." J Biol Chem **276**(44): 41310-41317.

Xu, W. (2011). "PSD-95-like membrane associated guanylate kinases (PSD-MAGUKs) and synaptic plasticity." Curr Opin Neurobiol **21**(2): 306-312.

Xu, W., O. M. Schluter, P. Steiner, B. L. Czervionke, B. Sabatini and R. C. Malenka (2008). "Molecular dissociation of the role of PSD-95 in regulating synaptic strength and LTD." Neuron **57**(2): 248-262.

Yamada, A., K. Irie, M. Deguchi-Tawarada, T. Ohtsuka and Y. Takai (2003). "Nectin-dependent localization of synaptic scaffolding molecule (S-SCAM) at the puncta adherentia junctions formed between the mossy fibre terminals and the dendrites of pyramidal cells in the CA3 area of the mouse hippocampus." Genes Cells **8**(12): 985-994.

Yan, X. X., Z. Toth, L. Schultz, C. E. Ribak and T. Z. Baram (1998). "Corticotropin-releasing hormone (CRH)-containing neurons in the immature rat hippocampal formation: light and electron microscopic features and colocalization with glutamate decarboxylase and parvalbumin." Hippocampus **8**(3): 231-243.

Yao, I., J. Iida, W. Nishimura and Y. Hata (2003). "Synaptic localization of SAPAP1, a synaptic membrane-associated protein." Genes Cells **8**(2): 121-129.

Yap, C. C., Y. Muto, H. Kishida, T. Hashikawa and R. Yano (2003). "PKC regulates the delta2 glutamate receptor interaction with S-SCAM/MAGI-2 protein." Biochem Biophys Res Commun **301**(4): 1122-1128.

Yavin, Z. and E. Yavin (1977). "Synaptogenesis and myelinogenesis in dissociated cerebral cells from rat embryo on polylysine coated surfaces." Exp Brain Res **29**(1): 137-147.

Ye, F. and M. Zhang (2013). "Structures and target recognition modes of PDZ domains: recurring themes and emerging pictures." Biochem J **455**(1): 1-14.

Yokomaku, D., H. Jourdi, A. Kakita, T. Nagano, H. Takahashi, N. Takei and H. Nawa (2005). "ErbB1 receptor ligands attenuate the expression of synaptic scaffolding proteins, GRIP1 and SAP97, in developing neocortex." Neuroscience **136**(4): 1037-1047.

Young, S., C. Griffante and G. Aguilera (2007). "Dimerization Between Vasopressin V1b and Corticotropin Releasing Hormone Type 1 Receptors." Cellular and Molecular Neurobiology **27**(4): 439-461.

Yudowski, G. A., O. Olsen, H. Adesnik, K. W. Marek and D. S. Bredt (2013). "Acute Inactivation of PSD-95 Destabilizes AMPA Receptors at Hippocampal Synapses." PLoS ONE **8**(1): e53965.

Zeitelhofer, M., J. P. Vessey, Y. Xie, F. Tubing, S. Thomas, M. Kiebler and R. Dahm (2007). "High-efficiency transfection of mammalian neurons via nucleofection." Nat Protoc **2**(7): 1692-1704.

Zhang, M., J. T. Xu, X. Zhu, Z. Wang, X. Zhao, Z. Hua, Y. X. Tao and Y. Xu (2010). "Postsynaptic density-93 deficiency protects cultured cortical neurons from N-methyl-D-aspartate receptor-triggered neurotoxicity." Neuroscience **166**(4): 1083-1090.

Zhang, X., Dong C, Wu QJ, Balch WE and W. G. (2011). "Di-acidic motifs in the membrane-distal C termini modulate the transport of angiotensin II receptors from the endoplasmic reticulum to the cell surface." J Biol Chem. **286**(23): 20525-20535.

Zhang, Y., H. Wang, H. Pan, X. Bao, M. Li, J. Jin and X. Wu (2006). "Gene delivery into primary cerebral cortical neurons by lentiviral vector." Cell Biol Int **30**(10): 777-783.

Zheng, C. Y., G. K. Seabold, M. Horak and R. S. Petralia (2011). "MAGUKs, synaptic development, and synaptic plasticity." Neuroscientist **17**(5): 493-512.

Zhou, W., L. Zhang, X. Guoxiang, J. Mojsilovic-Petrovic, K. Takamaya, R. Sattler, R. Huganir and R. Kalb (2008). "GluR1 controls dendrite growth through its binding partner, SAP97." J Neurosci **28**(41): 10220-10233.

Ziff, E. B. (1997). "Enlightening the Postsynaptic Density." Neuron **19**(6): 1163-1174.

Zmijewski, M. A. and A. T. Slominski (2009). "CRF1 receptor splicing in epidermal keratinocytes: potential biological role and environmental regulations." J Cell Physiol **218**(3): 593-602.

Zmijewski, M. A. and A. T. Slominski (2010). "Emerging role of alternative splicing of CRF1 receptor in CRF signaling." Acta Biochim Pol **57**(1): 1-13.

8 Acknowledgements